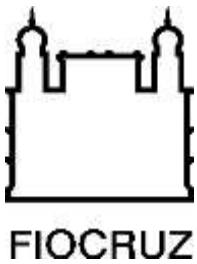


**FUNDAÇÃO OSWALDO CRUZ**
**INSTITUTO GONÇALO MONIZ**

**Programa de Pós-graduação em Biotecnologia em Saúde e Medicina Investigativa**

**TESE DE DOUTORADO**

# AVALIAÇÃO FARMACOLÓGICA DE COMPOSTOS HÍBRIDOS DE AÇÃO EM MÚLTIPLOS ESTÁGIOS OU DE DURAÇÃO LONGA PARA O TRATAMENTO DA MALÁRIA

**HELENITA COSTA QUADROS**

**Salvador - Bahia**
**2023**

**FUNDAÇÃO OSWALDO CRUZ**
**INSTITUTO GONÇALO MONIZ**

**Programa de Pós-graduação em Biotecnologia em Saúde e Medicina Investigativa**

# AVALIAÇÃO FARMACOLÓGICA DE COMPOSTOS HÍBRIDOS DE AÇÃO EM MÚLTIPLOS ESTÁGIOS OU DE DURAÇÃO LONGA PARA O TRATAMENTO DA MALÁRIA

**HELENITA COSTA QUADROS**

Tese apresentada ao Programa de Pós-graduação em Biotecnologia em Saúde e Medicina Investigativa para obtenção do grau de Doutora.

**Orientador**: Dr. Diogo Rodrigo de Magalhães Moreira
**Coorientadora**: Nicoletta Basilico
**Coorientador**: Dr. Fábio Rocha Formiga

**Salvador - Bahia**
**2023**

Ficha Catalográfica elaborada pela Biblioteca do
Instituto Gonçalo Moniz/ FIOCRUZ – Bahia - Salvador

**Q1a** Quadros, Helenita Costa

Avaliação farmacológica de compostos híbridos de ação em múltiplos estágios ou de duração longa para o tratamento da malária. / Helenita Costa Quadros. _ Salvador, 2023.

169 f.: il.: 30 cm

Orientador: Dr. Diogo Rodrigo de Magalhães Moreira
Coorientadora: Nicoletta Basilico
Coorientador: Dr. Fábio Rocha Formiga

Tese (Doutorado em Biotecnologia em Saúde e Medicina Investigativa) – Instituto Gonçalo Moniz, Fundação Oswaldo Cruz, Salvador, 2023.

1. Malária. 2. Plasmódio. Artemisininas. 4. Quinolinas. 5. Híbridos 6. Tratamento. I. Título.

CDU 616.936

"AVALIAÇÃO FARMACOLÓGICA DE COMPOSTOS HÍBRIDOS DE AÇÃO EM MÚLTIPLOS ESTÁGIOS OU DE DURAÇÃO LONGA PARA O TRATAMENTO DA MALÁRIA".

**HELENITA COSTA QUADROS**

FOLHA DE APROVAÇÃO

Salvador, **14 de fevereiro 2023**.

COMISSÃO EXAMINADORA

Dr. Daniel Youssef Bargieri
Professor Doutor
USP

Dr. Roberto Rudge de Moraes Barros
Professor Adjunto
UNIFESP

Dr. Leonardo de Farias Paiva
Pesquisador
IGM/FIOCRUZ

**FONTES DE FINANCIAMENTO**

"O presente trabalho foi realizado com apoio da Coordenação de Aperfeiçoamento de Pessoal de Nível Superior - Brasil (CAPES) - Código de Financiamento 001."

Fundação de Amparo à Pesquisa do Estado da Bahia – FAPESB.

*Dedico esta tese aos meus pais, Alberto e Sidnei, pelo apoio incondicional ao longo de toda a minha vida.*

## AGRADECIMENTOS

A Deus, por ser o meu melhor amigo e por conduzir a minha vida da melhor forma desde o meu nascimento até o momento presente.

Aos meus pais, Alberto e Sidnei, por me apoiarem em todas as minhas escolhas profissionais e, principalmente, por todas as orações em favor da minha felicidade e do meu sucesso. Vocês são inspiração e o meu combustível para continuar.

Aos meus irmãos, Larissa e Alberto, pelos suportes afetivo e emocional, vibrando pelas minhas conquistas e pelo meu sucesso em todos os momentos. Somos um tripé, cujo amor é a base de existirmos e continuarmos caminhando juntos até a eternidade.

As minhas avós, Helenita, Solange e Isaura, que com suas orações e palavras de conforto me fizeram continuar acreditando que sempre estive no caminho certo. Vocês foram essenciais para que eu me tornasse quem sou hoje.

A todos os meus familiares pelas orações e pelo carinho dispensados a mim durante todos esses anos. Mesmo com a distância, estamos sempre cuidando uns dos outros.

Ao meu orientador, Dr. Diogo Rodrigo de Magalhães Moreira pelo apoio durante a minha trajetória profissional, pelos ensinamentos, paciência e compreensão nos momentos em que precisei de um tempo para cuidar de coisas pessoais. Agradeço por ter me ensinado o significado da palavra "orientador" e por ser esse pesquisador excepcional. Você, verdadeiramente, sabe o que é fazer ciência com amor e dedicação. Me espelharei em você para trilhar o meu caminho a partir de agora.

A profª Nicoletta Basilico, Dra. Sarah D'Alessandro e toda a sua equipe pelo acolhimento na Università degli Studi di Milano durante o meu intercâmbio de doutorado sanduíche, e por tantas experiências adquiridas e trocadas neste período. Foi um presente inestimável trabalhar com vocês.

Aos meus coorientadores Dra. Nicoletta Basilisco (UNIMI, Milão) e Dr. Fábio Rocha Formiga (Fiocruz Pernambuco) pela ajuda em cada uma das suas áreas de pesquisas e supervisão na condução dessa tese.

Aos diversos colaboradores e coautores dos artigos frutos dessa tese, em especial ao Prof. Miguel Prudêncio (Lisboa) e sua equipe pelos ensaios com os esporozoítos; a Prof. Svetlana Tsogoeva (Erlanger, Alemanha) e a Prof. Maribel Navarro (UFJF, Minas Gerais) pelo envio dos fármacos híbridos; a Prof. Françoise Benoit-Vical (Toulouse, França) e equipe pelos ensaios com os parasitos ART-resistentes.

Aos amigos e colegas do LETI, por terem tornado a minha caminhada muito mais leve e divertida. Agradeço especialmente a Carol, Val, Mari, Adrielle, Rômulo, Renan, Breno, Sara, Luciano e todos os que, direta ou indiretamente, contribuíram para que eu finalizasse esse ciclo tão importante na minha vida. Sem vocês eu não chegaria tão longe.

A Monique, por ser a melhor amiga que eu poderia ter. Você me acolheu quando precisei e carregou comigo as minhas cargas mais pesadas. Muito obrigada! Você tornou todo esse processo mais leve e me fez acreditar a todo o tempo que eu conquistaria mais esse passo na minha vida.

A todos os funcionários do IGM-FIOCRUZ, pelo cuidado, carinho e atenção para com os alunos da instituição. Um agradecimento especial para Rute, secretária do LETI, Sr. Chico e Dona Vanda.

“Não to mandei eu? Sê forte e corajoso; não temas, nem te espantes; porque o Senhor teu Deus é contigo, por onde quer que andares”.

(**Josué 1:9**).

QUADROS, Helenita Costa. **Avaliação farmacológica de compostos híbridos de ação em múltiplos estágios ou de duração longa para o tratamento da malária**. 2023. 169 f. Tese (Doutorado em Biotecnologia em Saúde e Medicina Investigativa) - Fundação Oswaldo Cruz, Centro de Pesquisas Gonçalo Moniz, Salvador, 2023.

## RESUMO

**INTRODUÇÃO**: Nos últimos quatro anos, foram aprovados a vacina Mosquirix™ para a malária falcipária e o medicamento Tafenoquina para a malária vivax, os quais representam avanços importantes no combate à transmissão e no tratamento da malária, respectivamente. Todavia, ainda há inúmeros desafios a serem contornados para combater a malária, tais como o desenvolvimento de novos fármacos com ação antiparasitária frente a múltiplos estágios do ciclo evolutivo do plasmódio e o desenvolvimento de novos fármacos que contornem o tempo de meia-vida plasmático curto das artemisininas, os quais são a primeira linha de tratamento. Uma alternativa para superar tais desafios são os compostos híbridos, os quais podem exercer um papel importante no desenvolvimento de novos fármacos antimaláricos de amplo espectro de ação e com eliminação plasmática mais lenta do que das artemisininas. **OBJETIVO**: Investigar as bases farmacológicas de compostos híbridos como agentes antiplasmódicos. **MATERIAIS E MÉTODOS**: Os híbridos foram idealizados, sintetizados e caracterizados quimicamente através de colaborações entre o nosso grupo e outros grupos de pesquisadores. Os ensaios experimentais de potência *in vitro* foram realizados com o *P. falciparum* e *P. berghei*, enquanto os ensaios de eficácia *in vivo* foram realizados com o *P. berghei*. **RESULTADOS**: Os achados experimentais mostraram que a combinação química de grupos farmacofóricos quinolínicos, dando origem aos compostos híbridos MNCS59 (**1**) e MNCS60 (**2**), revelou potência, eficácia e espectro de ação mais amplos do que a monoterapia ou terapia combinada com os seus fármacos parentais. Dentre os diferentes estágios evolutivos do plasmódio, o estágio sanguíneo assexuado foi o mais susceptível ao tratamento com os compostos híbridos, seguido dos esquizontes teciduais; já os gametócitos maduros foram os menos susceptíveis ao tratamento. Coincidentemente, os estágios evolutivos mais susceptíveis ao tratamento com compostos híbridos MNCS59 (**1**) e MNCS60 (**2**) são aqueles onde o processo de homeostasia redox e de detoxificação do heme são essenciais ao plasmódio. Os achados experimentais encontrados com a combinação química do grupo farmacofórico endoperóxido existente nas artemisininas, dando origem aos compostos híbridos 163A (**3**) e LH70 (**4**), também demonstraram potência, eficácia e espectro de ação mais amplos do que a monoterapia ou terapia combinada com os seus fármacos parentais. Interessantemente, o composto híbrido (**4**) apresentou potência e eficácia superiores aos demais híbridos e as artemisininas. Estudos subsequentes para explicar o aumento da potência antiparasitária mostraram que o híbrido (**4**) possui uma estabilidade química e uma ação fenotípica mais duradoura do que as artemisininas. Por apresentar uma ação fenotípica mais duradoura, o composto híbrido (**4**) foi capaz de reduzir a proliferação de parasitos resistentes as artemisininas, porém não foi tão capaz de reduzir a viabilidade celular de parasitos quiescentes e resistentes as artemisininas. **CONCLUSÃO**: Com este conjunto de dados, nós concluímos que os compostos híbridos aqui estudados conservam os mecanismos de ação dos endoperóxidos e/ou quinolinas, e também apresentam um potencial terapêutico melhorado e um espectro de ação mais amplo do que a monoterapia ou a terapia combinada, podendo ser considerados como possíveis fármacos para a terapia combinada com as artemininas.

**Palavras-chave**: Malária. Plasmódio. Artemisininas. Quinolinas. Híbridos. Tratamento.

QUADROS, Helenita Costa. **Pharmacological assessment of multistage or long-acting hybrid compounds for the treatment of malaria**. 2023. 169 f. Tese (Doutorado em Biotecnologia em Saúde e Medicina Investigativa) - Fundação Oswaldo Cruz, Centro de Pesquisas Gonçalo Moniz, Salvador, 2023.

## ABSTRACT

**INTRODUCTION**: In the last four years, the Mosquirix™ vaccine for *falciparum* malaria and the Tafenoquine drug for *vivax* malaria have been approved, representing important advances in the combating of transmission and treating malaria, respectively. However, there are still several challenges to be overcome to combat malaria, such as the development of new drugs with antiparasitic action against multiple stages of the *Plasmodium* life cycle and the development of new drugs that circumvent the short plasma half-life of artemisinins, which are the first line of treatment. An alternative to overcome such challenges are hybrid compounds, which can play an important role in the development of new antimalarial drugs with broad spectrum of action and slower plasma elimination than artemisinins. **OBJECTIVE**: To investigate the pharmacological basis of hybrid compounds as antiplasmodium agents. **MATERIALS AND METHODS**: Hybrids were designed, synthesized, and chemically characterized through collaborations between our group and other research groups. *In vitro* potency assays were experimentally performed on *P. falciparum* and *P. berghei*, while *in vivo* efficacy assays were performed on *P. berghei*-infected mice. **RESULTS**: The experimental findings showed that the chemical combination of quinoline pharmacophore groups, giving rise to the hybrid compounds MNCS59 (**1**) and MNCS60 (**2**), showed a broader potency, efficacy, and spectrum of action higher than either monotherapy or combination therapy with their parent drugs. Among the different parasite stages of the *Plasmodium*, asexual blood stages were the most susceptible to treatment with the hybrid compounds, followed by tissue schizonts; while mature gametocytes were the least susceptible to treatment. Coincidentally, the parasite stages most susceptible to treatment with hybrid compounds MNCS59 (**1**) and MNCS60 (**2**) are those where the redox homeostasis and heme detoxification processes are essential for parasite survival. The experimental findings found with the chemical combination of the existing pharmacophore endoperoxide group of artemisinins, giving rise to the hybrid compounds 163A (**3**) and LH70 (**4**), also demonstrated potency, efficacy and a broader spectrum of action higher than monotherapy or combination therapy with their parent drugs. Interestingly, the hybrid compound (**4**) showed higher potency and efficacy than the other hybrids and the artemisinins. Subsequent studies to explain the increased antiparasitic potency showed that hybrid (**4**) has a longer lasting chemical stability and phenotypic action than the artemisinins. By presenting a longer lasting phenotypic action, hybrid compound (**4**) was able to reduce the proliferation of artemisinin-resistant parasites, but it was not as able to reduce the cell viability of a quiescent artemisinin-resistant parasites. **CONCLUSION**: With this data set, we concluded that the hybrid compounds studied here retain the mechanisms of action of endoperoxides and/or quinolines, and also exhibit an improved therapeutic potential and a broader spectrum of action than either monotherapy or combination therapy; thus, they may be considered as possible drugs for artemisinin combination therapy.

**Keywords**: Malaria. Plasmodium. Artemisinins. Quinolines. Hybrids. Treatment.

## LISTA DE FIGURAS E QUADRO

## LISTA DE ABREVIATURAS E SIGLAS

| | |
|---|---|
| **a.C** | Antes de Cristo |
| **ADME** | Absorção, distribuição, metabolismo e excreção |
| **AQ** | Amodiaquina |
| **ARS** | Artesunato |
| **ART** | Artemisinina |
| **ATQ** | Atovaquona |
| **BHIA** | Atividade Inibitória da β-hematina |
| **CDC** | Centro de Controle e Prevenção de Doenças Norte-Americano |
| **CQ** | Cloroquina |
| **$EC_{50}$** | Concentração efetiva para 50% |
| **$ED_{90}$** | Dose efetiva para 90% |
| **eEF2** | Fator de elongamento 2 da tradução |
| **FeIII-PPIX** | Hematina |
| **FeII-PPIX** | Heme |
| **FQ** | Ferroquina |
| **G6PD** | Enzima glicose-6-fosfato desidrogenase |
| **Hb** | Hemoglobina |
| **HIV** | Vírus da imunodeficiência humana |
| **HO-1** | Heme oxigenase-1 |
| **$IC_{50}$** | Concentração inibitória de 50% |
| **IPA** | Incidência parasitária anual |
| **LM** | Lumefantrina |
| **MFQ** | Mefloquina |
| **OMS** | Organização Mundial de Saúde |
| ***P. falciparum*** | *Plasmodium falciparum* |
| ***P. knowlesi*** | *Plasmodium knowlesi* |
| ***P. malariae*** | *Plasmodium malariae* |
| ***P. ovale*** | *Plasmodium ovale* |
| ***P. vivax*** | *Plasmodium vivax* |
| **Pfcrt** | Proteína conhecida como transportadora de resistência à cloroquina |

| | |
|---|---|
| **PfEMP1** | Proteína-1 de membrana expressa nas hemácias infectadas |
| **Pgh-1** | Glicoproteína P |
| **PPQ** | Piperaquina |
| **PQ** | Primaquina |
| **QN** | Quinina |
| **ROS** | Espécies Reativas de Oxigênio |
| **TACT** | Terapia tripla combinada com arteminina |
| **TCA** | Terapia combinada com artemisininas |
| **TFQ** | Tafenoquina |

**SUMÁRIO**

# 1 **INTRODUÇÃO**

A malária é uma doença causada por protozoários do gênero *Plasmodium* spp., os quais são transmitidos pelos mosquitos fêmeas do gênero *Anopheles* infectados. Dentre as cinco espécies de plasmódio capazes de infectar os humanos, o *Plasmodium falciparum* (*P. falciparum*) é o responsável por 98% de todas as mortes relatadas no mundo, sobretudo no continente africano. Além do *P. falciparum*, o *Plasmodium vivax* (*P. vivax*) também desempenha um papel importante na severidade da doença, acarretando números expressivos de casos de infecção e morte pela malária nas Américas (VARO; CHACCOUR; BASSAT, 2020).

De acordo com a Organização Mundial de Saúde (OMS), no ano de 2021 foram registrados 247 milhões de casos de malária e estimou-se 619 mil óbitos em todo o mundo. Em comparação ao ano de 2019, cerca de dois-terços do aumento dos números de casos de infecção e óbitos relatados em 2021 foram reflexo da interrupção do acesso aos sistemas de saúde pública durante o auge da pandemia do COVID-19. De fato, nos dois anos de pico da pandemia (2020 e 2021), foram estimados mais 13 milhões de casos de malária e 63 mil mortes. Além disso, as estratégias essenciais para o controle da transmissão da doença, tais como mosquiteiros tratados com inseticidas, spraying residual aplicado nas casas e medicamentos para a profilaxia e para o tratamento também tiveram baixa disponibilidade nesse período (WHO, 2022).

Com exceção deste período da pandemia do COVID-19 e dos períodos de surgimento das cepas resistentes, as medidas de controle do vetor e de profilaxia e tratamento da malária sempre foram eficientes em mitigar o número de casos da doença. Neste contexto, os tratamentos para a malária não complicada envolvem terapias medicamentosas combinadas de administração oral entre antimaláricos de classes diferentes, com regime de doses diárias durante três dias. Já o tratamento de escolha para a malária complicada geralmente é na forma de monoterapia medicamentosa injetável, e envolve primordialmente o artesunato (ARS) ou quinina (QN) (VARO; CHACCOUR; BASSAT, 2020). Contudo, em vista do surgimento de cepas do *P. falciparum* resistentes aos tratamentos atuais, novos compostos com potencial antimalárico e atuando em diferentes alvos terapêuticos são necessários e vêm sendo estudados (AMELO; MAKONNEN, 2021). Outrossim, há a necessidade por novos compostos antimaláricos que atuem não somente em suprimir a parasitemia, mas também impedir a transmissão da doença a nível dos esporozoítos, nos insetos, e gametócitos.

Um importante componente da terapia combinada são as artemisininas (ARTs) e os seus derivados ARS, dihidroartemisinina (DHA) e artemeter, os quais são antimaláricos que pertencem a classe dos peróxidos de lactona sesquiterpeno. Estes fármacos possuem uma atividade de ação rápida em suprimir a parasitemia, com ação nos estágios em anéis do ciclo eritrocítico da doença (QUADROS; SILVA; MOREIRA, 2022). No tocante à terapia combinada, as ARTs são utilizadas em combinações de doses fixas com outros antimaláricos com tempo de meia-vida plasmática mais longo do que as ARTs, tais como as quinolinas, visando a eficácia no tratamento da malária não complicada (HANBOONKUNUPAKARN; WHITE, 2022). Entretanto, cepas do *P. falciparum* resistentes às terapias combinadas também têm emergido em partes do mundo, levando a falhas destes tratamentos (MAIRET-KHEDIM et al., 2021). Uma opção para mitigar esta falha terapêutica é o desenvolvimento de derivados das ARTs com um tempo de meia-vida plasmática mais longo (O'NEILL et al., 2017).

Um outro importante componente da terapia combinada são as quinolinas QN, cloroquina (CQ), amodiaquina (AQ) e mefloquina (MFQ). As quinolinas apresentam uma ação potente frente ao estágio assexuado sanguíneo do plasmódio, por inibirem a detoxificação do heme durante a formação dos cristais de hemozoína. Porém, esta classe de fármacos possui uma ação pouco eficaz em impedir a transmissão da doença a nível dos esporozoítos e gametócitos. Uma alternativa para mitigar esta limitação terapêutica é o desenvolvimento de derivados das quinolinas com um espectro de ação mais amplo (MACEDO et al., 2016, 2017).

Considerando que a terapia combinada é bem estabelecida, porém apresenta algumas limitações, uma possibilidade é o desenvolvimento de compostos que recapitulem as propriedades farmacológicas da terapia combinada em um único composto, denominado como compostos híbridos ou duais. Estes compostos são sintetizados a partir da hibridização química de farmacóforos por combinar as características de dois ou mais agentes bioativos. Presumidamente, compostos híbridos podem atuar através de mecanismos de ação diferentes para reverter a resistência (farmacodinâmica) ou através das cinéticas de ação antiparasitária diferentes (farmacocinética), agindo em diferentes estágios do ciclo evolutivo do plasmódio (ALVEN; ADERIBIGBE, 2019; ÇAPCI et al., 2019; MOKHTARI et al., 2017). Além disso, os compostos híbridos têm o potencial de serem incluídos como um dos componentes nas terapias combinadas existentes, visto que há uma busca atual por uma terapia combinada usando três fármacos (terapia tripla) (DINI et al., 2018; PETO et al., 2022).

A presente tese de doutorado teve como objetivo desenvolver novos compostos híbridos derivados das classes dos endoperóxidos e quinolinas, e avaliá-los quanto aos seus mecanismos

de ação em diferentes alvos nos estágios do ciclo de vida do parasito e o potencial antimalárico através de ensaios em diferentes modelos experimentais *in vitro* e *in vivo* de malária.

# 2 **REFERENCIAL TEÓRICO**

## 2.1 HISTÓRICO E EPIDEMIOLOGIA GLOBAL DA MALÁRIA

De acordo com registros chineses de 2700 anos antes de Cristo (a.C), tabuletas da Mesopotâmia de 2000 a.C e papiros egípcios de 1570 a.C, casos semelhantes ao que hoje é conhecido por malária já haviam sido relatados. Com o desenvolvimento da teoria germinativa da infecção por Louis Pasteur e Robert Koch nos anos de 1878 e 1879, a busca pela causa da malária se intensificou, e, no ano seguinte, Louis Alphonse Laveran descreveu os parasitos envolvidos no ciclo intraeritrocítico da doença (COX, F. E. G., 2010; VERHAVE, 2022). Alguns anos mais tarde, Ronald Ross e Giovanni Battista Grassi identificaram que os mosquitos fêmeas do gênero *Anopheles* atuam como vetores dos parasitos causadores da malária (BYNUM, 2008).

A malária é uma doença febril aguda causada por protozoários e é considerada um dos problemas de saúde pública mais graves do mundo, cujos parasitos do gênero *Plasmodium* spp. são os agentes etiológicos (CDC; OMS, 2022). Em humanos, a malária pode ser causada pelas espécies do *P. falciparum*, *P. vivax*, *Plasmodium malariae* (*P. malariae*), *Plasmodium ovale* (*P. ovale*) e *Plasmodium knowlesi* (*P. knowlesi*). A distribuição atual das espécies pelo globo terrestre exibe uma preponderância de casos de infecção pelo *P. falciparum* na África, enquanto o *P. vivax* prevalece na América do Sul. No sudoeste asiático e oeste pacífico, tanto o *P. falciparum* quanto o *P. vivax* são prevalentes. O *P. malariae* apresenta uma distribuição ampla na América do Sul, Ásia e África, mas a incidência de casos é pouco frequente. Já o *P. ovale* é amplamente distribuído na África sub-Saariana, e o *P. knowlesi* é encontrado apenas em algumas áreas do sudeste da Ásia (AUTINO et al., 2012; MÜLLER; HYDE, 2010; OMS, 2022).

Devido à gravidade da malária, esta doença afeta metade da população mundial, sendo a maioria composta por indivíduos dos países tropicais e subtropicais (PANNU, 2019). A última atualização do Relatório Mundial de Malária 2022 publicada pela OMS estimou que em 2021 foram notificados 247 milhões de novos casos de infecções e 619 mil mortes em todo o mundo causados pela malária (OMS, 2022). Dentro deste contexto, a OMS da região africana indicou que 95% do número total de casos se concentraram nesta região, bem como 96% do número de mortes. Desta elevada percentagem de mortes, 80% representam crianças menores do que 5 anos de idade. Além disso, dados de 2018 registraram que o *P. vivax* gerou aproximadamente

3% dos casos em todo mundo; destes, 75% foram notificados nas Américas, <1% foi atribuído na África e o restante distribuído em outras regiões do globo (MACE; LUCCHI; TAN, 2022).

De acordo com os dados de morbidade e mortalidade divulgados pela OMS em 2022 referentes a 2021, durante os dois anos de pico da pandemia do COVID-19 houve um aumento de 13 milhões de casos de malária e 63 mil mortes em relação ao ano de 2019. Estes números foram relacionados à interrupção dos serviços de saúde durante a pandemia da COVID-19 (DASH et al., 2022; OMS, 2019, 2021). Além disso, a pandemia da COVID-19 exerceu uma enorme pressão sobre os sistemas de saúde dos países desenvolvidos e com elevado número de recursos. Do mesmo modo, os países africanos também sofreram fortes impactos com a pandemia, entretanto, diferente dos países desenvolvidos, enfrentaram e enfretam o desafio sem precedentes da COVID-19 com uma capacidade comparativamente menor do sistema de saúde e um nível elevado de casos de malária (WEISS et al., 2021).

Nas Américas, apesar dos avanços significativos em prol da eliminação da malária nos países endêmicos, esta doença ainda constitui um importante problema de saúde pública, visto que em 2020 foram registrados 232 mil casos de infecção no continente (OMS, 2021). Com elevado risco de infecção por malária, os países da América do Sul situados na região Amazônica concentram o maior número de casos, com destaque para o Brasil, Venezuela e Colômbia que, apesar de estarem em fase de controle, ainda continuam sendo os países mais acometidos. Argentina e Paraguai estão em fase de eliminação da doença e o Equador está progredindo para a pré-eliminação, que é quando o município ou o país apresenta a incidência parasitária anual (IPA) com menos de 10 casos de infecção por 1.000 habitantes sob risco (OMS, 2016; RECHT et al., 2017; SANTELLI et al., 2016). Apesar da alta incidência no Brasil, comparado com o ano de 2019, o número de casos de infecção foi reduzido pela metade em 2020 (OMS, 2021).

Por outro lado, há dezenas de anos os países de clima temperado erradicaram a malária, incluindo a América do Norte, Austrália, Japão e, mais recentemente, os países do continente Europeu (ASHLEY; PYAE PHYO; WOODROW, 2018; CDC, 2020; OMS, 2021). Isto ocorreu devido aos países desenvolvidos possuírem sistemas tecnológicos mais avançados e uma maior disponibilidade de recursos, os quais, por consequência, elevaram consideravelmente a expectativa de vida dos seus habitantes quando comparada aos de países menos desenvolvidos (RICCI, 2012). Além disso, o declínio da malária nestes países pode ser atribuído diretamente às intervenções de controle da doença, e indiretamente ao fato de os cidadãos terem um melhor acesso aos sistemas de saúde e maiores níveis de urbanização (WEISS et al., 2019).

De acordo com o Centro de Controle e Prevenção de Doenças Norte-Americano (CDC), em muitos países endêmicos para a malária a transmissão não ocorre em todas as regiões dos seus territórios (figura 1). Mesmo dentro de áreas tropicais e subtropicais, a transmissão não ocorre em condições tais como altitudes elevadas; temporadas de inverno; desertos; e nos países onde os programas de eliminação e controle da malária são bastante eficazes. Entretanto, em regiões muito quentes próximas à linha do Equador e distantes das condições mencionadas acima, a transmissão ocorre com mais frequência (CDC, 2020).

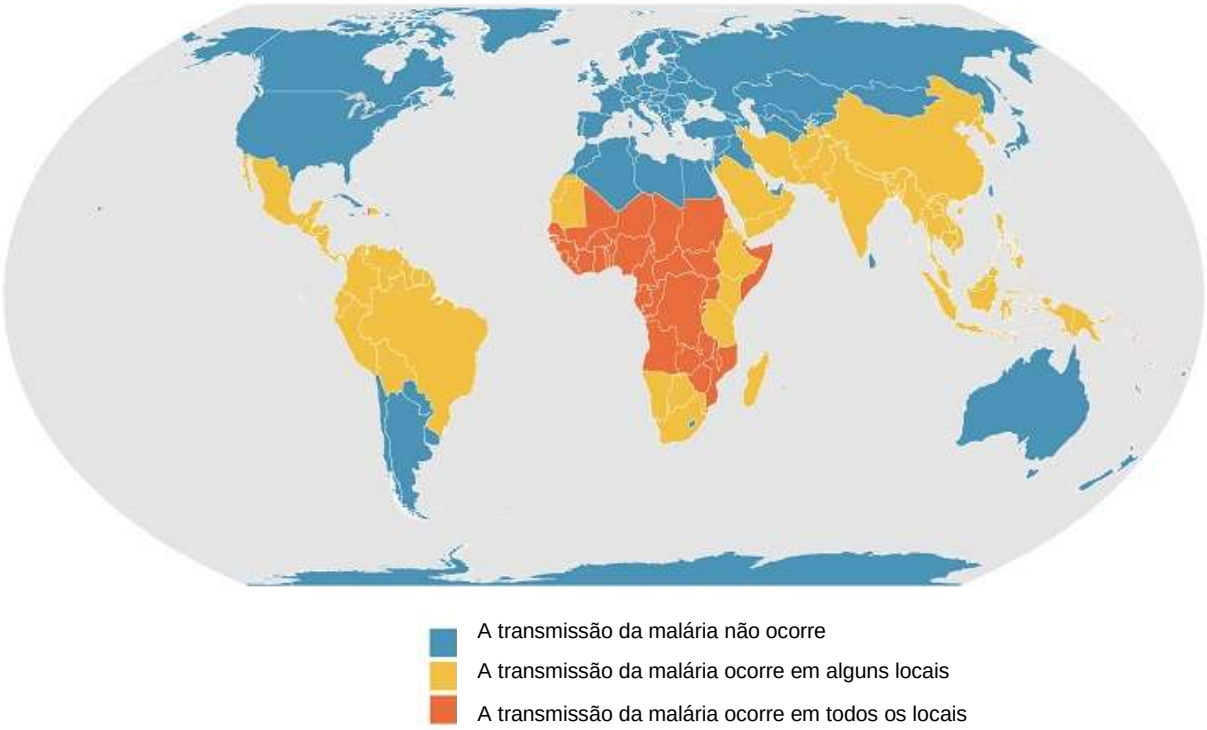


**Figura 1**- Distribuição global da malária estimada no ano de 2020
**Fonte**: adaptada do (CDC, 2020).

Falhas nos setores socioeconômicos, incluindo educação, renda per capita e moradia são apontadas como contribuintes diretos para a alta incidência de malária nos países subdesenvolvidos e em desenvolvimento. A falta de acesso à educação contribui para o desconhecimento sobre prevenção e estratégias de tratamento da malária, assim como a baixa renda dificulta o acesso fácil e rápido aos antimaláricos ou inseticidas nos países em que não são disponibilizados gratuitamente. Casas construídas em locais pouco assistidos e com baixa condição sanitária permitem mais facilmente a entrada dos vetores que carreiam o plasmódio, aumentando as chances de infecção dos residentes. Além destes fatores, o clima e condições

ambientais, bem como a resistência do agente etiológico e vetor aos antimaláricos também demonstram relevância na prevalência da malária (DEGAREGE et al., 2019).

## 2.2 CICLO DE VIDA DO PLASMÓDIO

As espécies de parasitos causadoras da malária pertencem ao gênero *Plasmodium* spp. e são organismos intracelulares eucarióticos do filo Apicomplexa. Os plasmódios apresentam um ciclo de vida complexo, alternando entre hospedeiros invertebrados (mosquitos) e vertebrados, e passam por múltiplas transições fenotípicas (COWMAN et al., 2016). No decorrer do ciclo, que ocorre tanto intracelular quanto extracelularmente, os principais locais de diferenciação e replicação incluem o intestino médio dos mosquitos fêmeas do gênero *Anopheles*, os hepatócitos no fígado e os eritrócitos (REAL; MANCIO-SILVA, 2022). As cinco espécies de plasmódio envolvidas na malária humana podem ser transmitidas por aproximadamente 40 espécies do mosquito fêmea do gênero *Anopheles*, sendo a *Anopheles gambiae* a mais eficiente em transmitir (PHILLIPS et al., 2017).

O ciclo de vida do *P. falciparum*, principal cepa responsável pelos casos de malária, se inicia quando o mosquito fêmea do gênero *Anopheles* infectado realiza o repasto sanguíneo através de uma picada na derme do hospedeiro e, ao mesmo tempo, inocula esporozoítos. Devido a sua motilidade, os esporozoítos atravessam os tecidos da pele, entram no fluxo sanguíneo e alcançam o fígado, escapando do sistema imune e drenagem do sistema linfático do hospedeiro. Uma vez no fígado, esta forma evolutiva invade os hepatócitos, estabelece um vacúolo parasitóforo e se multiplica gerando de 10.000 a 30.000 merozoítos por hepatócito em 5 a 8 dias. Em seguida, a partir do processo de esquizogonia, o qual é caracterizado por múltiplas fissões assexuadas, forma-se o esquizonte hepático. Após determinado tempo, o esquizonte se rompe e libera os merossomos, compreendidos por vesículas ligadas à membrana dos hepatócitos contendo os merozoítos agrupados. Uma vez liberados na corrente sanguínea, os merozoítos invadem exclusivamente os eritrócitos, iniciando o ciclo intraeritrocítico assexuado (figura 2) (REAL; MANCIO-SILVA, 2022; PHILLIPS et al., 2017; VENUGOPAL et al., 2020; WHITE et al., 2014).

Com a invasão nas hemácias, os merozoítos se desenvolvem para o estágio inicial intraeritrocítico chamado de anel, dentro do vacúolo digestivo formado. Neste estágio, para o seu crescimento, o parasito realiza a proteólise da hemoglobina (Hb) localizada nos citostomos; a globina, um dos substratos resultantes, torna-se uma fonte de aminoácidos necessária para o

desenvolvimento de anel para o e de trofozoíto e, por fim, a esquizonte. Em seguida, o esquizonte se rompe e libera milhares de merozoítos na corrente sanguínea, reiniciando o ciclo (WHITE et al., 2014).

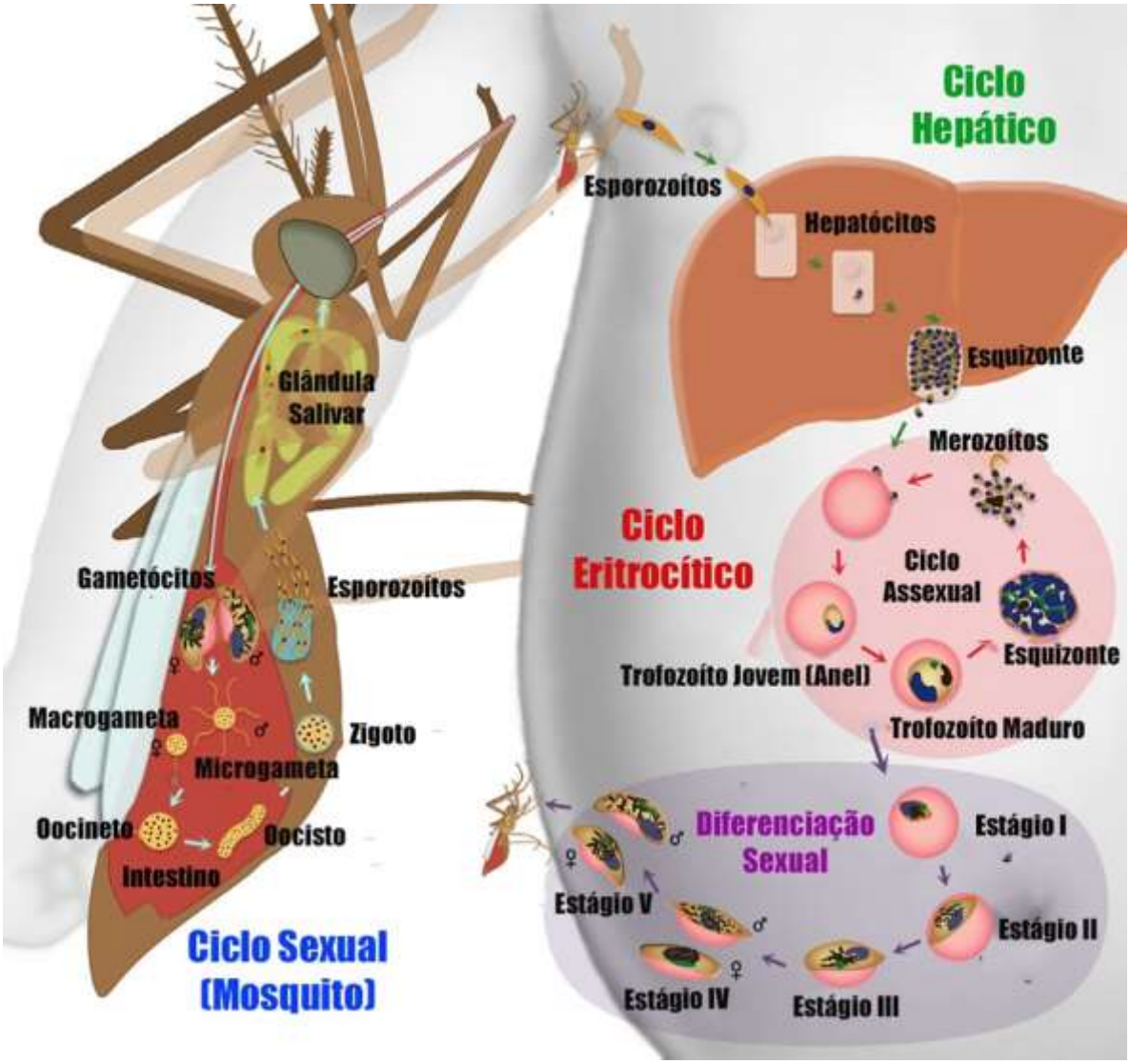


**Figura 2 -** Ciclo de vida do *Plasmodium* spp.
**Fonte**: adaptado de BIAMONTE; WANNER; LE ROCH, 2013.

Após vários ciclos de reprodução assexuada, cerca de 5% dos merozoítos passam pelo processo de diferenciação sexual, chamado de gametocitogênese, tornando-se gametócitos machos ou fêmeas (DASH et al., 2022). Assim, quando o mosquito faz o seu repasto sanguíneo em um hospedeiro infectado, o mesmo ingere estes gametócitos que se direcionam ao intestino médio e se tornam microgameta (macho) e macrogameta (fêmea) através do processo chamado gametogênese. Os gametas se fundem e formam o zigoto, que evolui para oocineto e, por fim, formam oocisto, que se rompe e libera os esporozoítos. Os esporozoítos migram para a glândula

salivar do mosquito e tornam-se disponíveis para infectar novos hospedeiros vertebrados quando o mosquito realiza um novo repasto sanguíneo (figura 2) (BIAMONTE; WANNER; LE ROCH, 2013).

O ciclo evolutivo assexuado dura aproximadamente 48 horas para o *P. falciparum*, *P. vivax* e *P. ovale*, 72 horas para *P. malariae*, e 24 horas para o *P. knowlesi*. Vale ressaltar que nas infecções causadas pelos *P. vivax* e *P. ovale*, os parasitos destas espécies desenvolveram a estratégia de persistir nos hospedeiros através dos hipnozoítos, os quais são formados a partir dos esporozoítos; estes podem permanecer no fígado por semanas ou até mesmo por anos e, eventualmente, culminarem em recidivas ou relapsos da doença (PHILLIPS et al., 2017; WHITE et al., 2014, 2018).

Com relação a gametocitogênese do *P. falciparum*, acredita-se que este processo seja desencadeado quando os parasitos no estágio sanguíneo assexuado respondem a estresses ambientais ou exógenos que levam à maturação de tipicamente 1% destes para formas sexuadas. Os estresses ambientais podem estar relacionados com a parasitemia elevada e o hematócrito baixo, ou seja, poucas hemácias saudáveis disponíveis para serem infectadas; e, também, podem estar relacionados com a baixa disponibilidade de lisofosfatidilcolina lipídica sérica humana do meio de cultura usado para o crescimento *in vitro* do parasito (método 'crash'). Já os estresses exógenos, tais como o tratamento com antiparasitários, podem acarretar o aumento da diferenciação de trofozoítos em formas sexuadas. Esta conversão sexual é marcada pela ativação epigenética da expressão do regulador principal e fator de transcrição PfAP2-G, o qual expressa proteínas específicas dos gametócitos (BRANCUCCI et al., 2017; LLORÀ-BATLLE et al., 2020; PORTUGALIZA et al., 2020, 2022).

Dessa forma, o *P. falciparum* apresenta cinco estágios de desenvolvimento dos gametócitos, sendo eles definidos em estágios I, II, III, IV e V, no qual apenas os gametócitos maduros do estágio V estão presentes na circulação periférica e ficam disponíveis para serem absorvidos pelo mosquito durante o repasto sanguíneo (DUFFY et al., 2016; JOSLING; LLINÁS, 2015).

Os gametócitos no estágio I são similares aos trofozoítos quanto a morfologia e não são facilmente distinguíveis. Contudo, podem ser identificados usando técnicas moleculares que determinem o início da diferenciação do parasito assexuado para sexuado. No estágio II, o gametócito começa a apresentar uma forma um pouco diferente da encontrada no estágio I, se assemelhando a um limão. Em seguida, no estágio III, ocorre um alongamento do parasito, no qual um lado se achata, e, no outro, a membrana se curva de modo semelhante a letra "D". Este

alongamento excede o tamanho da hemácia e gera uma deformação da mesma. Ainda em desenvolvimento, o gametócito alcança o estágio IV, em que o parasito se alonga ainda mais, se assemelhando a uma banana. Neste momento, o citoplasma da hemácia está quase completamente ocupado pelo parasito, exceto por uma pequena dobra de membrana conhecida como babete da Laveran. Por último, no estágio V, os gametócitos exibem extremidades arredondadas, ao contrário das extremidades pontiagudas dos gametócitos do estágio IV (figura 3) (NGOTHO et al., 2019).

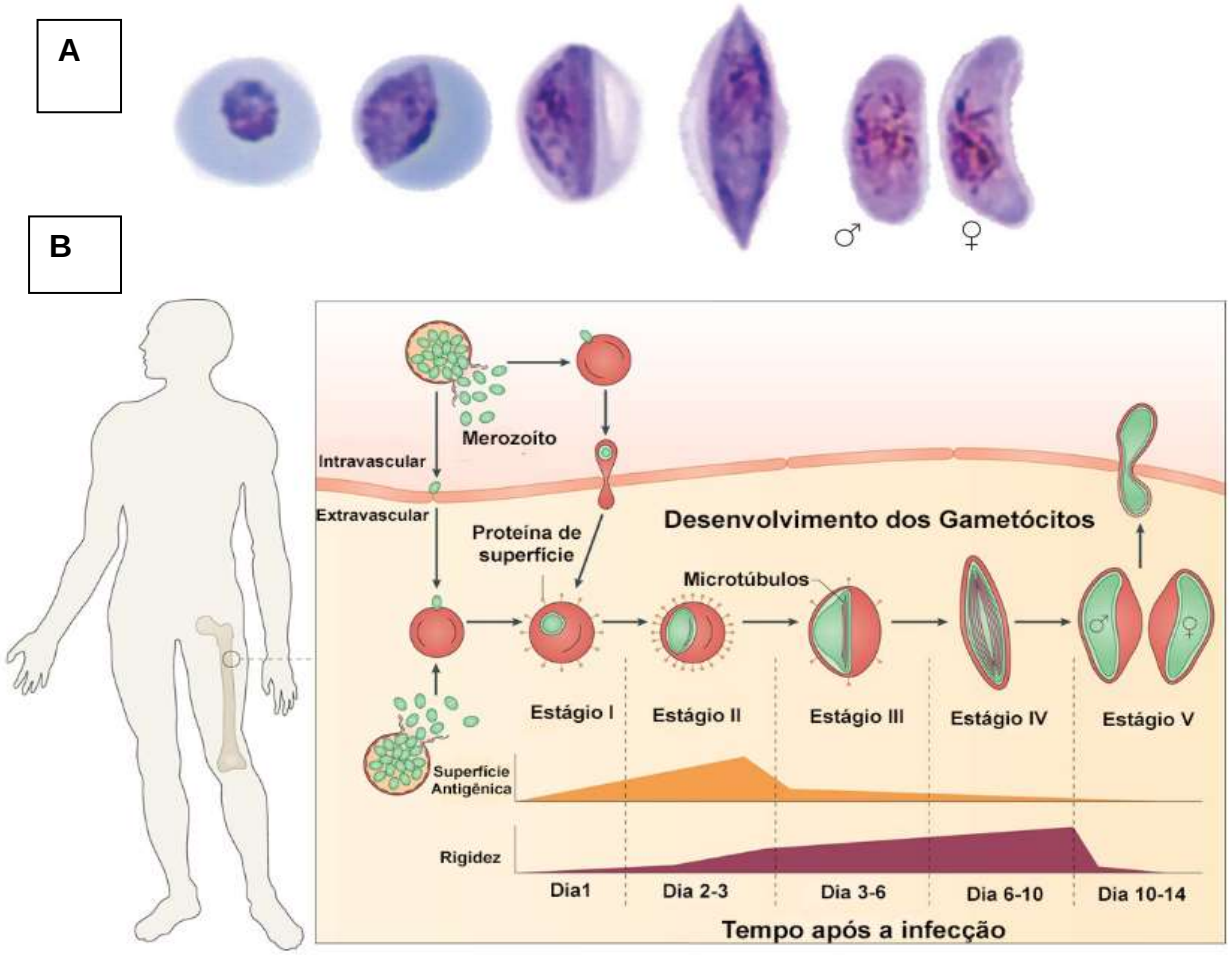


**Figura 3 -** Os estágios de desenvolvimento dos gametócitos do *P. falciparum*. A diferenciação dos gametócitos em cinco estágios pode ser analisada por microscópio óptico (A). Esquema do desenvolvimento dos gametócitos desde os merozoítos que se diferenciam em gametócitos até a formação dos gametas, em paralelo ao tempo de desenvolvimento em cada estágio (B).
**Fonte**: adaptado de (JOSLING; LLINÁS, 2015; VENUGOPAL et al., 2020).

## 2.3 PATOGÊNESE DA MALÁRIA

O primeiro contato do plasmódio com o sistema imunológico do hospedeiro ocorre quando os esporozoítos são inoculados na derme. Uma vez em contato com a derme do hospedeiro, esta forma evolutiva é fagocitada pelas células dendríticas, as quais apresentam antígenos do parasito ao linfonodo que drena o sítio onde houve a inoculação, e, assim, o sistema imunológico é ativado para combater o agente invasor. Entretanto, uma parte dos esporozoítos consegue escapar das células do sistema imunológico e alcança os hepatócitos, iniciando o ciclo hepático da doença. Neste sítio da infecção, as células de küpffer têm sua função suprimida e a expressão gênica do MHC de classe I é reprimida pelo patógeno (PHILLIPS et al., 2017).

Outro importante mecanismo patogênico do plasmódio é a hemólise, ocasionando anemia e febre. Os merozoítos infectam hemácias saudáveis e consomem a Hb, a qual é descrita como o principal componente das hemácias. A Hb compõe aproximadamente 95% das proteínas presentes no citosol, e entre 60 a 80% é metabolizada pelo parasito, principalmente nos estágios de trofozoítos e esquizontes, para ser utilizada como fonte de aminoácidos para o seu desenvolvimento. Entretanto, o grupo prostético heme também é liberado e, na sua forma livre, também conhecida como ferroprotoporfirina IX (FeII-PPIX), se acumula no vacúolo digestivo e é oxidado em ferriprotoporfirina IX (FeIII-PPIX), onde sua alta concentração torna-se tóxica ao parasito, levando à eliminação de uma fração destes. Para contornar isso, o parasito utiliza a via da biocristalização para detoxificar o heme livre. Nesta via ocorre uma conversão do FeIII-PPIX em um pigmento inerte e não tóxico chamado de hemozoína, o qual é encontrado nas hemácias infectadas (figura 4) (CORONADO; NADOVICH; SPADAFORA, 2014; HERRAIZ et al., 2019; KAPISHNIKOV et al., 2019, 2021; LIN et al., 2015).

Ressalta-se aqui que durante a replicação do parasito nas hemácias ocorre a hemólise, liberando Hb e os produtos do catabolismo da sua digestão, dentre eles o heme livre e os cristais de hemozoína. O heme livre no plasma pode ser inativado pela enzima heme oxigenase-1 (HO-1), porém esta inativação não é eficaz quando os níveis de heme livre são muito elevados, contribuindo para o quadro da malária complicada (SEIXAS et al., 2009). Já os cristais de hemozoína que não são inativados ficam retidos em infiltrados celulares a nível hepático, pulmonar e renal, contribuindo também para o quadro da malária complicada (RAMOS et al., 2019; SHAH; FIDOCK; PRINCE, 2021).

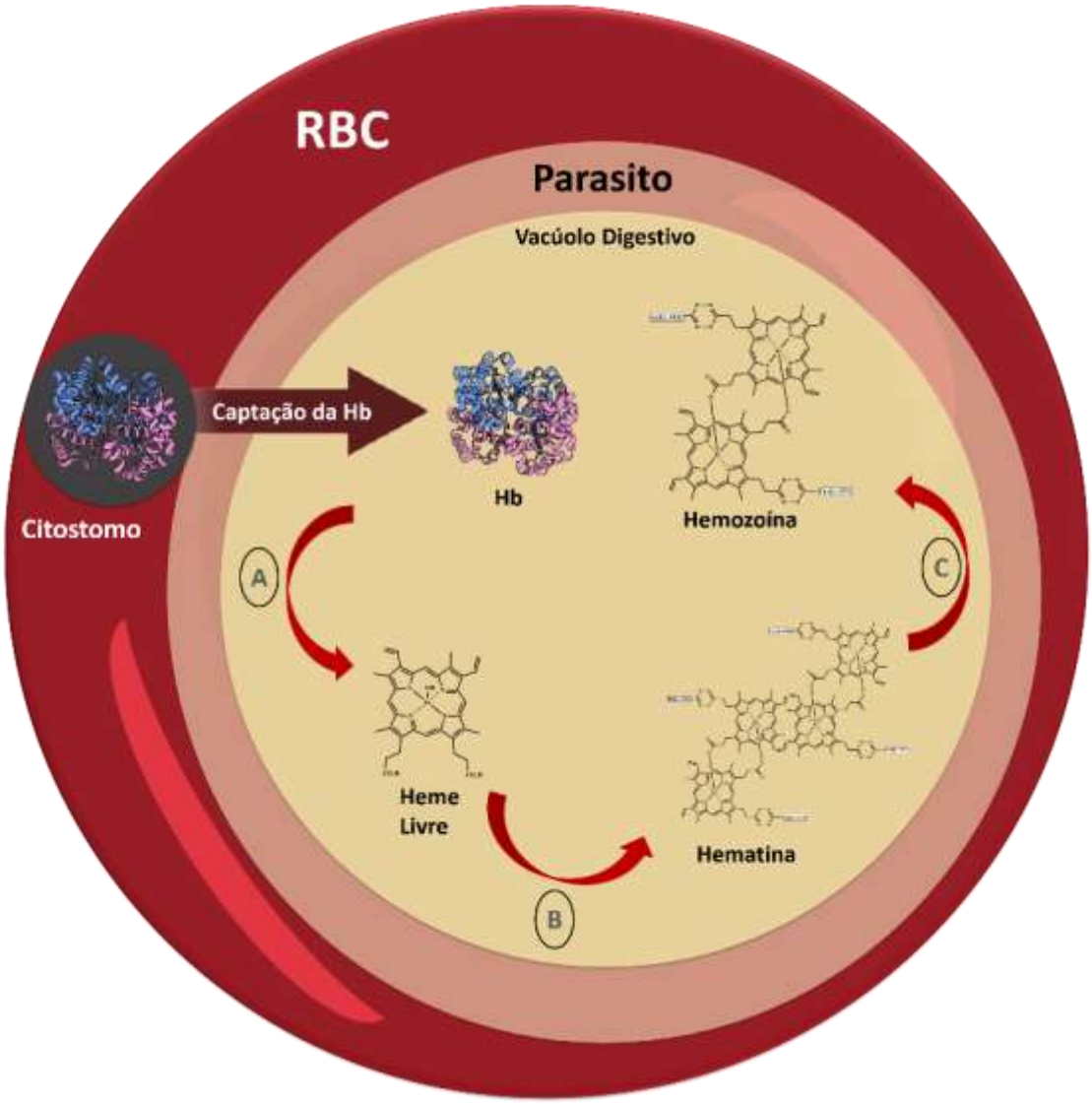


**Figura 4 -** Captação da hemoglobina pelo plasmódio e conversão do heme livre em hemozoína. Dentro do vacúolo digestivo, o parasito capta a hemoglobina presente nos citostomos e realiza a proteólise gerando globina e heme livre (A). O heme livre é oxidado em hematina e então biocristalizado pelo parasito, formando os dímeros de β-hematina (B) e, em seguida, a hemozoína (C).
**Fonte**: Elaborado pela autora

Além da participação do heme e da hemozoína para o agravamento da patologia, há ainda a participação do sistema imune e da citoaderência das hemácias neste processo. À medida que o ciclo de vida do plasmódio finaliza e outro se inicia através da infecção de novas hemácias saudáveis, uma parte da hemozoína liberada é reconhecida pelo receptor Toll-like 9, que funciona como um "sensor" de nucleotídeo capaz de detectar patógenos e estimular o aumento dos níveis do fator de necrose tumoral alfa, culminando nos sintomas clínicos como a febre. Outro mecanismo de defesa, além da degradação da Hb e rompimento das hemácias pelo parasito, é o endurecimento da membrana das hemácias infectadas. Em comparação com a forma bicôncava das hemácias não infectadas ou infectadas com o parasito no estágio de anel,

as hemácias infectadas com trofozoítos ou esquizontes são esféricas e menos deformáveis. Em função destes aspectos, o plasmódio pode induzir a citoaderência das hemácias infectadas ao endotélio dos capilares e vênulas causando a obstrução de órgãos vitais do indivíduo, o que pode acarretar, consequentemente, no quadro de malária complicada, caracterizado pelo desenvolvimento, principalmente, da malária cerebral, edema pulmonar, insuficiência renal aguda e anemia grave (MILNER, 2018; PARROCHE et al., 2007; TRAMPUZ et al., 2003; VENUGOPAL et al., 2020).

Vale ressaltar que o processo de aderência das hemácias infectadas pelos parasitos aos receptores endoteliais é realizado via proteína-1 de membrana, a qual é expressa nas hemácias infectadas (PfEMP1). Este processo é uma etapa normal do estágio de maturação final do ciclo assexuado do plasmódio, tornando-o competente para evitar sua eliminação pelo baço; desta forma, a aderência das hemácias infectadas possui um papel importante para o parasito, uma vez que a baixa densidade de parasitos circulantes não é detectada pelos testes diagnósticos, favorecendo posteriormente a recrudescência da infecção no estágio sanguíneo (ROE; O'FLAHERTY; FOWKES, 2022).

Outrossim, o estresse oxidativo e a inflamação também são fatores relacionados à patogênese da malária. O estresse oxidativo é causado pelas espécies reativas de oxigênio (ROS), as quais são descritas como átomos de nitrogênio ou oxigênio que possuem elétrons não pareados na sua camada externa. Estes radicais são agentes oxidantes que podem tanto causar danos à componentes celulares, como também estar envolvidos em processos celulares essenciais, como a sinalização intracelular e a resposta imune inata (LIGUORI et al., 2018).

O papel do estresse oxidativo nas doenças infecciosas é complexo, uma vez que está envolvido na eliminação do agente infeccioso e também nos danos moleculares que podem ocorrer no hospedeiro. A malária é uma doença altamente inflamatória e oxidativa, em que os baixos níveis de antioxidantes em pacientes infectados pelo *P. falciparum* e *P. vivax* caracterizam o elevado estresse oxidativo. Esta diminuição dos níveis de antioxidantes durante a malária evidencia a perda do equilíbrio da homeostasia entre os radicais livres e a capacidade antioxidante que é mantida em tecidos saudáveis (VASQUEZ; ZUNIGA; RODRIGUEZ, 2021).

Ainda neste contexto, o estresse oxidativo no combate ao plasmódio pode ser estimulado pela HO-1, a qual participa da degradação e o acúmulo do heme livre, acarretando no estresse ao parasito; ao mesmo tempo, exerce atividades protetoras ao hospedeiro através da modulação dos tecidos em resposta às injúrias. Dentre elas, destacam-se as atividades antiinflamatória,

antiapoptótica e antiproliferativa. Outrossim, outras vias também se convergem no estresse oxidativo ao hospedeiro, incluindo a resposta do hospedeiro à infecção, a explosão fagocítica oxidativa e os antimaláricos que possuem como mecanismo de ação a eliminação do parasito através do estresse oxidativo (PEREIRA; MARINHO; EPIPHANIO, 2018; VASQUEZ; ZUNIGA; RODRIGUEZ, 2021).

## 2.4 OS FÁRMACOS ANTIMALÁRICOS, OS SEUS MECANISMOS DE AÇÃO E O PERFIL FENOTÍPICO DE INIBIÇÃO DO PARASITO

A terapia medicamentosa para o tratamento de pacientes com a malária é ampla, compreendendo mais de dez fármacos. Exceto para a primaquina (PQ) e tafenoquina (TFQ), que são fármacos classificados como esquizonticidas teciduais utilizados em áreas endêmicas para o *P. vivax*, os demais fármacos antimaláricos são classificados como esquizonticidas sanguíneos e são utilizados em áreas endêmicas para o *P. falciparum* e outras espécies. Nesta subseção, foi realizada uma revisão dos fármacos antimaláricos que mecanisticamente atuam na homeostasia ou no bloqueio da detoxificação do heme.

A descoberta do primeiro tratamento antimalárico, há quase 400 anos, resultou da cura de pacientes com malária após o tratamento com infusões de extratos da casca de plantas da Amazônia peruana. Tal atividade exercida pelas plantas *Cinchona calisaya* e *Cinchona succirubra* foi mais tarde atribuída aos quininas alcaloides. A descoberta da QN foi considerada uma das mais importantes do século 17, e ficou marcada como o primeiro tratamento de sucesso para uma doença infecciosa. Entretanto, com o seu uso prolongado na malária não complicada, este antimalárico passou a revelar um baixo índice terapêutico e efeitos adversos. Assim, a QN permaneceu como o principal tratamento da malária não complicada de 1920 até a descoberta de antimaláricos sintéticos mais eficazes (AGUIAR, A. C. C. et al., 2012). Até o ano de 2018, a QN era administrada como terapia combinada com a clindamicina para a malária não complicada em gestantes, ou também como terapia combinada com doxiciclina, tetraciclina ou clindamicina quando o tratamento de primeira escolha não estava disponível (ACHAN et al., 2011; MACE; LUCCHI; TAN, 2022).

Como monoterapia, a QN apresenta baixa eficácia devido às reações adversas e ao surgimento de cepas resistentes. Dentre as reações adversas, o complexo de cinchonismo é o mais prevalente, no qual o paciente sofre de náusea, dor de cabeça, disforia, zumbido e também de sintomas de surdez (BERMAN, 2004; ISLAHUDIN et al., 2014). Assim, em função destes

problemas, outras moléculas, tais como as 4-aminoquinolinas, foram desenhadas e derivadas a partir da atividade antimalárica da QN (FIDOCK et al., 2004).

Dentre as 4-aminoquinolinas sintetizadas a partir da QN, a CQ se destacou durante várias décadas como o padrão-ouro para o tratamento da malária devido à sua eficácia elevada em suprimir a parasitemia, velocidade de ação antiparasitária rápida, baixa toxicidade e alta tolerabilidade. De um modo geral, o mecanismo de ação da CQ e dos demais fármacos desta classe envolve a ligação destes antimaláricos ao heme livre dentro do vacúolo digestivo, e também envolve a sua ligação na superfície da hemozoína já formada (figura 5 A). Quando não detoxificado, o heme livre se acumula no vacúolo digestivo causando alta toxicidade, danos na membrana e morte do parasito (Figura 5 B) (FIDOCK et al., 2004; KAPISHNIKOV et al., 2019; PILLAT et al., 2020).

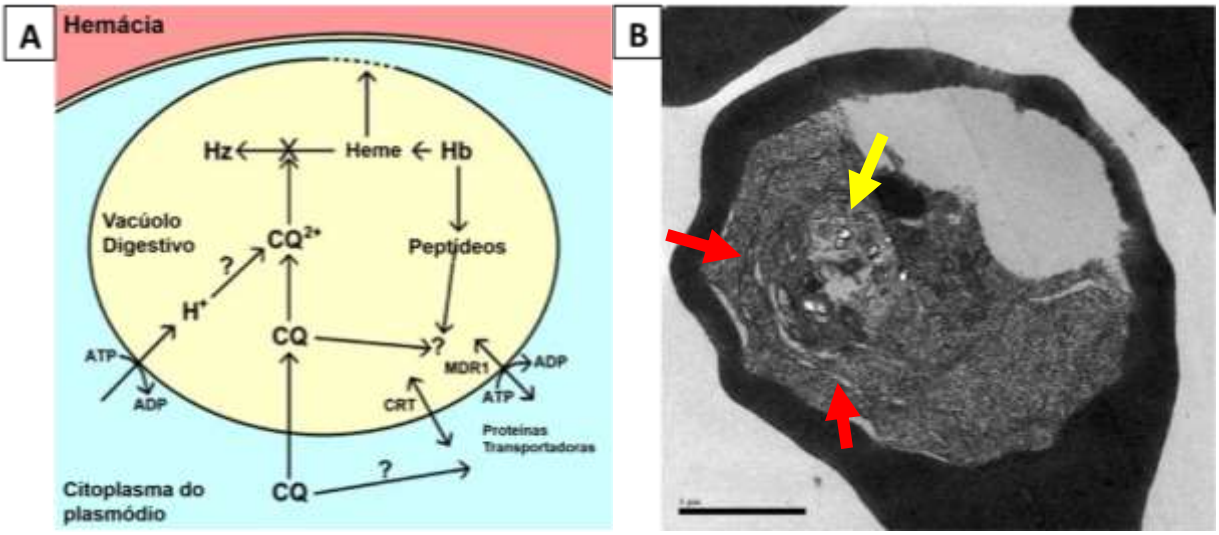


**Figura 5 -** Mecanismo de ação molecular da CQ no plasmódio e a observação das alterações ultra-estruturais no parasito após tratamento com a mesma. O acúmulo da CQ no vacúolo digestivo do parasito envolve a captação de íon seguido da protonação a $CQ^+$, com posterior transporte específico e/ou ligação ao heme livre, e, por fim, inibição da biossíntese de hemozoína. Os transportadores CRT e MDR1 parecem estar envolvidos no efluxo da CQ de dentro do vacúolo digestivo, entretanto, suas funções ainda não foram bem elucidadas (A). O parasito tratado com 4-aminoquinolina apresenta desorganização nas membranas (setas vermelhas), bem como uma diminuição no número e tamanho dos cristais de Hz (seta amarela) (B).
**Fonte**: Elaborado pela autora

Uma vez que a CQ alcança o interior da hemácia e o vacúolo digestivo, este se acumula em elevadas concentrações. A alta afinidade desse antimalárico ao vacúolo digestivo do parasito acontece em virtude desta organela possuir um pH ácido na faixa de 4,5 a 4,9, e a CQ ser uma base fraca, onde se protona em CQH ($CQ^+$). Ao ser protonada, a CQ não consegue fazer o caminho inverso e sair do vacúolo, e isto explica o porquê deste fármaco se acumular

de modo tão eficaz no plasmódio (KAPISHNIKOV et al., 2019). No vacúolo digestivo, a CQ pode se ligar tanto ao heme livre quanto à superfície dos cristais de hemozoína. Ao se ligar ao heme livre, a CQ suprime a nucleação inicial da hemozoína, enquanto que ao se ligar por adsorção a superfície dos cristais hemozoína, a CQ suprime a elongação do tamanho do cristais. Por atuar no bloqueio da detoxificação do heme, a CQ é eficaz em reduzir o crescimento dos esquizontes sanguíneos e teciduais, onde a formação de hemozoína é operante; todavia, a CQ é pouco eficaz em reduzir a viabilidade de gametócitos maduros, onde a formação de hemozoína é latente.

Entretanto, o uso massivo da CQ em 1960 acarretou a seleção dos parasitos que sofreram mutação nos genes *Pfmdr1* e *Pfcrt*; este último codifica uma proteína conhecida como proteína transportadora de resistência à CQ (Pfcrt), a qual vem gerando cepas resistentes do *P. falciparum* em muitas partes do mundo, dificultando o controle da doença (CHINAPPI et al., 2010; CDC, 2018; DAILY; MINUTI; KHAN, 2022; LAWRENSON et al., 2018; https://www.ncbi.nlm.nih.gov/books/NBK551512/).

A AQ também é uma 4-aminoquinolina com estrutura e mecanismo de ação similares à CQ. No processo de absorção pelo trato gastrointestinal, a AQ é rapidamente convertida pela enzima citocromo P450 (CYP) CYP2C8 no seu metabólito ativo chamado desetilamodiaquina, o qual age se acumulando dentro do vacúolo digestivo do parasito e interferindo na detoxificação do heme livre. Enquanto a AQ é eliminada rapidamente, o seu metabólito ativo é eliminado de forma mais lenta, com a meia-vida variando entre 4 a 10 dias. Apesar disso, este antimalárico é eficaz apenas frente a algumas cepas de plasmódio resistentes à CQ, e casos de resistência cruzada já foram datados (WHO, 2015).

Recomendada para a quimioprofilaxia medicamentosa, a MFQ tem sido amplamente utilizada por viajantes com destino a áreas endêmicas em malária. A MFQ é considerada um antimalárico potente e um dos mais eficazes, apesar da sua atividade antiparasitária ser limitada frente aos gametócitos. A combinação da MFQ com a ART tem sido recomendada para o tratamento e controle desta doença (WONG, W. et al., 2017). Apesar da MFQ já ser utilizada e amplamente estudada, o seu mecanismo de ação ainda não foi completamente elucidado; os dados mais convincentes indicam que a MFQ, ao contrário da CQ e AQ, possui uma ação pleiotrópica, agindo na detoxificaçao do heme, na síntese proteica a nível ribossomal através da ligação direta ao ribossomo citoplasmático Pf80S do *P. falciparum* (WONG, W. et al., 2017) e inibindo a atividade enzimática da fosforilase purina nucleosídeo (DZIEKAN et al., 2019).

A MFQ apresenta-se bastante eficaz contra cepas do *P. vivax* e *P. falciparum* resistentes à CQ (MAGUIRE et al., 2006). Além disso, cepas do *P. falciparum* resistentes à ART têm se mostrado sensíveis ao tratamento com a MFQ devido à diminuição do número de cópias do gene *Pfmdr*1, um biomarcador de resistência à MFQ. Este gene acarreta a codificação do transportador chamado glicoproteína-P (Pgh-1) no vacúolo digestivo, cuja função é realizar o efluxo do fármaco. Esses achados reforçam a importância do uso desse antimalárico na prevenção e no controle de parasitos resistentes aos tratamentos combinados com a ART ou outros antimaláricos; entretanto, apesar de eficaz, o uso substancial da MFQ tem sido associado com efeitos colaterais e com o surgimento de cepas resistentes (BLASCO; LEROY; FIDOCK, 2017; PINHEIRO et al., 2018; PRICE et al., 2004).

Ainda em relação a MFQ, faz-se necessário ressaltar que embora este seja um dos fármacos antimaláricos mais utilizado no momento, e a incidência de parasitos resistentes a MFQ seja relativamente pouco abundante, a MFQ apresenta uma velocidade de ação (48 h) no qual é relativamente lenta em comparação com a CQ (24 h), e mais rápida que a atovaquona (ATQ) (72 h). Outrossim, a MFQ é capaz de eliminar somente os parasitos no estágio de trofozoítos, ao contrário da CQ ou ART que são capazes de eliminar todas as formas do estágio sanguíneo assexuado. Por fim, a MFQ possui um tempo de meia-vida plasmático prolongado, que pode durar semanas. Embora esta característica seja interessante do ponto de vista profilático e de tratamento, o acúmulo da MFQ pode estar associado a toxicidade, incluindo eventos de neurotoxicidade.

Atualmente, o tratamento de primeira linha recomendado pela OMS para combater o *P. falciparum* em regiões onde há cepas resistentes à CQ é a terapia combinada da ART com outros fármacos com tempo de meia-vida plasmática longa (TCA). O fármaco do tipo endoperóxido pode ser ART, DHA, ARS ou artemeter. Essa terapia é indicada à malária não complicada causada pelo *P. falciparum*, uma vez que atua de modo eficaz frente a manifestação clínica e a transmissão da doença. Os fármacos recomendados para uso na TCA incluem a lumefantrina (LM), AQ, MFQ, sulfadoxina-pirimetamina, dentre outros (OMS, 2019).

A ART ou qinghaosu, o componente ativo da *Artemisia annua* L, planta medicinal bastante utilizada na China, foi isolada em 1972 e apresenta uma velocidade de ação antiparasitária rápida e eficaz nos estágios sanguíneo assexuado e sexuado da doença, além de uma eficácia relativa frente aos esquizontes teciduais (GOLENSER et al., 2006).

Como ações mecanísticas, a ART é ativada pelo heme, gerando espécies radicalares de capacidade reconhecida por alquilação. Estas espécies radicalares podem atuar alquilando o

heme livre e inibindo a formação da β-hematina, assim como o heme alquilado (isto é, conjugado ou adutos ART-hematina) pode atuar se ligando na superfície dos cristais de β-hematina já formados impedindo de maneira irreversível o seu crescimento (MA et al., 2021; RIBBISO et al., 2021). Os adutos ART-hematina, nos quais são produzidos através do consumo do heme, leva ao desequilíbrio na homeostasia redox do ferro (isto é, ferro oxidado *versus* ferro reduzido), afetando assim uma variedade de processos biológicos necessários para a sobrevivência e crescimento do parasito (QUADROS; SILVA; MOREIRA, 2022).

Como discutido acima, os antimaláricos do tipo esquizonticidas sanguíneos de primeira linha, tais como CQ, AQ, MFQ e ART, são eficazes contra a malária e, na sua maioria, possuem mecanismos de ação bem definidos e amplamente utilizados na clínica em terapias combinadas ou como monoterapia em regiões onde ainda há cepas sensíveis. Contudo, a atividade antimalárica destes fármacos vem sendo colocada à prova devido o surgimento e disseminação de parasitos resistentes aos fármacos existentes, requerendo, portanto, o desenvolvimento urgente de novos fármacos antimaláricos (FAN et al., 2018).

Além dos esquizonticidas sanguíneos que atuam na homeostasia e detoxificação do heme descritos acima, há os fármacos PQ e TFQ do grupo das 8-aminoquinolinas que são esquizonticidas teciduais, úteis ao tratamento da malária causada pelo *P. vivax* e especialmente importantes no contexto da malária no Brasil, onde o *P. vivax* é de alta prevalência (figura 6). Estes fármacos possuem atividade antiparasitária de potência relativamente baixa contra o estágio sanguíneo assexuado em comparação com a CQ; o mecanismo de ação neste estágio parece estar associado à interferência na homeostasia do heme e na geração de espécies reativas de oxigênio. Porém, estes fármacos são eficazes como esquizontes teciduais (hepáticos e hipnozoítos), e eficazes frente aos gametócitos (BAIRD, J. K., 2019).

A PQ foi desenvolvida no ano de 1950 pelas forças armadas dos Estados Unidos da América e desde então tem sido utilizada em combinação com algum esquizonticida sanguíneo. Recentemente, Camarda e colaboradores (2019) desvendaram que o mecanismo de ação da PQ envolve a produção e o acúmulo de peróxido de hidrogênio nos sítios de transformação de metabólitos, o qual acarreta a morte do parasito (CAMARDA et al., 2019). Entretanto, este fármaco apresenta toxicidade hemolítica em pacientes com deficiência da enzima glicose-6-fosfato desidrogenase (G6PD), sendo necessário a genotipagem antes do seu uso (FRAMPTON, 2018).

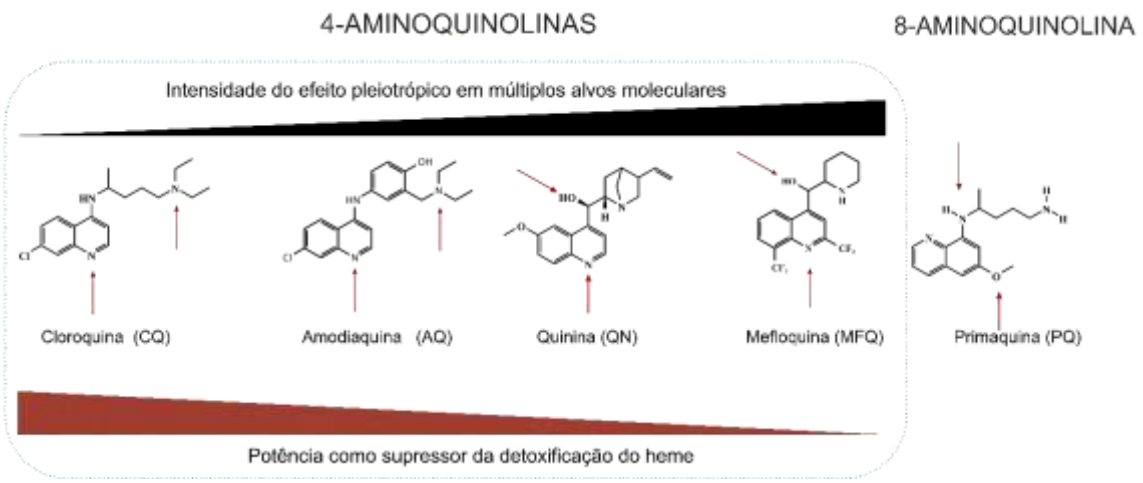


**Figura 6 -** Sumário das principais aminoquinolinas antimaláricas. Aqui, é plotado a ação dos antimaláricos em relação a supressão da detoxificação do heme *versus* a relação aos efeitos pleiotrópicos em múltiplos alvos moleculares no parasito. Destaca-se aqui a CQ como o fármaco mais potente e seletivo em suprimir a detoxificação do heme, sendo portanto o fármaco de menor ação pleiotrópica. De maneira inversa, destaca-se aqui a MFQ, onde apresenta-se como o fármaco menos potente e seletivo em suprimir a detoxificação do heme, sendo portanto o fármaco de maior ação pleiotrópica. Além das 4-aminoquinolinas, destaca-se aqui a 8-aminoquinolina (PQ), de potência e eficácia frente os esquizontes teciduais e gametócitos.
**Fonte**: Elaborado pela autora

A TFQ, comercialmente conhecida por Krintafel, é um análogo sintético da PQ e o antimalárico recentemente aprovado para o tratamento de relapso da malária causada por *P. vivax* após 70 anos do uso exclusivo da PQ. Este fármaco é caracterizado por ser metabolicamente estável e por ser eliminado mais lentamente do que outras 8-aminoquinolinas. Além disso, a TFQ é eficaz em prevenir o relapso da doença com uma única dose, a qual acarreta a cura radical, isto é, na eliminação dos parasitos sanguíneos e hepáticos do *P. vivax*; já a PQ previne o relapso da doença com 1-2 semanas do seu uso diário (LLANOS-CUENTAS et al., 2019; WATSON; NEKKAB; WHITE, 2021).

Na malária não complicada, estudos com *P. falciparum* sugerem que a TFQ tanto interfere nas funções mitocondriais do parasito, resultando em morte apoptótica, como também exerce atividade contra o estágio sanguíneo inibindo a polimerização da hematina. Outrossim, apesar dos mecanismos de ação ainda não totalmente elucidados, tem sido proposto que os metabólitos da TFQ e outras 8-aminoquinolinas aumentam o estresse oxidativo dentro dos gametócitos e de formas evolutivas do estágio hepático, ocasionando na morte do parasito (LLANOS-CUENTAS et al., 2022).

Por último, um aspecto que é importante citar a respeito das 8-aminoquinolinas PQ e TFQ é que estes são pró-fármacos, e que são metabolizados extensivamente a nível hepático, gerando cerca de cinco metabólitos no caso da PQ. Consequentemente, a eficácia da PQ e menos extensivamente da TFQ dependem da metabolização hepática do paciente, explicando o

porquê da eficácia apresentar certa variabilidade entre populações. Isto, associado a restrição aos pacientes deficientes em (G6PD), levam a limitações no uso e eficácia desta classe de esquizonticidas teciduais.

## 2.5 MEDIDAS DE CONTROLE E PROFILAXIA DA MALÁRIA

Em áreas endêmicas, medidas de controle dos mosquitos vetores do plasmódio envolvem o uso de mosquiteiros e inseticidas, além da realização da drenagem de água parada que funciona como criadouro dos mosquitos. Para os viajantes que se deslocam às áreas endêmicas, utilizar repelentes de insetos contendo DEET ou picaridina, realizar o tratamento de roupas com inseticida e evitar ficar ao ar livre entre o anoitecer e o amanhecer podem ajudar a diminuir o risco de contrair a malária associada a viagens (KOKO et al., 2022; WALTER; JOHN, 2022).

Além das medidas de controle da infecção e transmissão da doença pelos mosquitos, os antimaláricos atuais disponíveis para uso na clínica também atuam na quimioprofilaxia (AHMAD et al., 2021). O uso dos quimioprofiláticos orais é recomendado para os indivíduos que viajam para áreas endêmicas e que não tiveram nenhuma exposição prévia ao parasito, como também para àqueles que perderam a imunidade ao deixar a área endêmica, isto é, com menos exposição ao agente infeccioso. Além disso, os antimaláricos podem ser administrados diária ou semanalmente, antes e/ou após a viagem dependendo do antimalárico recomendado (WALTER; JOHN, 2022).

Tanto a OMS quanto o CDC Norte-Americano recomendaram os tratamentos com atovaquona–proguanil, doxiciclina, CQ, MFQ ou TFQ como profiláticos para viajantes em viagens de curta ou longa duração. Para viagens de longa duração (>6 meses) em áreas endêmicas, o uso dos quimioprofiláticos é prolongando e requer atenção especial devido aos possíveis efeitos colaterais. Um aspecto importante de um quimioprofilático oral seria a sua capacidade de inibir os estágios iniciais da infecção, ou seja, impedir a maturação de esporozoítos em esquizontes. Entretanto, poucos antimaláricos possuem tal eficácia atualmente.

Os antimaláricos quinolínicos CQ, AQ e MFQ possuem características que permitem o seu uso como agentes quimioprofiláticos, tais como velocidade de ação relativamente rápida em comparação com a ATQ, e uma duração plasmática longa; no entanto, estes antimaláricos exibem uma eficácia baixa em impedir a maturação de esporozoítos em esquizontes. Por outro lado, as ARTs possuem eficácia em impedir a maturação de esporozoítos; contudo, por

apresentarem um tempo de meia-vida de eliminação plasmática curta, não são factíveis para serem usados como agentes quimioprofiláticos.

Dito isto, novos fármacos têm sido investigados e julgados a partir dos seguintes critérios: baixo custo de produção; novos mecanismos de ação sem o desenvolvimento de resistência cruzada com antimaláricos já disponibilizados; cura com dose única; atividade contra os estágios assexuado (início da doença) e sexuado (gametócitos); ação anti-relapso, especialmente contra o hipnozoítos do *P. vivax*; e que possam atuar como quimioprofiláticos (DELVES et al., 2012; TSE; KORSIK; TODD, 2019).

Idealmente, fármacos de longa duração deveriam ser capazes de manter sua concentração plasmática eficaz por pelo menos 4 semanas, sobretudo para minimizar o número de administrações dos fármacos em áreas de transmissibilidade e taxas de reinfecção elevadas (BURROWS et al., 2017). Apesar dessa característica, identificar tais moléculas é um desafio, uma vez que são lipofílicas e frequentemente bases, aumentando assim as chances de maior distribuição de forma promíscua atingindo alvos celulares diferentes dos pretendidos (ABLA et al., 2017). Dentre os antimaláricos de longa duração com alvo no estágio sanguíneo, destaca-se a piperaquina (PPQ) (4-aminoquinolina) e MFQ (aminoálcool) com tempos de meia-vida de 33 dias e 14 a 30 dias, respectivamente (TARNING et al., 2005; FDA, 2009).

Ainda em relação a quimioprofilaxia oral, a MFQ é um fármaco clássico de longa duração, sendo o antimalárico mais recomendado para a quimioprofilaxia de viajantes em áreas endêmicas. Entretanto, a aderência pelos viajantes é geralmente baixa, devido aos efeitos colaterais, tempo de uso do antimalárico e fatores sociais (HOEFNAGEL; MASSAR; HAUTVAST, 2020). Com isso, estudos realizados vêm mostrando a importância do uso de quimioprofiláticos para a malária (SURYAPRANATA et al., 2022). Em um estudo conduzido por Grobusch e colaboradores (2021) com viajantes europeus que relataram alguma doença durante a viagem entre os anos de 1998 e 2018, observou-se que a malária ocupa a primeira colocação como a doença mais prevalente (GROBUSCH et al., 2021).

No estudo realizado por Abla e colaboradores (2017), um composto experimental chamado (-)-**1** [(3S,4S)-4-(3,6-bis(trifluoromethyl)-9Hcarbazol-9-yl)azepan-3-ol], caracterizado como um carbazol aminoálcool azepanil, possui como um possível mecanismo de ação a inibição da enzima Hsp90 do *P. falciparum*. Durante a investigação biológica do composto, os resultados revelaram que o (-)-**1** apresenta uma atividade antiparasitária excelente ($EC_{50}$ em nanomolar) em diversas cepas mutantes do *P. falciparum* resistentes à CQ, demonstrando também baixa propensão ao desenvolvimento de resistência. Além disso, o (-)-**1**

apresentou uma taxa de morte similar à CQ, e sua farmacocinética, após administração pelas vias intranvenosa e oral, revelou uma meia-vida acima de 24 horas em ratos. A dose estimada para reduzir 90% da parasitemia no 7º dia após a infecção ($ED_{90}$) foi de 3,6 mg/kg. Coletivamente, estes dados sugerem que este antimalárico experimental apresenta características de um fármaco de velocidade de ação rápida e de longa duração no plasma (ABLA et al., 2017).

A ATQ é uma quinona extremamente potente e eficaz, que possui uma meia-vida prolongada como uma característica essencial no combate ao plasmódio na malária não complicada e na profilaxia de viajantes, uma vez que possibilita a redução do número de administrações e aumenta a aderência dos indivíduos ao tratamento. De fato, a ATQ é um dos fármacos antimaláricos com eficácia excelente frente aos esporozoítos e gametócitos (BAKSHI et al., 2018; BLAGBOROUGH et al., 2013; PATON et al., 2019). No entanto, este fármaco apresenta um custo relativamente elevado e não é indicado como monoterapia devido ao rápido surgimento de cepas resistentes do *P. falciparum*, sendo, portanto, administrada como terapia combinada com o proguanil apenas para o tratamento, mas não para a prevenção (BAKSHI et al., 2018). Além disso, cepas resistentes à terapia combinada atovaquona-proguanil também já têm sido registradas (COTTRELL et al., 2014; SUTHERLAND et al., 2008).

Enquanto fármacos experimentais têm sido avaliados quanto à meia-vida plasmática de longa ou de curta duração, a ferroquina (FQ) permanece como o único antimalárico de longa duração em desenvolvimento clínico. Esse fato reforça uma maior necessidade de desenvolver novos fármacos com esta característica. Atualmente, em um estudo de fase 2a, um inibidor chamado DSM265, avaliado anteriormente em estudos pré-clínicos, foi investigado quanto à atividade antimalárica através de uma única dose em pacientes com malária não complicada causada pelo *P. falciparum* ou *P. vivax*. Apesar de ter sido eficaz em reduzir completamente a parasitemia da maioria dos pacientes infectados pelo *P. falciparum* com uma única dose, o DSM265 apresentou-se menos eficaz na cinética de eliminação do *P. vivax*. Seu perfil de longa duração torna-o potente para prevenir as reinfecções, contudo, estudos de combinação com outros fármacos ainda devem ser realizados (LLANOS-CUENTAS et al., 2018; MCCARTHY et al., 2017).

Além das medidas de controle para reduzir a transmissão do parasito pelos mosquitos e da quimioprofilaxia, a vacinação surgiu como uma vertente de profilaxia eficaz contra as infecções pelo plasmódio. Após mais de quatro décadas de pesquisas e ensaios clínicos, a OMS aprovou a vacina RTS,S/AS01 (Mosquirix™) para uso em crianças que vivem em áreas

endêmicas da malária. Esta vacina se baseia na imunização com proteínas dos esporozoítos do *P. falciparum* – estágio infectivo do plasmódio – para induzir resposta imunológica que protege contra a infecção (LAURENS, 2020). Em um extenso estudo de fase III em diferentes áreas endêmicas na África observou-se 74% de eficácia nas crianças de 5 a 17 anos após a última imunização, reduzindo para 28% e 9% após 1 e 5 anos pós vacinação, respectivamente. Em crianças de 6 a 12 semanas, a eficácia inicial estimada foi de 63%, com redução para 11% e 3% após 1 e 5 anos, respectivamente. A vacina ainda não é recomendada para adultos (ZAVALA, 2022).

Por fim, como discutido neste tópico e no anterior, há atualmente um arsenal terapêutico para a profilaxia e o tratamento da malária, que inclui medicamentos orais e a vacina Mosquirix™. Apesar deste conjunto de medidas, a prevalência e a gravidade nos casos da malária continuam altas. Isto se deve, em partes, ao constante surgimento de cepas do plasmódio resistentes aos fármacos. O surgimento de cepas resistentes aos fármacos é um fenômeno complexo e multifatorial, não abordados aqui; entretanto, é importante ressaltar que o uso de fármacos com amplo espectro de ação frente aos múltiplos estágios do plasmódio e o emprego de fármacos com longa duração no plasma podem mitigar o surgimento de cepas resistentes. Como revisaremos nos próximos tópicos, as duas principais classes de fármacos antimaláricos sofrem destes problemas, onde as quinolinas possuem um espectro de ação limitado somente ao estágio sanguíneo assexuado, e as ARTs possuem uma curta duração no plasma.

## 2.6 DESENVOLVIMENTO DOS ANTIMALÁRICOS QUINOLÍNICOS COM AÇÃO EM MÚLTIPLOS ESTÁGIOS DO PLASMÓDIO

Como citado anteriormente, a maioria dos fármacos antimaláricos atua na homeostasia e na detoxificação do heme. Este mecanismo de ação envolvendo o eixo heme/hemozoína é essencial no estágio sanguíneo assexuado; de fato, a maioria dos fármacos antimaláricos quinolínicos são esquizonticidas sanguíneos potentes e eficazes. Ressalva-se aqui que as ARTs em geral possuem uma eficácia alta frente aos esquizontes teciduais e aos gametócitos imaturos/jovens, porém, frente aos esporozoítos e aos gametócitos maduros a eficácia é comparativamente menor; além disso, é consenso que as ARTs são mais eficazes em curar os sintomas do paciente do que bloquear a transmissão (ação esterilizante).

Neste contexto, os dois principais desafios na busca por fármacos que atuem em múltiplos estágios são combater os gametócitos, que são formas evolutivas não-proliferativas,

e inibir a proliferação de esporozoítos no fígado (figura 7). Para isso, faz-se necessária a identificação de novos alvos e mecanismos de ação, assim como a busca por novos fármacos, a fim de ampliar o escopo de tratamentos e superar as vias de resistências já estabelecidas pelo parasito (DELVES et al., 2012; SHERIDAN et al., 2018).

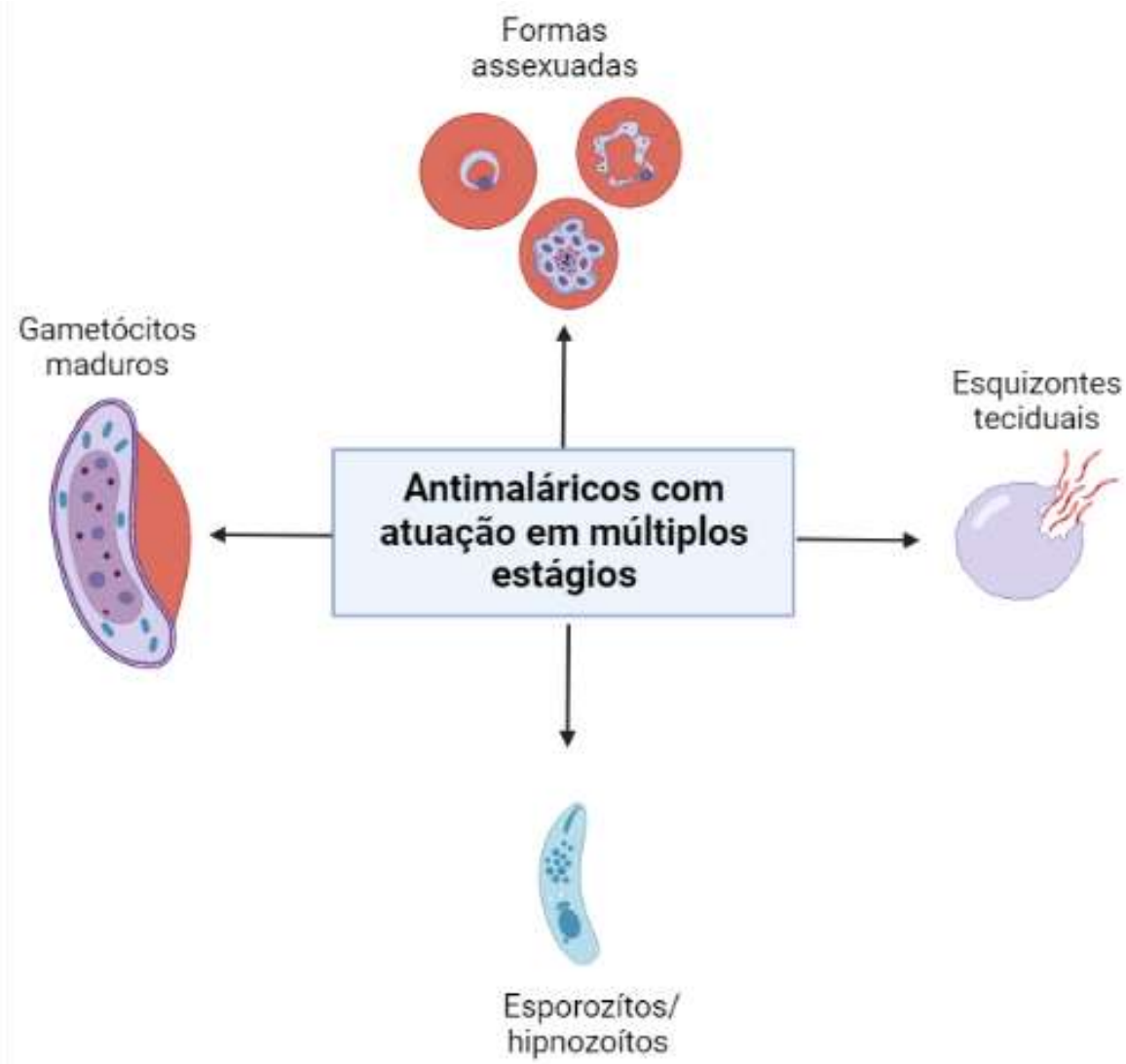


**Figura 7 -** Os fármacos antimaláricos que atuam em múltiplos estágios devem possuir atividade antiparasitária frente as formas assexuadas (anéis, trofozoítos e esquizontes sanguíneos), gametócitos e esporozoítos/hipnozoítos (inibidores da transmissão) e frente aos esquizontes teciduais.
**Fonte**: Elaborado pela autora

As quinolinas representam um importante arsenal terapêutico contra a malária, mas é importante que haja o desenvolvimento de novos compostos derivados das quinolinas que apresentem um espectro de ação mais amplo. Embora as quinolinas sejam reconhecidas por atuarem principalmente no eixo heme/hemozoína, é possível realizar modificações químicas e

combiná-las com outros farmacóforos para desenvolver quinolinas com um espectro de ação mais amplo, atuando também nos estágios sexuados e nos esquizontes teciduais.

A FQ, uma quinolina candidata à antimalárico para uso clínico, tem sido considerada para atuar em combinação com o ARS no enfrentamento à malária não complicada. Em estudos *in vivo* e em isolados clínicos, a FQ apresentou potência e eficácia superiores a CQ em inibir os esquizontes teciduais e os gametócitos (DUBAR et al., 2008). Um ensaio clínico de fase II demonstrou que as combinações destes dois fármacos com diferentes doses da FQ e dose fixa do ARS, culminaram numa alta taxa de cura dos pacientes e demonstraram ser seguras (HELD et al., 2015). Já um estudo clínico de fase IIb recentemente desenvolvido por Adoke e colaboradores (2021) revelou que a combinação de FQ e artefenomel, um endoperóxido, teve uma eficácia subótima em crianças da África com idade igual ou inferior a 5 anos (ADOKE et al., 2021).

Novas estratégias para ampliar o espectro de ação dos fármacos também têm sido investigadas. Dentre elas, o uso de metais para propostas terapêuticas tem sido adotado por apresentar inúmeras vantagens, tais como a possibilidade de preparação de complexos estáveis com estruturais predicáveis; a escolha seletiva de ligantes de acordo com sua afinidade; e possibilitar o aumento da compreensão do comportamento destes complexos metálicos no ambiente biológico. O acoplamento ou conjugação química de um metal na estrutura de antimaláricos já existentes é uma estratégica interessante usada para aprimorar a eficácia dos tratamentos atuais (MARCELINO et al., 2018).

A ligação de metais de transição à estrutura química de antimaláricos aprovados e seguros já disponíveis vem demonstrando um aprimoramento da atividade antiparasitária e ampliação do espectro de ação. Um estudo realizado por Macêdo e colaboradores (2016) mostrou que complexos de rutênio contendo CQ como ligante orgânico foram equipotentes à CQ em inibir formas evolutivas dos estágios sanguíneos assexuado e sexuado, e foram moderadamente eficazes frente ao estágio hepático (MACEDO et al., 2016).

Macêdo e colaboradores (2017) estudaram também a atividade antiplasmódio de complexos de platina (II) contendo a CQ como ligante orgânico. Neste estudo, observou-se que os complexos metálicos foram equipotentes com a CQ para inibir cepas do *P. falciparum* resistentes à CQ. Além disso, diferente da CQ, os complexos atuaram como agentes parasiticidas de forma irreversível contra os trofozoítos, no qual a formação da hemozoína é mais ativa. No fígado, demonstraram potência frente aos esporozoítos do *P. berghei*. Ademais, de forma superior à CQ, os complexos causaram uma perda da integridade mitocondrial e,

consequentemente, uma redução de sua atividade afetando todo o ciclo de vida do parasito (MACEDO et al., 2017).

Baragaña e colaboradores (2015) investigaram a quinolina DDD107498, um composto potente, com amplo espectro de ação e que atua em múltiplos estágios do ciclo evolutivo do plasmódio. O seu mecanismo de ação tem como alvo o fator de elongamento 2 da tradução (eEF2), o qual é responsável pela translocação dependente de GTP do ribossomo ao longo do RNA mensageiro e é essencial para a síntese proteica. Com elevada potência frente às cepas sensíveis e resistentes à CQ no estágio sanguíneo assexuado ($EC_{50}$ = 1 nM e 2,4 nM, respectivamente) e sexuado inibindo a formação dos gametas macho e fêmea em baixas concentrações ($IC_{50}$ = 1,8 nM e 1,2 nM, respectivamente), este composto demonstrou uma potente atividade antimalárica. Além disso, o DDD107498 também foi ativo contra o estágio hepático, atuando frente aos esquizontes hepáticos com o $EC_{50}$ menor do que 1 nM. Em conjunto, estes resultados sugerem que este composto possui características promissoras para um tratamento de única dose, o bloqueio da transmissão e a quimioproteção aos pacientes (BARAGAÑA et al., 2015).

Outro grupo de moléculas com potencial antimalárico foi estudado por Kato e colaboradores (2016), os quais identificaram uma série de azetidinas bicíclicas. Neste estudo, os autores elucidaram os mecanismos de ação de candidatos a antimaláricos que inibem um novo alvo molecular no ciclo de vida do plasmódio, a enzima fenilalanina-RNAt sintetase. As diferentes moléculas deste grupo foram capazes de bloquear a síntese proteica através da inibição da atividade da enzima fenilalanina-RNAt sintetase no citosol do *P. falciparum.* Ademais, demonstraram potência nos estágios sanguíneo (assexuado e sexuado) e hepático, bem como foram eficazes de curar animais infectados com apenas uma dose administrada por via oral (KATO, N. et al., 2016).

Pino e colaboradores (2017) relataram a atividade antiplasmódio do composto 49c, caracterizado como um *scaffold* à base de hidroxietilamina, o qual atua como um inibidor de plasmepsinas IX e X (proteases aspárticas). Estas proteases estão associadas com a clivagem inicial da Hb no vacúolo digestivo, gerando o desdobramento da proteína para que posteriormente a proteólise completa ocorra (LIN et al., 2015). Além disso, as proteases aspárticas são consideradas alvos terapêuticos potenciais para a quimioterapia, uma vez que são expressas principalmente nos esquizontes maduros do estágio sanguíneo, mas também em outras formas evolutivas, contribuindo para a patogenicidade do *P. falciparum*. Dito isto, o composto 49c foi capaz de inibir o desenvolvimento do plasmódio no estágio sanguíneo

assexuado com um $IC_{50}$ de 0,6 nM após 72 horas de tratamento, indicando que a inibição ocorre no processo de esquizogonia, bloqueando, por consequência, a liberação dos merozoítos. Outrossim, o composto foi capaz de inibir a esquizogonia no estágio hepático e o desenvolvimento e maturação dos gametócitos (PINO et al., 2017).

Os candidatos a novos antimaláricos quinolínicos com um espectro de ação mais amplo do que os que já existem na quimioterapia têm sido apontados como um importante avanço para erradicar a malária. Conforme apresentado acima, novos compostos estão sob investigação quanto à capacidade de atuar em pelo menos mais de um estágio do ciclo evolutivo do plasmódio (YAHIYA et al., 2019). Entretanto, a maioria ainda apresenta potência baixa frente aos gametócitos e os esporozoítos, sendo, portanto, ineficazes para impedir a transmissão ou o início da infecção em concentrações plasmáticas de relevância clínica. Uma possibilidade de contornar isso seria a combinação de grupos farmacofóricos de reconhecida ação frente aos gametócitos e os esporozoítos com as quinolinas, mimetizando a terapia combinada de fármacos, porém em um único composto (isto é, composto dual ou híbrido).

## 2.7 DESENVOLVIMENTO DOS ANTIMALÁRICOS ENDOPERÓXIDOS COM DURAÇÃO MAIS LONGA QUE AS ARTEMISININAS

Uma das principais características das ARTs é que elas apresentam um tempo de meia-vida de eliminação plasmática (t1/2) de 1-3 h, no qual é relativamente curto em relação a outros fármacos antimaláricos. Isto se deve principalmente a metabolização das ARTs pelas espécies de heme e de ferro (II) nos eritrócitos e nas células dos parasitos (figura 8). Em contraste com as ARTs, os demais antimaláricos apresentam uma metabolização hepática, e consequentemente, apresentam um tempo de meia-vida plasmática mais longo, variando de dias a semanas. Por isso, na TCA usa-se um antimalárico de t1/2 mais longo, tais como as quinolinas ou antibióticos, enquanto a TCA com dois componentes das ARTs (exemplo: ARS+ART) não são empregados (FAIRHURST; DONDORP, 2016). Aqui, faz-se necessário frisar que embora o t1/2 das ARTs seja um problema na terapêutica, as ARTs são uma classe de fármacos com velocidade de ação rápida, no qual reduz rapidamente a parasitemia, e consequentemente, os sintomas da malária. No momento, não há substitutos para as ARTs, e a busca por fármacos derivados das ARTs com um t1/2 mais longo é uma linha de pesquisa importante.

Considerando que a metabolização do grupo químico peróxido das ARTs pelas espécies de heme (II) nos eritrócitos e nas células dos parasitos é o responsável pelo t1/2 curto das ARTs, a maioria dos esforços tem sido realizados para desenvolver compostos do tipo peróxidos no

qual o processo de metabolização, onde a etapa de bioativação redutiva do grupo químico peróxido pelo ferro II ocorre, seja mais lento (QUADROS; SILVA; MOREIRA, 2022). Outrossim, a importância de desenvolver novos derivados das ARTs se refere ao fenômeno de resistência. Este fenômeno caracteriza-se, em partes, pelo atraso no tempo do ciclo evolutivo dos parasitos sanguíneos assexuado, aumentando o tempo de permanência do parasito em anéis. Ao estender o tempo durante a maturação em anéis, o plasmódio escapa do pico do tratamento com as ARTs, no qual é em torno de 3 horas.

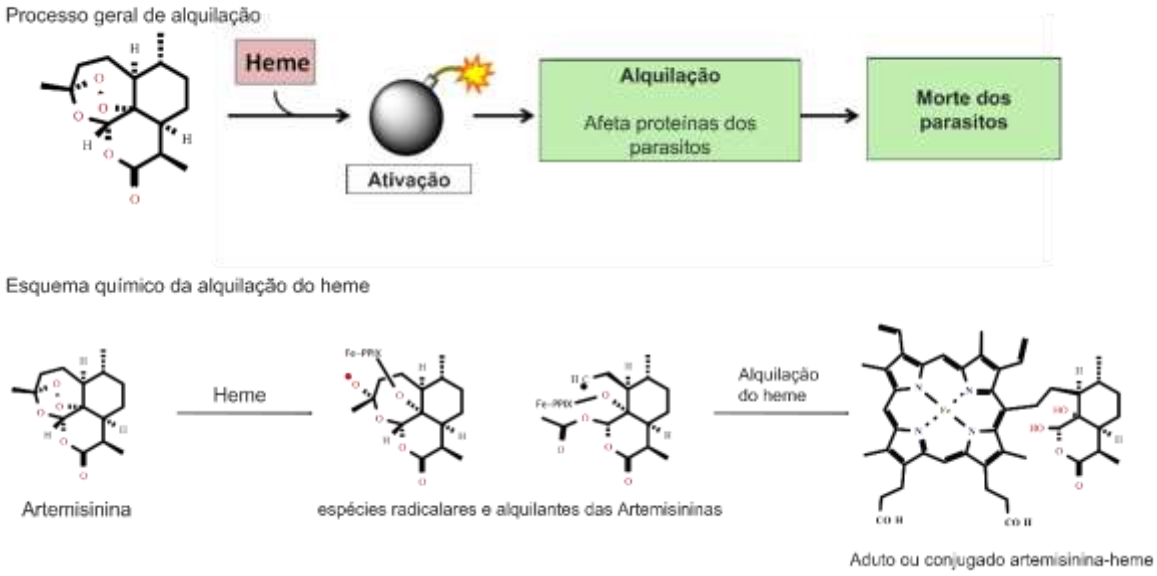


**Figura 8 -** As artemisininas são bioativadas quimicamente pelo heme. A bioativação produz uma espécie radicalar capaz de alquilar biomacromoléculas, entre estas proteínas (painel superior) ou até mesmo o heme. A alquilação de biomacromoléculas é um processo irreversível e que afeta a viabilidade e o crescimento do parasito.
**Fonte**: Elaborado pela autora

Diante do que foi discutido, presume-se que a metabolização lenta do peróxido resultaria em compostos com um t1/2 mais longo do que as ARTs, garantindo assim um tempo maior de exposição dos parasitos ao fármaco sem detrimento à diminuição da velocidade de ação antimalárica. Além disso, compostos derivados das ARTs com um t1/2 mais longo poderiam afetar alvos moleculares no qual as ARTs não afetam, apresentando um maior potencial terapêutico em inibir o crescimento dos parasitos.

Sem sombra de dúvidas, há uma busca muito intensa por novos compostos análogos as ARTs que, em comum, apresentem um grupamento químico peróxido na sua estrutura (BLANK et al., 2020; VENNERSTROM et al., 2004; WOODLEY et al., 2021) (figura 9). Diante do exposto, Kim e colaboradores (2017) estudaram o fármaco artefenomel (OZ439). Como resultados, eles encontraram que o OZ439 além de apresentar potência e eficácia

elevadas frente ao parasito, possui um t1/2 de 46 a 60 horas e uma concentração plasmática máxima mais alta do que as ARTs e o mais importante um t1/2 mais prolongado. Os resultados também mostraram que o tratamento com a dose única de 30 mg/kg com o OZ439 resultou na cura dos animais infectados com o *P. berghei*. Além disso, este fármaco apresentou atividade profilática 100% superior à MFQ quando administrado 96 horas antes da infecção (CHARMAN et al., 2011; KIM; HAMMILL; GUY, 2017).

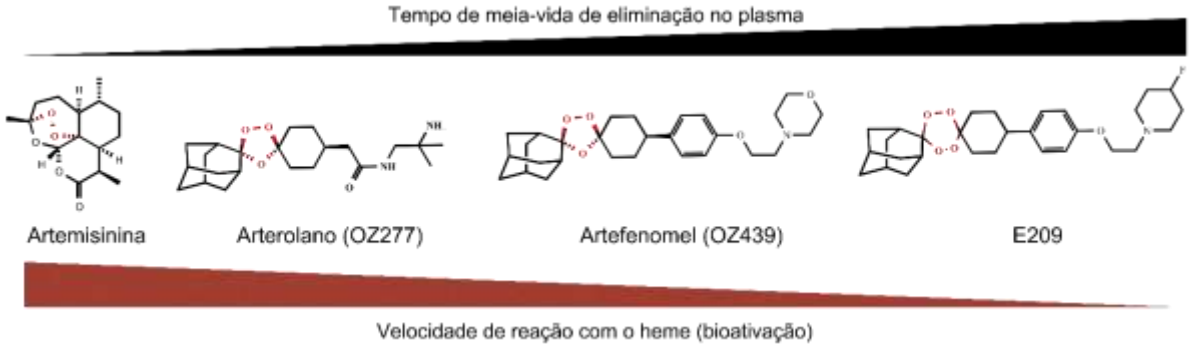


**Figura 9 -** As artemisininas são moléculas naturais onde o grupamento químico peróxido (destacado em vermelho) é essencial para a bioativação, no qual mediado pelo heme, pode produzir espécies radicalares capazes de alquilar biomacromoléculas no plasmódio. Alguns destes antimaláricos sintéticos são mais lentamente bioativados pelo heme, consequentemente apresentando um t1/2 mais longo do que as artemisininas.
**Fonte**: Elaborado pela autora

De forma semelhante ao OZ439, o endoperóxido E209 possui uma atividade antimalárica potente (em nanomolar) *in vitro* contra cepas do *P. falciparum* e *P. vivax*¸ e uma eficácia elevada *in vivo* contra o *P. falciparum* equivalente a DHA. Outrossim, suas características farmacocinéticas e farmacodinâmicas são compatíveis com os fármacos de administração em dose única, podendo ser caracterizado como um fármaco com características superiores às ARTs de uso atual (figura 9) (O'NEILL et al., 2017).

Por fim, esforços por parte de pesquisadores de diferentes lugares do mundo vêm sendo realizados para que novos fármacos antimaláricos possam ser aprovados para uso na terapia combinada, tal como o ozonídeo sintético OZ277 já em uso, o ozonídeo OZ439 em estágio clínico, e o E209 em estágio pré-clinico avançado. Até o momento, somente o ozonídeo sintético OZ277 está em uso clínico, embora este fármaco seja um endoperóxido semelhante as ARTs, o qual foi produzido e aprovado como uma terapia combinada com a PPQ para o combate à malária não complicada; entretanto, sua meia-vida é um pouco mais de apenas 3 horas em humanos, sendo destacada como uma limitação tal qual é encontrada nas ARTs (KIM;

HAMMILL; GUY, 2017b). É bem possível que no futuro próximo, o ozonídeo sintético OZ277 seja substituído por outro antimalárico endoperóxido de t1/2 maior.

## 2.8 TERAPIA COMBINADA DE FÁRMACOS *VERSUS* COMPOSTOS HÍBRIDOS

O conceito de terapia combinada de fármacos foi idealizado em 1965 pelos cientistas Emil Frei, James F. Holland e Emil J. Freireich, que postularam a possibilidade da primeira quimioterapia baseada em combinação de fármacos para combater a leucemia aguda em pacientes pediátricos (AYOUB, 2021; FREL et al., 1965). Além de aplicada ao câncer, a terapia combinada também é um tratamento comum para doenças infecciosas, tais como tuberculose e o vírus da imunodeficiência humana (do inglês, *human immunodeficiency virus*, HIV) (CUI; SU, 2009).

Na terapia combinada para a malária, é dito que os antimaláricos interagem quando a potência de dois ou mais antimaláricos combinados é maior (sinergismo ou potenciação) ou menor (antagonismo) do que seria esperado da atividade individual de cada fármaco. Se a combinação é sinérgica, ela é particularmente favorável, pois pode culminar na possibilidade de redução dos fármacos sem interferir na eficácia do tratamento. Do contrário, se a combinação é antagônica, a eficácia é reduzida. Quando não há interação dos fármacos em combinação, o efeito é denominado aditividade (figura 10) (BELL, 2005).

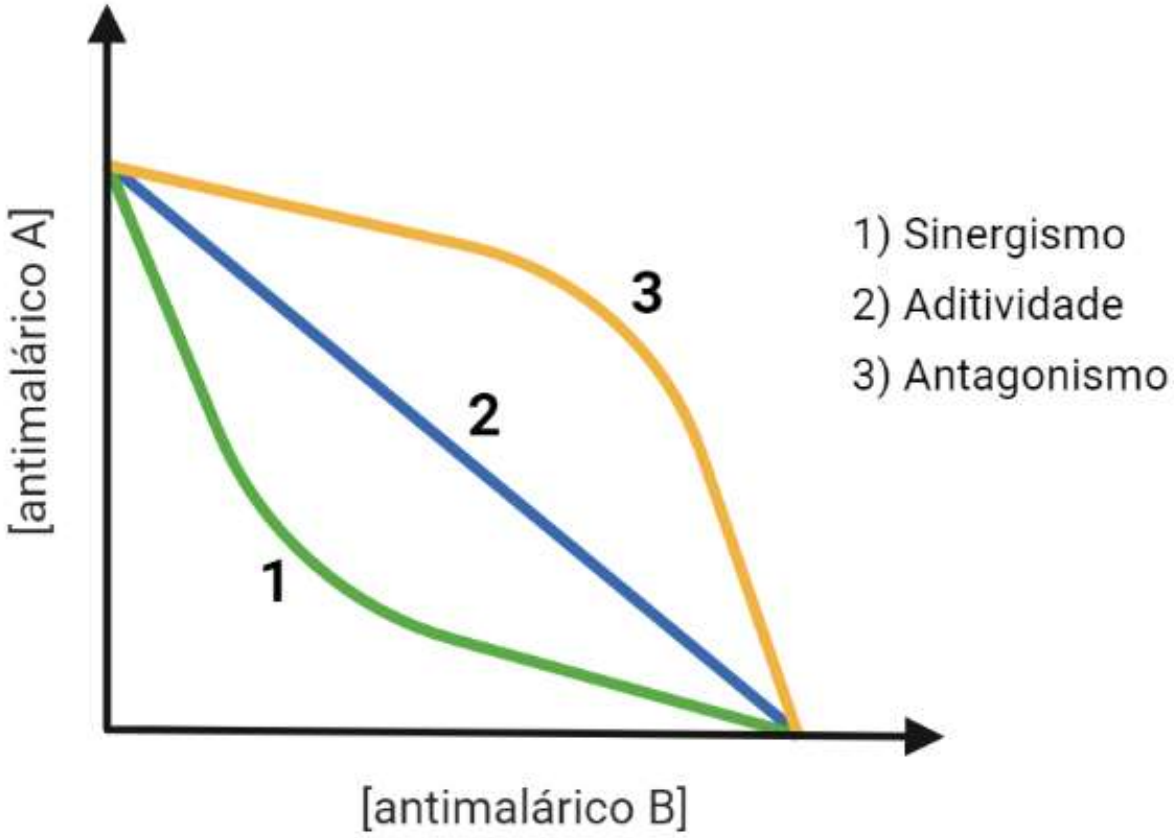


**Figura 10 -** Representação gráfica de um isobolograma mostrando possíveis interações entre dois antimaláricos, A e B. A curva 1 indica sinergismo (potenciação ou somação); a curva 2 indica aditividade (sem interação); e a curva 3 indica antagonismo (redução da potência) em relação à potência dos fármacos administrados individualmente.
**Fonte**: Elaborado pela autora

Na malária não complicada, a TCA é feita uma combinação da ART ou derivados de curta duração com outro fármaco de longa duração (TSE; KORSIK; TODD, 2019). Neste sentido, a TCA tem sido recomendada como uma das terapias mais eficazes para tratar infecções causadas por cepas do *P. falciparum* resistentes à CQ (PETER et al., 2021). Em regiões co-endêmicas para o *P. falciparum* e *P. vivax* resistentes à CQ, a TCA também tem sido recomendada (PRICE et al., 2014). Embora a terapia combinada de CQ e PQ seja eficaz para combater cepas do *P. vivax* resistentes à CQ e levar à cura radical (incluindo a eliminação dos hipnozoítos), existe uma relutância em indicar a PQ devido ao tempo padrão de tratamento de 14 dias e a possibilidade de causar hemólise nos pacientes. Nesse caso, a TFQ tem sido implementada gradativamente no esquema terapêutico (quadro 1) (DOUGLAS et al., 2010; PRICE et al., 2014).

De acordo com o Guia Prático de Tratamento da Malária no Brasil (2010), no Brasil e outros países com prevalência em *P. vivax* ou por outras espécies não-falcipárias, a terapia combinada medicamentosa pode ser sem ART, tais como CQ e PQ; doxiciclina e PQ, podendo a PQ ser substituída gradualmente pela TFQ, ou por último a combinação QN e clindamicina. De acordo com o guia de tratamento da malária no Brasil (2020), o objetivo do tratamento do *P. vivax* e de outras espécies não falcipárias é curar tanto a forma sanguínea quanto a forma hepática (cura radical) da doença, e, dessa forma, prevenir a recrudescência e a recaída, respectivamente (quadro 1).

**Quadro 1 -** Esquemas terapêuticos para a malária não complicada.

| Terapia combinada | Espécie do plasmódio |
|---|---|
| Artesunato + Mefloquina | *P. falciparum* |
| Artemeter + Lumefantrina | *P. falciparum* |
| Artesunato + Pironaridina | *P. falciparum* |
| Cloroquina + Primaquina ou Tafenoquina | *P. vivax* ou *P. ovale* |
| Doxiciclina + Primaquina | *P. vivax* ou *P. ovale* |
| Quinina + Clindamicina | *P. vivax* ou *P. ovale* |

**Fonte**: Elaborado pela autora

Desde o início do programa de terapia combinada na malária até o momento, a TCA tem revelado elevadas taxas de cura, tolerabilidade e segurança na administração, e uma redução significativa da mortalidade global (BASSAT et al., 2022). Todavia, a resistência ao fármaco de duração longa durante a TCA tem sido descrita como cada vez mais prevalente, em diversas partes do mundo. Ainda mais grave é o fato que na região do Greater Mekong na Ásia na fronteira da Tailândia com o Mianmar, Vietnã e o Camboja, o uso da terapia combinada DHA-PPQ tem falhado devido a presença de parasitos resistentes as ARTs, acarretando baixas taxas de cura (SAUNDERS; VANACHAYANGKUL; LON, 2014; VAN DER PLUIJM et al., 2020).

Novas estratégias são necessárias para retardar ou reverter a disseminação dos parasitos resistentes; como alternativa, a terapia tripla combinada baseada em ART (TACT), onde um terceiro fármaco de longa duração é incluído, tem emergido como uma possibilidade de tratamento para a malária não complicada (ANSBRO et al., 2020; DINI et al., 2018). O racional para a terapia tripla é que a adição do terceiro componente farmacêutico poderia minimizar a resistência às ARTs. Atualmente, os tratamentos Artemeter-LM-AQ e DHA-PPQ-MFQ estão em fase de testes clínicos, cujos controles são terapias combinadas padrão (VAN DER PLUIJM et al., 2020). Outra estratégia para retardar a disseminação dos parasitos resistentes é prolongar

o tempo de tratamento com a TCA de três para cinco dias, denominada de solução temporal da TCA (WANG et al., 2019).

No momento, a terapia tripla assim como a solução temporal da TCA está em estudos; todavia, as duas abordagens não solucionam o problema intrínseco da resistência dos parasitos as ARTs, no qual é, em partes, devido ao tempo de vida curto no plasma desta classe de fármacos. Por isso, a busca por fármacos do tipo ARTs de nova geração é tão importante. Entretanto, a terapia combinada com as ARTs não é a única a apresentar limitações. Em relação a terapia combinada com a PQ ou TFQ para o tratamento do *P. vivax*, um problema a ser destacado é que o tratamento com a PQ é duas vezes mais longo do que do outro fármaco parceiro (CQ, QN, doxiciclina); isto inviabiliza o desenvolvimento de um comprimido único com os dois fármacos e torna o tratamento mais complicado, diminuindo muitas vezes a adesão pelo paciente. Em virtude destes fatos, é nítido que tanto as terapias combinadas com as ARTs quanto com a PQ necessitam de novas tecnologias ou de novos fármacos.

Em função das limitações apresentadas pelas terapias combinadas, os compostos híbridos apresentam-se como uma alternativa, sobretudo por apresentar uma atividade em múltiplos estágios do ciclo de vida, bem como contra cepas resistentes. Geralmente, os fármacos híbridos podem ser desenhados partindo de três possibilidades: 1) usando ligantes químicos não-cliváveis; 2) ligantes cliváveis; e 3) através de metais de transição, como o ouro, que, de maneira dual podem atuar como ligantes químicos cliváveis e como antimaláricos. De fato, estudos já têm demonstrado que os metais de transição são farmacologicamente ativos contra os parasitos, enquanto tipicamente os ligantes químicos orgânicos são destituídos de tal capacidade (QUADROS et al., 2021).

A síntese de compostos híbridos ocorre a partir da hibridização de farmacóforos, nos quais dois ou mais agentes bioativos são combinados e atuam através de mecanismos de ação diferentes (ALVEN; ADERIBIGBE, 2019; MOKHTARI et al., 2017). A hibridização surgiu como uma alternativa para potencializar a eficácia farmacológica de antimaláricos já usados na clínica e/ou dos constituintes bioativos da molécula híbrida, além de driblar a resistência já encontrada contra os antimaláricos de amplo uso (ÇAPCI et al., 2019).

Neste contexto, híbridos de artemisinina-(iso)quinolina e artemisinina-quinolina foram desenvolvidos para combater o plasmódio (ÇAPCI et al., 2019). De acordo com o estudo de Çapci e colaboradores (2019), estes híbridos foram altamente potentes frente a cepas resistentes à CQ e cepas do *P. falciparum* multirresistentes ($EC_{50}$ (Dd2) < 1 nM; $EC_{50}$ (K1) < 0,78 nM) quando comparado com o tratamento clássico com a CQ ($EC_{50}$ (Dd2) = 165,3 nM; $EC_{50}$ (K1)

= 302,8 nM), e também foram eficazes em suprimir a parasitemia em animais infectados com *P. berghei*.

Outrossim, uma série de híbridos artemisinina-triazina e dímeros híbridos foi sintetizada e a atividade antiplasmódio e gametocida de cada híbrido experimental foi avaliada *in vitro* frente a cepas sensíveis e resistentes à CQ (NF54 e Dd2, respectivamente). Como resultados, os híbridos e dímeros híbridos foram ativos contra ambas as cepas do *P. falciparum* testadas, tendo como destaque o híbrido **22**, caracterizado um dímero híbrido triazina com o *p*anisidino substituído, o qual apresentou potências em nanomolar e uma seletividade expressiva ao parasito (CLOETE et al., 2014).

Os agentes quelantes do ferro também demonstram uma importante atividade na supressão da parasitemia *in vitro* e *in vivo.* Dito isto, um estudo desenvolvido por Dambuza et al. (2015) idealizou a hibridização da CQ com o N-alkyl-3-hydroxypyridin-4-ones gerando uma série de híbridos capazes de atuar no metabolismo do ferro e na supressão da parasitemia. Dessa forma, os efeitos antiplasmódio destes híbridos foram avaliados contra cepas sensíveis (3D7 e D10) e resistentes à CQ (K1 e Dd2) do *P. falciparum*. Como resultados, os híbridos **1** e **2** tiveram potências similares ou superiores a CQ. No estudo *in vivo*, a CQ na dose de 10 mg/kg/dia foi eficaz em suprimir a parasitemia em mais de 90% quando administrada via oral, enquanto os compostos híbridos foram capazes de suprimir a parasitemia em mais de 80% quando administrados pela via intravenosa, na dose de 8 mg/kg/dia (DAMBUZA et al., 2015).

# 3 **OBJETIVOS**

## 3.1 OBJETIVO GERAL

Avaliar a ação antimalárica de novos compostos híbridos derivados das classes dos endoperóxidos e quinolinas em diferentes modelos experimentais *in vitro* e *in vivo* de malária.

## 3.2 OBJETIVOS ESPECÍFICOS

- Avaliar a atividade antiparasitária, a citotoxicidade em células de mamíferos e a seletividade dos compostos híbridos (**1-4**) contra cepas do *P. falciparum* sensíveis ou resistentes a fármacos;
- Compreender a origem da potência antiparasitária a nível fenotípico ou molecular dos compostos híbridos em relação aos fármacos de referência ou protótipos;
- Estudar a eficácia *in vivo* e a ação antiparasitária dos compostos híbrido**s** no *P. berghei* e compará-los com os fármacos de referência;
- Avaliar a potência antiparasitária de compostos híbridos como componentes em terapias combinadas em comparação com a monoterapia ou terapia combinada clássica.

# 4 **DELINEAMENTO EXPERIMENTAL E RACIONAL**

## 4.1 DELINEAMENTO RACIONAL

A parte original da tese foi dividida em 2 capítulos. No capítulo 1, os compostos híbridos foram sintetizados, caracterizados quimicamente e estudados como fármacos antimaláricos experimentais, com o intuito de descobrir fármacos com ação frente aos múltiplos estágios evolutivos do plasmódio. Um enfoque foi realizado para compreender qual a origem e a razão, tanto a nível fenotípico quanto a nível molecular, do espectro de ação antiparasitário ser mais amplo ou mais estreito em relação aos fármacos de referência. Os seguintes artigos foram publicados:

1. Um novo híbrido de cloroquina e primaquina ligado pelo ouro(I): agente antiplasmódio multi-fase e multi-alvos;
2. Um híbrido de amodiaquina e primaquina ligado pelo ouro(I) é um agente antimalárico multi-estágio que tem como alvo a detoxificação do heme e a homeostasia redox de tióis;
3. Estudos de potência e eficácia de um híbrido quinolina-artemisinina contra múltiplos estágios do ciclo de vida do *Plasmodium*.

No capítulo 2, os dois compostos híbridos de ARTs mais potentes e eficazes como antimaláricos foram selecionados para estudos mais aprofundados. Mais especificamente, foram investigados a velocidade de ação antiparasitária, o perfil de ação antiparasitário frente a diferentes formas evolutivas no estágio sanguíneo assexuado (anéis, trofozoítos, esquizontes), a estabilidade química dos compostos na cultura do plasmódio e o perfil de duração prolongada nos eritrócitos. Por último, a avaliação dos compostos híbridos em cepas sensíveis ou resistentes as ARTs foram avaliadas em detalhes.

1. O artigo intitulado “Avaliação do potencial farmacológico de híbridos baseados em artemisininas para o tratamento da malária” será submetido a revista Antimicrobial Agents Chemotherapy.

## 4.2 REPRESENTAÇÃO ESQUEMÁTICA DO DELINEAMENTO EXPERIMENTAL

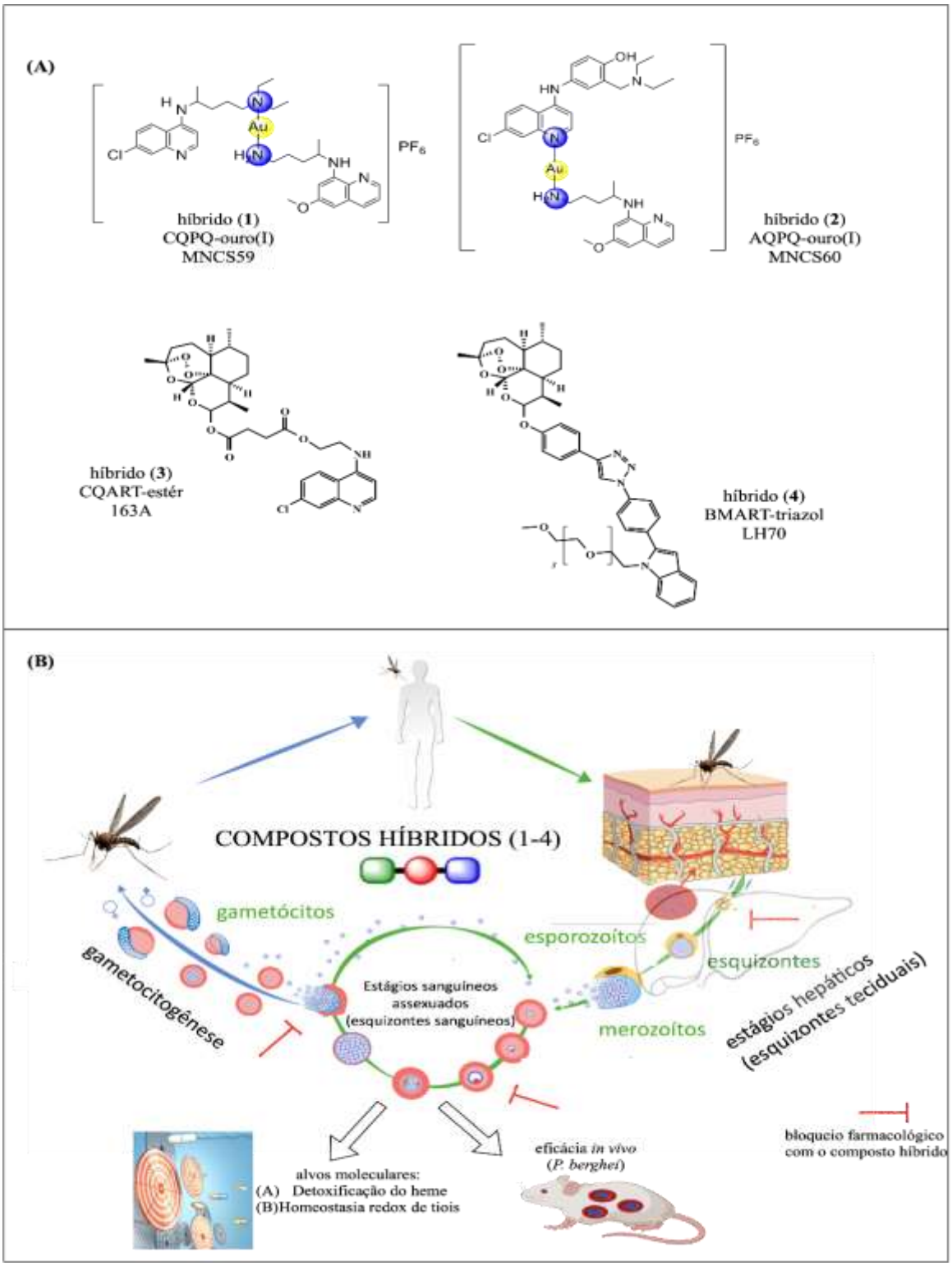


**Figura 11 -** Esquema gráfico dos compostos híbridos (**1-4**) estudados aqui (painel A) e um sumário dos estudos farmacológicos a nível fenotípico ou molecular e de eficácia *in vivo* conduzidos sob o tratamento com os compostos híbridos (**1-4**) (painel B). No painel A estão indicados os códigos dos compostos híbridos utilizados durante a tese, além dos códigos originais citados nos capítulos. No painel B estão indicados os estágios evolutivos do plasmódio onde os ensaios fenotípicos foram conduzidos. Exceto no ensaio de eficácia *in vivo* e de infecção em hepatócitos, onde a espécie de *P. berghei* foi utilizada, os demais ensaios foram conduzidos com o *P. falciparum*.
**Fonte**: Elaborado pela autora

## 4.3 CAPÍTULO 1

1 Um novo híbrido de cloroquina e primaquina ligado pelo ouro(I): agente antiplasmódio multi-fase e multi-alvos;

2 Um híbrido de amodiaquina e primaquina ligado pelo ouro(I) é um agente antimalárico multi-estágio que tem como alvo a detoxificação do heme e a homeostasia redox de tióis;

3 Estudos de potência e eficácia de um híbrido quinolina-artemisinina contra múltiplos estágios do ciclo de vida do *Plasmodium*.

# A Novel Hybrid of Chloroquine and Primaquine Linked by Gold(I): Multitarget and Multiphase Antiplasmodial Agent

Caroline de Souza Pereira,[a] Helenita Costa Quadros,[b] Diogo Rodrigo Magalhaes Moreira,[b] William Castro,[c] Romulo Ivisson Santos De Deus Da Silva,[b] Milena Botelho Pereira Soares,[b] Diana Fontinha,[d] Miguel Prudêncio,[d] Vinicius Schmitz,[a] Hélio F. Dos Santos,[a] Mathieu Gendrot,[e, f, g] Isabelle Fonta,[e, f, g, h] Joel Mosnier,[e, f, g, h] Bruno Pradines,[e, f, g, h] and Maribel Navarro*[a]

*Plasmodium* parasites kill 435 000 people around the world every year due to unavailable vaccines, a limited arsenal of antimalarial drugs, delayed treatment, and the reduced clinical effectiveness of current practices caused by drug resistance. Therefore, there is an urgent need to discover and develop new antiplasmodial candidates. In this work, we present a novel strategy to develop a multitarget metallic hybrid antimalarial agent with possible dual efficacy in both sexual and asexual erythrocytic stages. A hybrid of antimalarial drugs (chloroquine and primaquine) linked by gold(I) was synthesized and characterized by spectroscopic and analytical techniques. The CQPQ-gold(I) hybrid molecule affects essential parasite targets, it inhibits β-hematin formation and interacts moderately with the DNA minor groove. Its interaction with PfTrxR was also examined in computational modeling studies. The CQPQ-gold(I) hybrid displayed an excellent *in vitro* antimalarial activity against the blood-stage of *Plasmodium falciparum* and liver-stage of *Plasmodium berghei* and efficacy *in vivo* against *P. berghei*, thereby demonstrating its multiple-stage antiplasmodial activity. This metallic hybrid is a promising chemotherapeutic agent that could act in the treatment, prevention, and transmission of malaria.

## Introduction

Over a long period of time, a number of complementary strategies were employed to control malaria. The World Health Organization highlighted that the most advanced malaria vaccine candidate shows only partial protection against malaria in young children. It also called attention to insecticide-treated net as well as indoor residual spraying as powerful ways to immediately reduce malaria transmission. Regarding the chemotherapy strategy, the best available treatment for *Plasmodium falciparum* malaria is artemisinin-based combination therapy (ACT) using two or three well-known antimalarial drugs. Despite all the enormous efforts, malaria is still an important health problem, where in 2018, 228 million cases of malaria and 405 000 deaths around the world were reported.[1]

Malaria treatment with a cocktail of drugs or combination of drugs is showing critical limitations, such as poor patient compliance and a high risk of drug-drug interactions.[2] Further complications are reports of increased resistance to ACT.[3] Among many different approaches to antimalarial drug discovery and development, the antimalarial organic hybrid molecules must be cited. A plethora of examples of these kind of compounds have been studied so far.[4–6] A hybrid compound is defined as a chemical entity with two or more structural domains which acts on different or same biological function or with dual mode of action.[2] The most classic examples are trioxaquine,[7] trioxaferroquines[7] and primaquine/chloroquine hybrid.[5] The advantages of organic hybrid compounds are the possibility of additive or synergistic therapeutic response, improved druggable characteristics of the therapeutic compo-

[a] C. de Souza Pereira, V. Schmitz, Prof. H. F. Dos Santos, Prof. M. Navarro
Departamento de Química
Universidade Federal de Juiz de Fora, Rua José Lourenço Kelmer, s/n – Campus Universitário, Bairro Martelos CEP 36036-900, Juiz de Fora, Minas Gerais (Brasil)
E-mail: maribel.navarro@ufjf.edu.br
[b] H. Costa Quadros, Dr. D. R. Magalhaes Moreira,
R. I. Santos De Deus Da Silva, Dr. M. Botelho Pereira Soares
Instituto Gonçalo Moniz
Fundação Oswaldo Cruz, Av. Waldemar Falcão, 121, Candeal, Salvador, Bahia (Brasil)
[c] Dr. W. Castro
Centro de Química
Instituto Venezolano de Investigaciones Científicas (IVIC), Centro de Química, Carretera Panamericana, Km 11, Altos de Pipe, San Antonio de los Altos Miranda, 1020-A, Caracas (Venezuela)
[d] Dr. D. Fontinha, Dr. M. Prudêncio
Instituto de Medicina Molecular João Lobo Antunes
Faculdade de Medicina, Universidade de Lisboa
< Lisboa (Portugal)
[e] M. Gendrot, I. Fonta, J. Mosnier, Dr. B. Pradines
Unité Parasitologie et entomologie, Institut de recherche biomédicale des armées, 19–21 Bd Jean Moulin, 13005 Marseille (France)
[f] M. Gendrot, I. Fonta, J. Mosnier, Dr. B. Pradines
Aix-Marseille Univ, IRD, SSA, AP-HM, VITROME, 19–21 Bd Jean Moulin, 13005 Marseille (France)
[g] M. Gendrot, I. Fonta, J. Mosnier, Dr. B. Pradines
IHU Méditerranée Infection, 19–21 Bd Jean Moulin, 13005 Marseille (France)
[h] I. Fonta, J. Mosnier, Dr. B. Pradines
Centre National de Référence du Paludisme, 19–21 Bd Jean Moulin, 13005 Marseille (France)

Supporting information for this article is available on the WWW under https://doi.org/10.1002/cmdc.202000653

*This article belongs to the joint Special Collection with the European Journal of Inorganic Chemistry, "Metals in Medicine" and also to the Special Collection "BrazMedChem 2019: Medicinal Chemistry in Latin America".*

nent and prolonged antiparasitic duration.[2] A potential limitation for the two covalently linked antimalarial drug moieties is to reach localized targets. This, especially inside of digestive vacuole of the malarial parasite, can be a challenge.

A valuable approach is to connect two or more existing and well-known clinical antimalarial drugs with a transition metal to form a single chemical entity, named as metallic hybrids. It might be obvious to start designing this antimalarial metallic hybrid with the most successful antimalarial drug, chloroquine (CQ; Figure 1). Despite CQ-resistant (CQR) malaria parasites had spread worldwide, CQ is a potent hemozoin inhibitor,[8] and that reflects its remarkable accumulation inside digestive vacuole.[9] By inhibiting the formation of hemozoin[10] CQ kills the malarial parasites and acts in the intra-erythrocytic stage of the asexual *P. falciparum* life cycle.[11]

Another antimalarial drug for such metallic hybrid compound can be primaquine (PQ; Figure 1), This is one of few, commercially available gametocidal drugs, which acts in the sexual cycle of *P. falciparum* and blocks the transmission of the disease.[12] In addition, PQ has antiparasitic activity against the liver stage that is important for controlling the disease. As a limitation, PQ is extensive metabolized into approximately five major metabolites, where the concentration and composition vary according to different population, limiting PQ efficacy for transmission and controlling malaria.[13]

Gold(I)-based compounds, such as auranofin[14] and gold(I)-chloroquine complexes[15–17] have shown excellent antimalarial activity against *P. falciparum*, even against CQ-resistant strains. Recently, it was demonstrated that gold(I)-phosphine complexes were able to attenuate the viability of parasites,[18] reinforcing the potential of gold as a transition metal in antiparasitic therapy. Gold(I) compounds mainly act as inhibitors of the thioredoxin reductase (TrxR) system, which is present in parasites and also in cancer cells.[19,20] According to molecular modeling techniques gold(I) compounds can be capable to inhibit the *P. falciparum* thioredoxin reductase (PfTrxR),[21] which is an essential enzyme for the survival of this parasite.[22] Hence, a novel hybrid compound consisting of these two, well-known antimalarial drugs connected by gold atom has been developed in this work that fits with the 'master key' compounds and can favorably interact with multiple parasite targets.[23] Additionally, it was envisaged that this rational design would produce a multiple-stage antiparasitic agent which can be successful in the treatment, prevention and transmission of malaria.

Accordingly, the synthesis and characterization of this multitarget metal-antimalarial drugs hybrid, with possible dual efficacy in the sexual and asexual plasmodial stages. The mechanisms of action of our metallic hybrid molecule were evaluated through its interactions with three essential parasite targets: DNA (reversible and/or covalent interactions), heme (interaction with FPIX and inhibition of β-hematin formation), and PfTrxR using computational modelling studies. Importantly, antimalarial activity was estimated using both *in vitro* and *in vivo* models.

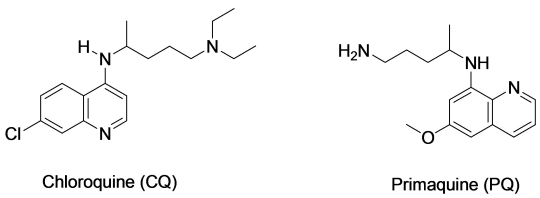


**Figure 1.** Structure of antimalarial drugs.

## Results and Discussion

### Synthesis and characterization of the hybrid gold(I) linker antimalarial drugs

The development of the hybrid of clinical antimalarial drugs linked by gold was inspired by the great antimalarial activity *in vitro* and *in vivo* of $[AuCQPPh_3]PF_6$ complex, which also acts at least in three distinct parasites targets (hemozoin, thioredoxin reductase and DNA) as we reported previously.[17,24,25] In view of that, we designed a gold(I) hybrid that contains not only chloroquine, but also primaquine, in order to investigate its potential to act as multitarget and be used against both sexual and asexual erythrocyte stages (dual phases) in the malarial parasite. This gold(I)-antimalarial drugs hybrid was obtained in a two-step reaction (Scheme 1). The first step consisted of the replacement of tetrahydrothiophene (THT) in the coordination sphere of Au(THT)Cl complex by primaquine that led to the AuPQCl intermediate. In the second step, this intermediate was dissolved in acetonitrile and mixed with an excess of $NH_4PF_6$ at room temperature to replace the chloride ligand, and the subsequent rapid coordination of chloroquine at low temperature which resulted in the hybrid $[AuCQPQ]PF_6$. It was isolated as brown solid. The stability of $[AuCQPQ]PF_6$, also known as CQPQ-gold(I) hybrid was evaluated in DMSO by $^1H$ and $^{31}P$ NMR

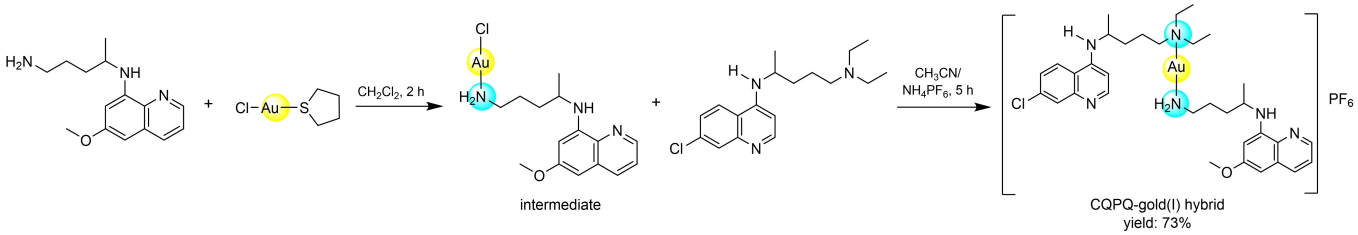


**Scheme 1.** Synthesis of $[AuCQPQ]PF_6$ hybrid.

studies after 31 days, in the interim, its stability in propylene glycol and in culture medium was followed by UV-visible, no changes were observed and this indicated that the hybrid [AuCQPQ]$PF_6$ molecule is stable in these solutions, which are also used in the biological tests (Figures S1–S4 in the Supporting information).

The CQPQ-gold(I) hybrid was characterized using several analytical and spectroscopic techniques. The IR spectrum showed the characteristic and relevant bands of the ligands CQ and PQ slightly displaced when compared to the same bands of the free ligands. The presence of others important bands at 557 and 844 $cm^{-1}$ correspond to $\nu$Au–N[26] and the counter ion $\nu PF_6$, respectively (Figure S5). Similarly, the UV/Vis absorption spectrum displayed the peaks associated with both ligands CQ and PQ slightly shifted (Figure S6). The results obtained from the elemental analyses and molar conductivity studies in DMSO confirmed the molecular formula proposed and that this compound is an electrolyte substance 1:1. The MALDI mass spectrum of metallic hybrid showed some important peaks attributed to the molecular fragment of $[Au\text{-}PQ]^+$ (456.14 *m/z*), and the corresponding peak of the free CQ at 320 m/z. Peak for the molecular ion was not observed (Figure S7).

One- and two-dimensional NMR spectra provided essential information for the full elucidation of the molecular structure of CQPQ-gold(I) hybrid, as described in our previous papers[25] and also reported by other investigation groups.[27,28] The variation in the $^1H$ and $^{31}C$ chemical shifts of each signal in the metal complex compared to those of the free ligands ($\Delta\delta$) can be used to deduce information about the coordination mode of the ligands to the metal. Both ligands, PQ and CQ, contain several, distinct donor nitrogen atoms that are able to coordinate to the gold ion. The coordination site is indicated by the largest variation in the $^1H$ and $^{31}C$ chemical shifts in the vicinity of these N atoms. The comparative analysis of the $^1H$ NMR spectra of the free ligands (CQ and PQ) and that of the gold(I)-antimalarial drugs hybrid (Figure S8) showed displacements of protons Hd′ ($\Delta\delta = 0.22$), H4′,5′ (0.43), H6′ (0.16) in the CQPQ-gold(I) hybrid, while the rest of the protons were not affected. These results suggest the coordination of PQ to gold through the primary amine $NH_2$, and that of CQ through the tertiary amine. The integration of each signal of $^1H$ NMR spectrum of CQPQ-gold(I) hybrid confirmed that its composition and that only one molecule of each antimalarial drug coordinated to gold(I) ion (Figure S9).

In the $^{13}C$ NMR spectrum of CQPQ-gold(I) hybrid (Figure S10) was observed all the carbon signals correspond to each carbon of the ligands (PQ and CQ), it was also noticed that C6′ ($\Delta\delta = 1.85$ ppm), Cb′ ($\Delta\delta = 1.28$ ppm), Cc′ ($\Delta\delta = 6.37$ ppm) and Cd′ ($\Delta\delta = 2.66$ ppm) were significantly shifted. This is consistent with $^1H$ NMR results, namely that the PQ and CQ coordination to gold occurred trough the nitrogen (N**3** for CQ and N**c** for PQ) atoms. CQ coordination to gold through N**3** was already described for $Au^{III}$–CQ complex.[15] In the $^{31}P$ NMR (Figure S11) a septuplet at −144 ppm was observed, confirming the presence of the counter ion $PF_6^-$.

$^1H$,$^{15}N$ gHMBC correlations (Figures S12–S14) were performed in order to provide additional structural data and to unequivocally establish the coordination of each ligand (PQ and CQ) to gold ion via the nitrogen atoms. Table 1 shows the chemical shifts of each signal for PQ, CQ and CQPQ-gold(I) hybrid which confirm that CQ binds to the gold ion by N**3** atom, corroborating the coordination mode described above. The values obtained are also in good agreement with the literature.[29]

The results discussed above suggest that the CQPQ-gold(I) hybrid, consisting of the gold linked the antimalarial drugs primaquine (gametocytocidal agent) and chloroquine (schizonticidal agent), which is a cationic metal complex with linear geometry and hybridization sp.

The density functional theory (DFT)-optimized structure of the CQPQ-gold(I) hybrid (Figure 2) shows two conformers. Structure **A** was found slightly more stable than **B** by only 3.1 kJ $mol^{-1}$, suggesting that both forms could coexist in a polar solvent. Of note, such ligand flexibility might be a favorable factor for a multitarget agent.

The $^1H$ and $^{13}C$ NMR chemical shifts were calculated for CQ and PQ ligands and for the CQPQ-gold(I) hybrid structure **A**. In the CQ ligand, low field shifts are predicted for H3′ ($\Delta\delta = 0.41$ ppm), H4′,5′ ($\Delta\delta = 0.39$ ppm) and H6′ ($\Delta\delta = 0.17$ ppm) and similarly, in the PQ ligand for Hc′ ($\Delta\delta = 0.19$ ppm) and Hd′ ($\Delta\delta = 0.09$ ppm). Concerning the $^{13}C$ NMR, low field shifts are predicted for C4′ ($\Delta\delta = 4.76$ ppm), C5′ ($\Delta\delta = 4.56$ ppm), C6′ ($\Delta\delta = 1.47$ ppm) in the CQ side, and in the PQ side for Cd′ ($\Delta\delta = 2.18$ ppm) and a high field shift for Cc′($\Delta\delta = -1.78$ ppm) and Cb′ ($\Delta\delta = -2.43$ ppm). These two latter results are distinct from experimental results, which suggest pronounced low field shifts for Cb′, Cc′ and Cd′ nuclei. The reason for such discrepancy between the experimental and calculated values has not been fully understood. One would not expect an error larger than 5% for $^{13}C$ calculated chemical shift, especially, when relative values are concerned. One possible reason for this is that the solvation model does not account for specific

**Table 1.** $^{15}N$ RMN chemical shifts ($\delta$) for the free ligands (PQ and CQ) and the [AuCQPQ]$PF_6$ hybrid in [$D_6$]DMSO.

| CQ $\delta$ (ppm) | PQ $\delta$ (ppm) | [AuCQPQ]$PF_6$ hybrid (ppm) | $\Delta\delta$ (ppm) |
|---|---|---|---|
| N**1** 268.02 | N**a** 295.26 | N**1** 265.16 | 2.86 |
| N**2** 94.08 | N**b** 81.82 | N**2** 93.94 | 0.14 |
| N**3** 43.68 | N**c** – | N**3** 52.35 | **8.67** |
| | | N**a** 295.27 | 0.01 |
| | | N**b** 80.53 | 1.29 |
| | | N**c** – | – |

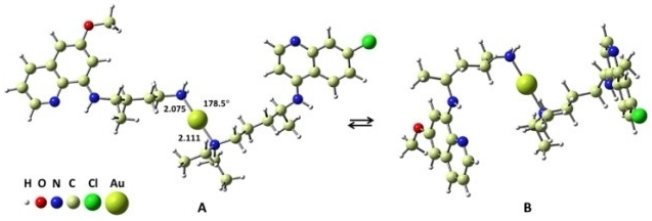


**Figure 2.** DFT-optimized structure of the CQPQ-gold(I) hybrid. Two distinct conformations are shown, with form **A** being 3.1 kJ $mol^{-1}$ more stable than **B**. The Au–N bond length is given in Å and the N–Au–N angle in degrees.

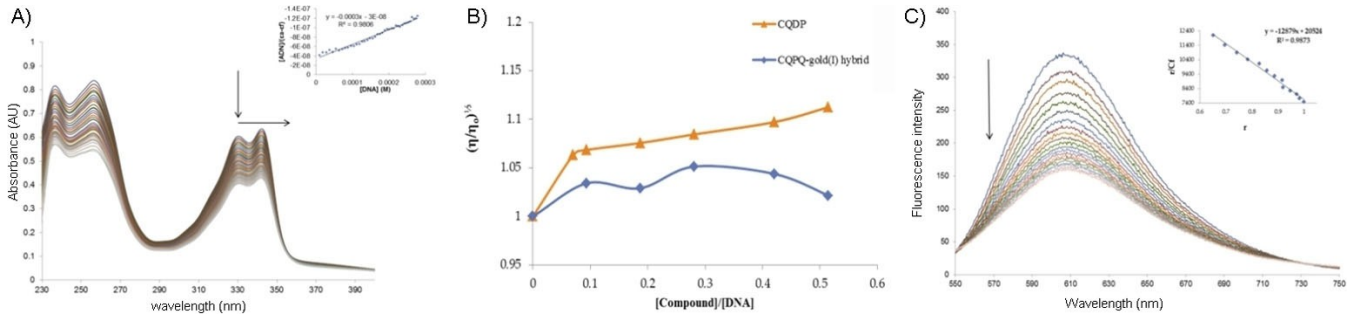


**Figure 3.** Interaction studies of [AuCQPQ]$PF_6$ with CT-DNA. A) Spectrophotometric titrations. B) Viscosity studies. C) Competitive DNA-binding studies.

solute-solvent interactions. Despite this disagreement with the experimental results, most of the relative chemical shifts from the theoretical NMR signals suggest complex structure **A** in alignment with the experimental interpretation of the proposed coordination mode as represented in Figure 2. The Figure S15 compares the calculated and experimental chemical shifts for all H and C atoms in the CQPQ-gold(I) hybrid structure. The average absolute errors were 7.4 ppm for $^{13}C$ and only 0.56 ppm for $^{1}H$, corresponding to an overall relative error of only 11%.

## Gold(I) linker antimalarial drugs hybrid as a multitarget drug

### *Interaction studies of [AuCQPQ]$PF_6$ with DNA*

Reversible interactions between [AuCQPQ]$PF_6$ with the DNA helix have been studied through the classical spectrophotometric titrations.[30–32] The results are displayed in Figure 3A, the hybrid [AuCQPQ]$PF_6$ exhibits two intense absorption bands in the range 200–270 nm and 310–370 nm which is attributed to n→π* and π→π* transition absorptions, respectively. The increased amount of DNA added to a solution of CQPQ-gold(I) hybrid until saturation caused hypochromism in both bands. The band maximums at 257 and 343 nm showed a significant decreased in the absorbance (32.8 and 34.4% respectively) and slight blue shift of 2 nm. These results are comparable to those observed with other compounds with known interactions with DNA, such as ethidium bromide (EB; Table 2) and with other metal complexes with antimalarial activity.[33] The binding constants ($K_b$) obtained for CQPQ-gold(I) hybrid, CQDP (chloroquine diphosphate) and EB are shown in Table 2. The $K_b$ value of our antimalarial gold(I) hybrid is similar than those listed or those previously reported for antitumor metal complexes.[34–36]

**Table 2.** Data obtained from different spectroscopic and analytical methods for DNA interaction with compounds.

| Property | EB | CQDP | [AuCQPQ]$PF_6$ |
|---|---|---|---|
| absorbance[a] (±1 nm) | 286 | 340 | 342 |
| hypochromism[a] (±0.2%) | 67.1% | 19.5% | 37.5% |
| $K_b$ x $10^4$ $(M^{-1})$[a] | 1.33±0.02 | 10.19±0.15 | 1.19±0.02 |
| $K_b$ x $10^5$ $(M^{-1})$[b] | – | 3.11±0.29 | 0.12±0.01 |

[a] Absorbance measurements. [b] Fluorescence measurements.

The constant is in the same range as that of the similar compound [Au(CQ)($PPh_3$)]$PF_6$ reported by us, that shows an antimalarial activity superior to the CQDP (chloroquine diphosphate) specifically in resistant strains,[24] the values of the constant are in the same range. Given all these results, some reversible interactions, such π–π stacking, and interaction dipole or hydrogen bridging appear to be taking place.

Additional information to explore the CQPQ-gold(I) hybrid-DNA interactions was collected from the viscosity measurements; these studies were performed using an Osward viscometer. The hydrodynamic behavior of DNA, specifically in the presence of small molecules (metallodrug) in different ratios [compound]/[DNA], can be examined through the changes in the viscosity of DNA, which is associated with the modes of binding. This can be distinguished effectively, as covalent and noncovalent binding modes display different hydrodynamic characteristics. Noncovalent interaction such as intercalators induce extension and unwinding of the DNA backbone, while for noncovalent major and minor groove binding compounds cause little or no distortion to the DNA.[37] The results for CQDP and CQPQ-gold(I) hybrid with DNA are shown in Figure 3B. Chloroquine increased the relative viscosities of DNA, acting predominantly as intercalate compound,[25,38] what was already expected, once free CQ intercalates into DNA.[38] CQPQ-gold(I) hybrid slightly increased the relative viscosity of the DNA at lower [compound]/[DNA] ratio, but at higher ratio only small variations of the relative viscosity of DNA were observed. The analyses of this data suggest that our metallic hybrid can interact with the DNA by reversible binding, and it can interact by intercalation or minor groove interaction with DNA. The mode of binding could be concentration dependent.[39]

In view of the results of the viscosity studies, the effect of interaction between the [AuCQPQ]$PF_6$ hybrid and DNA was also investigated using ethidium bromide as a fluorescence probe. EB emits intense fluorescence in the presence of DNA because of the strong interaction between the adjacent base pairs of DNA ($K_b = 1.4 \times 10^6$ $M^{-1}$).[40] The [AuCQPQ]$PF_6$ does not show any significant fluorescence at room temperature in the presence or absence of CT DNA, when excited at 471 nm. Furthermore, the addition of the CQPQ-gold(I) hybrid to a solution containing EB alone does not provoke quenching of free EB fluorescence and appearance of any new peak in the spectra. Therefore, any changes observed in the fluorescence emission spectra of a

solution containing the EB-DNA system at 471 nm when adding the metallic hybrid is because of the ability of the compound to interfere with the EB-DNA system. The addition of $[AuCQPQ]PF_6$ at different Cb/[DNA] ratio to the EB-DNA system, decreases the intensity of the emission band at 607 nm (Figure 3C). This demonstrates the moderate interaction of the compound with the EB-DNA system, possibly due to the displacement of EB resulting in fluorescence quenching.

According to the Scatchard equation,[41] a plot of $r/C_f$ versus $r$ gave $K_b$ values of $(0.12 \pm 0.05) \times 10^5$ and $(3.11 \pm 0.09) \times 10^5\ M^{-1}$ from the fluorescence data for the CQPQ-gold(I) hybrid and CQDP respectively, showing a possible displacement of EB similar to other metal complexes with reported biological activity.[42–44] This displacement can indicate intercalation or minor groove interaction.[45–48] The results also show that the DNA-binding affinity of CQPQ-gold(I) hybrid is mild, which agrees with the results obtained from electronic absorption spectra and viscosity measurements.

We also evaluated this interaction with the DNA by gel-electrophoresis, where the presence of interaction is determined through the variation of the electrophoretic mobility of the DNA. The pBR322 plasmid, is a supercoiled (SC) DNA, but it can be converted into open circular (OC) or linear (L) when in contact with some harmful agents. SC is the form that migrates faster, L is intermediate and OC is the one with greater difficulty to migrate in the agarose gel.[37] The effect of the interaction of CQPQ-gold(I) hybrid with the DNA plasmid on the variations of the electrophoretic mobility of the DNA plasmid was examined. The results obtained from this experiment (Figure S16) revealed no significant changes in the electrophoretic mobility between that of the free plasmid pBR322 and that with incubated with CQPQ-gold(I) hybrid for 17 h. The hybrid ($[AuCQPQ]PF_6$) does not cleave the DNA supercoil and does not alter the tertiary structure of the DNA under these conditions, suggesting that the CQPQ-gold(I) hybrid interacts with the DNA in a non-covalent manner, in the same way shown for metal-chloroquine complexes.[24,38]

The *in silico* analysis showed that the CQPQ-gold(I) hybrid binds to the minor groove of the DNA (Figure S17). The ligands do not intercalate between the base pairs, but instead the CQ moiety is hydrogen bonded to a phosphate group with distance of 1.82 Å, and the PQ ligand is twisted out from the minor groove. The binding energy ($\Delta E_b$) calculated over 500 frames from MD trajectory was $-94.4 \pm 0.3$ kcal mol$^{-1}$, ~85% due to electrostatic interaction and ~15% from van der Waals contributions. It is noted in Figure S17D that the DNA structure maintains its structure close to the solid state with an average root mean square deviation (RMSD) of only 1.98 Å. This is a consequence of the weak ligand-DNA interaction, in agreement with the experimental findings.

Collectively, our results suggest that our CQPQ-gold(I) hybrid binds the DNA primarily through noncovalent interactions through moderate electrostatic contacts at the minor groove region and π–π stacking interactions between them could also happen. Once the interaction of our metallic hybrid was evaluated with the DNA, one of the important parasite targets, we went further to validate our rational design of $[AuCQPQ]PF_6$ being a multitarget drug. The second identified essential target (inhibition of β-hematin formation) for malarial parasite was evaluated and the results are shown in the following section.

### *Heme as an important target for $[AuCQPQ]PF_6$*

Malaria parasites digest hemoglobin for their growth and to replicate, however in this process heme is accumulated which is toxic to the parasite. To avoid death, the parasite converts heme into the insoluble and inert hemozoin crystals in its digestive vacuole. This vital process for the parasite survival stands out as a selective target to be attacked by the antimalarial drug, in fact, this is the most accepted mechanism of action of chloroquine.[10]

CQ have been shown to form adducts with $Fe^{III}PPIX$[16] and consequently inhibiting the hemozoin formation. Converting $Fe^{III}PPIX$ is a target for anti-malarial drugs. Therefore, the interaction of CQPQ-gold(I) hybrid with ferriprotoporphyrin was first evaluated by UV/Vis spectroscopic titration to determine the association constant ($\log K$) of the compound with $Fe^{III}PPIX$, and also to monitor the presence of perturbations in the Soret's band of porphyrin (402 nm) with increasing concentration of the CQPQ-gold(I) hybrid. The observed $\log K$ for the CQPQ-gold (I) hybrid (Table 3) was similar to CQ. The increasing concentration of the metallic hybrid also caused a hypochromism of 65% (Figure 4). This result indicates that the CQPQ-gold(I) hybrid interacts with ferriprotoporphyrin similarly to CQ and metal-CQ complexes under same experimental condictions.[16] As the CQPQ-gold(I) hybrid interacts with ferriprotoporphyrin, it might have the ability to inhibit the β-hematin formation, therefore we evaluated the capacity of the hybrid to inhibit β-hematin formation.

Synthetic β-hematin is identical to hemozoin (malaria pigment).[49] The inhibition of β-hematin formation by a simple and cheap technique such as the Infrared spectroscopy, has

**Table 3.** Interaction with hemin, inhibition of β-hematin formation and lipophilicity studies.

| | Interaction with hemin | Inhibition of β-hematin formation | | | Lipophilicity studies | |
|---|---|---|---|---|---|---|
| Compound | $\log K$ [a] | IR | $HAI_{50}$ (mM) in buffer[c] | $HAI_{50}$ (mM) at interface[d] | $\log D$ (pH 5.1) | $\log D$ (pH 6.9) |
| $0.14 \pm 0.06$ (1,3) | $0.71 \pm 0.08$ (4) | + | | | −2.0 | 0.98 |
| CQ | $4.99 \pm 0.01$ | + | $0.11 \pm 0.03$ (1) | $2.82 \pm 0.09$ (1) | −1.53 | 0.38 |
| PQ | n.d.[b] | − | | | −0.41 | 2.0 |

$HAI_{50}$ is the drug-to-hemin ratio required to inhibit 50% of heme aggregation against a control experiment in the absence of drugs. [a] pH ~ 5. [b] Not detectable. [c] After 24 h of reaction. [d] After 2 h of reaction. Values in parentheses are the relative activity with respect to CQDP.

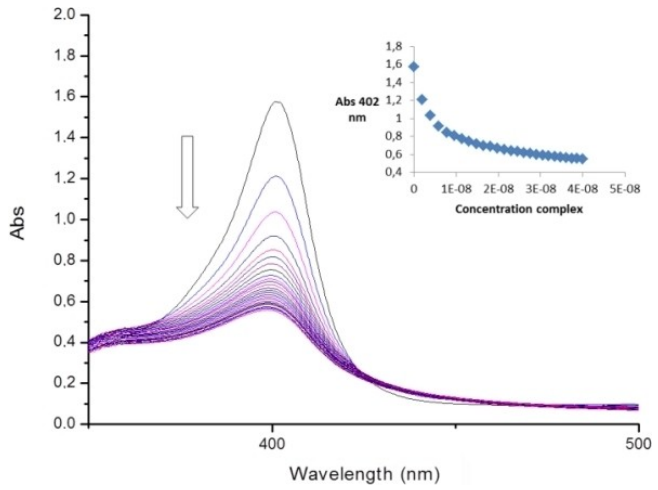


**Figure 4.** Spectroscopic titration of ferriprotoporphyrin with the CQPQ-gold (I) hybrid. Conditions: 40% DMSO, pH 7.5 and [CQPQ-gold(I) hybrid] = 0.02 mM.

been well documented by Egan et al.,[50] thus, this method was utilized in the present work for evaluating if our [AuCQPQ]$PF_6$ is able to inhibit β-hematin formation.

β-Hematin is a dimer of $Fe^{III}$PPIX, where the ionized heme-propionate side chain of one $Fe^{III}$PPIX coordinates to the Fe of the other, characterized by two bands in the infrared spectrum: 1663 $cm^{-1}$ from C═O and 1210 $cm^{-1}$ from C–O stretch of carboxylate group coordinated to the $Fe^{III}$ center.[51] Knowing that CQ inhibits the hemozoin formation, we first investigated the qualitative inhibition of β-hematin formation by our metallic hybrid in solid state, using FTIR spectroscopy to characterize the reaction products. The resulting IR spectrum (Figure 5) shows no IR bands corresponding to C═O and C–O stretch, while these bands are present for primaquine (negative control) and absent for CQ (control positive) indicating that our metallic hybrid inhibits β-hematin formation in a similar manner to CQ.[50]

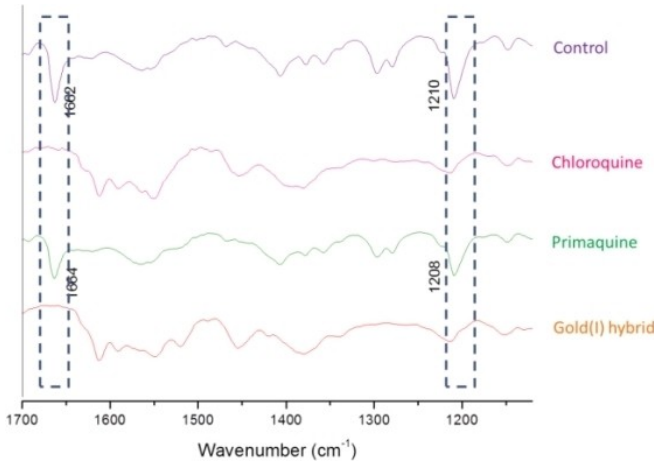


**Figure 5.** FTIR spectroscopic characterization of the inhibition of β-hematin formation by chloroquine, primaquine, CQPQ-gold(I) hybrid and the control.

In order to obtain quantitative data for the heme aggregation inhibition activity (HAIA) of [AuCQPQ]$PF_6$, a set of experiments were performed in acetate buffer and also at the interface of *n*-octanol/aqueous buffer; the results were then compared to those for CQDP as control. The $IC_{50}$ value measured for CQPQ-gold(I) hybrid in acetate buffer at pH 5 indicates that the metallic hybrid is able to inhibit the heme aggregation process and displays an activity very similar to that of CQDP in these conditions.

Subsequently in another experiment with more realistic conditions using the interfaces of *n*-octanol/water where the β-hematin assembles rapidly and spontaneously, following an adaptation of the procedure described by Egan et al.[52] and also reported by Sánchez-Delgado et al..[53] At this interface, the [AuCQPQ]$PF_6$ is significantly more potent than CQDP for inhibiting heme aggregation near the interface, more interesting, this result is similar to [Au(CQ)($PPh_3$)]$PF_6$, reported by us.[24] These results suggest that the CQPQ-gold(I) hybrid shows antiplasmodial activity similar to CQDP in sensitive strains, while in resistant strains enhanced activity, to avoid resistance, as was observed for other metal-CQ complexes with antimalarial activity, for example [$RuCl_2$(CQ)]$_2$,[32] [Au(CQ)($PPh_3$)]$PF_6$[24] or Au(CQ)(Cl).[16]

### *In silico study of interaction of CQPQ-gold(I) hybrid with* P. falciparum *thioredoxin reductase (PfTrxR) enzyme*

Molecular modeling techniques were applied to gain some molecular insights on the [AuCQPQ]$PF_6$–PfTrxR binding mode. The first approach was to perform a docking study in order to select representative poses for ligand-enzyme complex (see Figure S18 and the related discussion). Docking results are semi-quantitative only and more accurate potential need to be used to expand and quantify the analysis. This was done by MD simulation, in which the ligand-enzyme structures obtained from the docking study were used as starting point for MD simulation.

There are two equivalent binding sites in the enzyme, but just one ligand was considered as docked at the site formed by the C-terminal of monomer **2** and N-terminal of monomer **1**. Overall, the structure of the enzyme does not change significantly due to the ligand binding, as shown by the RMSD values along the MD trajectory in Figure S19A. When the root mean square fluctuation (RMSF) data are compared in Figure S19B we noted that the enzyme structure becomes more rigid (lower values of RMSF) in the ligand-enzyme complex in Pose 1 and 2 and more flexible in Pose 3 (higher values of RMSF). For the last Cys in the C-terminal motif (Cys540 in the original PDB numbering or Cys1007 in the current numbering scheme), the RMSF drops from 6.36 Å (free protein) to ~3 Å (Poses 1 and 2) and to 4.9 Å (Pose 3). An important parameter in these poses is the S(Cys540)–Au distance, which must be short enough to allow the approach of Cys540 by the metal center. The distance varies along the MD trajectory and the average values are (in Å): 11 ± 1 (Pose 1), 7.5 ± 0.7 (Pose 2) and 6.0 ± 0.9 Å (Pose 3). These results suggest that the CQPQ-gold(I) hybrid and S(Cys)

in Poses 2 and 3 are close enough to bind, and this state could be viewed as a pre-reactive arrangement, representing the Michaelis-Menten type complex.[54]

The [AuCQPQ]$PF_6$–PfTrxR binding modes are visualized in the snapshots of Figure 6 (Pose 2 – the most stable) and Figure S20 (Poses 1 and 3).

Only one frame is represented in Figure 6 and S20, which does not totally reflect the ligand-enzyme average contact throughout the entire MD trajectory, however, some important residues, which are in close contacts with the ligand, are highlighted and labeled. In Figure S21 A–C the total number of contacts calculated along the MD trajectory is plotted for every residue in the protein. Pose 1 (Figure S20 A, C) is found deep inside the binding site (close to the N-terminal motif). Pose 2 (Figure 6) and Pose 3 (Figure S20 B, D) are similar to each other, with contacts preserved in the α-helix including Phe106 and Ser103. Pose 2 (Figure 6) also showed some significant interactions between the ligand and Asp897 (weak H-bond = 2.47 Å) and Lys999 (weak H-bond = 2.35 Å) residues. Unlike in Pose 1, in Poses 2 and 3, the C-terminal cysteines are close to the ligand and these contacts are frequent in the MD trajectory (Figure S21 B, C).

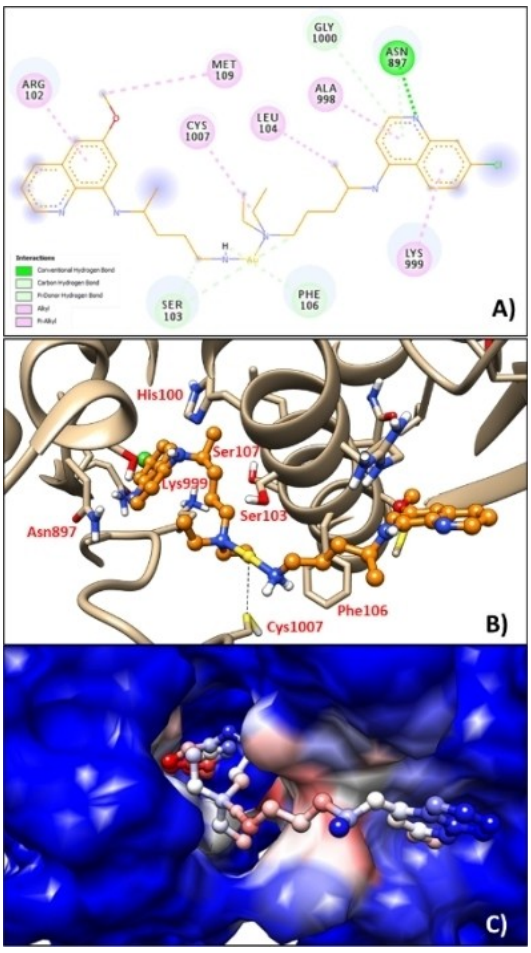


**Figure 6.** Binding mode of the CQPQ-gold(I) hybrid and PfTrxR enzyme obtained from MD simulation in aqueous solution (Pose 2). A) 2D diagram representing the main residues in contact with the ligand. B) 3D structure of the drug-receptor complex. C) Enzyme van der Waals surface with colors representing the frequency of drug-receptor contacts (scale: red: 60, white: 30, and blue: 0).

The binding energy was calculated from MD trajectory using the MMGBSA approach where 250 frames evenly spaced in time. The values are given in Table S1 which includes the overall binding energy and the individual contributions. Using a more accurate approach, Pose 2 was predicted as the most stable among those tested, followed by Pose 3. The Pose 1 was the least stable according to the MMGBSA. The values in Table S1 show that the VDW energy contribution is dominant and drives all binding processes, being more pronounced for the most extended ligand forms, which have a large contact surface with the enzyme. Summing up, the MD predicted the Pose 2 (Figure 6) as the most favorable binding mode, being the ligand-enzyme interaction driven mainly by the van der Waals contribution. Moreover, in Pose 2 the Cys540 at the C-terminal was at 7.5 Å on average apart from the Au center suggesting a pre-reactive arrangement necessary for enzyme inhibition. Our molecular modeling predicted that CQPQ-gold(I) hybrid complex can bind to the PfTrxR enzyme at the C-terminal motif where the ligand assumes an extended conformation with the Au center close to the Cys540. This arrangement is represented by Pose 2 (Figure 6) and might be viewed as the Michaelis-Menten complex prior the ligand exchange reaction. A detailed view of Pose 2 binding mode is represented in Figure 6C where we see the CQ moiety inside the binding site (in red) and the PQ ligand outside the interface tunnel (in blue). This suggests a primary role of CQ ligand to bind effectively to PfTrxR, which is an important finding to design new and potent hybrid complexes as inhibitors of PfTrxR.

### *Lipophilicity studies*

Table 3 shows the distribution coefficients (log *D*) for the CQPQ-gold(I) hybrid at pH 5 and 6.9, calculated by log *D* = log [compound in *n*-octanol]/[compound in water]. Log *D* < 0 suggest that the compound is more hydrophilic, log *D* > 0 more lipophilic and log *D* = 0 that it has the same affinity for both phases.[55] Based on the log *D* values obtained for [AuCQPQ]$PF_6$, it is noticeable that this compound presents similar behavior to CQ, that is, it is more hydrophilic at pH 5.1 and more lipophilic at pH 6.9. This fact indicates that at the pH of the malarial parasite vacuole (pH 5.1) the metallic hybrid accumulates in aqueous phase so it can act as a good antimalarial agent.

### *Biological studies of CQPQ-gold(I) hybrid molecule*

The growth inhibitory $IC_{50}$ values on the asexual blood stage of *P. falciparum* were determined against CQ-susceptible 3D7 and CQ-resistant W2 strains (Table 4). CQPQ-gold(I) hybrid presented activity in low nanomolar range against the susceptible *P. falciparum* strain 3D7, being almost as potent as CQ, and 1000-folds more potent than PQ. Against the resistant *P. falciparum* strain W2, CQPQ-gold(I) hybrid was at very least twice as potent

**Table 4.** Cytostatic activity against the intraerythrocytic *P. falciparum* stage, mammalian cell cytotoxicity and selectivity indexes of compounds.

| Compounds | *P. falciparum*, $IC_{50}$ ± S.D. [μM][a] | | Cells, $CC_{50}$ ± S.E.M. [μM][b] | | Selectivity index[c] | |
|---|---|---|---|---|---|---|
| | CQ-sensitive 3D7 | CQ-resistant W2 | J774 | HepG2 | 3D7 | W2 |
| PQ | 1.1173 ± 0.05 | 0.1823 ± 0.0189 | 24.6 ± 1.05 | 25.4 ± 2.65 | 22 | 135 |
| CQ | 0.018 ± 0.00167 | 0.460 ± 0.0174 | 51.5 ± 1.86 | ~80 | 2861 | 112 |
| CQPQ-gold(I) hybrid | 0.0277 ± 0.0039 | 0.166 ± 0.0257 | 20.9 ± 1.05 | 21.4 ± 7.5 | 753 | 126 |
| $AuCl(PPh_3)$ | > 2.0 | – | 19.74 | 4.53 | – | – |

[a] Determined 72 h after incubation with compounds. Values were calculated as mean of five independent experiments. [b] Determined 72 h after incubation with compounds. Values were calculated as mean of at least two independent experiments. $IC_{50}$ = inhibitory concentration at 50%. $CC_{50}$ = cytotoxic concentration at 50%. S.D. = standard deviation. S.E.M. = standard error of the mean. [c] Determined as $CC_{50}$ (J774 cells) /$IC_{50}$.

as CQ and as potent as PQ. Regarding cell toxicity, CQPQ-gold(I) hybrid presented a profile similar to PQ, being toxic in concentration equal or above 20 μM. As a result, the selectivity index of the metallic hybrid was similar to that of PQ and twice lower than CQ. Based on this, it can be stated that CQPQ-gold(I) hybrid has conserved the potency of CQ against the susceptible strain, and equally important, also retained the beneficial profile of PQ against the resistant strain of *P. falciparum*. Moreover, the evaluation of the interaction between these compounds and the red blood cells at 20 μM concentration, equivalent to 1000-fold of the $IC_{50}$ of CQPQ-gold(I) hybrid, the hemolysis was at 10% indicating no interaction with red blood cells at the proposed treatment concentration and presenting an acceptable safety profile (Figure S22).

After having ascertained the activity of the metallic hybrid at the blood stage, the growth inhibitory $IC_{50}$ values on the liver stage using *P. berghei* sporozoites-infected Huh-7 cells were determined (Table 5; Figure 7). In this parasite stage CQ has a very weak potency, while PQ has moderate. In contrast, CQPQ-gold(I) hybrid has been shown to be very potent, approximately 10-fold more than PQ. The enhanced potency of the CQPQ-gold hybrid at the liver stage in comparison to PQ led us to analyze the course of infection and the profile of parasite morphology following treatment (Figure 8). To this end, Huh-7 cells were infected with *P. berghei* sporozoites and treated with PQ or with CQPQ-gold(I) hybrid. After 24 h of treatment, parasites were imaged by transmission electron microscopy (TEM) and parasite burden as well as morphology were analyzed. In comparison to the untreated parasite control, the treatment with PQ and with the CQPQ-gold(I) hybrid at the same concentration reduced the parasite burden. This reduction induced by our metallic hybrid was approximately twice greater than by PQ. The course of infection imaged by TEM revealed that in comparison to uninfected Huh-7 cells, which typically exhibited large and intact nuclei, untreated infected cells presented fragmented nuclei and a number of schizonts surrounding cell membrane as well as being released. A close inspection of the morphology revealed that PQ treatment was able to delay the course of infection, where most the Huh-7 cells presented parasites arrested in the transition from sporozoites into schizonts. The treatment with the metallic hybrid resulted in the most efficient delay in the course of infection, where most of the Huh-7 cells presented parasites arrested in the sporozoite stage. It can be concluded that the hybrid acts on liver stage in a manner

**Table 5.** Antiparasitic activity of compounds in inhibiting of *P. berghei*-sporozoite development in Huh-7 cells.

| Compounds | Sporozoites-infected cells, $IC_{50}$ ± S.D. [μM][a] | Cells, $CC_{50}$ ± S.E.M. [μM][b] | |
|---|---|---|---|
| | | J774 | HepG2 |
| PQ | ~10 | 24.6 ± 1.05 | 25.4 ± 2.65 |
| CQ | ~15 | 51.5 ± 1.86 | ~80 |
| CQPQ-gold(I) hybrid | 0.63 ± 0.07 | 20.9 ± 1.05 | 21.4 ± 7.5 |

[a], [b] See footnotes in Table 4.

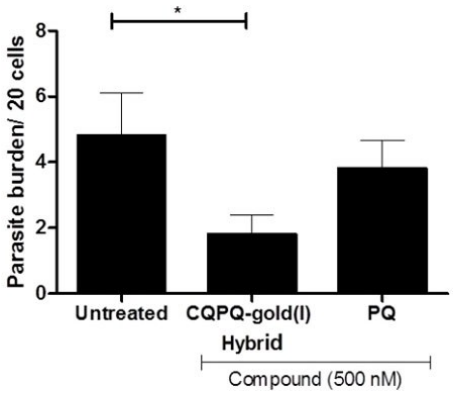


**Figure 7.** Quantification of parasite burden in the *P. berghei* sporozoite-infected Huh-7 cells. * $p < 0.01$ (one-way ANOVA).

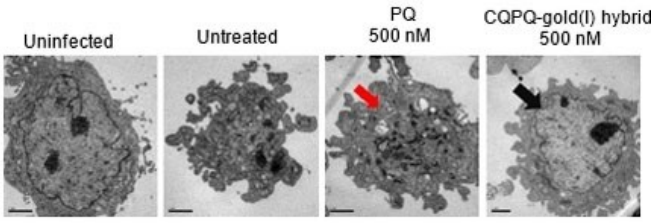


**Figure 8.** Transmission electron microscopy micrographs of Huh-7 cells, uninfected or infected with *P. berghei* sporozoites with no treatment or treated with primaquine or the CQPQ-gold(I) hybrid. Uninfected Huh-7 cells typically exhibited large and intact nuclei. Untreated infected cells presented fragmented nuclei and a number of schizonts surrounding the cell membrane, as well as being released. Huh-7 cells after treatment with CQPQ-gold(I) hybrid at 500 nM concentration 24 h post-infection have intact nuclei and healthy morphology (black arrow). Cells treated with primaquine under the same conditions presented diffuse parasites without a delimited membrane (red arrow). Scale bars: 2 μm.

similar to PQ, and it blocks the transition of sporozoites into schizonts, but with a superior potency. Considering that PQ is extensively metabolized that explains its modest activity on liver stage,[13,56] the enhanced potency of the CQPQ-gold(I) hybrid is likely due to the presence of the gold atom attached to PQ, which either affects the undesirable metabolism or enhance the PQ uptake.

After demonstrating the potency of the CQPQ-gold(I) hybrid against the parasite on both the blood and liver stages, we tested its efficacy against malaria in mice experiments. In the Peters suppressive test of parasitemia the metallic hybrid presented strong efficacy in reducing parasitemia and increasing mice survival when applied at the highest dose (33 μmol/kg). The same dose of CQ cured only 20% of the mice, while the metallic hybrid cured 100%. The efficacy of the CQPQ-gold(I) hybrid in curing mice was greater than PQ at a twofold dose, meaning that it is higher than CQ or PQ alone to confirm this finding, an experimental group also received an equimolar mixture of PQ and CQ (denoted here as CQPQ). The results show that our metallic hybrid at 33 μmol/kg dose was even more effective in curing mice than CQPQ at dose of 66 μmol/kg confirming that CQPQ-gold(I) hybrid has superior efficacy in suppressing the onset of infection (Table 6).

Next, we assessed if CQPQ-gold(I) hybrid can demonstrate efficacy in an established experimental infection setting (Thompson test), where treatment is given for mice displaying a patent parasitemia of 3–5% (Figure 9 A). In this experiment, the treatment with hybrid at 49 μmol/kg dose significantly reduced parasitemia and increased mice survival in comparison to untreated infected group (vehicle). In contrast, a similar efficacy was only observed with CQPQ at 66 μmol/kg dose, again denoting the higher efficacy of the metallic hybrid than CQPQ (Figure 9B and C; Table 7). The treatment with CQPQ-gold(I) hybrid ($[AuCQPQ]PF_6$) proved to be efficacious in reducing parasitemia and increasing survival of mice. However, it did not cure mice for good, suggesting that a successful therapy of an already established infection should also contain a fast-killing antimalarial component.[57] It is well-known that neither CQ nor PQ is a fast-killing antimalarial agent.[58] The observation from the Thompson test results indicates that the enhanced potency and efficacy of the CQPQ-gold(I) hybrid are not due to a rapid rate-of-kill property enhancement.

**Table 6.** Efficacy evaluation of CQPQ-gold(I) hybrid in suppressing parasitemia in *P. berghei*-infected mice.

| Compound | Dose μmol/kg [mg/kg] | Inhibition parasitemia [%][a] | Median survival [days] | Number of mice alive after 40 dpi [%][b] |
|---|---|---|---|---|
| saline (vehicle) | – | – | 20.3 | 0/15 (0) |
| CQ | 33 (11) | >99 | 27 | 1/5 (20) |
| PQ | 77 (20) | >99 | >41 | 3/5 (60) |
| CQPQ | 66[c] | >99 | >41 | 4/5 (80) |
| $[AuCQPQ]PF_6$ | 33 (30) | >99 | >41 | 5/5 (100) |
| | 11 (10) | 71.8±4.9 | 40 | 5/10 (50) |
| | 3.6 (3.3) | 5±3.9 | n.d. | 0/5 (0) |

[a] Values compared to vehicle group, errors are standard deviation. [b] DPI = days post-infection. [c] Ratio of 1:1 of CQ and PQ, using 33 μmol/kg each.

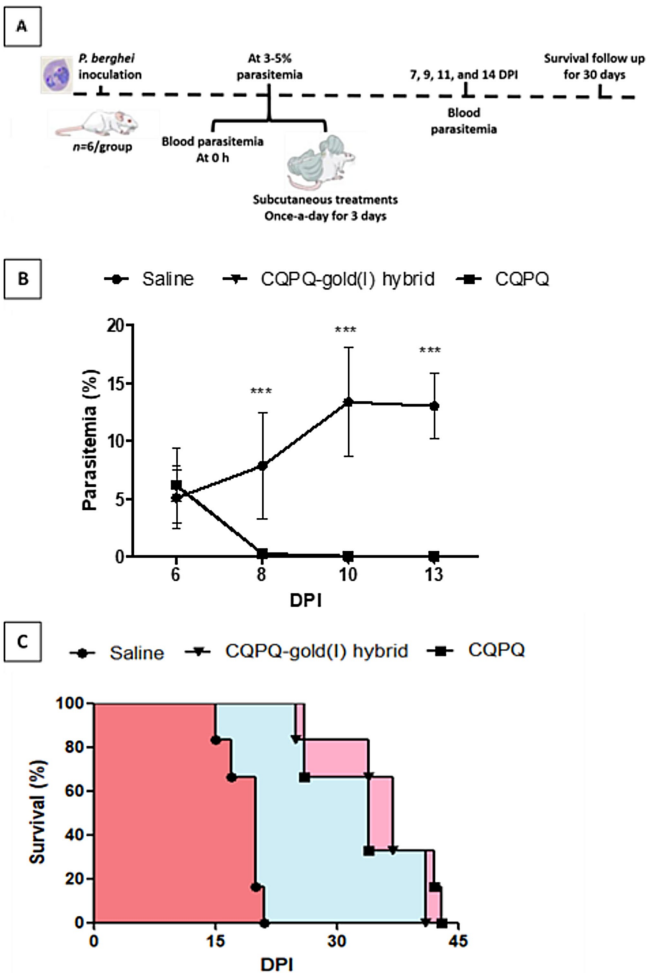


**Figure 9.** Evaluation of the efficacy of different compounds on *P. berghei*-infected mice in an established infection experimental setting (Thompson test). A) Experimental design of curative Thompson test, B) curve of parasitemia, and C) animal survival of *P. berghei*-infected mice. Parasitemia and animal survival were measured by using an $n = 6$/group. Error bars indicate S.D. *** $p < 0.01$ (two-way ANOVA) versus vehicle group. DPI = days post-infection.

**Table 7.** Survival evaluation of mice treated with compounds in an stablished infection experimental (Thompson test).

| Compound | Dose [μmol/kg] | Median survival [days] | Number of mice alive after 40 dpi [%][a] |
|---|---|---|---|
| saline (vehicle) | – | 20 | 0/6 (0) |
| CQPQ[b] | 66 | 34 | 0/6 (0) |
| CQPQ-gold(I) hybrid | 49 | 37 | 0/6 (0) |

[a] DPI = days post-infection. [b] Ratio of 1:1 of CQ and PQ, using 33 μmol/kg each.

Earlier the CQPQ-gold(I) hybrid demonstrated potent inhibition of the β-hematin formation in aqueous phase, similar to CQ, meanwhile, it was substantially more potent than CQ at the aqueous/*n*-octanol interface. This pointed out that the hybrid conserved the inhibition potency of CQ and that it displayed a fine-tuned distribution along digestive vacuole. Because of its

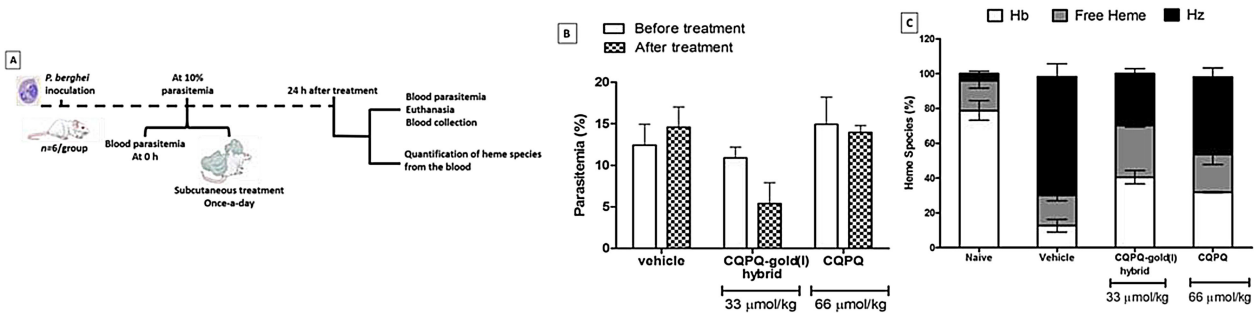


**Figure 10.** A) Experimental design, B) parasitemia, C) heme species, and summary of results (Table 8) from *P. berghei*-infected mice within 24 h of oral treatment. In (B), parasitemia was determined by GFP signal using flow cytometry. In (C), heme species were quantified from the peripheral blood after mouse euthanasia. Results show the pool of two independent experiments for $n = 3$/group for each experiment. Error bars are mean and 95% CI. $^{*}p < 0.05$ (one-way ANOVA and Newman-Keuls Multiple comparison test) between before versus after drug treatment. Hb, Hemoglobin; Hz, Hemozoin. CI = confidence interval.

inhibitory effect on hemozoin biosynthesis, the CQPQ-gold(I) hybrid demonstrated superior antimalarial potency and efficacy on the blood stage, which is a hallmark of the CQ treatment. This was investigated in *P. berghei*-infected mice by simultaneous monitoring of parasitemia and three heme species: hemoglobin, free heme and hemozoin (Figure 10 A). These experiments revealed that 24 h after administration of a single subcutaneous dose of 33 μmol/kg, CQPQ-gold(I) hybrid reduced parasitemia by 55.0 ± 8.7% and it was effective in impairing hemozoin formation by 44.2 ± 4.8% compared to untreated mice (Table 8). The treatment with 66 μmol/kg, 2-fold the dose of hybrid, showed that CQPQ did not reduce parasitemia, but it did significantly reduce hemozoin by 50.2 ± 10.0% (Table 8; Figure 10B and C). Concomitant to the decrease in the hemozoin levels, both CQPQ and CQPQ-gold(I) hybrid increased the levels of free heme, clearly showing that the treatment is efficient in interrupting the biosynthesis of hemozoin.

**Table 8.** Summary of results from *P. berghei*-infected mice after 24 h of subcutaneous treatment.

| Treatment [dose, μmol/kg] | Inhibition [%][a] Parasitemia | Hemozoin | Free heme increase [%][a] |
|---|---|---|---|
| CQPQ-gold(I) hybrid (33) | 55.0 ± 8.7 | 44.2 ± 4.8 | 38.4 ± 4.3 |
| CQPQ (66) | 0 | 50.2 ± 10.0 | 44.4 ± 7.9 |

[a] Compared to vehicle.

Once we ascertained that the superior potency and efficacy of CQPQ-gold(I) hybrid is in part due to its remarkable ability in simultaneously reducing parasitemia and modulating hemozoin formation, we investigated the effect of the primaquine component of CQPQ-gold(I) hybrid on the antiparasitic activity at the blood-stage. To this end, we determined the antiparasitic activity *in vitro* in cultured *P. berghei* and estimated the binding of compounds to reduced glutathione (GSH). We also investigated the ability of CQPQ-gold(I) hybrid and CQPQ combination to block or delay the maturation of *P. berghei* from rings to schizonts with *in vivo* Peters and Thompson tests. The CQPQ-gold(I) hybrid has reduced parasitemia by 50% at high and moderate concentrations in comparison to the untreated, unlike CQPQ which show potential on the rings only at fourfold concentration (1000 nM) (Figure 11 A and B). Moreover, in *in vitro* tests with *P. berghei* only CQPQ-gold(I) hybrid demonstrated activity at the common concentrations among the compounds (Figure 11 C). These findings suggest that the coordination of CQ and PQ to a gold ion and the creation of one single molecule is key to the enhanced antiparasitic activity that has been consistently demonstrated in both *in vitro* and *in vivo* models. It is likely due to the optimized pharmacodynamics rather than optimized pharmacokinetics. Furthermore,

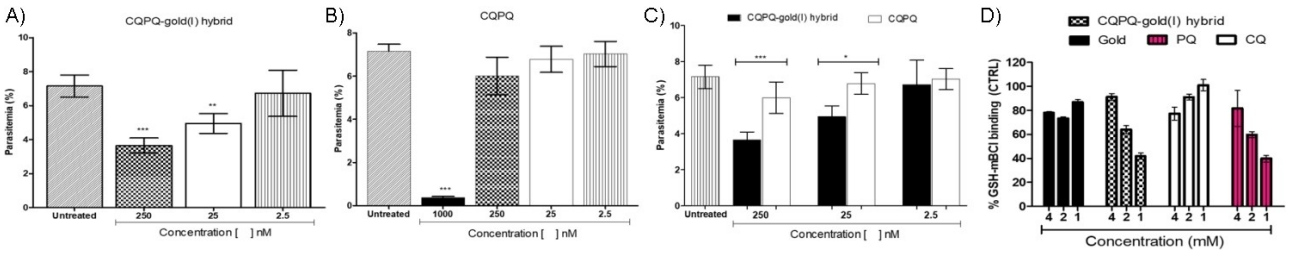


**Figure 11.** *In vitro* evaluation of the ability of CQPQ-gold(I) hybrid and CQPQ combination to block or delay of the maturation of *P. berghei* from rings to schizonts and the binding of compounds to reduced glutathione. A) The hybrid and B) CQPQ were tested at different concentrations on rings of *P. berghei*. C) The hybrid and CQPQ were tested at different concentrations, and the parasitemia was quantified; error bars indicate S.D. $^{***}p < 0.0002$ and $^{**}p < 0.001$ (one-way ANOVA) for hybrid or CQPQ versus untreated group and hybrid versus CQPQ. D) CQ, PQ or hybrid binding was measured by interaction with GSH in a cell-free assay.

we also observed that, unlike CQ, the CQPQ-gold(I) hybrid and PQ are able to interact with GSH in a cell-free assay (Figure 11 D), suggesting that the primaquine component of the metallic hybrid plays an important role in the blood-stage antiparasitic activity mediated by GSH depletion.

## Conclusion

The novel CQPQ-gold(I) hybrid molecule synthesized in this work is a multitarget drug that interacts with DNA, inhibits the β-hematin formation, and also displays potent antiparasitic activity and selectivity against two different stages of malaria, the liver and the blood (asexual) stages. Regarding the liver stage of *P. berghei* infection, the CQPQ-gold(I) hybrid presented significantly better potency compared to PQ, while CQ was not active at all. In the blood stage of infection, the CQPQ-gold(I) hybrid was as potent against a sensitive *P. falciparum* strain as CQ, and against a CQ-resistant strain it was as potent as PQ. In the experimental malaria infection model, this metallic hybrid exhibited superior efficacy to CQ and PQ and even to a combination of both. This synergistic effect is in part explained by the fact that the $[AuCQPQ]PF_6$ hybrid successfully combines the CQ ability to impair the hemozoin formation with the ability to reduce parasitemia in a dose range where both quinolines drugs are ineffective. In-silico assays suggested that $[AuCQPQ]^+$ interacts moderately with the DNA minor groove. In addition, the binding mode of $[AuCQPQ]^+$ with PfTrxR was also predicted and showed the CQ portion within the interface cavity towards the N-terminal region of the enzyme. Overall, the binding to the enzyme was 1.2 times stronger than DNA binding, suggesting the PfTrxR enzyme is a potential target for our CQPQ-gold(I) hybrid, and that the CQ ligand essential for binding both targets. Collectively, our data suggest that gold(I) linked to two quinoline drugs (CQ and PQ) explains the observed improved potency and efficacy, a feature which cannot be observed when only CQ and PQ are given together. The findings are in support of the idea that CQPQ-gold(I) hybrid presents more potential in the antimalarial intervention than in a combined therapy.

## Experimental Section

### Materials and methods

All reactions were made using Schlenk techniques[59] and the solvents were distilled using the appropriate distilling agents.[60] All reagents were used as received with no further purification. The extraction of chloroquine base and PQ base from their diphosphate salts were performed according to the literature.[61] The THT–Au–Cl was synthetized as described in the literature.[62] The NMR spectra were obtained at 298 K in $[D_6]$DMSO solution employing a Bruker Avance III HD 500 spectrometer, 9.4 T and the spectra were calibrated using deuterated solvent. The IR spectra were obtained in a Bruker Alpha FT-IR Spectrometer in the region of 4000–400 $cm^{-1}$ with a spectral resolution of 4 $cm^{-1}$. All UV/Vis experiments were performed on UV-1800 Spectrophotometer Shimadzu using quartz cuvettes. The mass spectroscopy experiments were performed on an AXIMA Performance matrix assisted laser desorption/ionization time of flight (MALDI-TOF) from Shimadzu Biotech, employing a nitrogen laser ($\lambda_{max}$ = 337 nm) for excitation in an α cyano matrix. Elemental analyses were obtained in a Perkin Elmer 2400 CHNS/O Series II microanalyzer. The conductivity data were obtained in a Meter Lab CDM2300 instrument and fluorescence measurements were carried out using a Perkin Elmer LS45 spectrophotometer with a pulse xenon lamp.

### Synthesis

*AuPQCl*: A solution of primaquine (535 mg, 1.99 mmol) in dichloromethane was added to a solution of Au(THT)Cl (400 mg, 1.25 mmol) previously synthesized in dichloromethane, and the solution remained in stirring for 2 h at 0 °C. The solvent was evaporated under vacuum and after diethyl ether addition, the solvent was evaporated again and the complex was obtained as a solid. The complex was washed with diethyl ether and dried under vacuum.

*$[AuCQPQ]PF_6$: (CQPQ-gold(I) hybrid)*: A solution of AuPQCl (153 mg, 0.31 mmol) in acetonitrile (10 mL) was added to $NH_4PF_6$ (90 mg, 0.56 mmol) the mixture was stirred for 2 h. The solution was then filtered through celite and added drop by drop in a solution of chloroquine (127 mg, 0.40 mmol) in acetonitrile (10 mL). After 4 h of agitation at 0 °C, the solvent was evaporated and brown oil was obtained. After washing by diethyl ether and evaporation, the brown precipitated product was washed with three portions of diethyl ether and dried under vacuum. Yield: 73%; Molar conductivity in DMSO, $\Lambda_M = 39.18 \pm 0.06$ $ohm^{-1}cm^2mol^{-1}$. $^1$H NMR ($(CD_3)_2SO$) ppm 8.54 (dd, $J$ = 1.5 Hz, 4 Hz, Hb); 8.35 (m, H2, H5); 8.07 (dd, $J$ = 8 Hz, $J$ = 1.5 Hz, Hd); 7.77 (d, $J$ = 2, H8); 7.42 (m, Hc,H6); 6.94 (d, $J$ = 7.5 Hz, N**2**H); 6.52 (d, $J$ = 5 Hz, H3); 6.49 (d, $J$ = 2 Hz, Hg); 6.29 (d, $J$ = 2 Hz, He); 6.15 (N**b**H); 3.82 (s, Hl); 3.76 (m, H1′); 3.67 (m, Ha′); 2.76 (m, Hd′, H4′, H5′); 1.57 (m, Hb′, Hc′, H2′, H3′); 1.22 (m, Ha″, H1″); 1.05 (t, $J$ = 7 Hz, H6′); $^{13}$C{$^1$H} NMR ($(CD_3)_2SO$) ppm 158.99 (Cf);151.75 (C2); 149.60 (C4); 149.07 (C9); 144.61 (Ci); 144.27 (Cb); 134.85 (Cd); 134.55 (Ch); 133.47 (C7); 129.61 (Cj); 127.30 (C8); 124.35 (C5);123.90 (C6); 122.15 (Cc); 117.47 (C10); 98.88 (C3); 96.29 (Ce); 91.73 (Cg); 55.01 (Cl); 51.31 (C4′); 47.41 (C1′); 46.81 (Ca′); 46.25 (C5′); 39.51 (Cd′); 32.75 (C2′, Cb′); 24.01 (Cc′); 21.61 (C3′); 20.27 (Ca″); 19.83 (C1″); 9.80 (C6′). $^{31}$P{$^1$H} NMR $PF_6^-$ ppm −144.2 (hep). IR $\nu$ (N–H) 3634, 3211; $\nu$ ($NH_2$) 3422, 3305; $\nu$ (C=C) 1615; $\nu$(C=N) 1580; $\nu$ ($PF_6$) 844; $\nu$(Au–N) 557. $\lambda_{max}$ nm in DMSO ($\varepsilon$, $M^{-1}cm^{-1}$): 340 (11767). MS (MALDI) (m/z) calcd for $[Au\text{-}PQ]^+ = 456.14$ $[CQ+H]^+ = 320.19$; found 456.14; 320.15; elemental analysis calcd. (%) for $C_{33}H_{47}AuClF_6N_6OP$.*3/2* $C_4H_{10}O$.*3/2*$CH_3CN$: C 46.11, H 6.13, N 9.60; found: C 46.41, H 5.71, N 9.56.

### Biotargets – metallic hybrid interaction studies

#### *DNA as a target*

*Spectrophotometric titrations*: Absorption titration experiments were carried out by stepwise additions of the calf thymus DNA (CT-DNA) solution (1.38 mM, in 5 mM Tris·HCl, pH 7.54 and 50 mM NaCl buffer) to the solution of each compound (0.4 μM) in DMSO, recording the UV/Vis spectra after each addition. Native DNA absorption was subtracted by adding the same amounts of CT-DNA to the blank cell. The binding affinity ($K_b$) was calculated from the spectrophotometric data according to the equation.[63]

$$\frac{[DNA]}{(\varepsilon_a - \varepsilon_f)} = \frac{[DNA]}{(\varepsilon_0 - \varepsilon_f)} + \frac{1}{Kb(\varepsilon_0 - \varepsilon_f)}$$

Where [DNA] is the concentration of DNA in base pairs, $\varepsilon_a$ is the extinction coefficient of the observed absorption band at the given DNA concentration (corresponding to $A_{obs}$/[compound]), $\varepsilon_f$ is the extinction coefficient of the free compound in solution, and $\varepsilon_b$ is the extinction coefficient of the compound when fully bound to DNA. A plot of [DNA]/[$\varepsilon_a-\varepsilon_f$] versus [DNA] gave a slope 1/[$\varepsilon_a-\varepsilon_f$] and a *y* intercept of 1/$K_b$[$\varepsilon_b-\varepsilon_f$]. $K_b$ is the ratio of the slope to the intercept.

*Viscosity study:* Viscosity measurements were carried out using an Ostwald viscometer immersed in a water bath maintained at 25 °C. The DNA concentration in buffer Tris·HCl was kept constant in all samples, however the [AuCQPQ]$PF_6$ hybrid concentration was increased from 0 to 147 μM. The flow time was measured at 3 times with a digital chronometer and the value was expressed as the mean. Data are presented as $(\eta/\eta_0)^{1/3}$ versus the ratio [complex]/[DNA], where $\eta$ and $\eta_0$ are the specific viscosity of DNA with the metallic hybrid and alone, respectively. The specific viscosity values were calculated using $(t-t_b)/t_b$, where *t* is the observed flow time and $t_b$ is the flow time of buffer.

*Competitive DNA-binding studies*: Ethidium bromide displacement assay was carried out essentially as per literature.[64] The maximum quantum yield for ethidium bromide was achieved at 471 nm; so this wavelength was selected as the excitation radiation for all samples at room temperature and in the emission range of 500–750 nm. The CT DNA-EB complex was prepared by adding 50 μL EB (1 mM) and 100 μL CT DNA (2 mM) in 5 mL of buffer (50 mM NaCl and 50 mM trizma at pH 7.3). The influence of the addition of each compound to the DNA–EB system solution was obtained by recording the variation of fluorescence emission spectra. [AuCQPQ]$PF_6$ hybrid did not exhibit emission in the presence of DNA and it did not influence the emission intensity of the free EB in the absence of DNA. Thus, the competitive DNA binding of the complex with EB could provide an evidence for interaction of the metallic hybrid with DNA base pairs. To quantify the affinity of the binding of the studied compound to DNA, the intrinsic binding constant ($K_b$) of the compound to DNA were obtained using the equation.

$$\frac{r}{Cf} = K_b x(n-r)$$

$C_b = C_t[(F-F_0)/(F_{max}-F_0)]$; where $C_t$ is the total compound concentration, *F* is the observed fluorescence emission intensity at a given DNA concentration, $F_0$ is the intensity in the absence of DNA, and $F_{max}$ is the fluorescence of the totally bound [AuCQPQ]$PF_6$ hybrid. Binding data were graphed as a Scatchard plot of $r/C_f$ versus *r*, where r is the binding ratio $C_b$/[DNA]*t*, $C_f$ is the free [AuCQPQ]$PF_6$ hybrid concentration and *n* is the number of binding sites.

*Electrophoresis*: For the DNA electrophoresis assays, 10 μL samples of the pBR322 plasmid (20 μg/mL) were combined with the [AuCQPQ]$PF_6$ hybrid at different ratios (molar ratios of [AuCQPQ]$PF_6$ hybrid / DNA (Ri) 1–4) and then incubated for 18 h at 37 °C. The reaction was then quenched by the addition of NaCl (1 M) to give a final chloride concentration of 0.2 M. Each sample (5 mL) was run (100 V for 40 min.) on a 0.7% agarose gel with TBE 1X (0.45 M Tris·HCl, 0.45 M boric acid, 10 mM EDTA) and stained with ethidium bromide. The bands were then viewed with a transilluminator and the image captured using a camera CoolSnapHQ2 (BIO-RAD), Universal HOOD III model 30.

### *Heme as a target*

*Interaction with ferriprotoporphyrin ($Fe^{III}$PPIX)*: The association constant of [AuCQPQ]$PF_6$ hybrid with ferriprotoporphyrin IX (hemin) was determined in 40% aqueous-DMSO as described previously.[65] The hemin stock solution (pH 7.5) were prepared with 3.5 mg of hemin in 10 mL of DMSO and the solution of $Fe^{III}$PPIX in 40% DMSO, were prepared with 140 μL of this hemin stock solution, 5 mL of distilled water, 3.86 mL of DMSO and 1 mL of 0.2 M Tris buffer (Tris; Tris(hydroxymethyl)aminomethane). CQPQ-gold(I) hybrid solution was prepared in 40% DMSO and aliquots of this solution was added to $Fe^{III}$PPIX and blank solutions in order to subtract the absorbance of the drug. The absorbance in Soret band (402 nm) was measured in presence and in absence of complex solution and the binding affinity was determined using the data and the equation $A = (A_0 + A_\infty K[C])/(1 + K[C])$ for a 1:1 complexation model using nonlinear least squares fitting, $A_0$ is absorbance of $Fe^{III}$PPIX, $A_\infty$ is the absorbance of the gold drug-hemin adduct at saturation and K is the association constant. The experiment measurements were made in triplicate.[66]

*Determination of inhibition of β-hematin formation by infrared spectroscopy*: The evaluation of the conversion of hemin to β-hematin was made as described by Egan et al.,[50] where 20 mg of hemin and two equivalents of the compound of interest were dissolved in 3 mL of 0.1 M NaOH solution and stirred for 30 minutes at 60 °C, then 0.3 mL of HCl 0.1 M solution and 1.7 mL of acetate buffer (10 M, pH 5) were added at the same temperature. After 120 min the mixture was cooled on ice for 10 min, centrifuged and washed with water to remove acetate salts. The solid was dried and infrared spectra were obtained with KBr pallets. Primaquine and chloroquine were used as negative and positive controls, respectively.[67]

*Inhibition of β-hematin formation in buffer and interface*: The assay of $IC_{50}$ of the β-hematin formation in buffer was performed as per Dominguez.[68] Briefly, a solution of hemin (50 μL, 4 mM), dissolved in DMSO, was distributed in 96-well microplates. The CQPQ-gold(I) hybrid was dissolved in DMSO and added in triplicate in test wells (50 μL) to final concentrations of 0–20 mM/well. Controls contained water and DMSO. Hemozoin formation was initiated by the addition of acetate buffer (100 μL of 0.2 M, pH 4.4). Plates were incubated at 37 °C for 48 h to allow completion of the reaction and centrifuged at 4000 RPM × 15 min. After discarding the supernatant, the pellet was washed twice with DMSO (200 μL) and finally dissolved in NaOH (200 μL, 0.2 N). The solutions were further diluted to 1:2 with NaOH (0.1 N) and absorbance recorded at 405 nm. The results were expressed as a percentage of inhibition of hemozoin formation.

β-Hematin formation at a water/octanol interface was followed with a method modified by Martínez et al..[53] Hemin was dissolved in 0.1 M NaOH solution to generate hematin. Acetone was added until the acetone to water ratio reached 4:6; the final solution contained 15 mg hematin/mL. A sample of this solution (200 μL) was carefully introduced close to the interface between *n*-octanol (2 mL) and aqueous acetate buffer (5 mL, 8 M; pH 4.9) in a cylindrical vial with an internal diameter of 2.5 cm. The mixture was incubated at 37 °C for 2 h, and at the end of the incubation the product (β-hematin) was isolated by centrifugation. The pellet was collected and washed twice with DMSO (2 mL), centrifuged again for 20 min, washed with 2 mL of ethanol and then dissolved in 25 mL of 0.1 M NaOH for spectrophotometric quantification. For the measurements of heme aggregation inhibition activity the appropriate amount of the CQPQ-gold(I) hybrid (23 mM in DMSO) was dissolved; after stirring for 30 min to equilibrate the drug between the two phases, the hematin solution was added close to the interface and the procedure was followed as described above. All experiments were performed in triplicate.

### Molecular modeling studies of the interaction of metallic hybrid with *P. falciparum* thioredoxin reductase enzyme and DNA

*Quantum mechanical calculations*: The 3D structure of [AuCQPQ]$PF_6$ was estimated by density functional theory calculation. The geometry was optimized in solution (using PCM approach) at B3LYP/SDD(f)/6-31 + G(2df) level. The same computational protocol was successfully applied for $Au^{I}$ and $Au^{III}$ complexes in our previous studies.[69–75] The vibrational frequencies were also calculated at the very same level of theory and the force constants estimated from the Hessian matrix using the Seminario method,[76] as implemented in the Visual Force Field Derivation Toolkit (VFFDT) program.[77] The final calculated geometry was also used to predict atomic charges (at HF/ SDD (f)/6-31 + G(2df) level) and $^{1}H$ and $^{13}C$ NMR chemical shifts relative to TMS standard (at B3LYP/SDD(f)/6-31 + G(2df) level). All calculations were carried out in the Gaussian-09 Rev. D.01 program.[78]

*Molecular docking studies*: Firstly, the interaction of [AuCQPQ]$PF_6$ with the *P. falciparum* thioredoxin reductase was analyzed. The PDB code 4J56 crystal structure was reported[22] for the mutant $PfTrxR^{C535S}$, which was reconstructed for the native form with Cys535 at the C-terminal motif. The enzyme structure is a homodimer containing 1008 residues (monomer 1: 1–504 and monomer 2: 505–1008-numbering scheme used in our edited structure) and two $FADH_2$ molecules. The goal of the present molecular modeling study was to predict and quantify the binding mode between [AuCQPQ]$PF_6$ and the PfTrxR enzyme.

Molecular docking studies were conducted in order to obtain some ligand-enzyme structures. The protocol was applied as in our previous papers for docking Au complexes in TrxR enzyme,[20,79] but with an update in the parameters file of the GOLD program[80] to account for gold atom (Atom type = Au, van der Waals radius = 1.51 Å, K value = 0.1, Ionization potential = 20.521 eV, Polarizability = 0.0, Atomic weight = 196.97, Formal charge = 1.0, Geometry = CO (coordinated metal ion), Number of neighbors = 0. The Au was defined as donor (D) with coordination number 2 and 4 and coordination distance of 2.29 Å. The maximum hydrogen bond energy was set to −15 to −10 kcal $mol^{-1}$ (same as Zn). The remaining parameters needed were set as for Zn (available in the original program).

The CHEMPLP function[81] was defined for scoring, and the docking searching used 100 GA runs setting to 200% of search efficiency. The C-terminal (Cys535 and Cys540; PDB numbering scheme) and N-terminal (Cys88 and Cys93; PDB numbering scheme) residues were used to define the centroid of the binding site (Figure S23A). The searching space covered a sphere of 15 Å around the centroid that included most of the interface cavity (Figure S23B).

Two different docking protocols were applied. The first one was carried out without any constraint and 100 ligand-enzyme poses were generated. In the second docking protocol, the same binding site definition was considered but the distance between S(Cys540; PDB numbering scheme) and Au was constrained within a 1.5–3.5 Å range. Technically, this means that if the S–Au distance is out of the boundaries the score is decreased by an amount proportional to the difference. This was done based on the most probable action mechanism of Au complexes as inhibitor of TrxR,[20,79] which passes through reaction of Au complex with Cys in the C-terminal motif.

Similar protocol was applied for the docking study of [AuCQPQ]$PF_6$ hybrid with the DNA. The structure of B-DNA dodecamer was taken from PDB ID: 1BNA.[82] The docking was performed over the entire DNA structure by defining the searching space as a 30 Å sphere centered at the geometric center of structure. In that way the minor and major grooves were mapped. The CHEMPLP scoring function was used to rank the 100 selected poses.

*Molecular dynamics simulation*: In order to improve the docking studies, the best selected poses were submitted to molecular dynamics (MD) simulations. The first step was to parametrize the classical potential GAFF2[83] for the gold coordination sphere. These parameters include atomic charges for all atoms, bond and angle force constants involving the first and second coordination spheres (Table S2) and van der Waals parameters for Au atom. Atomic charges were calculated at quantum mechanical level as described previously, but at Hartree-Fock (HF) level instead of B3LYP. The force constants were obtained at B3LYP level and for the van der Waals parameters the values adjusted for cisplatin (a $Pt^{II}$ complex) were used as described in our previous publication.[84] The remaining parameters are available in the GAFF2 as implemented in the Amber package.[85] The force field ff14SB[86] was used for the enzyme and the TIP3P model for solvent. For DNA, the OL15 force field[87] was used. The system containing the [AuCQPQ]$PF_6$ and PfTrxR enzyme (or the DNA dodecamer structure) (in distinct docking modes) was neutralized and immersed in a solvent box containing ~36000 water molecules (~7000 for DNA). The MD protocol involved the following steps: i) optimization of the solute, keeping the solvent molecules fixed; ii) optimization of the entire system; iii) NVT heating up to 310.0 K for 500 ps long; iv) NPT density equilibration for 1 ns long and v) NVT production for 100 ns long. Only the production phase data (considering the system in thermodynamic equilibrium) were analyzed and used to calculate the interaction properties.

### Distribution coefficient (D)

The water/*n*-octanol distribution coefficients were determined by the stir-flask method,[88,89] water-saturated *n*-octanol and *n*-octanol-saturated water were prepared by shaking equal volumes of *n*-octanol and water for one week and allowing the mixture to separate into the respective phases. A UV/Vis calibration curve for [AuCQPQ]$PF_6$ hybrid in *n*-octanol-saturated water in the 2–50 μM range was prepared. A mixture of 10 mL *n*-octanol and 10 mL water (each saturated in the other) was stirred for 1 h at 37 °C, after adding the sample to be analyzed. Once equilibrium was reached, the organic and aqueous phases were separated and centrifuged. Finally, the concentration of [AuCQPQ]$PF_6$ in each phase was measured spectrophotometrically to determine values for $\log D = \log$ [drug in *n*-octanol]/[drug in water]. Experiments were carried out three times.[90]

### Biological studies of metallic hybrids

*In vitro antimalarial activity*: The two strains, one of which is 3D7, the CQ-susceptible strain (isolated in West Africa; obtained from MR4, VA, USA), and the other is W2, the CQ-resistant strain (isolated in Indochina; obtained from MR4, VA, USA), were maintained in culture in Roswell Park Memorial Institute medium (RPMI 1640, Invitrogen), supplemented with 10% human serum (Abcys S.A. Paris, France) and buffered with 25 mM 4-(2-hydroxyethyl)-1-piperazineethanesulfonic acid (HEPES) and 25 mM $NaHCO_3$. Parasites were grown in A-positive human blood (Etablissement Français du Sang, Marseille, France) under controlled atmospheric conditions that consisted of 10% $O_2$, 5% $CO_2$ and 85% $N_2$ at 37 °C with a humidity of 95%.

The two strains were synchronized twice with sorbitol before use,[51] and clonality was verified every 15 days through PCR genotyping of the polymorphic genetic markers **msp1** and **msp2** and microsatellite loci.[52,53]

Chloroquine and primaquine were re-suspended in water in concentrations ranging between 3.2 to 3231 nM and 3.9 to 20 μM, respectively. [AuCQPQ]$PF_6$ was resuspended in DMSO and then diluted in RPMI/DMSO (99:1, *v*/*v*) to obtain final concentrations ranging from 3.9 to 20.1 μM.

For *in vitro* isotopic microtests, 25 μL/well of anti-malarial drug and 200 μL/well of the parasitized red blood cell suspension (final parasitemia, 0.5%; final hematocrit, 1.5%) were distributed into 96 well plates. The plates were incubated for 72 h at 37 °C in controlled atmosphere at 85% $N_2$, 10% $O_2$, 5% $CO_2$. After thawing the plates, hemolyzed cultures were homogenized by vortexing the plates. The drug susceptibility assay was performed using the HRP2 ELISA-based assay Malaria Ag Celisa kit (ref KM2159, Cellabs PTY LDT, Brookvale, Australia) as previously described.[54] The concentration at which the drugs were able to inhibit 50% of parasite growth ($IC_{50}$) was calculated with the inhibitory sigmoid $E_{max}$ model, with estimation of the $IC_{50}$ through nonlinear regression using a standard function of the R software (ICEstimator version 1.2). $IC_{50}$ values were validated only if the OD ratio (OD at concentration 0/OD at concentration max) was greater than 1.6 and the confidence interval ratio (upper 95% confidence interval of the $IC_{50}$ estimation/lower 95% confidence interval of the $IC_{50}$ estimation) was less than 2.0. $IC_{50}$ are expressed as means of 5 experiments.

*Cell toxicity*: In 96-well plates, HepG2 or J774 cells were seeded ((4.0×104 in 100 μL per well) of RPMI and Dulbecco's modified Eagle's medium (DMEM), respectively. Drugs were added 24 h later in a volume of 100 μL of medium and the plates were incubated for 72 h at 37 °C and under 5% $CO_2$. Drugs were tested in seven concentrations (1.25–80 μM), each one in triplicate. Doxorubicin chloridrate (Eurofarma, São Paulo, Brazil) was used as positive control, while untreated cells were employed as negative controls. Bioluminescence readings were performed using Filtermax™ F3 & F5 Multi-Mode instrument (Molecular Devices) using the kit CellTiter-Glo® (Promega). Mean $CC_{50}$ values were calculated using data from three independent experiments.

*Hemolysis assay*: Fresh uninfected human $O^+$ erythrocytes were washed three times with sterile phosphate-buffered saline (PBS), adjusted for 1% hematocrit and 100 μL dispensed in a 96-well round bottom plate. Then, 100 μL of drugs previously in DMSO and suspended in PBS were dispensed in the respective wells. Each drug was tested in seven concentrations (0.312–20 μM), assayed in triplicate. Untreated cells received 100 μL of PBS containing 1% (*v*/*v*) DMSO (negative control), while positive controls received saponin (Sigma-Aldrich) at 1% *v*/*v*. Plates were incubated for 1 h at 37 °C under 5% $CO_2$. Plates were centrifuged at 1500 rpm by 300 g for 10 min and 100 μL of supernatant were transferred to another plate, in which absorbance at 540 nm was measured using a SpectraMax 190 instrument. The % of hemolysis was calculated as follow: [(mean sample absorbance−mean negative control absorbance/mean positive control absorbance−mean negative control absorbance)]×100, and plotted against drug concentration generated using GraphPad Prism 5.01. Two independent experiments were performed.

*Activity against P. berghei liver stage*: The transgenic *P. berghei* parasites expressing green fluorescent protein (GFP) and firefly luciferase (Luc), (PbGFP-Luccon, parasite line 676 m1cl1) were freshly obtained through disruption of salivary glands of infected female *Anopheles stephensi* mosquitoes. Human hepatoma cell line Huh-7 was cultured in complete RPMI (RPMI-1640 medium supplemented with 10% (*v*/*v*) fetal bovine serum, 1% (*v*/*v*) nonessential amino acids, 1% (*v*/*v*) penicillin/streptomycin, 1% (*v*/*v*) glutamine, and 10 mM HEPES). Inhibition of hepatic infection was determined by measuring the luminescence intensity in Huh-7 cells infected with the firefly luciferase-expressing *P. berghei* parasites as previously described.[91] Briefly, for infection assays, Huh-7 cells ($1.0\times10^4$ per well) were seeded in 96-well plates one day before drug treatment and infection. The medium was replaced by medium containing the appropriate concentration of each compound, approximately 1 h prior to infection with sporozoites. An amount of the DMSO solvent equivalent to that present in the highest compound concentration was used as control. Sporozoite addition was followed by centrifugation at 1800×*g* for 5 min. Parasite infection load was measured 48 h post infection by a bioluminescence assay (Biotium, Hayward, CA, USA). The effect of the compounds on the viability of Huh-7 cells was assessed by the AlamarBlue assay (Life), using the manufacturer's protocol.

*Transmission electron microscopy of P. berghei liver stage*: Huh-7 cells ($1.0\times10^5$ per well) were seeded in 24-well plates. After drug treatment for 1 h, cells were infected with fresh sporozoites. After 24 h of incubation, cells were removed using trypsin, washed twice in PBS, then fixed with 2% formaldehyde and 2.5% glutaraldehyde (Electron Microscopy Sciences, Hatfield, PA, USA) in sodium cacodylate buffer (0.1 M, pH 7.2) for 40 min at room temperature. After fixation, cells were washed 3 times with cacodylate buffer and post-fixed with a 1.0% solution of osmium tetroxide containing 0.8% potassium ferrocyanide (Sigma-Aldrich) for 1 h. Cells were subsequently dehydrated in increasing concentrations of acetone (30, 50, 70, 90 and 100%) for 10 min in each step and embedded in Polybed resin (PolyScience family, Warrington, PA, USA). Ultrathin sections on copper grids were contrasted with uranyl acetate and lead citrate. Micrographs were taken using a JEM-1230 microscope (JEOL, Peabody, MA, USA).

*Animals, parasites and reagents*: Male Swiss Webster mice (18–22 g) were housed at Instituto Gonçalo Moniz (Fiocruz, Bahia, Brazil), maintained in sterilized cages under a controlled environment, receiving a rodent balanced diet and water ad libitum. All experiments were carried out in accordance with the recommendations of Ethical Issues Guidelines and were approved by the local Animal Ethics Committee (protocol number 02/2016). *P. berghei* expressing GFP was obtained as previously described[92] and kindly supplied by Prof. Antoniana Ursine Krettli (IRR/Fiocruz). Mitotracker™ deep red FM was purchased from Life Technology, ketamine and xylazine were purchased from Syntec (Sao Paulo, Brazil).

*Suppressive activity (Peters test)*: Male Swiss Webster mice (18–22 g) were infected by intraperitoneal injection of $1\times10^7$ GFP-*P. berghei*-infected erythrocytes per mouse and randomly divided into groups of $n=5$. Each compound was solubilized in propylene glycol/saline (20:80, *v*/*v*) prior to administration and treatment was initiated 24 h post infection and given once a day for four consecutive days by subcutaneous injection of 100 μL into the skin over the neck. Untreated infected mice receiving propylene glycol/saline (20:80, *v*/*v*) were used as negative control (vehicle). Parasitemia was determined by flow cytometry using GFP signal and co-staining with Mitotracker™ deep red FM (33 ng/mL), animal survival was observed daily until 40 days post-infection. The % of parasitemia reduction was calculated as follow: [mean vehicle group−mean treated

group/mean vehicle group]×100. Experiments were independently repeated for drug doses which inhibited >80% the parasitemia.

*Curative activity (Thompson test)*: Male Swiss Webster mice (18–22 g) were infected by intraperitoneal injection of $1\times10^7$ GFP–*P. berghei*-infected erythrocyte. Mice with parasitemia between 3–5% were randomly divided into groups of $n=6$ and treatment was performed daily for three consecutive days by subcutaneous route. Untreated infected mice receiving propylene glycol/saline (20:80, *v/v*) were used as a negative control (vehicle). The following parameters were evaluated: parasitemia counted at days 7, 9, 11 and 14 post-infection and 45 days post-infection animal survival. One experiment was performed.

*Schizont maturation assessment*: Male C57BL/6 mice (18–22 g) were infected by intraperitoneal injection of synchronized $1\times10^7$ GFP–*P. berghei*-infected erythrocytes per mouse and then the blood with 2–5% of parasitemia was collected. After successive washes with 0.9% sterile saline, 250 μL/well of GFP–*P. berghei*-infected blood was plated in 48-wells plate and the hematocrit adjusted to 2% when needed. Then, 250 μL/well of each compound solubilized in DMSO and diluted in RPMI medium in different concentrations (2.5, 25, 250 and 1000 nM) were dispensed in the respective wells in triplicate. The plate was maintained with a standard mixture of gases (3% $O_2$, 5% $CO_2$ and 91% $N_2$) and incubated at 37 °C for 24 h as described.[93] Untreated infected-blood was used as negative control. Parasitemia was determined by flow cytometry using GFP signal and co-staining with Mitotracker™ deep red FM (33 ng/mL). Three independent experiments were performed.

*Inhibition of hemozoin biosynthesis*: Male Swiss Webster mice (18–22 g) infected by *P. berghei* at parasitemia up to 10% were randomly divided into $n=3$/group. Treatment was performed by a single dose given by subcutaneous route. Untreated infected mice (vehicle) and uninfected mice (naïve) were included as control groups. Parasitemia was determined by flow cytometry before and after drug treatment. After 24 h treatment, mice were anesthetized using 70 mg/kg ketamine and 12.5 mg/kg xylazine (intraperitoneal), blood was gently aspirated in the brachial plexus using heparin coated tips and transferred into heparinized blood collection vials. Blood were centrifuged at 2500 rpm by 500 g at 4 °C for 5 min., plasma was discarded and cell pellet was washed with saline. Equal volumes of the remaining pellet were transferred to new tubes, suspended in 1.0 mL of 0.05% saponin and frozen overnight. Then, samples were centrifuged at 10000 rpmby 2500 g at 4 °C for 10 min., a volume of 0.5 mL of saline was added and centrifugation was repeated twice, the resulting cell pellets were processed to determining hemoglobin, free heme and hemozoin according to a previously described method.[94] At least two independent experiments were performed.

*Binding to reduced glutathione*: A solution of reduced glutathione (Sigma-Aldrich, 100 μL, 0.2 mM) dissolved in PBS pH 8.0 was distributed in a 96-well microplate. Testing compounds were dissolved in DMSO, diluted in PBS and then added in triplicate in the respective wells (50 μL) to final concentrations of 0.05 to 0.4 mM. Plate was incubated at 37 °C for 24 h to allow completion of the reaction, content was transferred into an opaque plate containing 20 μL of a solution of monochlorobimane at 1.0 mM. After 1 h of incubation at room temperature, fluorescence was recorded ($\lambda_{ex}=360$ nm, $\lambda_{em}=440$ nm). The results were expressed as a percentage of binding or inhibition in comparison to control without the testing compounds.

## Acknowledgements

*The authors are grateful to Dr. Roberto Rosas Pinho and Camila Condé for determining mass spectra, Mariana Borges for helping in the sporozoite assays and Dr. David Bátka for text editing. This work was supported by the Brazilian funding agencies: CAPES (grant no. 23038.006713/2013-88), CNPq (grant no. 305732/2019-6), FAPES grant number APP0088/2016) and Fiocruz/Inova (grant no.1642178247). MP was supported by grant PTDC-SAU-INF-29550-2017 (FCT, Portugal). HFDS and VS also thankful to FAPEMIG for the purchase of Nvidia graphics processing unit (GPU) used to speed up the MD simulations. CSP thanks CAPES for her Ph.D. scholarship.*

## Conflict of Interest

The authors declare no conflict of interest.

**Keywords:** chloroquine · DNA · gold · heme · malaria · primaquine

[1] World Health Organization (WHO), *Malaria.* March 2020. Accessed on 28.3.2020. https://www.who.int/malaria/en/.
[2] Y. Bansal, O. Silakari, *Eur. J. Med. Chem.* **2014**, *76*, 31–42.
[3] M. Ouji, J.-M. Augereau, L. Paloque, F. Benoit-Vical, *Parasite* **2018**, *25*, 24.
[4] A. Çapcı, M. M. Lorion, H. Wang, N. Simon, M. Leidenberger, M. C. B. Silva, D. R. M. Moreira, Y. Zhu, Y. Meng, J. Y. Chen, Y. M. Lee, F. Oliver, B. Kappes, J. Wang, L. Ackermann, S. B. Tsogoeva, *Angew. Chem. Int. Ed.* **2019**, *58*, 13066–13079.
[5] M. Lödige, L. Hiersch, *Int. J. Med. Chem.* **2015**, *2015*, 1–23.
[6] R. Oliveira, D. Miranda, J. Magalhães, R. Capela, M. J. Perry, P. M. O. Neill, R. Moreira, F. Lopes, *Bioorg. Med. Chem.* **2015**, *23*, 5120–5130.
[7] F. Bellot, F. Coslédan, L. Vendier, J. Brocard, B. Meunier, A. Robert, *J. Med. Chem.* **2010**, *53*, 4103–4109.
[8] K. N. Olafson, M. A. Ketchum, J. D. Rimer, P. G. Vekilov, *Proc. Natl. Acad. Sci. USA* **2015**, *112*, 4946–4951.
[9] J. G. Woodland, R. Hunter, P. J. Smith, T. J. Egan, *ACS Chem. Biol.* **2018**, *13*, 2939–2948.
[10] M. Navarro, W. Castro, C. Biot, *Organometallics* **2012**, *31*, 5715–5727.
[11] D. W. Wilson, C. Langer, C. D. Goodman, G. I. McFadden, J. G. Beeson, *Antimicrob. Agents Chemother.* **2013**, *57*, 1455–1467.
[12] I. Sutanto, S. Suprijanto, A. Kosasih, M. S. Dahlan, D. Syafruddin, R. Kusriastuti, W. A. Hawley, N. F. Lobo, F. O. Ter Kuile, *Clin. Infect. Dis.* **2013**, *56*, 685–693.
[13] G. Camarda, P. Jirawatcharadech, R. S. Priestley, A. Saif, S. March, M. H. L. Wong, S. Leung, A. B. Miller, D. A. Baker, P. Alano, M. J. I. Paine, S. N. Bhatia, P. M. O'Neil, S. A. Ward, G. A. Biagini, *Nat. Commun.* **2019**, *10*, 3226.
[14] A. R. Sannella, A. Casini, C. Gabbiani, L. Messori, A. R. Bilia, F. F. Vincieri, G. Majori, C. Severini, *FEBS Lett.* **2008**, *582*, 844–847.
[15] M. Navarro, F. Vásquez, R. A. Sánchez-Delgado, H. Pérez, V. Sinou, J. Schrével, *J. Med. Chem.* **2004**, *47*, 5204–5209.
[16] M. Navarro, W. Castro, M. Madamet, R. Amalvict, N. Benoit, B. Pradines, *Malar. J.* **2014**, *13*, 1–8.
[17] M. Navarro, H. Perez, R. A. Sanchez-Delgado *J. Med. Chem.* **1997**, *40*, 1937–1939.
[18] A. Ssemaganda, L. M. Low, K. R. Verhoeft, M. Wambuzi, B. Kawoozo, S. B. Nabasumba, J. Mpendo, B. S. Bagaya, N. Kiwanuka, D. I. Stanisic, S. J. Berners-Price, M. F. Good, *Metallomics* **2018**, *10*, 444–454.
[19] M. Navarro, W. Castro, S. González, M. J. Abad, P. Taylor, *J. Mex. Chem. Soc.* **2013**, *57*, 220–229.
[20] A. Garcia, R. C. Machado, R. M. Grazul, M. T. P. Lopes, C. C. Corrêa, H. F. Dos Santos, M. V. De Almeida, H. Silva, *J. Biol. Inorg. Chem.* **2016**, *21*, 275–292.

[21] A. Caroli, S. Simeoni, R. Lepore, *Biochem. Biophys. Res. Commun.* **2012**, *417*, 576–581.
[22] K. Fritz-Wolf, E. Jortzik, M. Stumpf, J. Preuss, R. Iozef, S. Rahlfs, K. Becker, *J. Mol. Biol.* **2013**, *425*, 3446–3460.
[23] J. L. Medina-Franco, M. A. Giulianotti, G. S. Welmaker, R. A. Houghten, *Drug Discovery Today* **2013**, *18*, 495–501.
[24] M. Navarro, W. Castro, A. Martínez, R. A. Martínez, *J. Inorg. Biochem.* **2011**, *105*, 276–282.
[25] M. Navarro, W. Castro, S. González, M. J. Abad, P. Taylor, *J. Mex. Chem. Soc.* **2013**, *57*, 220–229.
[26] J. D. S. Chaves, J. L. Damasceno, M. C. F. Paula, P. F. De Oliveira, G. C. Azevedo, R. C. Matos, M. C. S. Lourenço, D. C. Tavares, H. Silva, A. P. S. Fontes, M. V. De Almeida, *BioMetals* **2015**, *28*, 845–860.
[27] L. Glans, A. Ehnbom, C. De Kock, A. Martínez, J. Estrada, P. J. Smith, M. Haukka, R. A. Sánchez-Delgado, E. Nordlander, *Dalton Trans.* **2012**, *41*, 2764–2773.
[28] W. I. Sundquist, D. P. Bancroft, S. J. Lippard, *J. Am. Chem. Soc.* **1990**, *112*, 1590–1596.
[29] R. M. Silverstein, M. Webster, D. J. Kiemle, *Spectrometric Identification of Organic Compounds*, 7th ed., Wiley, **2005**, pp. 319.
[30] M. K. Nazeeruddin, S. M. Zakeeruddin, R. Humphry-Baker, R. Humphry-Baker, S. I. Gorelsky, A. B. P. Lever, M. Gratzel, *Coord. Chem. Rev.* **2000**, *208*, 213–225.
[31] V. A. Bloomfield, M. D. Crothers, I. Tinoco, *Physical Chemistry of Nucleic Acids*, 3rd ed., Harper & Row, **1974**, pp. 517.
[32] C. S. K. Rajapakse, A. Martínez, B. Naoulou, A. A. Jarzecki, L. Suárez, C. Deregnaucourt, V. Sinou, J. Schrével, E. Musi, G. Ambrosini, G. K. Schwartz, R. A. Sánchez-Delgado, *Inorg. Chem.* **2009**, *48*, 1122–1131.
[33] C. Biot, W. Castro, C. Y. Botté, M. Navarro, *Dalton Trans.* **2012**, *41*, 6335–6349.
[34] A. G. Quiroga, J. M. Pérez, E. I. Montero, J. R. Masaguer, C. Alonso, C. Navarro-Ranninger, *J. Inorg. Biochem.* **1998**, *70*, 117–123.
[35] G. Ibrahim, G. M. Bouet, I. H. Hall, M. A. Khan, *J. Inorg. Biochem.* **2000**, *81*, 29–34.
[36] R. W. Y. Sun, A. L. F. Chow, X. H. Li, J. J. Yan, S. S. Y. Chui, C. M. Che, *Cells. Chem. Sci.* **2011**, *2*, 728–736.
[37] A. Kellett, Z. Molphy, C. Slator, V. McKee, N. P. Farrell, *Chem. Soc. Rev.* **2019**, *48*, 971–988.
[38] L. Colina-Vegas, W. Villarreal, M. Navarro, C. R. De Oliveira, A. E. Graminha, P. I. D. S. Maia, V. M. Deflon, A. G. Ferreira, M. R. Cominetti, A. A. Batista, *J. Inorg. Biochem.* **2015**, *153*, 150–161.
[39] C. R. Brodie, J. G. Collins, J. R. Aldrich-Wright, *Dalton* **2004**, *21*, 1145–1152.
[40] J.-B. Lepecq, C. A. Paoletti, *J. Mol. Biol.* **1967**, *27*, 87–106.
[41] J. R. Lakowicz, *Principles of Fluorescence Spectroscopy*, 3rd., Springer, **2006**.
[42] D. Ajloo, M. E. Moghadam, K. Ghadimi, M. Ghadamgahi, A. A. Saboury, A. Divsalar, M. Sheikhmohammadi, K. Yousefi, *Inorg. Chim. Acta* **2015**, *430*, 144–160.
[43] M. Zampakou, M. Akrivou, E. G. Andreadou, C. P. Raptopoulou, V. Psycharis, A. A. Pantazaki, G. Psomas, *J. Inorg. Biochem.* **2013**, *121*, 88–99.
[44] A. Zianna, G. Psomas, A. Hatzidimitriou, E. Coutouli-Argyropoulou, M. Lalia-Kantouri, *J. Inorg. Biochem.* **2013**, *127*, 116–126.
[45] A. Banerjee, J. Singh, D. Dasgupta, *J. Fluoresc.* **2013**, *23*, 745–752.
[46] J. M. Fortune, N. Osheroff, *J. Biol. Chem.* **1998**, *273*, 17643–17650.
[47] I. Mitra, S. Mukherjee, V. P. Reddy, B. S. Dasgupta, J. C. Bose, K. S. Mukherjee, W. Linert, S. C. Moi, *RSC Adv.* **2016**, *6*, 76600–76613..
[48] A. Prisecaru, Z. Molphy, R. G. Kipping, E. J. Peterson, Y. Qu, *Nucleic Acids Res.* **2014**, *42*, 13474–13487.
[49] S. Pagola, P. W. Stephens, D. S. Bohle, A. D. Kosar, S. K. Madsen, *Nature* **2000**, *404*, 307–310.
[50] T. J. Egan, D. C. Ross, P. A. Adams, *FEBS Lett.* **1994**, *352*, 54–57.
[51] T. J. Egan, W. W. Mavuso, K. K. Ncokazi, *Biochemistry* **2001**, *40*, 204–213.
[52] T. J. Egan, *J. Inorg. Biochem.* **2006**, *100*, 916–926.
[53] A. Martínez, C. S. K. Rajapakse, D. Jalloh, C. Dautriche, R. A. Sánchez-Delgado, *J. Biol. Inorg. Chem.* **2009**, *14*, 863–871.
[54] M. N. Wenzel, A. F. Móska, V. Graziani, B. Aikman, S. R. Thomas, A. De Almeida, J. A. Platts, N. Re, C. Coletti, A. Marrone, G. Soveral, A. Cassini, *Inorg. Chem.* **2019**, *58*, 2140–2148.
[55] A. Martínez, C. S. K. Rajapakse, B. Naoulou, Y. Kopkalli, L. Davenport, R. A. Sánchez-Delgado, *J. Biol. Inorg. Chem.* **2008**, *13*, 703–712.
[56] L. Aguiar, M. Machado, M. Sanches-Vaz, M. Prudêncio, N. Vale, P. Gomes, *MedChemComm* **2019**, *10*, 221–226.
[57] G. W. Birrell, M. Chavchich, A. L. Ager, H. M. Shieh, G. D. Heffernan, W. Zhao, P. E. Krasucki, K. W. Saionz, J. Terpinski, G. A. Schiehser, L. R. Jacobus, G. D. Shanks, L. R. Jacobus, M. D. Edstein, *Antimicrob. Agents Chemother.* **2015**, 59, 170–177.
[58] L. M. Sanz, B. Crespo, C. De-Cózar, X. C. Ding, J. L. Llergo, J. N. Burrows, J. F. García-Bustos, F. J. Gamo, *PLoS One* **2012**, *7*, e30949.
[59] D. F. Shriver, M. A. Dredzon, *The Manipulation of Air-Sensitive Compounds*, 2nd ed., Wiley, **1986**.
[60] D. B. G. Williams, M. Lawton, *J. Org. Chem.* **2010**, *75*, 8351–8354.
[61] R. A. Sánchez-Delgado, M. Navarro, H. Pérez, J. A. Urbina, *J. Med. Chem.* **1996**, *39*, 1095–1099.
[62] R. Uson, A. Laguna, M. Laguna, D. A. Briggs, H. H. Murray, J. P. Fackler, *Inorg. Synth.* **1989**, *26*, 85–91.
[63] G. Scatchard, *Ann. N. Y. Acad. Sci.* **1949**, *51*, 660–672.
[64] A. J. Geall, I. S. Blagbrough, *J. Pharm. Biomed. Anal.* **2000**, *22*, 849–859.
[65] T. J. Egan, W. W. Mavuso, D. C. Ross, H. M. Marques, *J. Inorg. Biochem.* **1997**, *68*, 137–145.
[66] T. S. Macedo, W. Villarreal, C. C. Couto, D. R. M. Moreira, M. Navarro, M. Machado, M. Prudêncio, A. A. Batista, M. B. P. Soares, *Metallomics* **2017**, *9*, 1548–1561.
[67] T. S. Macedo, L. Colina-Vegas, M. Da Paixão, M. Navarro, B. C. Barreto, P. C. M. Oliveira, S. G. Macambira, M. Machado, M. Prudêncio, S. D'Alessandro, N. Basilico, D. R. M. Moreira, A. A. Batista, M. B. P. Soares, *Parasitology* **2016**, *143*, 1543–1556.
[68] J. N. Domínguez, C. León, J. Rodrigues, N. G. De Domínguez, J. Gut, P. J. Rosenthal, *Farmaco* **2005**, *60*, 307–311.
[69] H. F. Dos Santos, D. Paschoal, J. V. Burda, *Chem. Phys. Lett.* **2012**, *548*, 64–70.
[70] H. F. Dos Santos, D. Paschaol, J. V. Burda, *J. Phys. Chem. A.* **2012**, *116*, 11015–11024.
[71] H. F. Dos Santos, *Comput. Theor. Chem.* **2014**, *1048*, 95–101.
[72] H. F. Dos Santos, M. A. Vieira, G. Y. Sánchez Delgado, D. Paschoal, *J. Phys. Chem. A* **2016**, *120*, 2250–2259.
[73] G. Y. Sánchez Delgado, D. Paschoal, H. F. Dos Santos, *Comput. Theor. Chem.* **2017**, *1108*, 86–92.
[74] G. Y. S. Delgado, D. Paschoal, H. F. Dos Santos, *J. Biol. Inorg. Chem.* **2018**, *23*, 1283–1293.
[75] G. Y. S. Delgado, D. Paschoal, M. A. L. De Oliveira, H. F. Dos Santos, *J. Inorg. Biochem.* **2019**, *200*, 110804.
[76] J. M. Seminario, *Int. J. Quantum Chem. Quantum Chem. Symp.* **1996**, *30*, 1271–1277.
[77] S. Zheng, Q. Tang, J. He, S. Du, S. Xu, C. Wang, Y. Xu, F. Lin, *J. Chem. Inf. Model.* **2016**, *56*, 811–818.
[78] M. Frisch, G. W. Trucks, H. Schlegel, G. Scuseria, M. Robb, J. Cheeseman, G. Scalmani, V. Barone, B. Mennucci, G. A. Petersson, H. Nakatsuji, M. Caricato, X. Li, H. P. Hratchian, A. F. Izmaylov, J. Bloino, G. Zheng, J. L. Sonnerberg, M. Hada, M. Ehara, K. Toyota, R. Fukuda, J. Hasegawa, M. Ishida, T. Nakajima, Y. Honda, O. Kitao, H. Nakai, T. Vreven, J. A. Montgomery, J. E. Peralta, F. Ogliaro, M. Bearpark, J. J. Heyd, E. Brothers, K. N. Kudin, V. N. Staroverov, R. Kobayashi, J. Normand, K. Raghavachari, A. Rendell, J. C. Burant, S. S. Iyengar, J. Tomasi, M. Cossi, N. Rega, J. M. Millam, M. Klene, J. E. Knox, J. B. Cross, V. Bakken, C. Adamo, J. Jaramillo, R. Gomperts, R. E. Stratmann, O. Yazyev, A. J. Austin, R. Cammi, C. Pomelli, J. W. Ochterski, R. L. Martin, K. Morokuma, V. G. Zakrzewski, G. A. Voth, P. Salvador, J. J. Dannenberg, S. Dapprich, A. D. Daniels, Ö. Farkas, J. B. Foresman, J. V. Ortiz, J. Cioslowski, D. J. Fox, *Gaussian 09*; Gaussiann Inc.: Wallingford, CT, 2009.
[79] T. T. Tavares, G. C. Azevedo, A. Garcia, A. G. Carpanez, P. M. Lewer, D. Paschoal, B. L. Müller, H. F. Dos Santos, R. C. Matos, H. Silva, R. M. Grazul, A. P. S. Fontes, *Polyhedron* **2017**, 132, 95–104.
[80] M. L. Verdonk, J. C. Cole, M. J. Hartshorn, C. W. Murray, R. D. Taylor, *Proteins Struct. Funct. Genet.* **2003**, *52*, 609–623.
[81] O. Korb, T. Stu, T. E. Exner, *J. Chem. Inf. Model.* **2009**, 49, 84–96.
[82] H. R. Drew, R. M. Wing, T. Takano, C. Broka, S. Tanaka, K. Itakura, R. E. Dickerson, *Proc. Natl. Acad. Sci. USA* **1981**, *78*, 2179–2183.
[83] J. Wang, R. M. Wolf, J. W. Caldwell, P. A. Kollman, D. A. Case, *J. Comput. Chem.* **2004**, 25, 1157–1174.
[84] J. F. Lopes, V. S. A. Menezes, H. A. Duarte, W. R. Rocha, W. B. De Almeida, H. F. Dos Santos, *J. Phys. Chem. B.* **2006**, *110*, 12047–12054.
[85] D. A. Case, R. M. Betz, D. S. Cerutti, T. E. Cheatham III, T. A. Darden, R. E. Duke, T. J. Giese, H. Gohlke, A. W. Goetz, N. Homeyer, S. Izadi, P. Janowski, J. Kaus, A. Kovalenko, T. S. Lee, S. LeGrand, P. Li, C. Lin, T. Luchko, R. Luo, B. Madej, D. Mermelstein, K. M. Merz, G. Monard, H. T. Nguyen, I. Omelyan, A. Onufriev, D. R. Roe, A. Roitberg, C. Sagui, C. L. Simmerling, W. M. Botello-Smith, J. Swails, R. C. Walker, J. Wang, R. M.

Wolf, X. Wu, L. Xiao, P. A. Kollman, *AMBER 2016*, University of California, San Francisco, **2016**.
[86] J. A. Maier, C. Martinez, K. Kasavajhala, L. Wickstrom, K. E. Hauser, C. Simmerling, *J. Chem. Theory Comput.* **2015**, *11*, 3696–3713.
[87] M. Zgarbová, J. Šponer, M. Otyepka, T. E. Cheatham, R. Galindo-Murillo, P. Jurečka, *J. Chem. Theory Comput.* **2015**, *11*, 5723–5736.
[88] C. Rappel, M. Galanski, A. Yasemi, L. Habala, B. K. Keppler, *Electrophoresis* **2005**, *26*, 878–884.
[89] L. G. Danielsson, Y. H. Zhang, *TrAC Trends Anal. Chem.* **1996**, *15*, 188–196.
[90] M. Kah, C. D. Brown, *Chemosphere* **2008**, *72*, 1401–1408.
[91] I. H. J. Ploemen, M. Prudêncio, B. G. Douradinha, J. Ramesar, J. Fonager, G. J. Van Gemert, A. J. F. Luty, C. C. Hermsen, R. W. Sauerwein, F. G. Baptista, M. M. Mota, A. P. Waters, I. Que, C. W. G. M. Lowik, S. M. Khan, C. J. Janse, B. M. D. Franke-Fayard, *PLoS One* **2009**, *4*, 1–12.
[92] A. A. Sultan, V. Thathy, V. Nussenzweig, R. Ménard, *Infect. Immun.* **1999**, *67*, 2602–2606.
[93] Z. W. Chang, B. Malleret, B. Russell, L. Rénia, C. Claser, *Antimicrob. Agents Chemother.* **2016**, *60*, 6859–6866.
[94] M. Vanaerschot, L. Lucantoni, T. Li, J. M. Combrinck, A. Ruecker, T. R. S. Kumar, K. Rubiano, P. E. Ferreira, G. Siciliano, S. Gulati, P. P. Henrich, C. L. Ng, J. M. Murithi, V. C. Corey, S. Duffy, O. J. Lieberman, M. I. Veiga, R. E. Sinden, P. Alano, M. J. Delves, K. L. Sim, E. A. Winzeler, T. J. Egan, S. L. Hoffman, V. M. Avery, D. A. Fidock, *Nat. Microbiol.* **2017**, *2*, 1403–1414.

Manuscript received: August 25, 2020
Revised manuscript received: November 2, 2020
Version of record online: ■■, ■■■

# FULL PAPERS

**Three in one**: A novel multitarget metallo-hybrid of chloroquine and primaquine linked by gold(I) with potent antiparasitic activity and selectivity against two different stages of malaria – the blood (asexual) and the liver stage – has been developed. It acts on at least three identified targets of the parasite: it inhibits the β-hematin formation, interacts with DNA and interacts of PfTrxR.

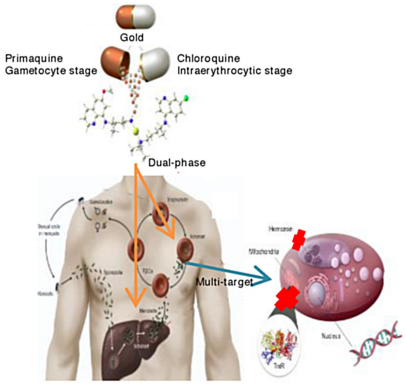


*C. de Souza Pereira, H. Costa Quadros, Dr. D. R. Magalhaes Moreira, Dr. W. Castro, R. I. Santos De Deus Da Silva, Dr. M. Botelho Pereira Soares, Dr. D. Fontinha, Dr. M. Prudêncio, V. Schmitz, Prof. H. F. Dos Santos, M. Gendrot, I. Fonta, J. Mosnier, Dr. B. Pradines, Prof. M. Navarro**

*pharmaceutics*

MDPI

*Article*

# A Hybrid of Amodiaquine and Primaquine Linked by Gold(I) Is a Multistage Antimalarial Agent Targeting Heme Detoxification and Thiol Redox Homeostasis

**Caroline De Souza Pereira [1], Helenita Costa Quadros [2], Samuel Yaw Aboagye [3], Diana Fontinha [4], Sarah D'Alessandro [5], Margaret Elizabeth Byrne [3], Mathieu Gendrot [6,7,8,9], Isabelle Fonta [6,7,8,9], Joel Mosnier [6,7,8,9], Diogo Rodrigo M. Moreira [2], Nicoletta Basilico [10], David L. Williams [3], Miguel Prudêncio [4], Bruno Pradines [6,7,8,9] and Maribel Navarro [1,*]**

1 Laboratório de Química Bioinorgânica e Catálise, Departamento de Química, Universidade Federal de Juiz de Fora, Juiz de Fora 36036-900, Brazil; carolsp_jf@yahoo.com.br
2 Instituto Gonçalo Moniz, Fundação Oswaldo Cruz, Salvador 40296-710, Brazil; helenita_quadros@hotmail.com (H.C.Q.); diogo.magalhaes@fiocruz.br (D.R.M.M.)
3 Department of Microbial Pathogens and Immunity, Rush University Medical Center, Chicago, IL 60612, USA; samuel_y_aboagye@rush.edu (S.Y.A.); margaret_byrne@rush.edu (M.E.B.); david_williams@rush.edu (D.L.W.)
4 Instituto de Medicina Molecular, Faculdade de Medicina, Universidade de Lisboa, 1649-028 Lisboa, Portugal; dfontinha@medicina.ulisboa.pt (D.F.); mprudencio@medicina.ulisboa.pt (M.P.)
5 Dipartimento di Scienze Farmacologiche e Biomolecolari, Università degli Studi di Milano, 20133 Milan, Italy; sarah.dalessandro@unimi.it
6 Unité Parasitologie et Entomologie, Institut de Recherche Biomédicale des Armées, 13005 Marseille, France; ma.gendrot@laposte.net (M.G.); isabelle.fonta.09@gmail.com (I.F.); joelmosnier@orange.fr (J.M.); bruno.pradines@gmail.com (B.P.)
7 Aix-Marseille Université, VITROME, 13005 Marseille, France
8 IHU Méditerranée Infection, 13005 Marseille, France
9 Centre National de Référence du Paludisme, 13005 Marseille, France
10 Dipartimento di Scienze Biomediche, Chirurgiche e Odontoiatriche, Universitá Degli Studi di Milano, 20133 Milan, Italy; nicoletta.basilico@unimi.it
* Correspondence: maribel.navarro@ufjf.br

**Abstract:** Hybrid-based drugs linked through a transition metal constitute an emerging concept for *Plasmodium* intervention. To advance the drug design concept and enhance the therapeutic potential of this class of drugs, we developed a novel hybrid composed of quinolinic ligands amodiaquine (AQ) and primaquine (PQ) linked by gold(I), named [AuAQPQ]$PF_6$. This compound demonstrated potent and efficacious antiplasmodial activity against multiple stages of the *Plasmodium* life cycle. The source of this activity was thoroughly investigated by comparing parasite susceptibility to the hybrid's components, the annotation of structure–activity relationships and studies of the mechanism of action. The activity of [AuAQPQ]$PF_6$ for the parasite's asexual blood stages was influenced by the presence of AQ, while its activity against gametocytes and pre-erythrocytic parasites was influenced by both quinolinic components. Moreover, the coordination of ligands to gold(I) was found to be essential for the enhancement of potency, as suggested by the observation that a combination of quinolinic ligands does not reproduce the antimalarial potency and efficacy as observed for the metallic hybrid. Our results indicate that this gold(I) hybrid compound presents a dual mechanism of action by inhibiting the beta-hematin formation and enzymatic activity of thioredoxin reductases. Overall, our findings support the potential of transition metals as a dual chemical linker and an antiplasmodial payload for the development of hybrid-based drugs.

**Keywords:** malaria; *Plasmodium*; antimalarial drugs; quinolines; gold; heme detoxification; redox homeostasis; hemozoin; flavoenzymes

check for updates

**Citation:** De Souza Pereira, C.; Quadros, H.C.; Aboagye, S.Y.; Fontinha, D.; D'Alessandro, S.; Byrne, M.E.; Gendrot, M.; Fonta, I.; Mosnier, J.; Moreira, D.R.M.; et al. A Hybrid of Amodiaquine and Primaquine Linked by Gold(I) Is a Multistage Antimalarial Agent Targeting Heme Detoxification and Thiol Redox Homeostasis. *Pharmaceutics* **2022**, *14*, 1251. https://doi.org/10.3390/pharmaceutics14061251

Academic Editor: Maria João Castro Gouveia

Received: 4 May 2022
Accepted: 7 June 2022
Published: 12 June 2022

**Publisher's Note:** MDPI stays neutral with regard to jurisdictional claims in published maps and institutional affiliations.

## 1. Introduction

Malaria is a parasitic disease caused by six *Plasmodium* species: *P. falciparum*, *P. vivax*, *P. malariae*, *P. knowlesi*, *P. ovale curtisi* and *P. ovale wallikeri*. Among these, the deadliest species are *P. falciparum* and *P. vivax*. According to the World Health Organization (WHO) in 2020, there were 241 million cases of malaria, leading to an estimated 627,000 deaths [1]. The most important strategies to prevent the disease, control infection and transmission are vaccines [2], pharmaceuticals [3] and insecticides [4]. With respect to vaccines, only one vaccine (RTS,S/AS01, Mosquirix) has been approved and recommended by the WHO for children in sub-Saharan Africa and in other areas with moderate to high *P. falciparum* transmission [5]. In the case of treatments and insecticides, the drawbacks are related to resistance and limited efficacy for certain parasite stages [3,4].

For complete elimination of malaria, new drugs acting against the hepatic, asexual blood and sexual *Plasmodium* life cycle stages are urgently needed [6]. The synthesis of hybrid-based drugs has emerged as a novel approach to obtain antiplasmodial compounds with potent activity against multiple parasite stages and strains resistant to common antimalarials [7–9]. The initial concept was that hybrid-based drugs could combine the antiplasmodial effects of its components (i.e., additivity or synergism) in a single molecule, facilitating the evaluation of pharmacokinetics, pharmaceutical formulation, and other aspects [7,8]. Among the concepts for designing hybrid-based drugs, there are three main possibilities: using non-cleavable chemical linkers [9,10], cleavable linkers (triggered by proteases or pH) [11,12] and transition metals that all play dual roles as cleavable chemical linkers and as antimalarials [13] (Figure 1). While all these possibilities have been investigated and have yielded promising results, the use of metals as chemical linkers offers the advantage of being pharmacologically active against parasites, while typically, organic chemical linkers are devoid of such effects.

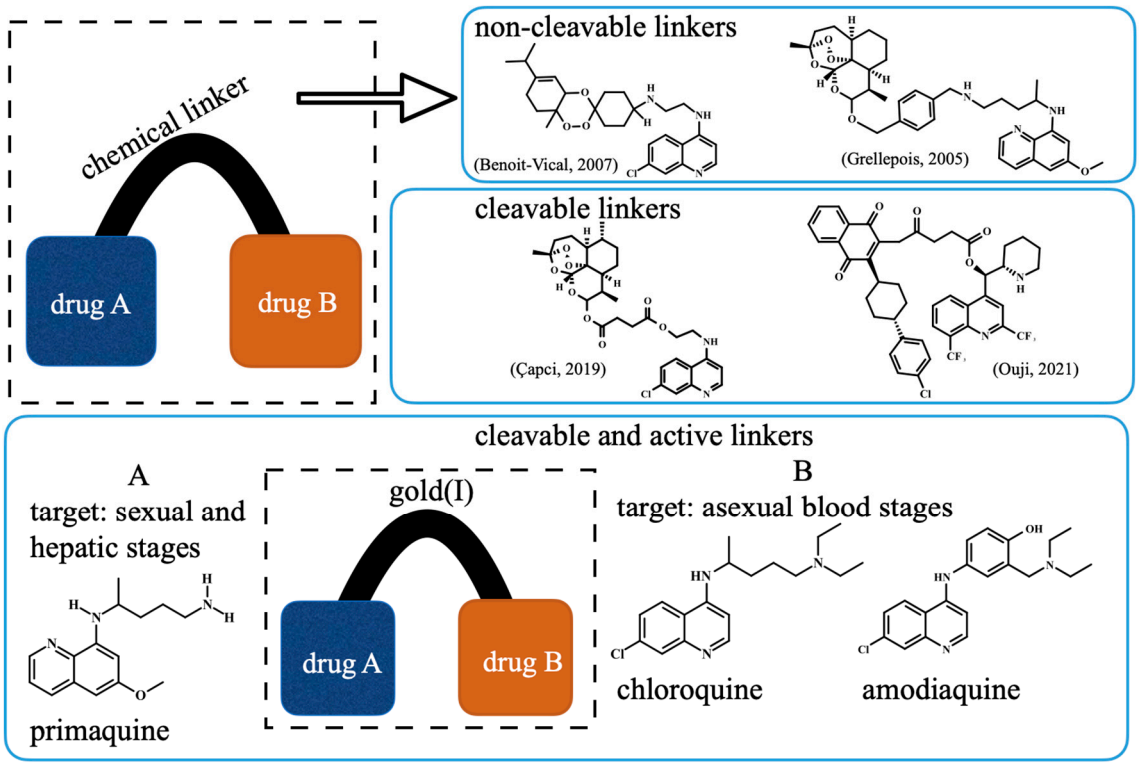


**Figure 1.** Panel (**A**) Schematic of the concept of hybrid-based drugs against malaria, highlighting the nature of chemical linkers and showing representative hybrids containing aminoquinolines as one of the components (references given in brackets). Panel (**B**) The concept of designing hybrid compounds containing gold(I) as a dual cleavable chemical linker and an antimalarial payload [9–12].

Our strategy for metallic hybrid-based drugs was designed in line with the current combined therapy of chloroquine (CQ) and primaquine (PQ) for non-*falciparum* malaria treatment in many areas with a high incidence of *P. vivax* and *P. ovale* [14]. This combination was developed for targeting different parasite stages, with CQ killing the asexual blood stages and PQ killing hypnozoites and gametocytes. A limitation of this therapeutic combination is that while there is a consistent summation of activity for the hepatic stages of the parasite [15,16], summation of activity for the asexual blood stages is variable and depends on the parasite strain and drug ratio [17,18]. To overcome this, we previously reported the synthesis of a hybrid of PQ and CQ linked by gold(I), denoted [AuCQPQ]$PF_6$ (**1**); this "three-in-one-molecule" was active against two stages of the *Plasmodium* life cycle and against three molecular targets of the parasite, confirming that it has multiple parasite stages and is a pleiotropic antimalarial agent [13]. However, hybrid (**1**) was not enough to overcome resistance to CQ when tested in vitro against CQ-resistant *P. falciparum* strains. The strategy employed here was to replace CQ by amodiaquine (AQ), leading to the [AuAQPQ]$PF_6$ (**2**) compound, also referred to as hybrid (**2**) (Figure 1).

The structure of this novel hybrid (**2**) includes components active against three parasite stages. The first component is PQ, which is active against the hepatic and sexual stages [19]. The second component is AQ, which similar to CQ, is active against the asexual blood stages through suppression of the heme detoxification process [20] and is relatively potent in vitro against hepatic stages [21]. In laboratory-cultured strains of *P. falciparum*, the CQ-resistant parasites are relatively susceptible to AQ [20]; however, in malaria patients, there is a cross-resistance of AQ to CQ and a reduced susceptibility to AQ treatment [22]. Gold(I) was chosen as the third component due to its inhibitory activity for flavoenzymes, especially the thioredoxin reductase (TrxR) of *P. falciparum* (*Pf*TrxR), which is essential for the parasite's survival [23–25]. A limitation of gold(I) compounds as antimalarials is their relatively low efficacy to reduce the parasitemia in infected mice after auranofin treatment [25].

The hybrid compound [AuAQPQ]$PF_6$ (**2**) was synthesized, and its structure was fully characterized. Multiple pharmacological studies, including a thorough investigation of its antiparasitic activity against the multiple stages of the *Plasmodium* life cycle, a comparison of parasite susceptibility to the hybrid's components and a combination of quinoline components (AQ + PQ), and a detailed study of the mechanism of action, revealed some of the structural determinants and compelling explanations for the potency enhancement of gold(I) hybrid's activity in comparison to its components, whether individually or in combination.

## 2. Experimental Section

### *2.1. Materials and Methods*

All the gold(I) complexes were prepared under argon using common Schlenk techniques and distilled solvents prior to use. All reagents were used without prior purification. The THT-Au-Cl (THT: tetrahydrothiophene) and AuPQCl were synthesized as described in the literature [13]. All NMR experiments were recorded on a Bruker Avance III HD 500 spectrometer, 11.7 T at 298 K and using DMSO-$d_6$ as solvent. Infrared (IR) spectra were obtained in a Bruker Alpha FT-IR Spectrometer in the region of 4000–400 $cm^{-1}$ with a spectral resolution of 4 $cm^{-1}$ and 64 scans. UV–Vis spectra were performed on UV-1800 Spectrophotometer Shimadzu using quartz cuvettes. Mass spectra (ESI-MS) were obtained on a 6530 Accurate-Mass Q-TOF system equipped with a dual AJS ESI source and a 1260 Infinity II high-performance liquid chromatography instrument as injection system, both from Agilent Technologies. Elemental analyses of carbon, nitrogen and oxygen were obtained in a Perkin Elmer 2400 CHNS/O Series II microanalyzer. Conductivity values were determined with a MS Tecnopon NI-CVM instrument.

### *2.2. Synthesis of [AuAQPQ]$PF_6$ (2)*

To a solution of AuPQCl (153 mg, 0.31 mmol) in tetrahydrofuran (10 mL), $NH_4PF_6$ (88 mg, 0.54 mmol) was added to the mixture and stirred for 1 h. The solution was then

filtered through a celite pad and added dropwise to a solution of amodiaquine free base (140 mg, 0.39 mmol) in tetrahydrofuran (10 mL). After 5 h of stirring at 0 °C, the solvent was evaporated, and a brownish oil was obtained. To remove unreacted amodiaquine, acetonitrile was added leading to precipitation of final compound. The solution was separated by filtration and the solvent was evaporated to obtain a brownish oil again. Finally, the oil was washed with diethyl ether and vacuum dried, giving rise to a brownish crystalline solid. Yield: 54%; Molar conductivity in DMSO $\Lambda_M$ DMSO = 49.30 ± 0.12 ohm$^{-1}$ cm$^2$ mol$^{-1}$. ESI-MS (*m*/*z*): $[PQ + H]^+$ = 260.1741, $[AQ + H]^+$ = 356.15 $[Au(AQ) + 2H]^+$ = 554.9641. IR ν 3632 (O-H); 3392, 3278 (N-H); 2972, 2942 (C-H aliphatic); 1615 (C=C); 1578 (C=N); 846 (P-F); 557 (Au-N). $^1$H NMR ($(CD_3)_2SO$) ppm 9.13 (sl, N2H); 8.39 (m, H2, H5, Hb); 8.07 (dd, J = 2 Hz, J =8 Hd); 7.87 (d, J = 2.5 Hz, H8); 7.56 (dd, J = 2 Hz, J = 9 Hz, H6); 7.42 (dd, J = 4 Hz, J = 8 Hz, Hc); 7.31 (d, J = 2.5 Hz, H3′); 7.22 (dd, J = 2.5 Hz, J = 8.5 Hz, H5′); 6.96 (d, J = 8.5 Hz, H6′); 6.61 (d, J = 5.5 Hz, H3), 6.48 (d, J = 2.5 Hz, Hg); 6.29 (d, J = 2.5 Hz, He); 6.14 (d, 9 Hz, NbH); 4.09 (s, H7′); 3.82 (s, Hl); 3.67 (m, Ha″); 2.95 (m, H8′); 2.81 (m, Hd′); 1.60 (m, Hb′, c′); 1.19 (m, H9′, a″). $^{13}$C{$^1$H} NMR ($(CD_3)_2SO$) ppm 159.04 (Cf); 154.62 (C2′); 150.81 (C9); 149.83 (C2); 146.84 (C10); 144.66 (Ci); 144.34 (Cb); 135.09 (C7); 134.91 (Cd); 134.59 (Ch); 130.37 (Cj); 129.67 (C3′); 128.55 (C5′); 127.66 (C8); 125.60 (C4′); 125.51 (C6); 124.60 (C5); 122.21 (Cc); 118.46 (C1′); 117.28 (C4); 116.56 (C6′); 100.68 (C3); 96.34 (Ce); 91.78 (Cg); 55.05 (Cl); 50.79 (C7′); 46.88 (Ca′); 46.73 (C8′); 39.94 (Cd′); 32.81 (Cb′); 24.04 (Cc′); 20.31 (Ca″); 8.69 (C9′). $^{31}$P{$^1$H} NMR ($(CD_3)_2SO$) $PF_6^-$ ppm -144.21 (hep.). Anal. Calcd. (%) $C_{35}H_{43}AuClF_6N_6O_2P.3/2C_4H_8O$: C 46.23, H 5.20, N 7.89; found: C 46.16, H 4.64, N 7.53.

### *2.3. Interaction with Ferriprotoporphyrin (Fe(III)PPIX)*

The association constant (log *K*) of $[AuAQPQ]PF_6$ compound with ferriprotoporphyrin IX (hemin chloride) was determined as described by Egan et al. [26] in 40% aqueous-DMSO. A hemin stock solution (pH 7.5) was prepared by adding 3.5 mg of hemin to a 10 mL of DMSO. The working solution of Fe(III)PPIX in 40% DMSO was prepared by a mixture of 140 µL of hemin stock solution, 5 mL of distilled water, 3.86 mL of DMSO and 1 mL of 0.2 M tris buffer (tris(hydroxymethyl)aminomethane). Aliquots of compounds were added to working (Fe(III)PPIX) and blank solutions in order to subtract the absorbance of the compound. The absorbance in Soret band (402 nm) was measured in the presence and absence of compound solution. The binding affinity was determined using the equation $A = (A_0 + A_\infty K[C])/(1 + K[C])$ for a 1:1 complexation model using nonlinear least squares fitting, where $A_0$ is absorbance of Fe(III)PPIX, $A_\infty$ is the absorbance of the compound-hemin adduct at saturation and *K* is the association constant. Three independent experiments were performed.

### *2.4. Determination of β-Hematin Formation Inhibition by Infrared Spectroscopy*

The conversion of hemin to β-hematin was determined by infrared (IR) spectroscopy as described by Egan et al. [26]. In a microtube, 20 mg of hemin and three equivalents of the compounds were dissolved in 3 mL of 0.1 M NaOH solution and stirred for 30 min at 60 °C. Then, 0.3 mL of 0.1 M HCl and 1.7 mL of sodium acetate buffer (10 M, pH 5) were added at the same temperature. After incubation for 120 min, the reaction mixture was cooled on ice for 10 min, and then, it was centrifuged and washed with water to remove sodium acetate salts. The solid was dried and IR spectra were obtained using attenuated total reflection (ATR) using chloroquine as a positive control.

### *2.5. β-Hematin Inhibition Activity (BHIA)*

A hemin chloride (10 µL of 4 mM stock in 80% DMSO) aliquot was dispensed in a U bottom 96-well microplate, and then, 10 µL of 0.1 M NaOH (O-BHIA) or 4 mM reduced glutathione in PBS at pH 7.0 (R-BHIA) was added, and plates were sealed and incubated at 37 °C for 2 h. After this, 10 µL of the drug dissolved in DMSO was added and incubated for 2 h, followed by the addition of 180 µL of sodium acetate buffer (1.0 M, pH 5.2) and 10 µL of nonionic detergent IGEPAL-CA-630 solution in methanol (10 mg/mL). Plates were

sealed and incubated at 37 °C for 18 h. Each drug was tested in a range from 1000 to 17 μM final concentration. The reaction was stopped by the addition of 50 μL of a sodium dodecyl sulfate solution (5.0% *v*/*v* in 0.1 M bicarbonate buffer at pH 9.0). Plates were centrifuged at 3700 rpm for 5 min, and 100 μL of supernatant was placed in a separate plate. Absorbance was quantified at 405 nm using a SpectraMax 190 microplate reader (Molecular Devices, Sunnyvale, CA, USA). The % inhibition was compared to untreated and unreacted controls (no acetate buffer), and $IC_{50}$ values were estimated by using non-linear regression curve calculated in Prism version 5.01. Two independent experiments were performed, and each drug concentration was tested in quadruplicate concentrations.

### *2.6. Interaction with Reduced Glutathione (GSH) by Fluorescence Assay*

Ten microliters per well of a solution of 2.0 mM reduced glutathione (Sigma-Aldrich, St. Louis, MO, USA, dissolved in PBS pH 7.2) was distributed in a 96-well microplate containing 170 μL/well of DMSO/PBS (1:1; *v*/*v*). Stock solutions of compounds were diluted in DMSO, and 10 μL was added in quadruplicate in the respective wells to a final concentration of 0.015 to 0.5 mM. The plate was sealed and incubated at 37 °C for 2 or 24 h, an d then, the contents were transferred to an opaque plate containing 10 μL of a solution of monochlorobimane (Sigma-Aldrich) at 4.0 mM in methanol. After 1 h incubation at room temperature, fluorescence was recorded ($\lambda$ex = 360 nm, $\lambda$em = 440 nm). Blank subtraction was performed prior to monochlorobimane addition, and controls included untreated wells (no drug) and no GSH. The results were expressed as a percentage of inhibition of GSH binding to monochlorobimane in comparison to control without compound. At least two independent experiments were performed.

### *2.7. Interaction with Reduced Glutathione by NMR*

Compound (**2**) (19.7 mg, 0.021 mmol) dissolved in 300 μL of DMSO-$d_6$ and 15 mg (0.049 mmol) of reduced glutathione (GSH) dissolved in 200 μL of $D_2O$ were added to an NMR tube, mixed and sealed. In parallel, the same reaction mixture but containing PQ or AQ (0.021 mmol) was prepared. The $^1$H NMR spectra were recorded at different times.

### *2.8. Inhibition of Enzymatic Activity of Recombinant Flavoenzymes*

The codon-optimized sequence for *Pf*TrxR [27,28] was synthesized and subcloned into pET-15b (Genscript) and expressed and purified as for human glutathione reductase (hGR). Recombinant *Schistosoma mansoni* (*S. mansoni*) thioredoxin glutathione reductase (*Sm*TGR), human TrxR (hTrxR), and hGR proteins were expressed and purified as described [29–31]. TrxR and TGR enzyme inhibition assays were performed in triplicate at 25 °C in 0.1 M potassium phosphate (pH 7.4), 10 mM EDTA, 100 μM NADPH and 0.01% Tween-20. *Sm*TGR (4 nM), hTrxR (4 nM), and *Pf*TrxR (50 nM) were preincubated with the compounds for 15 min. The reaction was started with addition of an equal volume of 5,5′-dithiobis(2-nitrobenzoic acid) (6 mM) and NADPH (100 μM). The increase in $A_{412}$ during the first 3 min was recorded. To determine inhibition of GR, hGR (120 pM) was added to an assay mixture (100 μM NADPH, 0.1 M potassium phosphate pH 6.9, 200 mM KCl, and 1 mM EDTA) with and without inhibitors, and the reaction was preincubated for 15 min. Activity was initiated with the addition of 1 mM oxidized glutathione and 100 μM NADPH, and initial rates of NADPH oxidation were monitored at 340 nm. The reactions were performed in triplicate. The $IC_{50}$s were calculated in Prism version 5.01.

### *2.9. Cytotoxicity against Mammalian Cells*

In vitro cytotoxicity was assayed against two mammalian cell lineages, J774 (murine macrophages) and HepG2 (human hepatocellular carcinoma). Lineages were maintained in RPMI-1640 (HepG2) or DMEM (J774) containing 10% fetal bovine serum and supplemented with L-glutamine, vitamins and amino acids in 75-cm$^2$ flasks at 37 °C, with the medium changed twice weekly. Cell cultures from 60 to 80% confluence were trypsinized, washed in complete medium, and $4 \times 10^4$ cells were plated in 100 μL per well with complete

medium in 96-well flat-bottom white plates for 24 h at 37 °C prior to the addition of the compounds. Triplicate aliquots of compound and the reference drugs (stock solution in DMSO) covering 7 different concentrations at 2-fold dilutions were added to the wells, and plates were incubated for 72 h more. After incubation for 72 h at 37 °C, plates were maintained at room temperature, the culture medium was removed, and 100 µL volume of CellTiter-Glo reagent was added to each well. The bioluminescence was measured using a microplate reader Filtermax F5 Multi-Mode instrument (Molecular Devices) and Softmax software. $CC_{50}$ data were obtained from at least two independent experiments for each cell line and analyzed using Prism version 5.01. The selectivity index (S.I.) was estimated using the $IC_{50}$s from mammalian cells divided by the $IC_{50}$ obtained against the asexual blood stage *P. falciparum*.

### *2.10. P. falciparum Asexual Blood Stages*

The asexual blood stages of CQ-susceptible strain (3D7) and CQ-resistant strain (W2) of *P. falciparum* were maintained in culture in RPMI-1640 supplemented with 10% human serum (Abcys S.A., Paris, France) and buffered with 25 mM 4-(2-hydroxyethyl)-1-piperazineethanesulfonic acid (HEPES) and 25 mM $NaHCO_3$. Parasites were grown in A-positive human blood (Etablissement Français du Sang, Marseille, France) under controlled atmospheric conditions of 10% $O_2$, 5% $CO_2$ and 85% $N_2$ at 37 °C with a humidity of 95%. For determination of antiparasitic activity, a volume of 25 µL/well of drug and 200 µL/well of the parasitized red blood cells at final parasitemia of 0.5% and hematocrit of 1.5% were distributed into 96-well plates. The plates were incubated for 72 h at 37 °C in controlled atmosphere. After frozen and thawing the plates, hemolyzed cultures were homogenized by vortexing the plates. The antiparasitic activity was determined using the HRP2 ELISA-based assay Malaria Ag Celisa kit (ref KM2159, Cellabs PTY LDT, Brookvale, Australia). The concentration at which the drugs were able to inhibit 50% of parasite growth ($IC_{50}$) was calculated with the inhibitory sigmoid $E_{max}$ model, with estimation of the $IC_{50}$ through nonlinear regression using a standard function of the R software (ICEstimator version 1.2). $IC_{50}$s are expressed as means of three to five experiments.

### *2.11. P. berghei Hepatic Stages*

Human hepatoma cell line Huh-7 was cultured in 1640 RPMI medium supplemented with 10% *v*/*v* fetal bovine serum, 1% *v*/*v* nonessential amino acids, 1% *v*/*v* penicillin/streptomycin, 1% *v*/*v* glutamine, and 10 mM HEPES at pH 7 and maintained at 37 °C with 5% $CO_2$. Huh-7 cells at $1.0 \times 10^4$ per well were seeded in 96-well plates the day before drug treatment and infection. The culture medium was replaced by infection medium (culture medium supplemented with gentamicin (50 µg/mL) and amphotericin B (0.8 µg/mL)) containing the appropriate concentration of each compound for approximately 1 h prior to infection with sporozoites of firefly luciferase-expressing *P. berghei*, freshly obtained through the disruption of salivary glands of infected female *Anopheles stephensi* mosquitoes. An amount of the DMSO solvent equivalent to that present in the highest compound concentration was used as negative control. Sporozoite addition was followed by centrifugation at 1800× *g* for 5 min. and parasite infection load was measured 48 h after infection by using a bioluminescence assay (Biotium, Hayward, CA, USA). The effect of the compounds on the viability of Huh-7 cells was assessed by performing the AlamarBlue (Invitrogen, Waltham, MA, USA) assay according to the manufacturer's protocol.

### *2.12. P. falciparum Gametocytes*

The activity of compounds was assessed against young gametocytes (stages I/III) and against mature gametocytes (stage V). Drugs were serially diluted in a 96-well flat bottom plate (concentration range 29.0–0.22 µM) in 100 µL per well, and each drug was tested in triplicate at seven different concentrations. Methylene blue was used as positive control. A volume of 100 µL of 3D7elo1-pfs16-CBG99 gametocytes of 3D7 *P. falciparum* at 0.5–1% parasitemia and 2% hematocrit were dispensed. Plates were incubated for 72 h at 37 °C

under 1% $O_2$, 5% $CO_2$, 94% $N_2$ atmosphere. Luciferase activity was used to determine gametocytes viability. A volume of 100 µL of culture medium was removed from each well to increase hematocrit; 70 µL of resuspended culture was transferred to a black 96-well plate; 70 µL of D-luciferin (1 mM in citrate buffer 0.1 M, pH 5.5) was added. Luminescence measurements were performed after 10 min with 500 ms integration time. The $IC_{50}$ was extrapolated from nonlinear regression analysis of the concentration–response curve. The percentage of gametocytes viability was calculated as 100 × ((OD treated sample − OD blank)/(OD untreated sample − µc-blank)) where "blank" is the sample treated with 500 nM of methylene blue, which completely kills gametocytes.

### *2.13. Mice and Parasites*

Male Swiss mice (4 to 8 weeks old) for the experimental study were obtained from the Animal Resource Facility at Instituto Gonçalo Moniz (Salvador, Brazil). Male or female Swiss mice (7 to 8 weeks old) were used for weekly passage of *P. berghei* parasites. Animals were housed under a 12 h light/dark cycle with free access to sterilized food pellets and sterilized water. These studies were approved by the Instituto Gonçalo Moniz Animal Ethics Committee (protocol 019/2021). NK-65 strain of *P. berghei* parasites expressing green fluorescent protein (GFP) was maintained by continuous weekly blood passage in mice. Mice were euthanized by tribromoethanol (300 mg/kg animal weight), blood was collected by brachial plexus, and a standard inoculum of $10^7$ parasitized erythrocytes per 200 µL was prepared by dilution in 0.9% saline and inoculated by intraperitoneal (i.p.) injection to experimental mice. Parasite enumeration in infected mice was determined in the peripheral blood collected from the tail veins. For determination of parasitemia in passage mouse, blood smear slides were mounted and stained by May–Grunwald–Giemsa. For experimental study, parasite enumeration was performed by flow cytometry using GFP signal and co-staining with a 50 nM of Mitotracker deep red FM (Life Invitrogen, Carlsbad, CA, USA) for 15 min.

### *2.14. Parasitemia Suppression in P. berghei-Infected Mice (Peters Test)*

*P. berghei*-infected mice were randomly divided in $n$ = 5/group. After 3 h (oral treatment by gavage) or 24 h (i.p. treatment), mice were treated once per day with 100 µL of drug or vehicle for four consecutive days. Each drug was solubilized in DMSO and diluted in a solution of kolliphor (cremophor, 4%), polysorbate 80 (5%), sorbitol (5%), glucose (5%), and tween 20 (5%) in 0.9% saline to a final concentration of 10% ($v/v$) of DMSO. Experimental compound [AuAQPQ]$PF_6$ (**2**) was administered at 10.8 µmol/kg of animal weight (10 mg/kg), fixed-dose of drug combination (AQ + PQ) was administered at 10 µmol/kg of animal weight (using 5.0 µmol/kg each drug) or at 30 µmol/kg of animal weight (using 15 µmol/kg each drug), and untreated group received vehicle only. Twenty-four hours after last drug administration, parasitemia was determined at regular intervals for 10 days. Animal survival was monitored twice per day for at least 40 days after infection. Parasitemia reduction was determined in comparison to vehicle. Unless indicated, one single experiment was performed.

### *2.15. Statistical Analysis*

Data are presented as the median ± standard error of the mean (S.E.M.) or the mean ± standard deviation (S.D.). Statistical analysis was performed using the Prism version 5.01 software (GraphPad Software, La Jolla, CA, USA). Statistical significance was assessed by performing the one-way analysis of variance (ANOVA) followed by post-test for multiple comparisons as indicated in each figure. Differences with $p$ values < 0.05 were considered significant.

## 3. Results

### *3.1. Synthesis of Metallic Hybrid and Characterization of Its Coordination Mode*

The [AuAQPQ]$PF_6$ (**2**) compound was synthesized in a two-step reaction as shown in Figure 2. The first step consisted of replacing the tetrahydrothiophene (THT) in the coordination sphere of the Au(THT)Cl complex with primaquine, leading to the AuPQCl intermediate. In the second step, this intermediate was dissolved in tetrahydrofuran and mixed with an excess of $NH_4PF_6$ at room temperature to remove the chloride ligand and then rapidly coordinated with amodiaquine at low temperature, which resulted in the hybrid [AuAQPQ]$PF_6$. This final product was isolated as a brownish solid with a yield of 54%. [AuAQPQ]$PF_6$ (**2**) was characterized by analytical and spectroscopic techniques. The IR spectrum (Figure S1) showed the characteristic and relevant bands of the quinolinic ligands. There was a slight displacement of the bands of the ligands coordinated with metal ions vis a vis the metal-free ligands. In addition to the bands of the ligands, the IR spectrum revealed the presence of bands at 557 and 846 $cm^{-1}$, which correspond to νAu-N and νP-F, respectively, therefore confirming the formation of hybrid gold(I) linked to quinolinic ligands. The molar conductivity obtained in a DMSO solution was in a range of 1:1 electrolyte [32], and the elemental analyses confirmed the proposed molecular formula.

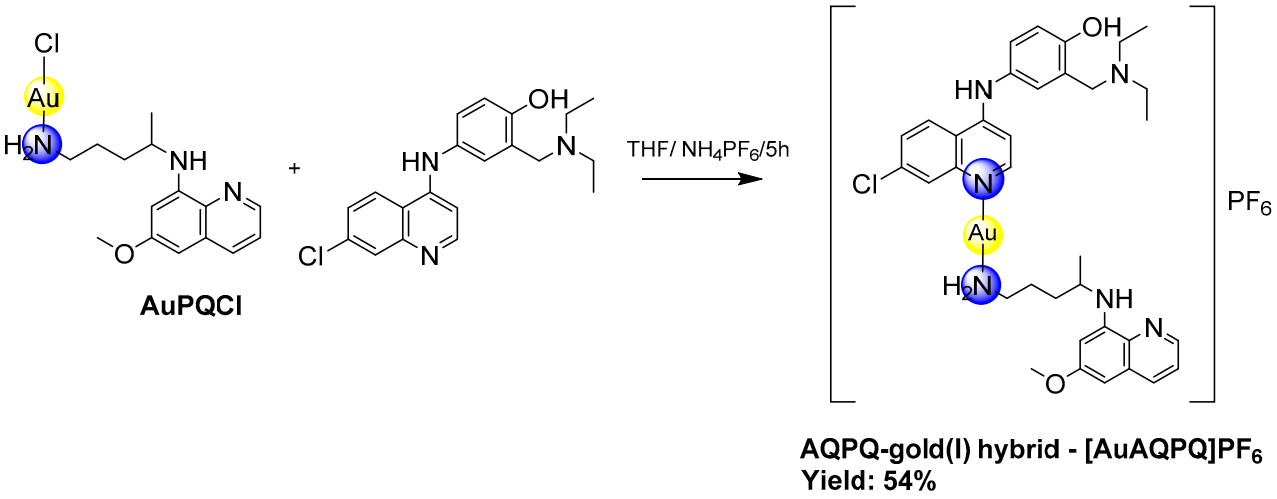


**Figure 2.** Synthesis of [AuAQPQ]$PF_6$ (**2**).

The chemical assignment of proton, carbon, and phosphorus atoms was ascertained through a combination of 1D NMR spectroscopy ($^1H$, $^{13}C$ and $^{31}P$) and 2D NMR spectroscopy techniques, such as gradient correlation spectroscopy ($^1H$-$^1H$ gCOSY), heteronuclear single quantum coherence ($^1H$-$^{13}C$ gHSQC), and heteronuclear multiple bond coherence ($^1H$-$^{13}C$ and $^1H$-$^{15}N$) HMBC. The $^1H$ NMR spectra (Figures S2 and S3) showed all the characteristic signals of quinolinic ligands and indicated that the peak integrations were consistent with the proposed molecular structure depicted in Figure 2.

Chemical shift variation (Δδ) was used as a parameter to identify the site of coordination of the ligands to the gold(I) in comparison to the metal-free ligands. In the case of AQ, the largest Δδ values were observed for the aliphatic protons of the tertiary amine (Δδ = 0.40 ppm for H7′, Δδ = 0.44 ppm for H8′), the aromatic proton of the quinolinic ring (Δδ = 0.47 ppm for H6), and a shift in the NH proton of 0.51 ppm, all indicating that this ligand was coordinated with gold. In contrast, the main chemical shift for PQ was 0.27 ppm, which corresponds to the hydrogen Hd′ from the $NH_2$ group, indicating that PQ binds gold(I) through the nitrogen in $NH_2$.

In the spectra for $^{13}C\{^1H\}$NMR (Figures S4 and S5), the signals corresponding to both ligands (AQ and PQ) were observed. The $^{13}C$ assignment was supported by the information derived from the $^1H$-$^{13}C$ HMBC spectrum (Figure S6). The signals for Cd′ (Δδ = 2.18 ppm) of PQ, and C9′ (Δδ = 2.13 ppm), C7′ (Δδ = 3.76 ppm), C1′ (Δδ = 5.09 ppm),

C8 (Δδ = 1.91 ppm), C6′ (Δδ = 2.06 ppm), C3′ (Δδ = 3.66 ppm), C7 (Δδ = 1.29 ppm), C10 (Δδ = 2.56 ppm) and C9 (1.01 ppm) of AQ were the ones most displaced in comparison with the metal-free ligands. An inspection of the $^{1}$H-$^{15}$N HMBC spectra (Figures S7–S9) further revealed that AQ coordinated with gold(I) through its quinolinic nitrogen (N1), which was inferred by the size of its shift (Δδ = −34.52) in comparison to the other nitrogen atoms from AQ (N2, Δδ = 6.98; N3, Δδ =12.55).

The signals corresponding to the hydroxyl proton located at C1′ on the AQ were observed at 7.62 ppm. A plausible explanation is an interaction between the hydroxyl group and the nitrogen of the tertiary aliphatic amine, which would explain the observed displacements for the protons near the tertiary amine. Finally, the spectrum of $^{31}$P{$^{1}$H}NMR (Figure S10) exhibited the septuplet at −144 ppm, which is a well-known characteristic of $PF_6$ as a counter ion, and the ESI-MS spectrum of [AuAQPQ]$PF_6$ (**2**) showed peaks at $m/z$ = 260.17 and $m/z$ = 356.15, which were attributed to the ligands PQ and AQ, respectively, in addition to a fragment detected at $m/z$ =554.96 attributed to the cationic fragment [Au(AQ) + 2H]$^{+}$ (Figure S11). Based on these, we propose that compound (**2**) is cationic with a linear geometry and hybridization sp. In addition to the chemical characterization, we also determined its chemical stability in DMSO solution by $^{1}$H and $^{31}$P NMR (Figures S12 and S13). No changes in the spectrum were observed for up to 25 days, indicating that [AuAQPQ]$PF_6$ (**2**) is remarkably stable in solution.

### *3.2. Metallic Hybrid Is a Potent and Selective Antiparasitic for Asexual Blood Stages*

The antiplasmodial activity of compounds was first evaluated in vitro against the asexual blood stage of *P. falciparum*, and their toxicity toward mammalian cells was determined in J774 lineage (Table 1). AQ was more potent for CQ-susceptible than CQ-resistant strains of *P. falciparum*. PQ, albeit of low potency, was more active for CQ-resistant than CQ-susceptible strains. After ascertaining this, the activity of [AuAQPQ]$PF_6$ (**2**) was determined, and it displayed potent activity. For the CQ-susceptible strain, it was slightly less potent than CQ and AQ. For the CQ-resistant strain, [AuAQPQ]$PF_6$ (**2**) was 29-fold more potent than AQ and 154-fold more potent than CQ.

**Table 1.** In vitro activity of compounds against the asexual blood stages of *P. falciparum*, cytotoxicity for mammalian cells and the selectivity profile.

| Compounds | *P. falciparum*, $IC_{50}$ ± S.E.M. (nM) [a] | | $CC_{50}$ ± S.E.M. (nM) [b] | Selectivity Index [c] | |
|---|---|---|---|---|---|
| | CQ-Susceptible 3D7 | CQ-Resistant W2 | | 3D7 | W2 |
| Primaquine (PQ) | 1117 ± 53 | 182 ± 16 | 36,500 ± 1100 | 32 | 200 |
| Amodiaquine (AQ) | 18.0 ± 1.6 | 86.2 ± 9.4 | 23,800 ± 700 | 1322 | 276 |
| [AuAQPQ]$PF_6$ (**2**) | 35.5 ± 2.1 | 2.97 ± 0.96 | 16,400 ± 700 | 461 | 5655 |
| Chloroquine (CQ) | 18.0 ± 2.0 | 459 ± 21 | 51,500 ± 1860 | 2861 | 112 |

[a] Inhibitory concentration for 50% ($IC_{50}$) determined 72 h after incubation with compounds using the histidine-rich protein 2 ELISA kit. Values were calculated as mean ± S.E.M. of at least three independent experiments. [b] Cytotoxic concentration for 50% ($CC_{50}$) against the macrophages of the J774 cell lineage, determined 72 h after incubation with compounds using the CellTiterGlo kit. Values were calculated as mean ± S.E.M. of at least two independent experiments. [c] Determined as $CC_{50}/IC_{50}$. S.E.M., standard error of the mean; AQ, amodiaquine hydrochloride hydrate; PQ, primaquine diphosphate; CQ, chloroquine diphosphate.

Determination of cytotoxicity for mammalian cells revealed that [AuAQPQ]$PF_6$ (**2**) has a profile that is similar to its quinoline components with a cytotoxic effect that is lower than the reference drug (doxorubicin, $CC_{50}$ = 0.44 ± 0.31 μM for J774; $CC_{50}$ < 0.12 μM for HepG2). Both PQ and AQ were more cytotoxic for J774 cells than cancerous HepG2 cells, while [AuAQPQ]$PF_6$ (**2**) was equally cytotoxic regardless of the lineage (Tables 1 and 2). The overall cytotoxicity of [AuAQPQ]$PF_6$ (**2**) was in the micromolar range, providing a selectivity index superior to PQ and comparable to AQ.

**Table 2.** In vitro activity of compounds against multiple stages of *Plasmodium* life cycle. Inset shows the infection of Huh-7 cells by *P. berghei* sporozoites (black bars) and the Huh-7 cell confluency (red dots).

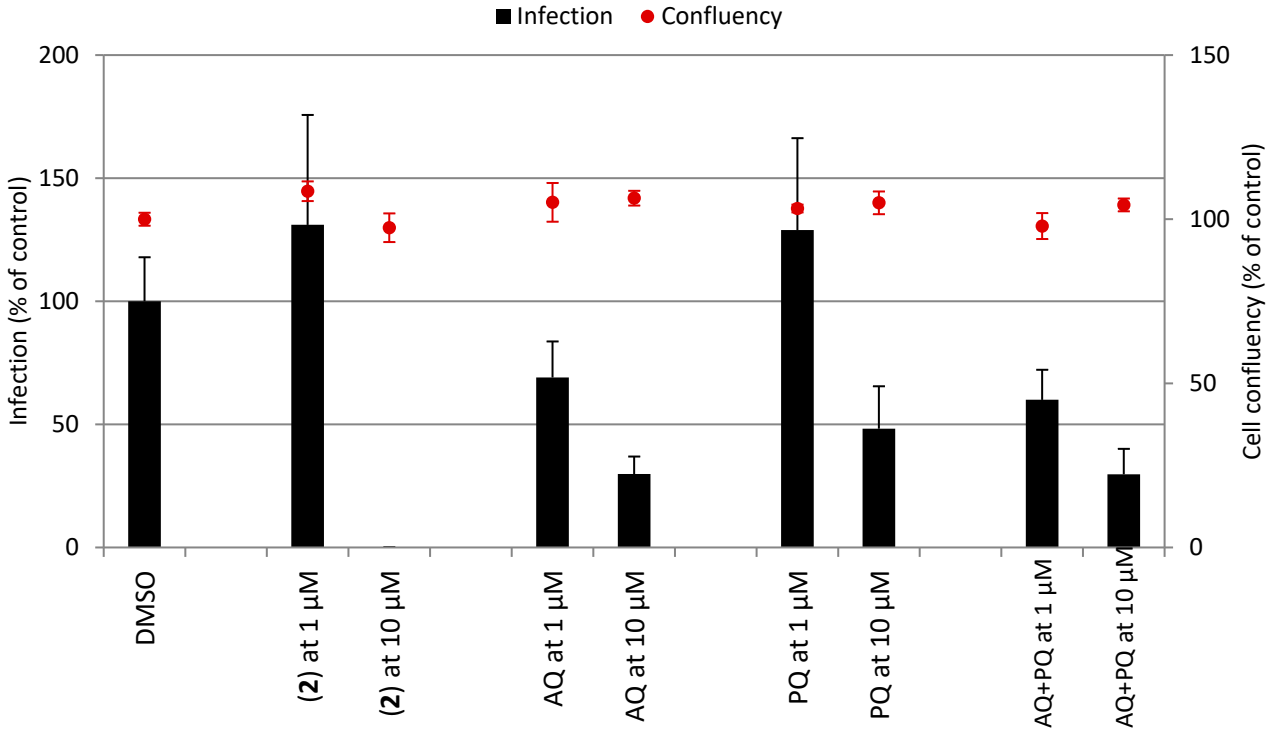


| Compounds | $IC_{50}$ (µM) and Parasite Stages | | | |
|---|---|---|---|---|
| | Sporozoites (Inhibition of Infection, %) [a] | Uninfected Hepatic Cells [b] | GAMETOCYTES of *P. falciparum* [c] | |
| | | | Stages I/III | Stage V |
| Primaquine (PQ) | 52 | >80 | 13.7 ± 7.6 | 43.2 ± 10.6 |
| Amodiaquine (AQ) | 71 | >80 | 0.061 ± 0.02 | 23.6 ± 5.0 |
| [AuAQPQ]$PF_6$ (**2**) | 100 | 14.4 ± 2.7 | 0.035 ± 0.01 | 9.5 ± 3.1 |
| AQ + PQ [d] | 70 | 41.0 ± 3.2 | N.D. | N.D. |
| Reference | 52 (PQ) | <0.12 (DOXO) | 0.0123 ± 0.0054 (DHA) | 0.038 ± 0.014 (MB) |

[a] Assay against Huh-7 cells infected by *P. berghei* sporozoites and activity was determined after 48 h of drug (10 µM) incubation. Values are the % of inhibition in comparison to untreated control from one experiment. [b] Cytotoxicity in uninfected HepG2 cells determined 72 h after drug incubation. [c] Assay against gametocytes of 3D7 strain of *P. falciparum* and activity was determined after 72 h. Values are mean ± S.D. of one experiment, with each concentration tested in triplicate. [d] Refers to 1:1 mixture of AQ and PQ. Reference drug for each assay: DOXO, doxorubicin; DHA, dihydroartemisinin; MB, methylene blue.

Given the high selectivity index of [AuAQPQ]$PF_6$ (**2**) as an antiplasmodial agent for the asexual blood stages of *P. falciparum*, we tested its efficacy as a blood schizonticidal agent in *P. berghei*-infected mice using a standard 4-day regime. A dose of 10.8 µmol/kg of animal weight of [AuAQPQ]$PF_6$ (**2**) was chosen based on a previous dose–response curve for hybrid (**1**) [13]. Efficacy of [AuAQPQ]$PF_6$ (**2**) was evaluated both by intraperitoneal injection and orally by gavage. As shown in Figure 3, compound (**2**) given by intraperitoneal injection was efficacious in reducing parasitemia and increasing animal survival in comparison to untreated infected group. When given orally, (**2**) suppressed parasitemia, but with a cure rate of only 50% from a pool of two independent experiments. Tested in parallel at the same dose by oral administration, a fixed-dose drug combination (AQ + PQ) reduced parasitemia but did not extend the median of animal survival. This drug combination only extended the median of animal survival when given at a dose of 30 µmol/kg, although this was not enough to cure the mice. Based on this, we estimated

that the [AuAQPQ]$PF_6$ (**2**) is at least three-fold more efficacious as a blood schizonticidal agent in *P. berghei*-infected mice than a drug combination (AQ + PQ).

(**A**)

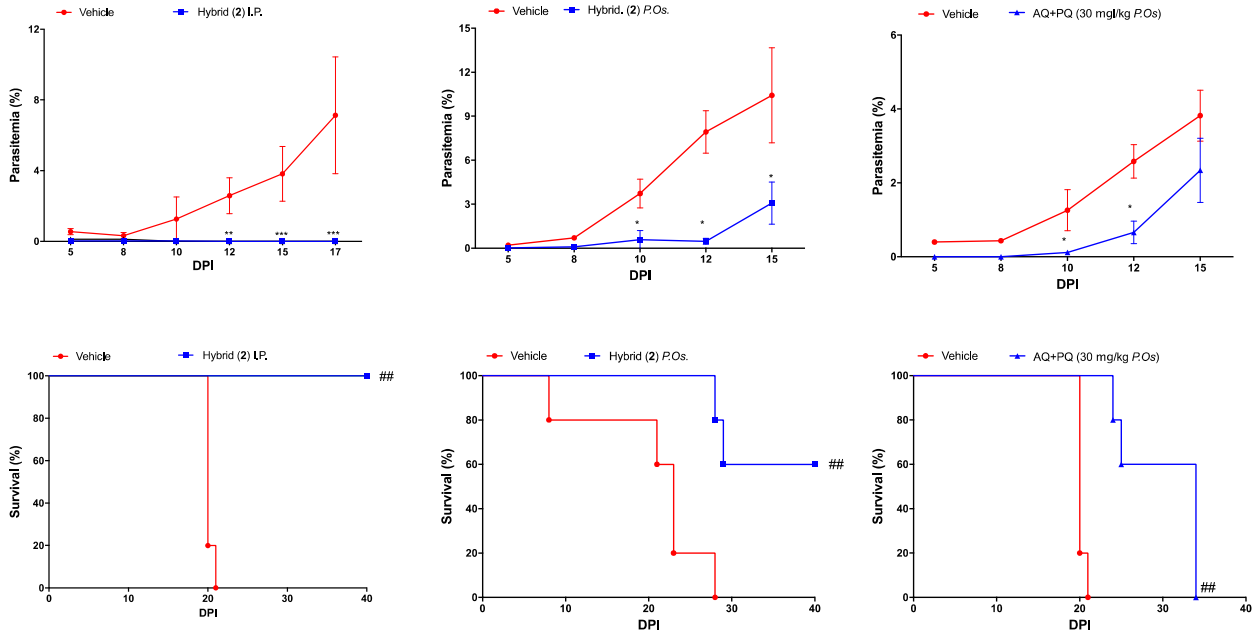


(**B**)

| Groups | Dose µmol/kg (mg/kg)/Route | Parasitemia Inhibition (%) [a] | Median of Animal Survival (Days) | Number of Mice Alive after 40 dpi (%) [b] |
|---|---|---|---|---|
| Vehicle | - | -,- | 19; 23 | 0/10 (0) |
| [AuAQPQ]$PF_6$ (**2**) | 10.8 (10)/*P.Os* | 84.5 ± 7.0 | 34.5 | 5/10 (50) |
| [AuAQPQ]$PF_6$ (**2**) | 10.8 (10)/I.P. | >99 | >40 | 5/5 (100) |
| AQ + PQ [c] | 10.8/*P.Os* | 43.3 ± 10 | 20 | 0/5 (0) |
| AQ + PQ [c] | 30/*P.Os* | 74.4 ± 5.0 | 34 | 0/5 (0) |

**Figure 3.** Efficacy of compounds to suppress the parasitemia in *P. berghei*-infected Swiss mice. Panel (**A**): Representative graphs of parasitemia and animal survival. Panel (**B**): Table summarizing the results. Footnotes for table: [a,b] Values are from a single experiment, using $n = 5$/group unless indicated. [a] Values are mean and standard deviation determined in comparison to vehicle group. [c] Refers to a 1:1 mixture of AQ and PQ. * $p < 0.05$, ** $p < 0.01$, *** $p < 0.001$ (one-way ANOVA) versus vehicle. ## $p < 0.05$ (log-rank and Mantel–Cox test) versus vehicle. DPI, days post-infection. *P.Os.*, orally by gavage; I.P., intraperitoneal injection.

### *3.3. Metallic Hybrid Is Active against the Sexual and Hepatic Stages*

The antiplasmodial activity of [AuAQPQ]$PF_6$ (**2**) was subsequently evaluated against the hepatic stages using Huh-7 cells infected with sporozoites of *P. berghei* and against the sexual blood stage (gametocytes) of the 3D7 strain of *P. falciparum* (Table 2). AQ is relatively potent against the *Plasmodium* hepatic stage, being more potent than PQ and other quinolines; however, AQ has a low potency for the gametocytes. PQ is active against the sexual and hepatic stages, but it depends on *in vivo* metabolism [20], as it typically exhibits low in vitro potency. Of note, a representative gold(I) complex lacking quinolinic ligand [AuClP$Ph_3$] exhibits low activity for these parasite stages ($IC_{50}$ of 15.2 ± 2.6 µM for gametocytes V; no inhibitory activity for the hepatic stages up to 10 µM).

Having ascertained the antiplasmodial profile of hybrid components, [AuAQPQ]$PF_6$ (**2**) was tested and found to have potent activity against both parasite stages. For the hepatic

stages, [AuAQPQ]$PF_6$ (**2**) at 10 μM was more potent than PQ, AQ, and their combination, and its activity was achieved with an excellent selectivity index, as it was not cytotoxic for Huh-7 cells. For the sexual stages, the activity was assessed in young (stages I to III) and in mature gametocytes (stage V). For young gametocytes, the [AuAQPQ]$PF_6$ (**2**) compound displayed $IC_{50}$ value in low nanomolar range, comparable to the reference drug dihydroartemisinin. Moreover, the activity of hybrid (**2**) against young gametocytes was similar to the activity against the asexual blood stages. For mature gametocytes, it presented potency in micromolar range, which is higher than PQ or AQ but lower than the gametocidal drug of reference methylene blue. We further compared the activity of [AuAQPQ]$PF_6$ (**2**) against gametocytes with its analog [AuCQPQ]$PF_6$ (**1**, $IC_{50}$ of $0.057 \pm 0.012$ and $8.3 \pm 0.91$ μM for gametocytes I to III and V, respectively), and the results revealed that, in essence, gold(I) hybrids have a similar gametocidal activity, i.e., a potent activity against young gametocytes but limited activity against mature gametocytes.

### *3.4. Metallic Hybrid Targets the Plasmodium Heme Detoxification*

To study the potential of [AuAQPQ]$PF_6$ (**2**) for suppressing *Plasmodium* heme detoxification, the association constant (log *K*) values of compounds to bind to the soluble Fe(III)-PPIX and the ability of compounds to suppress formation of the β-hematin crystals (the synthetic counterpart of hemozoin) were determined.

The binding of [AuAQPQ]$PF_6$ with Fe(III)-PPIX was examined by spectroscopic titration of UV–Vis using the Soret band. In this experiment, a quenching of the Soret band is typically observed upon increasing concentration of compounds, indicating the drug:heme binding process. Based on the log *K* values tabulated in Figure 4, it was observed that the affinity of [AuAQPQ]$PF_6$ (**2**) for binding Fe(III)-PPIX is similar as observed for AQ. This contrasts to a previous hybrid [AuCQPQ]$PF_6$ (**1**), which had a higher affinity than its quinoline component CQ (Figure 5). We posit that a decrease in the Fe(III)-PPIX affinity by [AuAQPQ]$PF_6$ is due to AQ being coordinated through its quinolinic nitrogen, which is a structural requirement for Fe(III)-PPIX binding.

The inhibition of β-hematin formation was monitored by infrared spectroscopic analysis of the two bands at 1660 and 1207 $cm^{-1}$ that are observed with the dimer but are absent from the monomer [26]. The β-hematin formation was inhibited by [AuAQPQ]$PF_6$ as well as by the quinolinic compounds (AQ and CQ) but not by PQ (negative control) (Figure 3 and Figure S14). To determine a compound's potency in inhibiting β-hematin formation, the β-hematin inhibitory activity (BHIA) was assayed in oxidized iron (Fe(III)PPIX, O-BHIA) and reduced iron (Fe(II)PPIX, R-BHIA) conditions [33]. [AuAQPQ]$PF_6$ (**2**) displayed potent BHIA against the ferric hematin with a potency that is twice that of CQ and almost as potent as AQ, while PQ and artemisinin lacked inhibitory activity. [AuAQPQ]$PF_6$ was only slightly more potent for ferrous heme than ferric hematin, while CQ was twice as potent for ferrous heme than ferric hematin. Both hybrid (**2**) and AQ were potent for R-BHIA, albeit they were less potent than artemisinin, which is a strong inhibitor in this assay. Based on this, we can infer that [AuAQPQ]$PF_6$ (**2**) is an inhibitor of β-hematin crystal formation, which is consistent with its strong binding to Fe(III)-PPIX.

(**A**)

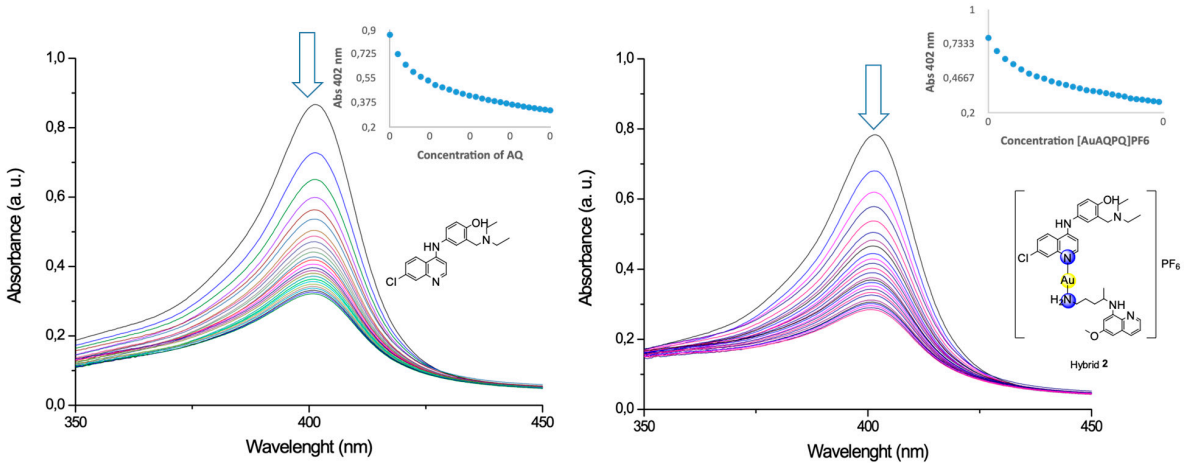


(**B**)

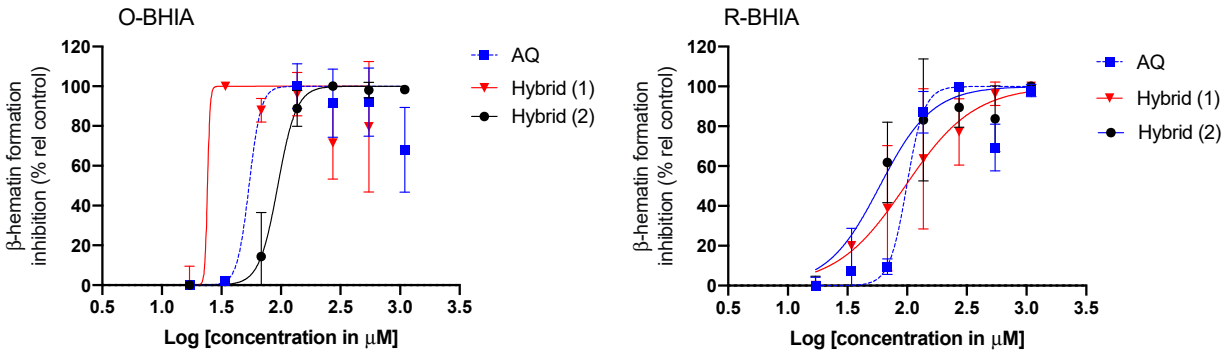


(**C**)

| Compounds | log *K* to Hemin (Soluble) [a] | β-Hematin Inhibitory Activity (BHIA) | | |
|---|---|---|---|---|
| | | Determined by IR [b] | O-BHIA (Hematin) [c] | R-BHIA (Heme) [c] |
| Primaquine (PQ) | N.D. | No | >1000 | >1000 |
| Amodiaquine (AQ) | 4.84 ± 0.03 | Yes | 140 ± 30 | 100 ± 10 |
| [AuAQPQ]$PF_6$ (**2**) | 4.70 ± 0.03 | Yes | 160 ± 50 | 90 ± 30 |
| Chloroquine (CQ) | 4.99 ± 0.01 | Yes | 230 ± 40 | 130 ± 30 |
| Artemisinin (ARS) | N.D. | N.D. | >1000 | 60 ± 10 |

**Figure 4.** Effects of compounds on the suppression of heme detoxification as inferred by drug:hemin binding and inhibition of the β-hematin formation. Panel (**A**) Titration of ferriprotoporphyrin IX [Fe(III)-PPIX, hemin]. Panel (**B**) Inhibition of the β-hematin formation; dots are the median ± S.E.M and lines are the data fitted into the log(concentration) versus response with a variable slope equation. Panel (**C**) Table summarizing the properties. Arrow in panel (**A**) indicates the decrease in absorbance upon increasing concentration of compounds. Footnotes for table: [a] Association constant to [Fe(III)-PPIX]. Values are median ± S.E.M. of three independent experiments. [b] β-hematin formation upon incubation of a 3:1 ratio of drug:hematin for 30 min. and qualitatively determined by infrared (IR). Yes indicates β-hematin inhibition; No indicates β-hematin formation. [c] β-hematin formation determined after 18 h of incubation. Values are median ± S.E.M. of $IC_{50}$ μM from three independent experiments. O-BHIA, oxidizing BHIA using hematin as reactant; R-BHIA, reducing BHIA using heme as reactant; S.E.M., standard error of the mean; AQ, amodiaquine (free base); PQ, primaquine (free base); CQ, chloroquine (free base); ARS, artemisinin; N.D., not determined.

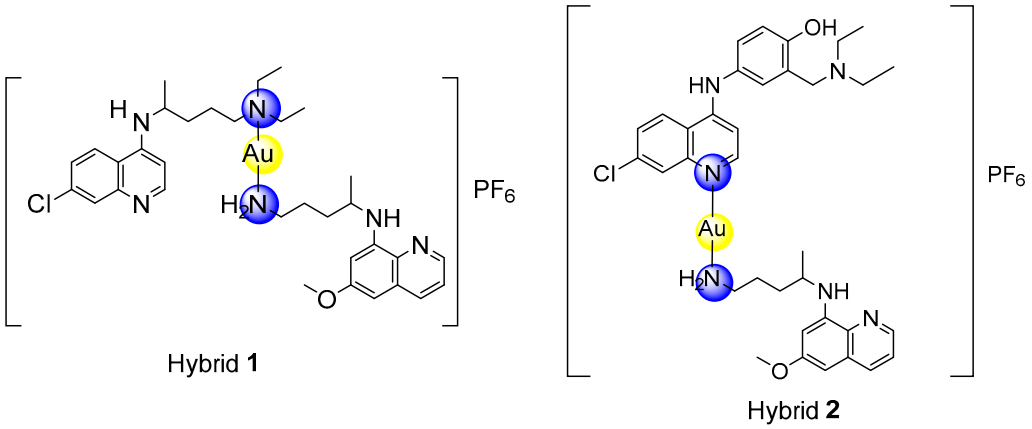


| Property | Hybrid (1) | Hybrid (2) | Reference Drugs |
|---|---|---|---|
| CQ-susceptible *P.f.* (μM) | 0.027 ± 0.0039 | 0.035 ± 0.0021 | 0.018 ± 0.002 (CQ) |
| CQ-resistant *P.f.* (μM) | 0.166 ± 0.025 | 0.0029 ± 0.00096 | 0.086 ± 0.009 (AQ) |
| log*K* (Fe-PPIX) | 5.2 ± 0.03 | 4.7 ± 0.03 | 4.99 ± 0.01 (CQ) |
| BHIA (mM) | 0.13 ± 0.06 | 0.16 ± 0.05 | 0.23 ± 0.04 (CQ) |
| *Pf*TrxR (μM) | 0.73 | 66.4 | 0.062 (Auranofin) |

**Figure 5.** Summary of the structure–activity relationships and drug properties for the gold(I) hybrids. CQ, chloroquine; AQ, amodiaquine.

### *3.5. Metallic Hybrid Inhibits Flavoenzymes Involved in the Thiol Redox Homeostasis*

*Plasmodium* relies on the flavoenzymes glutathione reductase (GR) and TrxR to control its thiol redox homeostasis [34], and gold(I) compounds such as auranofin can presumably cause an imbalance of this homeostasis by inhibiting the enzymatic activity of these enzymes. To understand the effects of [AuAQPQ]$PF_6$ (**2**) in this homeostasis, its inhibition of the enzymatic activity was determined against a panel of flavoenzymes: *Pf*TrxR, hTrxR, hGR, and *Sm*TGR. The results, displayed in Table 3, show that AQ did not inhibit the enzymatic activity of any flavoenzyme with appreciable potency. In contrast, [AuAQPQ]$PF_6$ (**2**) inhibited hTrxR and *Sm*TGR with potency in the low micromolar range; in common, these two are selenocysteine (Sec) TrxRs. For *Pf*TrxR, which is a cysteine (Cys) TrxR, [AuAQPQ]$PF_6$ (**2**) did not show appreciable inhibition. This inhibitory profile was explained when [AuAQPQ]$PF_6$'s activity was compared to its analog [AuCQPQ]$PF_6$ (**1**) and to the gold(I) phosphine compounds auranofin and [AuCl($PPh_3$)]. Similar to the [AuAQPQ]$PF_6$ (**2**), the CQ analog [AuCQPQ]$PF_6$ (**1**) had more potent inhibition of the Sec-TrxRs than the Cys-TrxR and hGR. Auranofin was found to be a pan-inhibitor for all TrxRs but not for GR, while [AuCl$PPh_3$] was found to be an inhibitor for all flavoenzymes tested.

Mechanistically, gold(I) compounds can undergo a ligand exchange reaction with the thiolates and selenolates in the flavoenzyme's catalytic site, resulting in enzyme–gold adducts [35,36]. To further understand the inhibition of Cys-TrxRs by hybrid compounds, we set up a cell-free assay to monitor the consummation of reduced glutathione (GSH) as a mimetic model for nucleophiles. Initially, GSH was incubated for 2 or 24 h at compound concentrations ranging from 10 to 0.3 drug:GSH molar ratio, and the consummation of GSH was determined by fluorescence of monochlorobimane (Figure S15). When compounds were incubated for 2 h, [AuCl$PPh_3$] was able to interact with GSH in a drug-concentration manner, while neither CQ nor phenanthroline interacted with GSH (negative controls). [AuCl$PPh_3$] was more potent than [AuAQPQ]$PF_6$ (**2**) in interacting with GSH; however, when compounds were incubated for 24 h, binding of [AuCl$PPh_3$] for GSH remained almost unaltered, and presumably, it reacted with GSH by a ligand exchange reaction. Differently, the binding of [AuAQPQ]$PF_6$ (**2**) with GSH increased during 2 versus 24 h incubation, indicating that, over time, [AuAQPQ]$PF_6$ (**2**) was consuming GSH. AQ interaction with

GSH had a similar behavior: its reaction after 2 h incubation seems to be incomplete; meanwhile, at 24 h incubation, GSH consummation increased. It was interpreted that the interaction of [AuAQPQ]$PF_6$ (**2**) with GSH is more similar to that observed for AQ than for [AuClPPh$_3$].

**Table 3.** Effects of compounds on the thiol redox homeostasis as inferred by the inhibitory effects on the enzymatic activity of recombinant flavoproteins.

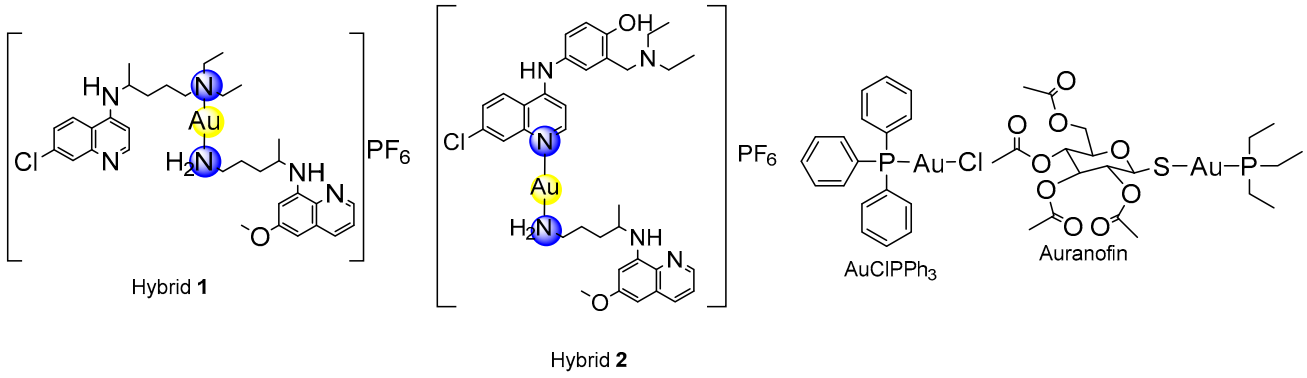


| Compounds | $IC_{50}$ (μM) for TrxRs [a] | | | Human GR [a] | *P. falciparum* 3D7 (Cell Based Activity) [c] |
|---|---|---|---|---|---|
| | Human (Sec) | *S. mansoni* (Sec) [b] | *P. falciparum* (Cys) | | |
| Amodiaquine (AQ) | 26.5 | 42.0 | >66.7 | >66.7 | 0.018 ± 0.002 |
| [AuAQPQ]$PF_6$ (**2**) | 4.98 | 0.75 | 66.4 | >66.7 | 0.035 ± 0.0021 |
| [AuCQPQ]$PF_6$ (**1**) | 0.0068 | 0.0038 | 0.73 | 0.053 | 0.027 ± 0.0039 |
| [AuClPPh$_3$] | 0.00065 | 0.0005 | 0.0019 | 0.00118 | 4000 ± 512 |
| Auranofin | 0.020 | 0.007 | 0.062 | 40.0 | 0.060 [d] |

[a] $IC_{50}$ values are in μM and the mean of one experiment, where each drug was tested in five different concentrations in triplicate. TrxR, thioredoxin reductase; GR, glutathione reductase. [b] *S. mansoni* thioredoxin–glutathione reductase (*Sm*TGR). [c] In vitro antiplasmodial activity expressed as $IC_{50}$ values in μM. [d] Value taken from reference [25]. Sec, redox-active site composed of selenocysteine; Cys, redox-active site composed of cysteine.

To reproduce the findings above and to characterize them at the molecular level, the interaction of compounds with GSH was monitored by NMR. After ascertaining the interaction of quinolinic compounds PQ and AQ with GSH, the GSH interaction with [AuAQPQ]$PF_6$ was analyzed (Figure S16). This step allowed us to unequivocally ascertain that GSH binds to the quinolinic ring of the primaquine component of hybrid (**2**). GSH conjugation to the primaquine component of hybrid (**2**) was inferred by the absence of the peak corresponding to Hg hydrogen of PQ after the addition of GSH. This behavior was also observed in an experiment using metal-free PQ (data not shown), and it was previously observed by others [37]. Gold(I) reduction to Au(0) species, ligand-exchange reactions or the appearance of the signals corresponding to metal-free quinolinic ligands were not observed. Although both PQ and AQ can bind to GSH, because of the dissimilar mode of coordination, the PQ component in the complex is more prone to bind to GSH than to gold(I) or AQ.

## 4. Discussion

We have demonstrated the chemistry, potency and efficacy of [AuAQPQ]$PF_6$ (**2**) as an antimalarial agent. In the strategy to synthesize [AuAQPQ]$PF_6$ (**2**), the PQ component was coordinated with the gold(I) atom via its aliphatic nitrogen, while the AQ component was coordinated via its quinolinic nitrogen. This mode of coordination for AQ was an unexpected finding, especially considering that in the same synthesis strategy for its analog [AuCQPQ]$PF_6$ (**1**), the CQ component was coordinated with gold(I) through its aliphatic nitrogen. Despite the dissimilarity in terms of metal coordination, [AuAQPQ]$PF_6$ (**2**) was

quite stable in the air, in aqueous solution, and in DMSO solutions as previously observed for its analog (**1**).

Against the asexual blood stages of *P. falciparum*, [AuAQPQ]$PF_6$ (**2**) was twice less potent than AQ for the drug-sensitive strain but was significantly more potent than AQ for the drug-resistant strain. This is because in the sensitive strain, the activity of [AuAQPQ]$PF_6$ (**2**) is largely due to the presence of the AQ component, while PQ makes little or no contribution to antimalarial activity in this stage. However, PQ can contribute to antimalarial activity against drug-resistant parasite strains since these strains are typically hypersensitive to treatment [16,21]. Moreover, toxicity to mammalian cells was low for the hybrid (**2**), resulting in a high selectivity index.

The efficacy of [AuAQPQ]$PF_6$ (**2**) against the asexual blood stages using *P. berghei*-infected mice revealed that it is a powerful antimalarial agent. It was at least three times more efficacious than a combination of its components (AQ + PQ). PQ has low potency and subsequently limited efficacy against asexual blood stages. Conceivably, the summation of the efficacies against these stages upon PQ co-administration could only be achieved if a high PQ dosage was deployed. However, [AuAQPQ]$PF_6$ (**2**) is composed of a fixed ratio of AQ + PQ; therefore, the superior efficacy of [AuAQPQ]$PF_6$ (**2**) versus a drug combination of AQ + PQ could be partly due to its pharmacokinetic profile and an increase in the cellular accumulation of PQ in the parasite cells upon [AuAQPQ]$PF_6$ (**2**) exposure. While further investigation of this interpretation is beyond the scope of the present study, we note that previous studies have also observed a potency enhancement of *in vivo* efficacy for hybrid molecules containing PQ in comparison to PQ alone or its drug combination [38,39].

[AuAQPQ]$PF_6$ (**2**) has an improved spectrum of inhibitory activity against multiple stages of the *Plasmodium* life cycle, spanning from sporozoites to gametocytes. The enhanced potency of the hybrid compared to drug combinations is most likely due to a cooperation of two quinolinic drugs with distinct modes of actions; specifically, PQ, causing an augmentation of oxidative species toxic for the parasite [20], and AQ, suppressing heme detoxification and decreasing the levels of antioxidant GSH in egressing hepatic schizonts and in young gametocytes [19,40]. The reason for the superior potency of [AuAQPQ]$PF_6$ over a drug combination remains less clear, but it is plausible that it affects thiol redox homeostasis while metal-free quinolines do not.

Mechanistically, the activity of [AuAQPQ]$PF_6$ (**2**) could be partly ascribed to the suppression of heme detoxification, inhibition of the activity of flavoenzymes involved in the thiol redox homeostasis, and the cooperation of both effects. In support of this hypothesis, [AuAQPQ]$PF_6$ (**2**) binds to Fe(III)-PPIX and inhibits β-hematin crystal formation, demonstrating the potential of (**2**) to suppress parasite heme detoxification. In contrast, [AuAQPQ]$PF_6$ (**2**) inhibits flavoenzyme activity, including *Pf*TrXR, relatively weakly in comparison to its inhibition of in vitro parasite growth. We observed that while both [AuAQPQ]$PF_6$ (**2**) and its quinolinic components react with GSH, they do so in a different way from [AuCl($PPh_3$)]: while the latter reacts quickly with GSH, the former react slowly. Furthermore, the $^1$H-NMR analysis did not display evidence of ligand exchange, such as a displacement of quinoline from the sphere of coordination of gold(I), but it did display evidence of GSH binding to the PQ component of [AuAQPQ]$PF_6$ (**2**). Therefore, the multiple analyses suggested that [AuAQPQ]$PF_6$ (**2**) has relatively low reactivity for thiol reactants, indicating that quinoline dissociation in the hybrid compounds may only occur inside parasite cells. Moreover, this may explain the relatively low inhibitory activity of [AuAQPQ]$PF_6$ (**2**) for recombinant flavoenzymes.

The dissimilarity in the coordination of 4-aminoquinoline CQ or AQ to the gold(I) atom has implications for the mechanism of action of hybrid compounds as well as for their antimalarial activity. Our previous hybrid compound [AuCQPQ]$PF_6$ (**1**) was more potent in inhibiting β-hematin than CQ, while [AuAQPQ]$PF_6$ (**2**) was equipotent to AQ. It is well known that CQ and AQ interact with Fe(III)-PPIX by iron–quinoline coordination and the stacking of quinoline over protoporphyrin [41,42]. In the [AuCQPQ]$PF_6$ (**1**) hybrid, the 4-aminoquinolinic heterocyclic is available to interact with Fe(III)-PPIX by both modes,

while in the [AuAQPQ]$PF_6$ (**2**) hybrid, quinoline is coordinated with gold(I). Thus, only stacking interactions between Fe(III)-PPIX and (**1**) are possible. This is one explanation for why [AuAQPQ]$PF_6$ (**2**) did not display superior potency to AQ as a heme detoxification suppressor (Figure 4). The coordination of 4-aminoquinoline CQ or AQ to gold(I) also has consequences for the mechanisms affecting thiol redox homeostasis, and it can be inferred by observing that [AuCQPQ]$PF_6$ (**1**) is more potent in inhibiting the enzymatic activity of flavoenzymes than [AuAQPQ]$PF_6$ (**2**). This supports the hypothesis that compound (**1**) is more prone to interact with flavoenzymes than compound (**2**); namely, [AuCQPQ]$PF_6$ (**1**) is liable to undergo a ligand exchange reaction [43,44] in the presence of flavoenzymes. While much work remains to be conducted to clearly define the gold(I) hybrids' effect on thiol redox homeostasis in parasite cells, we were intrigued to find that the metallic hybrids displayed selectivity for inhibiting Sec-TrxRs versus Cys-TrxR, indicating that the gold(I) compounds share some reactivity to interact with Sec-TrxR. This agrees with the prevailing model that the inhibitory activity of gold(I) compounds for flavoenzymes is explained by the kinetics of a ligand exchange reaction rather than the selective affinity of gold species for Sec versus Cys [35].

## 5. Conclusions and Perspectives

The [AuAQPQ]$PF_6$ (**2**) compound is of remarkable stability, of facile preparation and displays high potency and strong efficacy as a blood schizonticidal agent and of improved spectrum of activity against multiple stages of the *Plasmodium* life cycle. It achieves suppression of heme detoxification process, as inferred by drug binding to [Fe(III)PPIX] and β-hematin inhibitory activity (BHIA), and it may cause an imbalance in the thiol redox homeostasis of the parasite, as inferred by its inhibition on the enzymatic activity of flavoenzymes. Future work needs to determine the contribution of each mechanism (heme detoxification versus redox homeostasis) for hybrid antiparasitic activity, but the findings presented here indicate the mutual benefits of combining gold(I) to quinolines. Thus, this study provides compelling evidence that hybrid-based drugs featuring gold(I) as a chemical linker represent a potential approach for drug design.

**Supplementary Materials:** The following supporting information can be downloaded at: https://www.mdpi.com/article/10.3390/pharmaceutics14061251/s1. Figure S1. Infrared spectra for the quinolinic ligands and the [AuAQPQ]PF6 hybrid. Figure S2. 1H NMR (DMSO-d6, 298K, 500 MHz) of [AuAQPQ]PF6 hybrid. Figure S3. 1H NMR (DMSO-d6, 298K, 500 MHz) of the metal-free quinolines and of [AuAQPQ]PF6 hybrid. Figure S4. 13C NMR (DMSO-d6, 298K, 125 MHz) of the quinolinic ligands and of [AuAQPQ]PF6 hybrid. Figure S5. Expansion of 13C NMR (DMSO-d6, 298K, 125 MHz) in the aromatic region for the [AuAQPQ]PF6 hybrid. Figure S6. 13C-1H HMBC (DMSO-d6, 298K) of the [AuAQPQ]PF6 hybrid. Figure S7. 15N-1H HMBC (DMSO-d6, 298K) of the [AuAQPQ]PF6 hybrid. Figure S8. 15N-1H HMBC (DMSO-d6, 298K) of amodiaquine (AQ). Figure S9. 15N-1H HMBC (DMSO-d6, 298K) of primaquine (PQ). Figure S10. 31P{1H} NMR (DMSO-d6, 298K, 202 MHz) of the [AuAQPQ]PF6 hybrid. Figure S11. ESI-MS spectrum of the [AuAQPQ]PF6 hybrid. Figure S12. Stability of [AuAQPQ]PF6 hybrid in a DMSO-d6 solution at 298K monitored by 1H NMR (500 MHz). Figure S13. Evaluation of stability of [AuAQPQ]PF6 hybrid in a DMSO solution at 298K monitored by 31P{1H} (202 MHz). Figure S14. Formation of β-hematin monitored by IR and its inhibition by [AuAQPQ]PF6 hybrid (2). Figure S15. Interaction of compounds with reduced glutathione (GSH) at indicated time of incubation. Values are the mean ± S.D. from two independent experiments. GSH was detected using monochlorobimane and the percent of drug:GSH binding was determined in comparison to untreated samples (no drug). AuP = [AuClPPh3]. Figure S16. Evaluation of the interaction of the [AuAQPQ]PF6 hybrid and glutathione by H1-NMR (DMSO-d6:D2O/300:200 µL, 298K, 500 MHz).

**Author Contributions:** Study design, M.N. and D.R.M.M.; experimental work, C.D.S.P., H.C.Q., S.D., D.F., S.Y.A., M.G., M.E.B., I.F. and J.M.; writing—original draft preparation, C.D.S.P., D.R.M.M. and M.N.; writing—review and editing, S.Y.A., D.L.W., M.P., N.B., D.R.M.M., B.P. and M.N.; funding acquisition, D.L.W., M.P., N.B., D.R.M.M., B.P. and M.N. All authors have read and agreed to the published version of the manuscript.

**Funding:** C.S.P. and H.C.Q. were supported through a CAPES doctoral scholarship (Brazil). M.N. acknowledges FAPEMIG (grant APQ-01543-18, Brazil) and CNPq (grant 306009/2020-0, Brazil). D.R.M.M. acknowledges CNPq (grant 305732/2019-6, Brazil), FAPESB (grant APP0088/2016, Brazil) and Proep/Fiocruz (grant IGM-002-FIO-20-2-25, Brazil). M.P. was supported by grant PTDC-SAU-INF- 29550-2017 (FCT, Portugal). S.D.-A. and N.B. were supported by Fondazione Cariplo (grant 2017–0846, Italy), the Ministero dell'Istruzione, dell'Università e della Ricerca (grant PRIN 2015.4JRJPP_004, Italy) and the Ministero degli Affari Esteri e della Cooperazione Internazionale (Progetti di grande rilevanza, grant 00949–2018, Italy). S.Y.A., M.E.B., and D.L.W. were supported by US NIH/NIAID R33AI127635 (United States of America). B.P. was supported by the French Institute for Public Health Surveillance (Santé Publique France, grant CNR du Paludisme) and the Délégation Générale pour l'Armement (grant PDH-2-NRBC-4-B-4104).

**Institutional Review Board Statement:** The use of mice was approved by the animal ethics committee (Fiocruz Bahia, Brazil, protocol number 019/2021 approved in 29 January 2021).

**Informed Consent Statement:** Blood donor consent was waived since erythrocytes were used for *P. falciparum* culture and no personal data were collected.

**Data Availability Statement:** Supporting information is available enclosed.

**Acknowledgments:** The authors are thankful to Rodrigo M. Justo (UFJF, Brazil) for the valuable assistance in the determination of the elemental analyses and to Olívia Moreira and Marcone A. L. de Oliveira (UFJF, Brazil) for the valuable assistance in the determination of ESI-MS, supported through the MCT/FINEP/CT-INFRA 01/2013-REF 0633/13S grant. S.D.-A. and N.B. thank the Transfusion Medicine Service, Department of Laboratory Medicine, ASST Grande Ospedale Metropolitano Niguarda (Milan, Italy) for providing blood samples for the parasite culture. H.C.Q. and D.R.M.M. thank the flow cytometry facility at Fiocruz (Brazil) for data acquisition.

**Conflicts of Interest:** The authors declare no conflict of interest.

## References

1. World Malaria Report 2021. Available online: https://www.who.int/teams/global-malaria-programme/reports/world-malaria-report-2021 (accessed on 3 May 2022).
2. Penny, M.A.; Camponovo, F.; Chitnis, N.; Smith, T.A.; Tanner, M. Future use-cases of vaccines in malaria control and elimination. *Parasite Epidemiol. Control.* **2020**, *10*, e00145. [CrossRef] [PubMed]
3. Achan, J.; Mwesigwa, J.; Edwin, C.P.; D'Alessandro, U. Malaria medicines to address drug resistance and support malaria elimination efforts. *Expert Rev. Clin. Pharmacol.* **2017**, *11*, 61–70. [CrossRef] [PubMed]
4. Matiya, D.J.; Philbert, A.B.; Kidima, W.; Matowo, J.J. Dynamics and monitoring of insecticide resistance in malaria vectors across mainland Tanzania from 1997 to 2017: A systematic review. *Malar. J.* **2019**, *18*, 102. [CrossRef] [PubMed]
5. Available online: https://www.who.int/news/item/06-10-2021-who-recommends-groundbreaking-malaria-vaccine-for-children-at-risk (accessed on 27 September 2021).
6. Smith, P.W.; Diagana, T.T.; Yeung, B.K.S. Progressing the global antimalarial portfolio: Finding drugs which target multiple *Plasmodium* life stages. *Parasitology* **2014**, *141*, 66–76. [CrossRef]
7. Vandekerckhove, S.; D'hooghe, M. Quinoline-based antimalarial hybrid compounds. *Bioorg. Med. Chem.* **2015**, *23*, 5098–5119. [CrossRef]
8. Sampath Kumar, H.M.; Herrmann, L.; Tsogoeva, S.B. Structural hybridization as a facile approach to new drug candidates. *Bioorg. Med. Chem. Lett.* **2020**, *30*, 127514. [CrossRef]
9. Benoit-Vical, F.; Lelièvre, J.; Berry, A.; Deymier, C.; Dechy-Cabaret, O.; Cazelles, J.; Loup, C.; Robert, A.; Magnaval, J.F.; Meunier, B. Trioxaquines are new antimalarial agents active on all erythrocytic forms, including gametocytes. *Antimicrob. Agents Chemother.* **2007**, *51*, 1463–1472. [CrossRef]
10. Grellepois, F.; Grellier, P.; Bonnet-Delpon, D.; Bgu, J.P. Design, Synthesis and antimalarial activity of trifluoromethylartemisinin—Mefloquine dual molecules. *ChemBioChem* **2005**, *6*, 648–652. [CrossRef]
11. Çapci, A.; Lorion, M.M.; Wang, H.; Simon, N.; Leidenberger, M.; Silva, M.C.B.; Moreira, D.R.M.; Zhu, Y.; Meng, Y.; Chen, J.Y.; et al. Artemisinin-(Iso)quinoline hybrids by C-H activation and click chemistry: Combating multidrug-resistant malaria. *Angew. Chem. Int. Ed.* **2019**, *58*, 13066–13079. [CrossRef]
12. Ouji, M.; Nguyen, M.; Mustière, R.; Jimenez, T.; Augereau, J.M.; Benoit- Vical, F.; Deraeve, C. Novel molecule combinations and corresponding hybrids targeting artemisinin-resistant *Plasmodium falciparum* parasites. *Bioorg. Med. Chem. Lett.* **2021**, *39*, 127884. [CrossRef]
13. Pereira, C.S.; Quadros, H.C.; Moreira, D.R.M.; Castro, W.; Da Silva, R.I.S.D.; Soares, M.B.P.; Fontinha, D.; Prudêncio, M.; Schmitz, V.; Dos Santos, H.F.; et al. A Novel hybrid of chloroquine and primaquine linked by Gold(I): Multitarget and multiphase antiplasmodial agent. *ChemMedChem* **2021**, *16*, 662–678. [CrossRef] [PubMed]

14. Commons, R.J.; Simpson, J.A.; Thriemer, K.; Humphreys, G.S.; Abreha, T.; Alemu, S.G.; Añez, A.; Anstey, N.M.; Awab, G.R.; Baird, J.K.; et al. The effect of chloroquine dose and primaquine on *Plasmodium vivax* recurrence: A WorldWide Antimalarial Resistance Network systematic review and individual patient pooled meta-analysis. *Lancet Infect. Dis.* **2018**, *18*, 1025–1034. [CrossRef]
15. Gorka, A.P.; Jacobs, L.M.; Roepe, P.D. Cytostatic versus cytocidal profiling of quinoline drug combinations via modified fixed-ratio isobologram analysis. *Malar. J.* **2013**, *12*, 332. [CrossRef] [PubMed]
16. Cabrera, M.; Cui, L. In Vitro activities of primaquine-schizonticide combinations on asexual blood stages and gametocytes of *Plasmodium falciparum*. *Antimicrob. Agents Chemother.* **2015**, *59*, 7650–7656. [CrossRef] [PubMed]
17. Dembélé, L.; Franetich, J.F.; Soulard, V.; Amanzougaghene, N.; Tajeri, S.; Bousema, T.; van Gemert, G.J.; Le Grand, R.; Dereuddre-Bosquet, N.; Baird, J.K.; et al. Chloroquine potentiates primaquine activity against active and latent hepatic plasmodia ex vivo: Potentials and pitfalls. *Antimicrob. Agents Chemother.* **2020**, *65*, e01416-20. [CrossRef] [PubMed]
18. Maher, S.P.; Vantaux, A.; Chaumeau, V.; Chua, A.C.Y.; Cooper, C.A.; Andolina, C.; Péneau, J.; Rouillier, M.; Rizopoulos, Z.; Phal, S.; et al. Probing the distinct chemosensitivity of *Plasmodium vivax* liver stage parasites and demonstration of 8-aminoquinoline radical cure activity in vitro. *Sci. Rep.* **2021**, *11*, 19905. [CrossRef] [PubMed]
19. Camarda, G.; Jirawatcharadech, P.; Priestley, R.S.; Saif, A.; March, S.; Wrong, M.H.L.; Leung, S.; Miller, A.B.; Baker, D.A.; Alano, P.; et al. Antimalarial activity of primaquine operates via a two-step biochemical relay. *Nat. Commun.* **2019**, *10*, 3226. [CrossRef]
20. O'Neol, P.M.; Shone, A.E.; Stanford, D.; Nixon, G.; Asadollahy, E.; Park, B.K.; Maggs, J.L.; Roberts, P.; Stocks, P.A.; Biagini, G.; et al. Synthesis, antimalarial activity, and preclinical pharmacology of a novel series of 4′-fluoro and 4′-chloro analogues of amodiaquine. identification of a suitable "back-up" compound for n-tert-butyl isoquine. *J. Med. Chem.* **2009**, *52*, 1828–1844. [CrossRef]
21. Delves, M.; Plouffe, D.; Scheurer, C.; Meister, S.; Wittlin, S.; Winzeler, E.A.; Sinden, R.E.; Leroy, D. The activities of current antimalarial drugs on the life cycle stages of Plasmodium: A comparative study with human and rodent parasites. *PLoS Med.* **2012**, *9*, e1001169. [CrossRef]
22. Diawara, S.; Madamet, M.; Kounta, M.B.; Lo, G.; Wade, K.A.; Nakoulima, A.; Bercion, R.; Amalvict, R.; Gueye, M.W.; Fall, B.; et al. Confirmation of plasmodium falciparum in vitro resistance to monodesethylamodiaquine and chloroquine in Dakar, Senegal, in 2015. *Malar. J.* **2017**, *16*, 118. [CrossRef]
23. Sannella, A.R.; Casini, A.; Gabbiani, C.; Messori, L.; Bilia, A.R.; Vincieri, F.F.; Majori, G.; Severini, C. New uses for old drugs. Auranofin, a clinically established antiarthritic metallodrug, exhibits potent antimalarial effects in vitro: Mechanistic and pharmacological implications. *FEBS Lett.* **2008**, *582*, 844–847. [CrossRef] [PubMed]
24. Feng, L.; Pomel, S.; Latre de Late, P.; Taravaud, A.; Loiseau, P.M.; Maes, L.; Cho-Ngwa, F.; Bulman, C.A.; Fischer, C.; Sakanari, J.A.; et al. Repurposing auranofin and evaluation of a new gold(I) compound for the search of treatment of human and cattle parasitic diseases: From protozoa to helminth infections. *Molecules* **2020**, *25*, 5075. [CrossRef] [PubMed]
25. Ssemaganda, A.; Low, L.M.; Verhoeft, K.R.; Wambuzi, M.; Kawoozo, B.; Nabasumba, S.B.; Mpendo, J.; Bagaya, B.S.; Kiwanuka, N.; Stanisic, D.I.; et al. Gold(I) phosphine compounds as parasite attenuating agents for malaria vaccine and drug development. *Metallomics* **2018**, *10*, 444–454. [CrossRef] [PubMed]
26. Egan, T.J.; Mavuso, W.W.; Ross, D.C.; Marques, H.M. Thermodynamic factors controlling the interaction of quinoline antimalarial drugs with ferriprotoporphyrin IX. *J. Inorg. Biochem.* **1997**, *68*, 137–145. [CrossRef]
27. Müller, S.; Gilberger, T.W.; Färber, P.M.; Becker, K.; Schirmer, R.H.; Walter, R.D. Recombinant putative glutathione reductase of *Plasmodium falciparum* exhibits thioredoxin reductase activity. *Mol. Biochem. Parasitol.* **1996**, *80*, 215–219. [CrossRef]
28. Kanzok, S.M.; Schirmer, R.H.; Turbachova, I.; Iozef, R.; Becker, K. The thioredoxin system of the malaria parasite *Plasmodium falciparum*. Glutathione reduction revisited. *J. Biol. Chem.* **2000**, *275*, 40180–40186. [CrossRef] [PubMed]
29. Cheng, Q.; Arnér, E.S. Selenocysteine Insertion at a predefined UAG codon in a release factor 1 (RF1)-depleted Escherichia coli host strain bypasses species barriers in recombinant selenoprotein translation. *J. Biol. Chem.* **2017**, *292*, 5476–5487. [CrossRef]
30. Silvestri, I.; Lyu, H.; Fata, F.; Boumis, G.; Miele, A.E.; Ardini, M.; Ippoliti, R.; Bellelli, A.; Jadhav, A.; Lea, W.A.; et al. Fragment-based discovery of a regulatory site in thioredoxin glutathione reductase acting as "doorstop" for NADPH entry. *ACS Chem. Biol.* **2018**, *13*, 2190–2202. [CrossRef]
31. Lyu, H.; Petukhov, P.A.; Banta, P.R.; Jadhav, A.; Lea, W.A.; Cheng, Q.; Arnér, E.S.J.; Simeonov, A.; Thatcher, G.R.J.; Angelucci, F.; et al. Characterization of lead compounds targeting the selenoprotein thioredoxin glutathione reductase for treatment of schistosomiasis. *ACS Infect. Dis.* **2020**, *6*, 393–405. [CrossRef]
32. Geary, W.J. The use of conductivity measurements in organic solvents for the characterisation of coordination compounds. *Coord. Chem. Rev.* **1971**, *7*, 81–122. [CrossRef]
33. Ribbiso, K.A.; Heller, L.E.; Taye, A.; Julian, E.; Willems, A.V.; Roepe, P.D. Artemisinin-based drugs target the plasmodium falciparum heme detoxification pathway. *Antimicrob. Agents Chemother.* **2021**, *65*, e02137-20. [CrossRef] [PubMed]
34. Jortzik, E.; Becker, K. Thioredoxin and glutathione systems in *Plasmodium falciparum*. *Int. J. Med. Microbiol.* **2012**, *302*, 187–194. [CrossRef] [PubMed]
35. Angelucci, F.; Sayed, A.A.; Williams, D.L.; Boumis, G.; Brunori, M.; Dimastrogiovanni, D.; Miele, A.E.; Pauly, F.; Bellelli, A. Inhibition of *Schistosoma mansoni* thioredoxin-glutathione reductase by auranofin: Structural and kinetic aspects. *J. Biol. Chem.* **2009**, *284*, 28977–28985. [CrossRef] [PubMed]

36. Saccoccia, F.; Angelucci, F.; Boumis, G.; Brunori, M.; Miele, A.E.; Williams, D.L.; Bellelli, A. On the mechanism and rate of gold incorporation into thiol-dependent flavoreductases. *J. Inorg. Biochem.* **2012**, *108*, 105–111. [CrossRef] [PubMed]
37. Garg, A.; Prasad, B.; Takwani, H.; Jain, M.; Sing, S. Evidence of the formation of direct covalent adducts of primaquine, 2-tert-butylprimaquine (NP-96) and monohydroxy metabolite of NP-96 with glutathione and N-acetylcysteine. *J. Chromatogr. B* **2011**, *879*, 1–7. [CrossRef]
38. Capela, R.; Cabal, G.G.; Rosenthal, P.J.; Gut, J.; Mota, M.M.; Moreira, R.; Lopes, F.; Prudêncio, M. Design and evaluation of primaquine-artemisinin hybrids as a multistage antimalarial strategy. *Antimicrob. Agents Chemother.* **2011**, *55*, 4698–4706. [CrossRef]
39. Miranda, D.; Capela, R.; Albuquerque, I.S.; Meireles, P.; Paiva, I.; Nogueira, F.; Amewu, R.; Gut, J.; Rosenthal, P.J.; Oliveira, R.; et al. Novel endoperoxide-based transmission-blocking antimalarials with liver- and blood-schizontocidal activities. *ACS Med. Chem. Lett.* **2013**, *5*, 108–112. [CrossRef]
40. Bray, P.G.; Hawley, S.R.; Ward, S.A. 4-Aminoquinoline resistance of *Plasmodium falciparum*: Insights from the study of amodiaquine uptake. *Mol. Pharmacol.* **1996**, *50*, 1551–1558.
41. Dodd, E.L.; Tazoo, D.; Bohle, D.S. Solution and solid state correlations of antimalarial drug actions: NMR and crystallographic studies of drug interactions with a heme model. *Inorg. Chem.* **2017**, *56*, 7803–7810. [CrossRef]
42. Olafson, K.N.; Nguyen, T.Q.; Vekilov, P.G.; Rimer, J.D. Deconstructing quinoline-class antimalarials to identify fundamental physicochemical properties of beta-hematin crystal growth inhibitors. *Chemistry* **2017**, *23*, 13638–13647. [CrossRef]
43. Goetzfried, S.K.; Kapitza, P.; Gallati, C.M.; Nindl, A.; Cziferszky, M.; Hermann, M.; Wurst, K.; Kircher, B.; Gust, R. Investigations of the reactivity, stability and biological activity of halido (NHC)gold(I) complexes. *Dalton Trans.* **2022**, *51*, 1395–1406. [CrossRef] [PubMed]
44. Zou, T.; Lum, C.T.; Lok, C.N.; Zhang, J.J.; Che, C.M. Chemical biology of anticancer gold(III) and gold(I) complexes. *Chem. Soc. Rev.* **2015**, *44*, 8786–8801. [CrossRef] [PubMed]

*pharmaceuticals*

MDPI

*Article*

# Studies of Potency and Efficacy of an Optimized Artemisinin-Quinoline Hybrid against Multiple Stages of the *Plasmodium* Life Cycle

**Helenita C. Quadros [1], Aysun Çapcı [2], Lars Herrmann [2], Sarah D'Alessandro [3], Diana Fontinha [4], Raquel Azevedo [4], Wilmer Villarreal [5], Nicoletta Basilico [6], Miguel Prudêncio [4], Svetlana B. Tsogoeva [2,*] and Diogo R. M. Moreira [1,*]**

1 Instituto Gonçalo Moniz, Fundação Oswaldo Cruz (Fiocruz), Salvador 40296-710, Brazil; helenita_quadros@hotmail.com
2 Organic Chemistry Chair I and Interdisciplinary Center for Molecular Materials (ICMM), Friedrich-Alexander University of Erlangen-Nürnberg, Nikolaus Fiebiger-Straße 10, 91058 Erlangen, Germany; aysun.capci@icloud.com (A.Ç.); lars.herrmann@fau.de (L.H.)
3 Dipartimento di Scienze Farmacologiche e Biomolecolari, Università degli Studi di Milano, 20133 Milan, Italy; sarah.dalessandro@unimi.it
4 Instituto de Medicina Molecular, Faculdade de Medicina, Universidade de Lisboa, Av. Prof. Egas Moniz, 1649-028 Lisboa, Portugal; dfontinha@medicina.ulisboa.pt (D.F.); raquel.azevedo@medicina.ulisboa.pt (R.A.); mprudencio@medicina.ulisboa.pt (M.P.)
5 Grupo de Química Inorgânica Medicinal e Reações Aplicadas, Instituto de Química, Universidade Federal do Rio Grande do Sul (UFRGS), Porto Alegre 91501-970, Brazil; wilmer.villarreal@ufrgs.br
6 Dipartimento di Scienze Biomediche, Chirurgiche e Odontoiatriche, Universitá degli Studi di Milano, 20133 Milan, Italy; nicoletta.basilico@unimi.it
* Correspondence: svetlana.tsogoeva@fau.de (S.B.T.); diogo.magalhaes@fiocruz.br (D.R.M.M.)

**Abstract:** A recently developed artemisinin-quinoline hybrid, named 163A, has been shown to display potent activity against the asexual blood stage of *Plasmodium*, the malaria parasite. In this study, we determined its in vitro cytotoxicity to mammalian cells, its potency to suppress *P. berghei* hepatic infection and to decrease the viability of *P. falciparum* gametocytes, in addition to determining whether the drug exhibits efficacy of a *P. berghei* infection in mice. This hybrid compound has a low level of cytotoxicity to mammalian cells and, conversely, a high level of selectivity. It is potent in the prevention of hepatic stage development as well as in killing gametocytes, denoting a potential blockage of malaria transmission. The hybrid presents a potent inhibitory activity for beta-hematin crystal formation, in which subsequent assays revealed that its endoperoxide component undergoes bioactivation by reductive reaction with ferrous heme towards the formation of heme-drug adducts; in parallel, the 7-chloroquinoline component has binding affinity for ferric hemin. Both structural components of the hybrid co-operate to enhance the inhibition of beta-hematin, and this bitopic ligand property is essential for arresting the growth of asexual blood parasites. We demonstrated the in vivo efficacy of the hybrid as an erythrocytic schizonticide agent in comparison to a chloroquine/artemisinin combination therapy. Collectively, the findings suggest that the bitopic property of the hybrid is highly operative on heme detoxification suppression, and this provides compelling evidence for explaining the action of the hybrid on the asexual blood stage. For sporozoite and gametocyte stages, the hybrid conserves the potency typically observed for endoperoxide drugs, and this is possibly achieved due to the redox chemistry of endoperoxide components with ferrous heme.

**Keywords:** malaria; *Plasmodium*; hemozoin; heterobivalent; artemisinin; hybrids



**Citation:** Quadros, H.C.; Çapcı, A.; Herrmann, L.; D'Alessandro, S.; Fontinha, D.; Azevedo, R.; Villarreal, W.; Basilico, N.; Prudêncio, M.; Tsogoeva, S.B.; et al. Studies of Potency and Efficacy of an Optimized Artemisinin-Quinoline Hybrid against Multiple Stages of the *Plasmodium* Life Cycle. *Pharmaceuticals* **2021**, *14*, 1129. https://doi.org/10.3390/ph14111129

Academic Editor: Pascal Sonnet

Received: 18 October 2021
Accepted: 3 November 2021
Published: 6 November 2021



## 1. Introduction

Malaria, caused by the unicellular pathogen *Plasmodium*, still represents a major public health problem worldwide. In the last few years, the overall number of cases and estimated

deaths due to malaria has remained constant rather than declined [1]. This is most likely due to a combination of factors, including interruption of public health and basic assistance, civil wars, resistance to multiple drug therapies, massive movement of refugees, and changes in climate conditions [2]. Yet, in 2019, 27 countries were able to eliminate malaria transmission, a remarkable number in comparison to only six countries in 2000. This outcome is most likely due to a solid implementation of public health programs to combat malaria using insecticide-treated mosquito nets and newer antimalarial medicines [1–3].

Many scientific studies spanning from basic parasitology to applied pharmacology have been performed to understand how antimalarial medicines work and how the parasites can escape treatment through drug resistance mechanisms [4,5]. Among them, the obligate parasite's heme detoxification process has received considerable attention [6,7]. An example of masterly evolutionary adaptation by an intracellular parasitic pathogen, the parasite digests at least 80% of red blood cell hemoglobin as it grows inside the unfriendly environment of mature and/or immature human red blood cells, depending on the species. Hemoglobin digestion releases cytotoxic ferrous heme (iron II protoporphyrin, $Fe^{II}$-PPIX), which is oxidized to ferric hematin (iron III protoporphyrin, $Fe^{III}$-PPIX) and detoxified by crystallization to an inert form known as hemozoin (Hz, also known as malaria pigment) which is harmless to the parasite [6,7]. This detoxification process essentially converts a soluble iron-containing molecule into an insoluble β-hematin dimer, which then adds to growing Hz crystals [6,7]. As the parasite grows and destroys human red blood cells, lysed cells release Hz crystals into the bloodstream, where Hz is sequestered and deposited within the deep endothelial vasculature. Mounting evidence has shown that tissue inflammation that typically accompanies the disease is in part due to Hz deposition in the inflammatory infiltrate. This is associated with the acute stage of malaria, which may present severe manifestations [4,8].

*Plasmodium* is one of only three genera on the planet that produce Hz and depends on its formation as a mechanism of heme detoxification [6,7]. Hz appears as a unique target for antimalarial drug therapies, as the pharmacological blockage of this process is deleterious for parasite survival. This has been the main mode of action of antimalarial quinolines quinine, chloroquine, and amodiaquine, among other drugs used for treating patients, for many decades. These drugs slow the growth of the parasite by targeting multiple steps of the heme detoxification (Figure 1). The underlying mechanisms this action may include: targeting the soluble ferric hematin to result in an augmentation of free hematin levels, which is cytotoxic for parasites; targeting the soluble ferric hematin by forming even more cytotoxic drug–heme complexes; and finally adsording the drugs to the Hz crystal surfaces, blocking its growth. All these mechanisms involve drug binding to ferric hematin, which ultimately leads to an increase in the levels of the exchangeable heme species [9,10]. In contrast, antimalarial peroxides, such as artemisinins and ozonides, lack strong affinity for ferric hematin but undergo a mandatory process of activation that entails drug bioreduction through a redox reaction with intracellular ferrous heme, involving intermediate radical species and ultimately producing heme-drug adducts [11–14]. New compelling evidence has shown that the intermediate species can cause a radical-induced protein alkylation by leading to inactivation of proteins essential for the parasite survival, whereas the heme-drug adducts are cytotoxic to the parasites by suppressing the heme detoxification process [15].

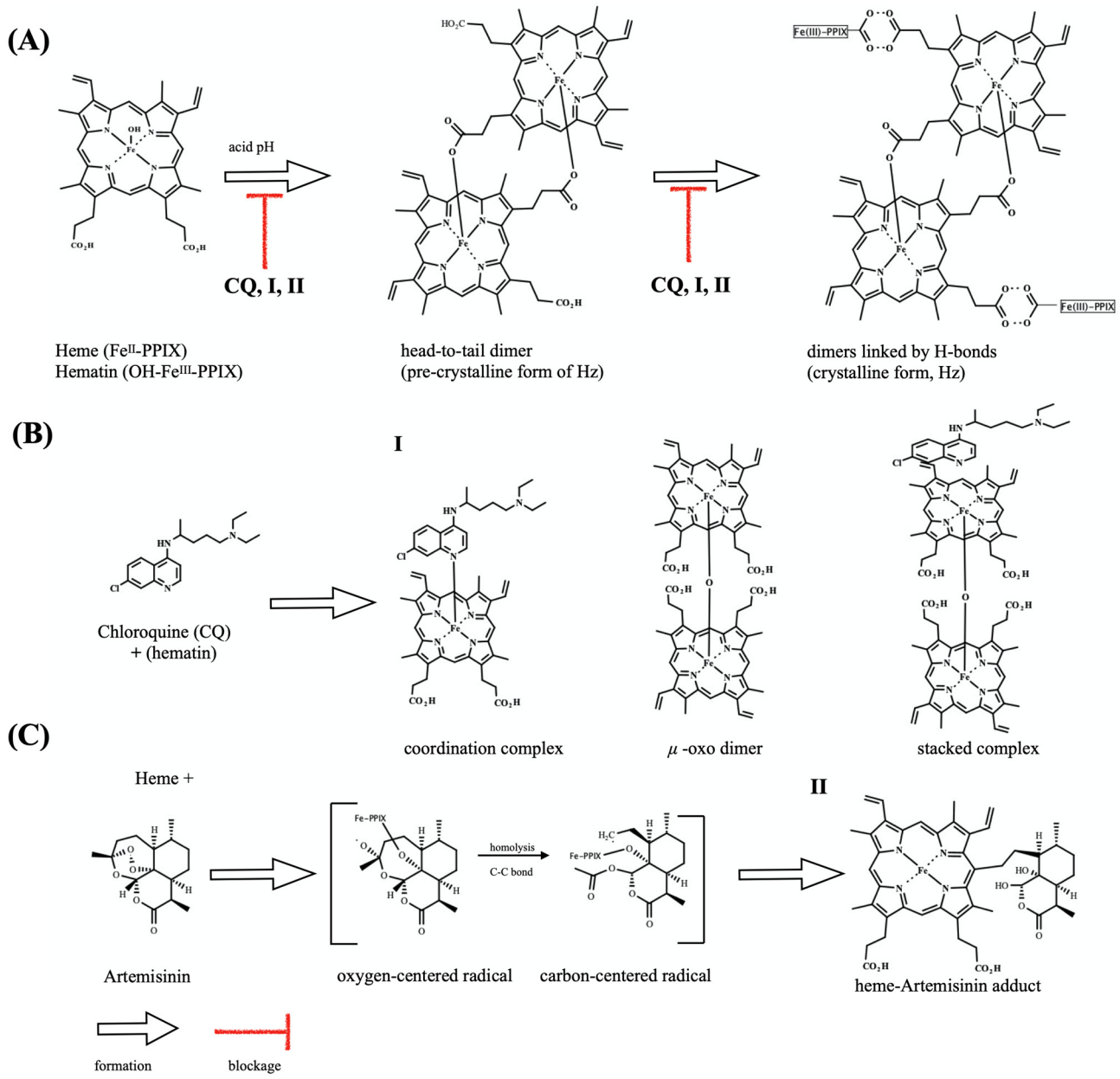


**Figure 1.** Overview of the heme detoxification process and drug blockage. (**A**) shows the dimerization of hematin through the reciprocal coordination of iron and propionate moieties and subsequent formation of hydrogen-bonds between dimers to form hemozoin (Hz) crystals. (**B**) shows the structure of chloroquine (CQ) and its speciation in the presence of hematin. Formation of hematin species μ-oxo-dimer is induced under CQ exposure and does not form Hz crystals. (**C**) shows the structure of antimalarial endoperoxide artemisinin, and its bioreductive activation by heme, leading to radical species responsible for alkylation of proteins as well as of Fe-PPIX. After alkylation, there occurs formation of a heme-artemisinin adduct. Unless specified, iron is in its ferric state.

In this context, the combination of antimalarial peroxides with antimalarial quinolines offers a unique possibility of spanning multiple ways to suppress heme detoxification and simultaneously act through an irreversible mechanism of alkylation of essential parasite proteins to ultimately achieve the antiplasmodial activity. Yet, the parasite may be able to escape this therapy through drug resistance mechanisms. To overcome this, different strategies have been considered, such as the addition of a third drug partner [16], prolonged therapy [17], improved pharmaceutical formulations [18], and chemically conjugation of drug partners [19,20]. The last strategy typically includes the molecular hybridization of

antimalarial structures towards a single molecule of bitopic ligand property (i.e., bivalency in regard to pharmacophore property), which can offer a simpler pharmacokinetic profile than that of drug combinations while conserving the pleiotropic antimalarial effects of the drug combination [21,22].

We and others have demonstrated that various classes of antimalarial compounds can be hybridized with antimalarial peroxides such as artemisinins and ozonides to form hybrid-based drugs, resulting in potent activity due to summation of effects [13,23–29]. To identify the optimal position for molecular combination and the chemical linkers for molecular hybridization, we recently launched a campaign to design peptide-cleavable linkers, non-cleavable linkers, and molecular combinations by using refined synthetic methodologies [27,29]. This work resulted in the discovery of a potent antimalarial hybrid of artemisinin and 7-chloroquinoline, the hybrid-based drug named 163A [29] (Figure 2). The 163A hybrid presented superior potency for the asexual blood stage of *P. falciparum* in comparison with established single drugs. Furthermore, the potent in vitro antimalarial activity of 163A was translated into excellent efficacy against *P. berghei* in a mouse model, revealing higher efficacy than established single drugs [29]. Despite the progress achieved by this and other antimalarial hybrid-based drugs in recent years, little is known regarding the drug profiling towards stages of the *Plasmodium* life cycle other than the asexual blood stage. Another fundamental question relies on whether hybrid-based drugs, theoretically designed as heterobivalent molecules, can indeed exhibit a bitopic ligand property on heme detoxification process by simultaneously displaying affinity for ferric hematin, as classically observed for quinolines, as well as undergo redox chemistry reactivity with ferrous heme, as typically observed for endoperoxide antimalarials like artemisinin. Here, we aimed to study the antiplasmodial therapeutic breadth and drug activity profile for this hybrid-based drug and to assess its potency and efficacy compared to those of established single drugs or drug combinations.

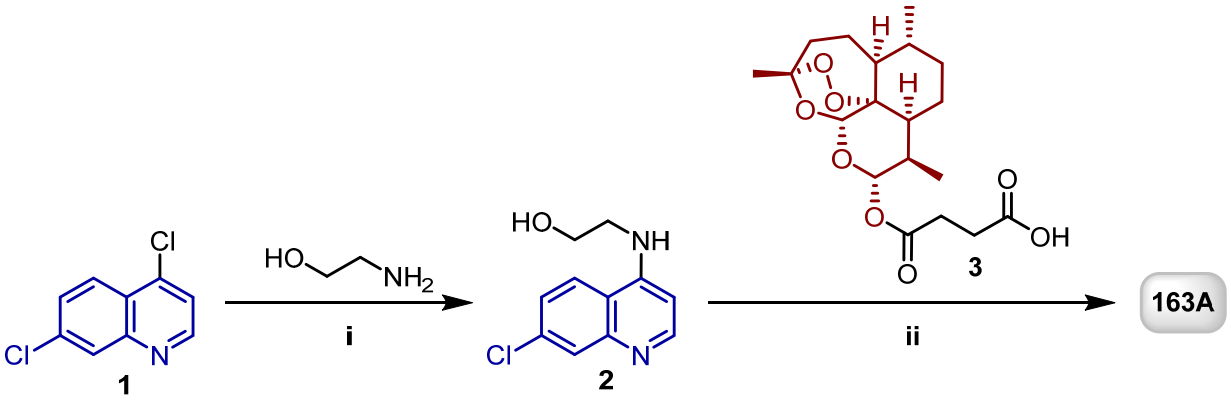


(**A**)

| Compounds | Drug-sensitive 3D7 | Drug-sensitive Dd2 | Drug-resistant K1 |
|---|---|---|---|
| Quinoline **2** | 760 | 1600 | 2400 |
| Artesunic acid **3** | 14.4 ± 2.0 | 10.9 ± 0.7 | 5.2 ± 0.8 |
| Artemisinin | 26.8 ± 2.4 | 11.3 ± 1.8 | 5.4 ± 0.5 |
| Hybrid 163A | 4.5 ± 0.5 | 2.3 ± 0.6 | 1.7 ± 0.3 |

(**B**)

**Figure 2.** (**A**) shows the synthesis of artemisinin and 7-chloroquinoline hybrid 163A. Reagents and conditions: (i) $Et_3N$, 120 °C, 2 h; (ii) DCC, DMAP, $CH_2Cl_2$, 0 °C to rt, 18 h, $N_2$. (**B**) shows a table summarizing the $IC_{50}$ values in nM against the asexual blood stage of *P. falciparum*. Adapted with permission from ref. [29]. Copyright 2019 John Wiley & Sons, Inc.

## 2. Results

### *2.1. Toxicity for Host Cells and Selectivity*

The 163A hybrid has been previously shown to inhibit *P. falciparum* parasite growth by both CQ-sensitive and CQ-resistant strains of the asexual blood stage [29]. We sought to assess the cytotoxicity of 163A by using both J774 (a non-cancerous macrophage cell line) and HepG2 (hepatic cells as potential host for sporozoites) lineages under the same conditions used to determine antimalarial potency. Toxicity of 163A was assayed in parallel to established single antimalarial drugs artemisinin and chloroquine as representative parental drug components of 163A, and doxorubicin was used as a standard cytotoxic drug. These experiments were subsequently used to estimate an in vitro selectivity index (S.I.), which measures the 163A concentration resulting in 50% cytotoxicity ($CC_{50}$) over the concentration needed for 50% parasite growth inhibition ($IC_{50}$) (Figure 3).

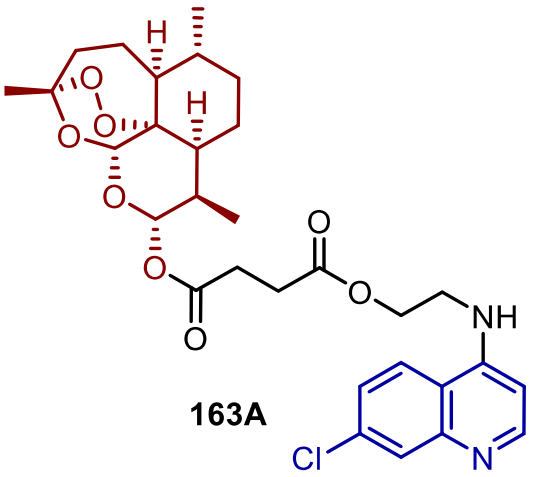


(**A**)

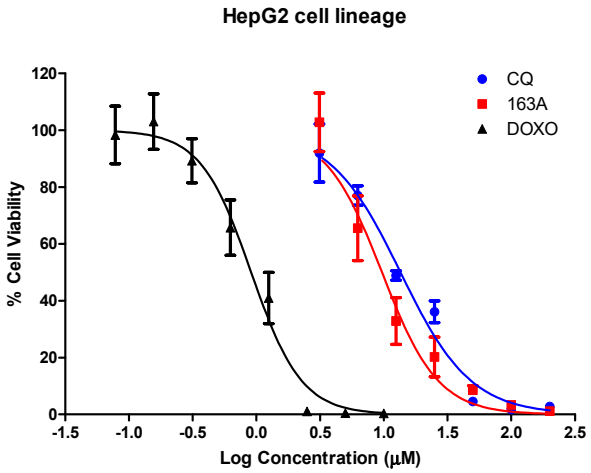


(**B**)

| Compounds | Chloroquine | Artemisinin | 163A | Doxorubicin |
|---|---|---|---|---|
| **Cell lines** | **Cytotoxicity ($CC_{50}$ ± S.D., μM)** | | | |
| HepG2 [a] | 12.1 ± 2.0 | 9.9 ± 2.4 | 9.8 ± 0.2 | 0.6 ± 0.5 |
| J774 [a] | 87.1 ± 18.2 | >200 | 28.7 ± 5.7 | 1.3 ± 0.3 |
| **Cell lines** | **Selectivity index (S.I.)** | | | |
| HepG2 [b] | 952 | 369 | 2177 | N.D. |
| J774 [b] | 6858 | 7463 | 6378 | N.D. |

(**C**)

**Figure 3.** (**A**) Molecular structure of hybrid-based drug 163A highlighting the main structural components. (**B**) Uninfected HepG2 cells were cultured in the presence of the compound (163A, parental or reference drugs) for 72 h. Cell viability was detected by the ATP activity in the cell lysates by CellTiter-Glo. Data were normalized to the signal from untreated cells, which was set at 100% cell viability, and data were fit to a logistic curve by Prism version 5.01. (**C**) shows a Table with a summary of cytotoxic concentration for 50% ($CC_{50}$) and selectivity index values. Footnotes for table: [a] Values are median ± S.D. of at least three independent experiments, each concentration tested in triplicate. [b] Selectivity index determined as $CC_{50}/IC_{50}$; values of $IC_{50}$ performed for asexual blood stage of 3D7 strain of *P. falciparum* and determined after 72 h incubation time. CQ = chloroquine diphosphate; DOXO = doxorubicin. S.D. = standard deviation; N.D. = not determined.

Like the parental drugs, 163A hybrid showed cytotoxicity for non-infected cells in the micromolar range, being at least 15 fold less cytotoxic than anticancer agent doxorubicin. Next, we determined the S.I. for the individual components and observed that in HepG2 cells, the 163A hybrid is 3 to 4 fold more selective than parental drugs. For J774 cells, 163A hybrid exhibited twice more cytotoxicity than chloroquine, whereas artemisinin is devoid of cytotoxicity in concentrations up 200 μM. Despite superior cytotoxicity than parental drugs, the 163A hybrid is still several fold less cytotoxic than anticancer agent

doxorubicin. For selectivity index calculated for J774 cells, the 163A hybrid and its parental drugs presented a similar selectivity. The molecular hybridization of artemisinin and 7-chloroquinoline towards the 163A hybrid did not negatively affect the toxicity profile when compared to parental drugs. A previous study has suggested an augmentation of the toxicity profile of antimalarial hybrids in comparison to the parental drugs, possibly related to the chemical nature of the linker [26], however, we can infer that the chemical linker, employed on 163A structure, has cytocompatibility to a cellular environment.

### *2.2. Inhibition on Hepatic and Sexual Stages*

In addition to its activity against the parasite's asexual blood stages, it is desirable for a novel antimalarial agent to also demonstrate activity against the hepatic stage of infection, which is obligatory for the onset of blood infection and, depending on the parasite species, can be involved in disease relapses (as is the case of *P. vivax* infection) [30,31]. Additionally, activity against the sexual blood stages of *Plasmodium* is desirable for a novel antimalarial, as these stages are involved in parasite transmission to the invertebrate host [32,33]. To address this, we used an in vitro model of Huh-7 hepatic cells infected with *P. berghei* sporozoites to determine the activity of 163A against hepatic infection [34]. For the sexual blood stage of *P. falciparum* 3D7 strain, a standard protocol for gametocytogenesis was employed [35], and gametocyte viability was measured by bioluminescence of luciferase (Figure 4).

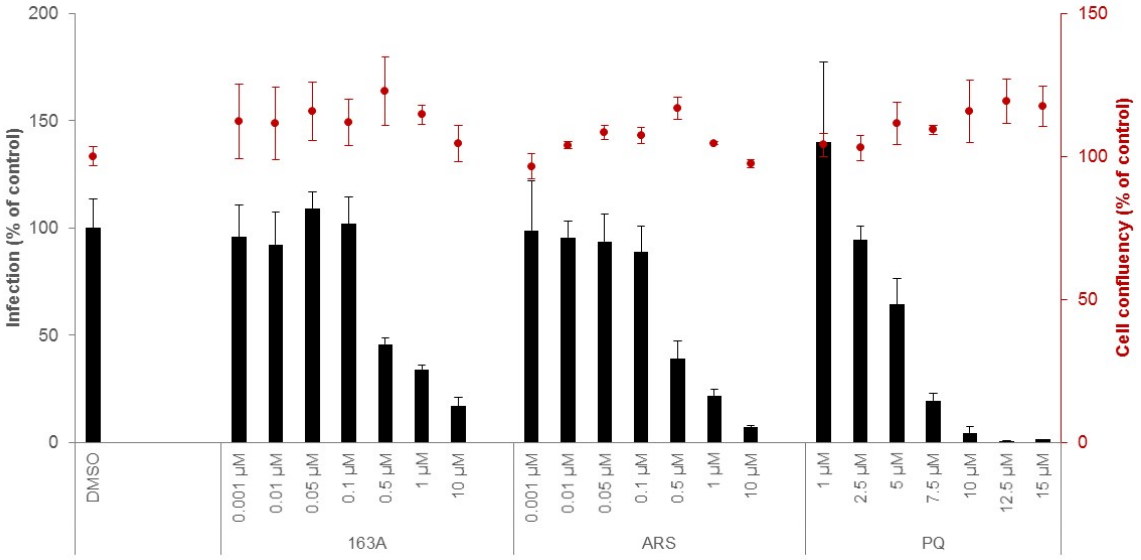


(**A**)

| Parasite stage | IC$_{50}$ (nM) for compounds | | | |
|---|---|---|---|---|
| | **Chloroquine** | **Artesunate** | **Dihydroartemisinin** | **163A** |
| Hepatic (sporozoites) [a] | 15,000 | 390 | N.D. | 350 |
| Sexual (gametocytes I–III) [b] | N.D. | N.D. | 14.0 ± 1.1 | 37.3 ± 5.1 |
| Sexual (gametocytes V) [c] | >20,000 | N.D. | 2785 ± 40.3 | 5195 ± 2544 |

(**B**)

**Figure 4.** Characterization of 163A in vitro activity against hepatic sporozoites and sexual blood stage. (**A**) shows the % of infection (left y axis) and host cell confluency (right y axis) of Huh-7 cells infected by *P. berghei* sporozoites. (**B**) shows a table with a summary of inhibitory concentration for 50% (IC$_{50}$) for multiple stages of the *Plasmodium* life cycle. Experimental details (footnotes in the table): [a] Activity was determined after 48 h of drug incubation. Two independent experiments were performed; values are mean of one experiment, each concentration tested in triplicate. Reference drug is primaquine (IC$_{50}$ = 4700 nM). [b] Assayed against gametocytes at stages I to III of 3D7elo1-pfs16-CBG99 strain of *P. falciparum* and activity was determined after 72 h of drug incubation. [c] Assayed against gametocytes at V stage and the reference drug is Methylene blue (IC$_{50}$ = 60 ± 10 nM). [b,c] Values are mean ± S.D. of three experiments, each concentration tested in duplicate. ART = artesunate; PQ = primaquine. N.D. = not determined.

Our results show that 163A inhibits hepatic infection but has no impact on the viability of the host hepatic cells. In terms of potency, it is 10-fold more potent to inhibit *Plasmodium* liver schizont development than the standard drug in the therapy (primaquine) and it is as potent as artesunate. In marked contrast, the parental drug artemisinin has low inhibitory activity for liver schizonts [36,37] and dihydroartemisinin has variable inhibitory activity depending on *Plasmodium* species and host, in part due to its low stability [38]. In addition, 4-aminoquinolines such as chloroquine present low potency in the hepatic stage of *Plasmodium* infection [39], suggesting that the observed inhibitory activity of 163A against this phase of the parasite's life cycle can be attributed to the molecule's endoperoxide compartment.

Next, an assessment of the effect of 163A on the viability of gametocytes was performed for young (stages I to III) and mature gametocytes (stage V). For young gametocytes, results showed that this was strongly inhibited by both dihydroartemisinin and the 163A hybrid, with $IC_{50}$ values in low nanomolar range and similar to observed for $IC_{50}$ values against the asexual blood stage. In contrast, both compounds presented potency in micromolar range for mature gametocytes. For both young and mature gametocytes, the 163A hybrid was 2- to 3-fold less potent than dihydroartemisinin, whereas chloroquine is at least 20-fold less potent than dihydroartemisinin for arresting viability in mature gametocytes. Based on this, it is possible to deduce that the 163A hybrid preserves the gametocyte killing property typically observed for antimalarial endoperoxides.

### *2.3. Dual Role on the Heme Detoxification Process*

The bitopic ligand property of the 163A hybrid is related to the feasibility of endoperoxide to target ferrous heme and the 7-chloroquinoline to target ferric hematin, possibly generating a single heterobivalent molecule able to display a dual role in the heme detoxification process. The 163A hybrid has been shown to inhibit β-hematin formation and to suppress the in vivo parasite heme detoxification [29]; however, this heterobivalency property was not previously examined in terms of 163A targeting ferrous heme and its underlying redox chemistry reactivity. To examine this heterobivalency property (Figure 5), we employed a recent methodology that allows the simultaneous examination of β-hematin inhibitory activity (BHIA) under an oxidizing condition (ferric hematin) and under a reducing condition (ferrous heme) [40], in addition to determining the association constant of drugs for ferric hematin (log *K*) [41].

The 163A hybrid greatly inhibited β-hematin formation assayed using the conventional ferric hematin by displaying a potency twice as high as chloroquine, whereas artemisinin lacked inhibitory activity. The 163A hybrid was as potent as chloroquine in inhibiting β-hematin formation under ferrous heme and it was only slightly less potent than artemisinin, which is a strong inhibitor assayed in the presence of ferrous heme. The inhibitory activity on the β-hematin formation was higher when assayed for ferrous heme than ferric hematin, which is also a behavior observed for 7-chloroquinoline [40]. Other hybrid-based drugs have displayed potency equal or superior to parental drug and antimalarial quinolines of reference, such as amodiaquine and chloroquine [13,26]. Consistent with this notion and based on a model of structural determinants for 7-chloroquinolines inhibiting β-hematin formation [42], a plausible reason for increased inhibitory potency of hybrid for β-hematin crystal formation is a combination of binding affinity of 7-chloroquinoline component for ferric Fe-PPIX and the chemical linker playing a role as a side chain by assisting further binding property.

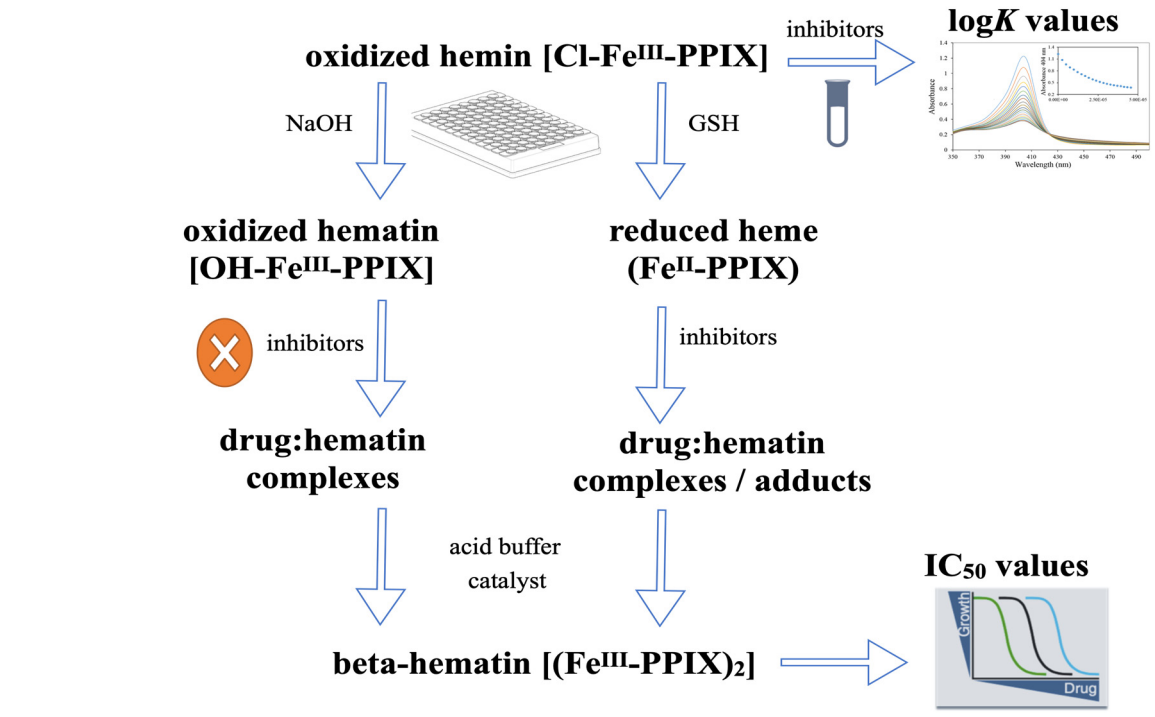


(**A**)

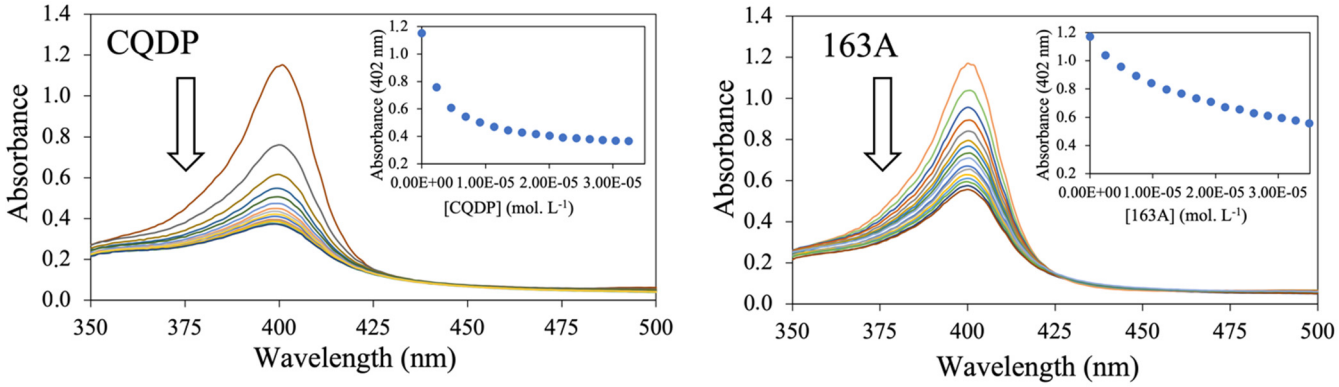


(**B**)

| Compounds | log*K* (mean ± S.D.)[a] | β-hematin inhibitory activity (IC$_{50}$ ± S.E.M. (mM)[b] | |
|---|---|---|---|
| | | oxidized-BHIA | reduced-BHIA |
| Chloroquine | 5.55 ± 0.02 | 0.23 ± 0.04 | 0.13 ± 0.03 |
| Artemisinin | N.D. | >1.0 | 0.06 ± 0.01 |
| 163A | 4.72 ± 0.03 | 0.13 ± 0.05 | 0.10 ± 0.03 |
| Primaquine | N.D. | >1.0 | >1.0 |

(**C**)

**Figure 5.** Dual role of 163A on the *Plasmodium* heme detoxification. (**A**) shows the experimental assays of β-hematin inhibitory activity (BHIA) for oxidized-BHIA and reduced-BHIA and subsequent assays. (**B**) shows titration of hemin to increasing concentration of drugs. Spectrophotometric characterization of hemin–drug complexes upon increasing drug concentration is indicated by the arrow. (**C**) is a table summarizing the association constant (log*K*) values of compounds for ferric hemin and inhibitory concentration for 50% (IC$_{50}$) values of compounds for oxidized-BHIA and reduced-BHIA. Experimental details for table: [a] Log*K* values were calculated from three independent experiments. [b] IC$_{50}$ were calculated from three independent experiments after 18 h of drug incubation. S.E.M. = standard error of the mean values. CQDP = chloroquine diphosphate; GSH = glutathione, reduced. N.D. = not determined due to lack of binding.

To understand the reason for the 163A hybrid to inhibit β-hematin formation in an oxidizing condition, measurement of the association constant for ferric hematin (log *K*) was determined. Titration of the 163A hybrid to ferric hemin revealed that it has binding affinity by suggesting a hematin–drug complexation, with a log *K* value lower than observed for chloroquine, whereas artemisinin did not exhibit binding property. This result indicates that binding of 163A to ferric hemin is weaker than to chloroquine. Literature has shown the aminoalkyl side chain of chloroquine is essential for its binding to Fe-PPIX [42] and based on this, a formal possibility is that the chemical linker of the 163A hybrid may not reproduce an optimal binding affinity as observed for chloroquine. Furthermore, the speciation of hematin–drug complexation observed in titration experiments may not be the same as observed for β-hematin assays, justifying the increased potency of hybrid for inhibiting β-hematin formation than chloroquine.

### *2.4. Parasitemia Profile in P. berghei-Infected Mice*

Typically, a single drug therapy requires a much higher dose for curing established infection (Thompson test) than suppressing onset infection (Peters test). However, 163A has previously demonstrated success as an efficacious antimalarial by observing that the same 163A dosage for suppressing parasitemia also presented curative potential in an established infection [29]. As a limitation, 163A treatment was previously studied by subcutaneous administration, which is an optimal route of high absorption for lipophilic drugs such as artemisinin, but here, we wanted to determine in a more stringent way whether 163A could result in a decline in parasitemia and could cure mice when administered by intraperitoneal injection, a route of drug administration that is typically employed for severe malaria patients. In *P. berghei*-infected Swiss mice with a patent parasitemia > 3.0%, we evaluated in a 3-day dose regime at 140 μmol/kg of 163A or a fixed-dose drug combination (chloroquine plus artemisinin). Twenty-four hours after cession of treatment (day 9 post-infection), parasitemia was measured in different intervals, in addition to a follow up of animal survival up to 40 days post-infection.

As observed in Figure 6, 163A was efficacious at inhibiting parasitemia in comparison to the untreated group, with a reduction larger than 89% at the peak of parasitemia. In the group receiving the drug combination, parasitemia reduction was > 99% in comparison to the untreated group, which is consistent with the notion that this drug combination has summation of efficacies on reducing parasitemia in *P. berghei*-infected mice [43]. Importantly, we found that 24 h after cession of treatment, 163A or drug combination treatment was able to decrease parasitemia, a feature typically observed for artemisinin but not for chloroquine. The period of maximum parasitemia reduction for 163A was 96 h posttreatment. Recrudescent parasite was monitored daily and observed at day 14 for 163A therapy and at day 19 for drug combination. The median survival time was twice as high for the drug combination in comparison to the untreated group or the group receiving 163A treatment.

Consistent with previous reports in the Thompson malaria model [43,44], therapy using a single antimalarial drug given once-a-day does not cure mice. Exceptions are the therapies of high-dose regimens, multiple daily doses, drug combinations, and specific route of administration (such as the subcutaneous administration for highly lipophilic drugs). Based on this, we inferred that in comparison to subcutaneous administration, intraperitoneal administration of 163A at the same dose regime provides a sharp decline of parasitemia; however, with intraperitoneal administration this drug dosage is not enough to resolve infection and cure mice. In addition, we inferred that the non-superior efficacy of 163A observed in comparison to drug combinations is probably because the 7-chloroquinoline component from the 163A structure is a less potent antimalarial than chloroquine employed in the drug combination [29].

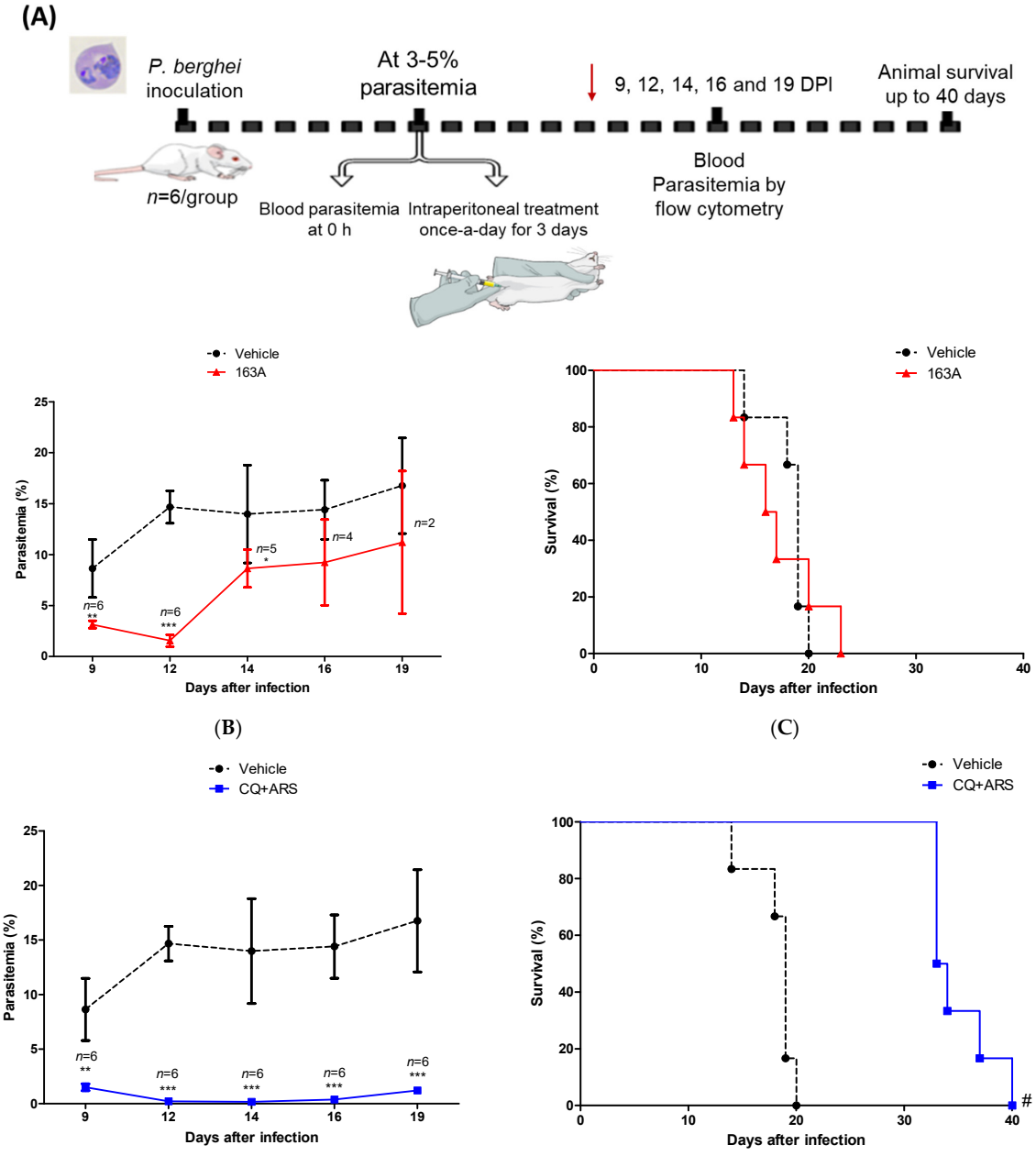


| Groups | Dose µmol/kg (mg/kg) | Parasitemia Inhibition (%) | Median of Animal Survival (days) | Number of Mice Alive after 40 dpi |
|---|---|---|---|---|
| Vehicle | - | - | 19 | 0/6 (0) |
| 163A | 140 (82.5) | 89.4 ± 1.5 | 16.5 | 0/6 (0) |
| CQ + ARS | 140 | >99 | 33.5 | 0/6 (0) |

(F)

**Figure 6.** Efficacy of 163A in an established *Plasmodium* infection in mice. (**A**) Experimental design of Thompson therapy test. (**B**,**D**) Parasitemia profile in *P. berghei*-infected Swiss mice following therapy once-a-day by intraperitoneal administration of 163A or a fixed-dose drug combination (CQ + ARS). (**C**,**E**) Animal survival of *P. berghei*-infected Swiss mice following therapy. (**F**). Summary of parasite reduction and median of animal survival. Values are from one single experiment, using $n = 6$/group. Parasitemia inhibition was determined in comparison to vehicle, values are median ± S.D. Error bars indicate S.D. * $p < 0.01$, ** $p < 0.001$, *** $p < 0.0001$ (One-way ANOVA) versus vehicle; $^{\#}$ $p = 0.0007$ (Log-rank and Mantel-Cox test) for CQ + ARS versus vehicle. DPI = days post-infection. Red arrow in panel A indicates the last day of drug administration.

## 3. Discussion

The presented findings of potency and selectivity of hybrid 163A as an antimalarial agent for the multiple stages of *Plasmodium* life cycle, illustrated in Figure 7, argues in favor of drug development of hybrid-based drugs in comparison to single antimalarial drugs. For asexual blood stage of *P. falciparum*, hybrid 163A presents superior potency and higher selectivity indexes in comparison to single antimalarial drugs. We interpreted that both components, 7-chloroquinoline and endoperoxide, can suppress the heme detoxification process, which is a biochemical process highly active in the asexual blood stage. For sexual and hepatic stages, hybrid 163A presents potency and selectivity indexes in comparison to endoperoxide drugs artesunate/dihydroartemisinin, whereas the quinoline component is typically devoid of antiparasitic activity for these stages.

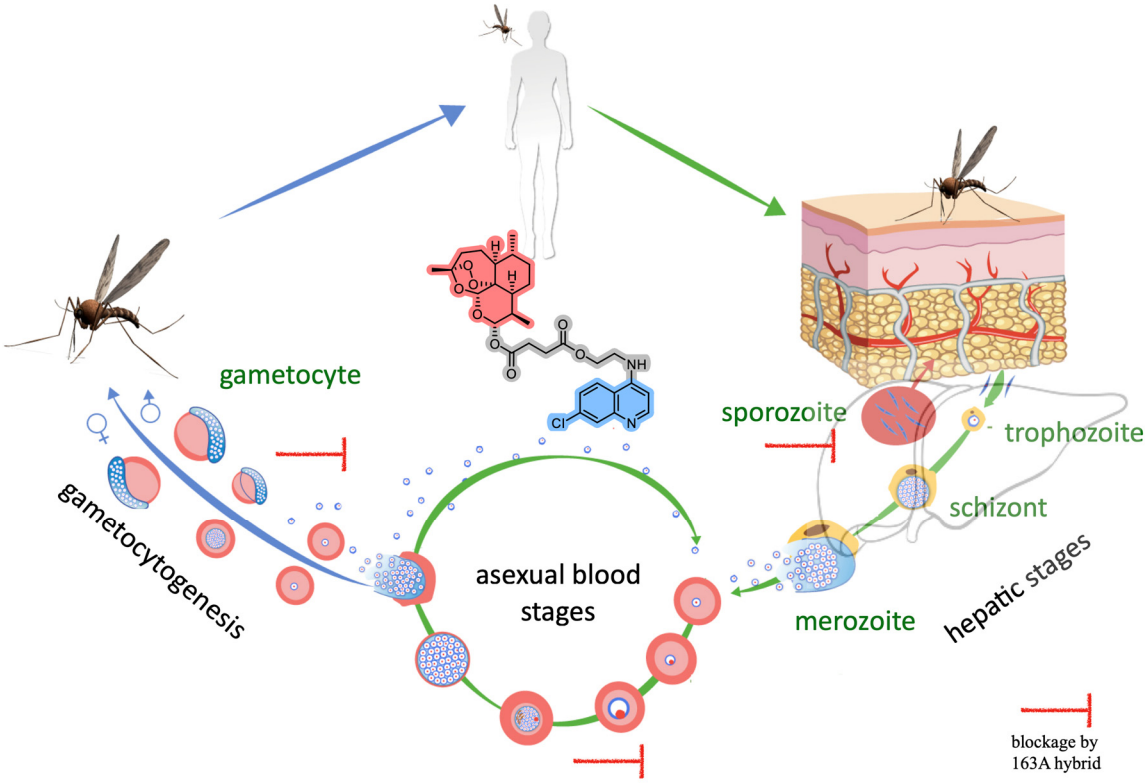


**Figure 7.** Overview of *Plasmodium* life cycle, denoting the three stages where the antimalarial activity of the 163A hybrid blocks the parasite growth and viability.

For the asexual blood stage, the heme detoxification process is an important drug target. It has been well known for decades that 4-aminoquinolines such as chloroquine and amodiaquine strongly suppress this process in multiple ways and target soluble ferric hematin and adsorb on surfaces of hemozoin crystals [6,7]. However, only in recent years has it become clear that antimalarial endoperoxides, such as artemisinin and ozonides, can suppress the heme detoxification process by a redox chemical process involving ferrous heme towards the formation of heme-drug adducts. This not only leads to a depletion of cytosolic heme levels and alters iron redox homeostasis but also produces heme-drug adducts that are endogenous antiparasitics [16]. Based on this, a more compelling hypothesis is that the enhanced antimalarial profile, i.e., the summation of effects by additivity or a synergism phenomenon, for drug combination between 4-aminoquinolines and endoperoxides is in part due to pleiotropic effects on the heme detoxification. The summation of effects has important consequences for antimalarial activity at the asexual blood stage. Consistent with this notion, the 163A hybrid presents superior potency, higher selectivity indexes, and stronger efficacy in comparison to single antimalarial drugs. Our experimental approach

using multiples assays on soluble Fe-PPIX and β-hematin crystal formation, which is a compelling model to study the *Plasmodium* heme detoxification, argues that both components, 7-chloroquinoline and endoperoxide, can simultaneously act to suppress the heme detoxification process.

We observed that 163A has a potent antiparasitic activity against the liver stage. Typically, 8-aminoquinolines such as primaquine and tafenoquine have antiparasitic activity for the liver stage [45] whereas 4-aminoquinolines are devoid ofantiparasitic activity for this stage. For antimalarial endoperoxides, artemisinin lacks inhibitory activity for the liver stage when assayed up to 10 μM, whereas artesunate and artemisone inhibit liver schizonts [37]. Based on this, we can infer that the 163A hybrid activity is mostly due to the presence of the endoperoxide compartment, as artesunate is active whereas chloroquine is not. It was previously observed that an artemisinin/primaquine hybrid-based drug containing a cleavable-linker displayed enhanced potency and efficacy for *Plasmodium* liver stage in comparison to an analogous hybrid containing a non-cleavable-linker or to single parental drugs [36], which is in line with the observations disclosed here for hybrid 163A. Our data indicate that the hybrid can preserve the activity against the liver stage of antimalarial endoperoxides, which is a remarkable feature if considering not all antimalarial endoperoxides can inhibit liver stage parasites. Moreover, considering the importance of this stage for controlling infection and relapse, further investigation into the potency and efficacy of the 163A hybrid is required to address whether it fully eliminates liver stage parasites or solely delays their development.

We further observed that the 163A hybrid has a strong antiparasitic activity for young gametocytes, with potency comparable to dihydroartemisinin, the reference drug in the assay. The potency of these compounds for young gametocytes is very close to the asexual blood stage, denoting a potential for blocking parasite development towards mature gametocytes and possibly reducing gametocyte carriage in patients. Our findings are consistent with a previously described hybrid-based drug composed of 1,2,4-trioxane and quinoline that exhibited stronger activity for gametocytes than the quinoline component and the same potency as its endoperoxide component [23].

For less metabolically active sexual parasites in stage V, endoperoxide compounds as well as other clinically relevant antimalarials typically require a higher drug concentration to kill them [35,46,47]; an exception is the experimental drug methylene blue. Although certainly the 163A hybrid and dihydroartemisinin have inferior efficiency against late stage, of note, both drugs presented $IC_{50}$ values ranging 2–5 μM, whereas the maximum concentration of dihydroartemisinin in patient serum is approximately 4 μM [48], a concentration closer to $IC_{50}$ values necessary for killing mature gametocytes. Furthermore, we have inferred that, as in the liver stage, the activity against gametocytes is greatly influenced by the endoperoxide component, as chloroquine is devoid of gametocytocidal activity. To fully assess 163A action on late stage, further experiments using exflagellation are necessary, but to date the potency of 163A against immature gametocytes denotes a potential for blocking malaria transmission to the invertebrate host.

Regarding the mode of action, the heme detoxification process is one of the parasite targets for 163A against asexual blood stages, followed by a 163A bioreductive activation through heme towards the process of radical-induced protein alkylation [29]. For the mode of action against the liver and sexual stages, this remains less clear. Gametocytes are nonreplicating and lack substantial hemozoin synthesis as compared to the asexual blood stage; in addition, in the liver stage, the hepatic cells have less abundant cytosolic heme than red blood cells, which is necessary for bioreductive activation of artemisinin by heme. Despite differences in parasite metabolism and heme abundance within the *Plasmodium* life cycle, a plausible explanation is that antimalarial endoperoxides, including hybrid 163A, may arrest parasite growth by the same mechanism of drug bioreductive activation *via* heme and alkylation of proteins and heme. Apart from this mechanism, another plausible explanation for the preserved or even superior potency of hybrid-based drugs in comparison to single quinoline drugs is the enhanced lipophilicity for the hybrid 163A in

comparison to parental drugs, possibly enhancing drug permeability and accumulation. In line with this, a recent work has indicated that enhanced lipophilicity is an important aspect for explaining superior antimalarial activity of homobivalent drugs based on artemisinin dimers in comparison to monomers [49].

Previously, we demonstrated the superior efficacy of 163A therapy in comparison to single antimalarial drugs [29]. Here, we extended the efficacy profile by testing 163A therapy using intraperitoneal administration, performed in parallel to a group receiving a fixed-dose of drug combination. Both therapies produced a sharp decline in parasitemia in comparison to untreated infected mice, and the drug combination therapy was able to prolong animal survival. The 163A therapy demonstrated non-superior efficacy to drug combination and the reason for this could be that the in vivo metabolization of ester chemical linker of 163A hybrid to yield the 7-chloroquinoline component (compound 2, Figure 2) [29]. At least in vitro, this 7-chloroquinoline component is a less potent antimalarial agent than the quinoline component of the drug combination (chloroquine). The non-superior efficacy of hybrid-based therapy versus drug combination has also been observed by others [23,24], and this profile does not undermine the antimalarial potential of this class of drugs. The initial concept of hybrid-based therapy was to replace fixed-dose drug combinations [50]; however, a new potential use is to replace one of the components of drug combinations with a hybrid-based drug.

## 4. Materials and Methods

### *4.1. General Materials*

Chloroquine diphosphate, artemisinin, and hemin chloride (BioXtra) were obtained from Sigma-Aldrich (St. Louis, MO, USA). Primaquine phosphate was manufactured by FarManguinhos (Rio de Janeiro, Brazil). May-Grunwald-Giemsa stain was obtained from the Panotico (Laborclin, Pinhais, Brazil). Tribromoethanol was supplied from Sigma-Aldrich (St. Louis, MO, USA) and dissolved in 2-propanol:water 20% (*v*/*v*). All other general laboratory chemicals and solvents were of analytical or HPLC grade. Experimental drug 163A was synthesized and purified as previously described [29].

### *4.2. Cytotoxicity Assay in Mammalian Cells*

Compounds were tested for in vitro cytotoxicity against two mammalian cell lineages, J774 (murine macrophages) and HepG2 (human hepatocellular carcinoma), and cellular viability was determined by bioluminescence using CellTiter-Glo kit (Promega, Madison, USA). Lineages were maintained in RPMI-1640 (hepG2) or DMEM (J774) containing 10% fetal bovine serum and supplemented with L-glutamine, vitamins, and amino acids in 75-cm$^2$ flasks at 37 °C, with the medium changed twice weekly. Cells from 60 to 80% confluent cultures were trypsinized, washed in complete medium, and plated at 4 × 10$^4$ cells per well in 100 µL of complete medium in 96-well flat-bottom white plates for 24 h at 37 °C prior to the addition of the compounds. Triplicate aliquots of compounds and the reference drugs (stock solution in DMSO) covering 7 different concentrations (200–3.125 µM) at 2-fold dilutions were added to the wells, and plates were incubated for 72 h more. Controls included compound-free wells with DMSO (vehicle) as positive controls and cell-free wells with medium only, which were used for background subtraction. Following incubation for 72 h at 37 °C, plates were maintained at room temperature, the culture medium was removed, and a 100 µL volume of CellTiter-Glo kit was added to each well. The bioluminescence was measured using a microplate reader Filtermax™ F3 & F5 Multi-Mode instrument (Molecular Devices, San Jose, USA) and Softmax software. $CC_{50}$ data were obtained from at least two independent experiments for each cell line and analyzed using GraphPad Prism Version 5.01. The selectivity index (S.I.) was calculated using the $CC_{50}$s from mammalian cells divided by the $IC_{50}$ obtained against the asexual blood stage *P. falciparum* 3D7.

### *4.3. P. berghei Liver Stage*

Human hepatoma cell line (Huh-7) cells were cultured in 1640 RPMI medium supplemented with 10% $v/v$ fetal bovine serum, 1% $v/v$ nonessential amino acids, 1% $v/v$ penicillin/streptomycin, 1% $v/v$ glutamine, and 10 mM HEPES, pH 7, and maintained at 37 °C with 5% $CO_2$. Huh-7 cells at $1.0 \times 10^4$ per well were seeded in 96-well plates the day before drug treatment and infection. The medium was replaced by medium containing the appropriate concentration of each compound approximately 1 h prior to infection with sporozoites of firefly luciferase-expressing *P. berghei* line freshly obtained through disruption of salivary glands of infected female *Anopheles stephensi* mosquitoes. An amount of the DMSO solvent equivalent to that present in the highest compound concentration was used as a control. Sporozoite addition was followed by centrifugation at $1700\times g$ for 5 min. Parasite infection load was measured 48 h after infection by a bioluminescence assay (Biotium, Hayward, CA, USA). The effect of the compounds on the viability of Huh-7 cells was assessed by the AlamarBlue assay (Life) using the manufacturer's protocol.

### *4.4. P. falciparum Gametocytes*

Drugs were serially diluted in a 96-well flat bottom plate (concentration range 29.0–0.22 µM) in 100 µL per well, and each drug was tested in duplicate, in seven different concentrations. A volume of 100 µL of *P. falciparum* gametocytes from the luminescent strain 3D7elo1-pfs16-CBG99 (stages I to III or stage V) at 0.5–1% parasitemia and 2% hematocrit were dispensed. For mature gametocytes, a culture containing more than 90% of stage V gametocytes was employed. Methylene blue was used as positive control. Luciferase activity was used for measuring gametocyte viability. Plates were incubated for 72 h at 37 °C under 1% $O_2$, 5% $CO_2$, and 94% $N_2$ atmosphere. A volume of 100 µL of culture medium was removed from each well to increase hematocrit, and 70 µL of resuspended culture were transferred to a black 96-well plate. A volume of 70 µL of D-luciferin (1 mM in citrate buffer 0.1 M, pH 5.5) was added. Luminescence measurements were performed after 10 min with 500 ms integration time using a microplate reader Sinergy 4 (Biotek). The $IC_{50}$ was extrapolated from the non-linear regression analysis of the concentration–response curve. The percentage of gametocytes viability was calculated as $100 \times$ [(OD treated sample − OD blank)/(OD untreated sample − µc-blank)] where "blank" is the sample treated with 500 nM of methylene blue, which completely kills gametocytes.

### *4.5. β-Hematin Inhibition Activity (BHIA)*

A 10 µL sample of hemin chloride at 4 mM dissolved in 80% DMSO was aliquoted to a U bottom 96-well microplate. A 10 µL sample of 0.1 M NaOH (O-BHIA) or a 4 mM reduced glutathione in PBS at pH 7.0 (R-BHIA) was then added and plates were sealed and incubated at 37 °C for 2 h. A 10 µL sample of drug dissolved in DMSO were added and after incubation for 2 h, 180 µL of acetate buffer (2.0 M, pH 5.2) and 10 µL of nonionic detergent IGEPAL-CA-630 solution in methanol (10 mg/mL) were added, plates were sealed and incubated at 37 °C for 18 h. Each drug was tested in a range from 1000 to 17 µM at final concentration. The reaction was stopped by the addition of 50 µL of a sodium dodecyl sulfate (5.0% $v/v$ in 0.1 M bicarbonate buffer at pH 9.0). Plates were centrifuged at 3700 rpm for 5 min., and a 100 µL of supernatant was placed on a separate plate containing 100 µL/well of a pyridine solution (20% $v/v$ in HEPES 1 M) according to a previous method [51]. Absorbance was quantified at 405 nm using a SpectraMax 190 microplate reader (Molecular Devices, Sunnyvale, CA). The percentage of inhibition was compared to untreated and unreacted controls (no acetate buffer), and $IC_{50}$ values were estimated by using a non-linear regression curve calculated in GraphPad Prism. At least two independent experiments were performed, each concentration in quadruplicate.

### *4.6. Determination of the Association Constant to Ferriprotoporphyrin IX*

The association constant of compounds to ferriprotoporphyrin IX (hemin chloride) was measured essentially as previously described [41]. Titration of a 2 mL solution (7.5 µM

of ferriprotoporphyrin IX in 40% of DMSO, apparent pH 7.5) in presence of compound (500 μM in 40% of DMSO, pH 7.5) was performed by UV absorbance at λ = 402 nm using Hewlett Packard spectrophotometer, diode array model 8452 (Santa Clara, CA, USA). The volume of each titration was 5 μL, and the relative molar ratio varied from 0 to 10 with regard to [$Fe^{III}$-PPIX]. Spectra were recorded about 1 min after each addition. The absorption of all compounds was subtracted by adding the same amounts to the blank (40% of DMSO, pH 7.5). Fitting model with a 1:1 drug:association was used by the equation described by Egan [41]:

$$A = A_0 + A\,K_\infty\,[C]$$

$$1 + K\,[C]$$

where $A_0$ is the absorbance of hemin before addition of complex or free chloroquine, $A_\infty$ is the absorbance for the drug-hemin complex at saturation, A is the absorbance at each point of the titration, and *K* is the conditional association constant. Three independent experiments were performed.

### *4.7. Mice*

Male Swiss mice (4 to 8 weeks old) for experimental study were obtained from the Animal Resource Facility at Instituto Gonçalo Moniz (Salvador, Brazil). Male or female BALB/c mice (7 to 8 weeks old) were used for weekly passage of malaria parasites. Animals were housed under a 12-h light/dark cycle with free access to sterilized food pellets and sterilized water. These studies were approved by the Instituto Gonçalo Moniz Animal Ethics Committee (protocol 014/2018).

### *4.8. Parasites*

Drug-sensitive *P. berghei* parasites expressing green fluorescent protein (GFP) [52] were maintained by continuous weekly blood passage in Swiss mice. Mouse was euthanized by tribromoethanol (300 mg/kg animal weight), blood was collected by cardiac puncture, and a standard inoculum of $10^7$ parasitized erythrocytes per 200 μL was prepared by dilution in 0.9% saline and administered by intraperitoneal (i.p.) injection to experimental mice. Parasite enumeration in infected mice was determined in the peripheral blood collected from the tail veins. For determination of parasitemia in passage mice, blood smears were mounted in slides and stained by May-Grunwald-Giemsa. For experimental study, parasite enumeration was performed by flow cytometry using GFP signal and co-staining with 5.0 nM of Mitotracker deep red FM (Life Invitrogen) for 15 min. of incubation.

### *4.9. P. berghei-Infected Mice (Thompson Test)*

Male Swiss mice were inoculated with a $2 \times 10^6$ parasitized erythrocytes per 200 μL by i.p. injection. After infection reaches a parasitemia between 3 to 5% (determined by flow cytometry, BD LSRFortessa™ Cell Analyzer, Piscataway, NJ, USA), mice were randomly divided in *n* = 6/group and treated once-a-day per 100 μL by i.p. injection of respective drug or vehicle for three consecutive days. Drugs were solubilized in DMSO and diluted in a solution of Kolliphor (Cremophor, 4%), Polysorbate 80 (5%), Sorbitol (5%), glucose (5%), and Tween 20 (5%) in 0.9% saline to a final concentration of 10% (*v*/*v*) of DMSO. Experimental compound 163A was administered at 140 μmol/kg of animal weight (82.5 mg/kg), a fixed-dose of drug combination (chloroquine plus artemisinin) was administered at 140 μmol/kg of animal weight (using 70 μmol/kg each drug), and the untreated group received vehicle only. Twenty-four hours after the last drug administration, parasitemia was determined in regular intervals for 5 days. Animal survival was monitored twice a day for 40 days after infection. Parasitemia reduction was determined in comparison to the vehicle drug. One single experiment was performed.

### *4.10. Statistical Analysis*

Data are presented as median ± standard error of the mean (S.E.M.) or mean ± standard deviation (S.D.). Statistical analysis was performed using the Prism version 5.01 software (GraphPad Software, La Jolla, CA, USA). Statistical significance was assessed by performing the one-way analysis of variance (ANOVA) followed by post-test for multiple comparisons as indicated in each figure. Differences with $p$ values < 0.05 were considered significant.

## 5. Conclusions

We found that 163A has low cytotoxicity for host cells and has a broad inhibition profile spanning the *Plasmodium* life cycle, including hepatic stage and gametocytes, which indicates a potential of this drug to block malaria transmission. The broad spectrum of antimalarial activity is achieved in part because the hybrid has pleiotropic effects on the heme detoxification, targeting both ferrous heme and ferric hematin. The efficacy of the hybrid is strong, superior to single antimalarial drugs, such as quinolines or artemisinins, and it is only reproduced when heterobivalent structures or a combination of drugs are employed. These findings support the continuation of drug development towards a single molecule with heterobivalency properties into antiparasitics for combating *Plasmodium* infection. The safety and potential of antimalarial profile of hybrid 163A merits further investigation of pharmacokinetics and efficacy in drug combination regimens.

**Author Contributions:** Study design, S.B.T. and D.R.M.M.; experimental work, H.C.Q., A.Ç., L.H., D.F., R.A., W.V. and S.D.; writing—original draft preparation, H.C.Q. and D.R.M.M.; writing—review and editing, M.P., N.B., S.B.T. and D.R.M.M.; funding acquisition, M.P., N.B., S.B.T. and D.R.M.M. All authors have read and agreed to the published version of the manuscript.

**Funding:** H.C.Q. work was supported through a CAPES doctoral scholarship (Finance Code 001, Brazil). S.B.T. acknowledges the Deutsche Forschungsgemeinschaft (DFG) for funding (grant number TS87/17-1; TS87/23-1, Germany) and the Bavarian State Ministry for Science, Research and Art (Germany). D.R.M.M. acknowledges CNPq (grant No. 305732/2019-6, Brazil), FAPESB (grant number APP0088/2016, Brazil), and Fiocruz/Proep (grant number IGM-002-FIO-20-2-25, Brazil). M.P. was supported by grant PTDC-SAU-INF-29550-2017 (FCT, Portugal). S.D. and N.B. were supported by the by Fondazione Cariplo (grant number 2017-0846), the Ministero dell'Istruzione, dell'Università e della Ricerca (grant number PRIN 2015.4JRJPP_004), and the Ministero degli Affari Esteri e della Cooperazione Internazionale (Progetti di grande rilevanza, grant number 00949-2018). W.J.V.P. acknowledges FAPERGS (grant number ARD#21/2551-0000686-2).

**Institutional Review Board Statement:** The use of mice was approved by the animal ethics committee (Fiocruz Bahia, Brazil, protocol number 014-2018).

**Informed Consent Statement:** Blood donor consent was waived since erythrocytes were used for P. falciparum culture and no personal data were collected.

**Data Availability Statement:** Data is contained within the article.

**Acknowledgments:** S.D. and N.B. thank AVIS Comunale Milano for providing blood samples for parasite culture. H.C.Q. and D.R.M.M. thank the flow cytometry at Fiocruz for data acquisition.

**Conflicts of Interest:** The authors declare no conflict of interest.

## References

1. Tam, G.; Cowling, B.J.; Maude, R.J. Analysing human population movement data for malaria control and elimination. *Malar. J.* **2021**, *20*, 294. [CrossRef] [PubMed]
2. Lindsay, S.W.; Thomas, M.B.; Kleinschmidt, I. Threats to the effectiveness of insecticide-treated bednets for malaria control: Thinking beyond insecticide resistance. *Lancet Glob. Health* **2021**, *9*, e1325–e1331. [CrossRef]
3. Hughes, E.; Wallender, E.; Ali, A.M.; Jagannathan, P.; Savic, R.M. Malaria PK/PD and the Role Pharmacometrics Can Play in the Global Health Arena: Malaria Treatment Regimens for Vulnerable Populations. *Clin. Pharm. Ther.* **2021**, *110*, 926–940. [CrossRef]
4. Moxon, C.A.; Gibbins, M.; McGuinness, D.; Milner, D.A.; Marti, M. New Insights into Malaria Pathogenesis. *Annu. Rev. Pathol. Mech. Dis.* **2020**, *15*, 315–343. [CrossRef] [PubMed]

5. Duffey, M.; Blasco, B.; Burrows, J.N.; Wells, T.N.; Fidock, D.A.; Leroy, D. Assessing risks of Plasmodium falciparum resistance to select next-generation antimalarials. *Trends Parasitol.* **2021**, *37*, 709–721. [CrossRef] [PubMed]
6. De Villiers, K.A.; Egan, T.J. Heme Detoxification in the Malaria Parasite: A Target for Antimalarial Drug Development. *Accounts Chem. Res.* **2021**, *54*, 2649–2659. [CrossRef]
7. Kapishnikov, S.; Hempelmann, E.; Elbaum, M.; Als-Nielsen, J.; Leiserowitz, L. Malaria Pigment Crystals: The Achilles′ Heel of the Malaria Parasite. *ChemMedChem* **2021**, *16*, 1515–1532. [CrossRef]
8. Hanscheid, T.; Egan, T.J.; Grobusch, M.P. Haemozoin: From melatonin pigment to drug target, diagnostic tool, and immune modulator. *Lancet Infect. Dis.* **2007**, *7*, 675–685. [CrossRef]
9. Openshaw, R.; Maepa, K.; Benjamin, S.J.; Wainwright, L.; Combrinck, J.M.; Hunter, R.; Egan, T.J. A Diverse Range of Hemozoin Inhibiting Scaffolds Act on Plasmodium falciparum as Heme Complexes. *ACS Infect. Dis.* **2021**, *7*, 362–376. [CrossRef]
10. Olafson, K.N.; Nguyen, T.Q.; Rimer, J.D.; Vekilov, P.G. Antimalarials inhibit hematin crystallization by unique drug–surface site interactions. *Proc. Natl. Acad. Sci. USA* **2017**, *114*, 7531–7536. [CrossRef]
11. Garah, F.B.-E.; Wong, M.H.-L.; Amewu, R.K.; Muangnoicharoen, S.; Maggs, J.L.; Stigliani, J.-L.; Park, B.K.; Chadwick, J.; Ward, S.A.; O'Neill, P.M. Comparison of the Reactivity of Antimalarial 1,2,4,5-Tetraoxanes with 1,2,4-Trioxolanes in the Presence of Ferrous Iron Salts, Heme, and Ferrous Iron Salts/Phosphatidylcholine. *J. Med. Chem.* **2011**, *54*, 6443–6455. [CrossRef] [PubMed]
12. Creek, D.J.; Charman, W.N.; Chiu, F.C.K.; Prankerd, R.J.; Dong, Y.; Vennerstrom, J.L.; Charman, S.A. Relationship between Antimalarial Activity and Heme Alkylation for Spiro- and Dispiro-1,2,4-Trioxolane Antimalarials. *Antimicrob. Agents Chemother.* **2008**, *52*, 1291–1296. [CrossRef] [PubMed]
13. Loup, C.; Lelièvre, J.; Benoit-Vical, F.; Meunier, B. Trioxaquines and Heme-Artemisinin Adducts Inhibit the In Vitro Formation of Hemozoin Better than Chloroquine. *Antimicrob. Agents Chemother.* **2007**, *51*, 3768–3770. [CrossRef] [PubMed]
14. Wang, J.; Zhang, C.-J.; Ni Chia, W.; Loh, C.C.Y.; Li, Z.; Lee, Y.M.; He, Y.; Yuan, L.-X.; Lim, T.K.; Liu, M.; et al. Haem-activated promiscuous targeting of artemisinin in Plasmodium falciparum. *Nat. Commun.* **2015**, *6*, 10111. [CrossRef]
15. Ma, W.; Balta, V.A.; West, R.; Newlin, K.N.; Miljanić, O.Š.; Sullivan, D.J.; Vekilov, P.G.; Rimer, J.D. A second mechanism employed by artemisinins to suppress Plasmodium falciparum hinges on inhibition of hematin crystallization. *J. Biol. Chem.* **2021**, *296*, 100123. [CrossRef]
16. Van der Pluijm, R.W.; Tripura, R.; Hoglund, R.M.; Phyo, A.P.; Lek, D.; Islam, A.U.; Anvikar, A.R.; Satpathi, P.; Satpathi, S.; Behera, P.K.; et al. Triple artemisinin-based combination therapies versus artemisinin-based combination therapies for uncomplicated Plasmodium falciparum malaria: A multicentre, open-label, randomised clinical trial. *Lancet* **2020**, *395*, 1345–1360. [CrossRef]
17. Wang, J.; Xu, C.; Liao, F.L.; Jiang, T.; Krishna, S.; Tu, Y. A Temporizing Solution to "Artemisinin Resistance". *N. Engl. J. Med.* **2019**, *380*, 2087–2089. [CrossRef]
18. Santos-Magalhães, N.S.; Mosqueira, V.C.F. Nanotechnology applied to the treatment of malaria. *Adv. Drug Deliv. Rev.* **2010**, *62*, 560–575. [CrossRef]
19. Fröhlich, T.; Çapcı Karagöz, A.; Reiter, C.; Tsogoeva, S.B. Artemisinin-Derived Dimers: Potent Antimalarial and Anticancer Agents. *J. Med. Chem.* **2016**, *59*, 7360–7388. [CrossRef]
20. Çapcı, A.; Herrmann, L.; Kumar, H.M.S.; Fröhlich, T.; Tsogoeva, S.B. Artemisinin-derived dimers from a chemical perspective. *Med. Res. Rev.* **2021**, *41*, 2927–2970. [CrossRef]
21. Tsogoeva, S.B. Recent Progress in the Development of Synthetic Hybrids of Natural or Unnatural Bioactive Compounds for Medicinal Chemistry. *Mini Rev. Med. Chem.* **2010**, *10*, 773–793. [CrossRef]
22. Walsh, J.; Bell, A. Hybrid Drugs for Malaria. *Curr. Pharm. Des.* **2009**, *15*, 2970–2985. [CrossRef]
23. Benoit-Vical, F.; Lelièvre, J.; Berry, A.; Deymier, C.; Dechy-Cabaret, O.; Cazelles, J.; Loup, C.; Robert, A.; Magnaval, J.-F.; Meunier, B. Trioxaquines Are New Antimalarial Agents Active on All Erythrocytic Forms, Including Gametocytes. *Antimicrob. Agents Chemother.* **2007**, *51*, 1463–1472. [CrossRef]
24. Coslédan, F.; Fraisse, L.; Pellet, A.; Guillou, F.; Mordmüller, B.; Kremsner, P.G.; Moreno, A.; Mazier, D.; Maffrand, J.-P.; Meunier, B. Selection of a trioxaquine as an antimalarial drug candidate. *Proc. Natl. Acad. Sci. USA* **2008**, *105*, 17579–17584. [CrossRef] [PubMed]
25. Horwedel, C.; Tsogoeva, S.B.; Wei, S.; Efferth, T. Cytotoxicity of Artesunic Acid Homo- and Heterodimer Molecules toward Sensitive and Multidrug-Resistant CCRF-CEM Leukemia Cells. *J. Med. Chem.* **2010**, *53*, 4842–4848. [CrossRef] [PubMed]
26. Feng, T.-S.; Guantai, E.; Nell, M.; van Rensburg, C.E.; Ncokazi, K.; Egan, T.J.; Hoppe, H.C.; Chibale, K. Effects of highly active novel artemisinin–chloroquinoline hybrid compounds on β-hematin formation, parasite morphology and endocytosis in Plasmodium falciparum. *Biochem. Pharmacol.* **2011**, *82*, 236–247. [CrossRef] [PubMed]
27. Fröhlich, T.; Hahn, F.; Belmudes, L.; Leidenberger, M.; Friedrich, O.; Kappes, B.; Couté, Y.; Marschall, M.; Tsogoeva, S.B. Synthesis of Artemisinin-Derived Dimers, Trimers and Dendrimers: Investigation of Their Antimalarial and Antiviral Activities Including Putative Mechanisms of Action. *Chemistry* **2018**, *24*, 8103–8113. [CrossRef]
28. Zhan, W.; Liu, Y.J.; Yang, C.; Zhang, H.; Harris, J.C.; Wang, R.; Zhu, S.; Sherman, J.; Sukenick, G.; Rodriguez, A.; et al. Artemisinin-based hybrids produce intracellular proteasome inhibitors that overcome resistance in Plasmodium falciparum. *bioRxiv* **2021**. [CrossRef]
29. Çapcı, A.; Lorion, M.M.; Wang, H.; Simon, N.; Leidenberger, M.; Silva, M.C.B.; Moreira, D.R.M.; Zhu, Y.; Meng, Y.; Chen, J.Y.; et al. Artemisinin–(Iso)quinoline Hybrids by C−H Activation and Click Chemistry: Combating Multidrug-Resistant Malaria. *Angew. Chem. Int. Ed.* **2019**, *58*, 13066–13079. [CrossRef] [PubMed]

30. Fontinha, D.; Moules, I.; Prudêncio, M. Repurposing Drugs to Fight Hepatic Malaria Parasites. *Molecules* **2020**, *25*, 3409. [CrossRef] [PubMed]
31. White, N.J. Anti-malarial drug effects on parasite dynamics in vivax malaria. *Malar. J.* **2021**, *20*, 161. [CrossRef]
32. Ngotho, P.; Soares, A.B.; Hentzschel, F.; Achcar, F.; Bertuccini, L.; Marti, M. Revisiting gametocyte biology in malaria parasites. *FEMS Microbiol. Rev.* **2019**, *43*, 401–414. [CrossRef]
33. Dechy-Cabaret, O.; Benoit-Vical, F. Effects of Antimalarial Molecules on the Gametocyte Stage of Plasmodium falciparum: The Debate. *J. Med. Chem.* **2012**, *55*, 10328–10344. [CrossRef]
34. Ploemen, I.H.J.; Prudêncio, M.; Douradinha, B.; Ramesar, J.; Fonager, J.; Van Gemert, G.-J.; Luty, A.; Hermsen, C.C.; Sauerwein, R.W.; Baptista, F.G.; et al. Visualisation and Quantitative Analysis of the Rodent Malaria Liver Stage by Real Time Imaging. *PLoS ONE* **2009**, *4*, e7881. [CrossRef]
35. D'Alessandro, S.; Silvestrini, F.; Dechering, K.; Corbett, Y.; Parapini, S.; Timmerman, M.; Galastri, L.; Basilico, N.; Sauerwein, R.; Alano, P.; et al. A Plasmodium falciparum screening assay for anti-gametocyte drugs based on parasite lactate dehydrogenase detection. *J. Antimicrob. Chemother.* **2013**, *68*, 2048–2058. [CrossRef]
36. Capela, R.; Cabal, G.; Rosenthal, P.J.; Gut, J.; Mota, M.M.; Moreira, R.; Lopes, F.; Prudêncio, M. Design and Evaluation of Primaquine-Artemisinin Hybrids as a Multistage Antimalarial Strategy. *Antimicrob. Agents Chemother.* **2011**, *55*, 4698–4706. [CrossRef] [PubMed]
37. Delves, M.; Plouffe, D.; Scheurer, C.; Meister, S.; Wittlin, S.; Winzeler, E.; Sinden, R.E.; Leroy, D. The Activities of Current Antimalarial Drugs on the Life Cycle Stages of Plasmodium: A Comparative Study with Human and Rodent Parasites. *PLoS Med.* **2012**, *9*, e1001169. [CrossRef]
38. Parapini, S.; Olliaro, P.; Navaratnam, V.; Taramelli, D.; Basilico, N. Stability of the Antimalarial Drug Dihydroartemisinin under Physiologically Relevant Conditions: Implications for Clinical Treatment and Pharmacokinetic and In Vitro Assays. *Antimicrob. Agents Chemother.* **2015**, *59*, 4046–4052. [CrossRef] [PubMed]
39. Macedo, T.S.; Villarreal, W.; Couto, C.C.; Moreira, D.R.M.; Navarro, M.; Machado, M.; Prudêncio, M.; Batista, A.A.; Soares, M.B.P. Platinum(II)–chloroquine complexes are antimalarial agents against blood and liver stages by impairing mitochondrial function. *Metallomics* **2017**, *9*, 1548–1561. [CrossRef]
40. Ribbiso, K.A.; Heller, L.E.; Taye, A.; Julian, E.; Willems, A.V.; Roepe, P.D. Artemisinin-Based Drugs Target the Plasmodium falciparum Heme Detoxification Pathway. *Antimicrob. Agents Chemother.* **2021**, *65*, e02137-20. [CrossRef] [PubMed]
41. Egan, T.J.; Mavuso, W.W.; Ross, D.C.; Marques, H. Thermodynamic factors controlling the interaction of quinoline antimalarial drugs with ferriprotoporphyrin IX. *J. Inorg. Biochem.* **1997**, *68*, 137–145. [CrossRef]
42. Olafson, K.N.; Nguyen, T.Q.; Vekilov, P.G.; Rimer, J.D. Deconstructing Quinoline-Class Antimalarials to Identify Fundamental Physicochemical Properties of Beta-Hematin Crystal Growth Inhibitors. *Chemistry* **2017**, *23*, 13638–13647. [CrossRef] [PubMed]
43. Moore, B.R.; Page-Sharp, M.; Stoney, J.R.; Ilett, K.F.; Jago, J.D.; Batty, K.T. Pharmacokinetics, Pharmacodynamics, and Allometric Scaling of Chloroquine in a Murine Malaria Model. *Antimicrob. Agents Chemother.* **2011**, *55*, 3899–3907. [CrossRef] [PubMed]
44. Birrell, G.W.; Chavchich, M.; Ager, A.L.; Shieh, H.-M.; Heffernan, G.D.; Zhao, W.; Krasucki, P.E.; Saionz, K.W.; Terpinski, J.; Schiehser, G.A.; et al. JPC-2997, a New Aminomethylphenol with High In Vitro and In Vivo Antimalarial Activities against Blood Stages of Plasmodium. *Antimicrob. Agents Chemother.* **2015**, *59*, 170–177. [CrossRef] [PubMed]
45. Camarda, G.; Jirawatcharadech, P.; Priestley, R.S.; Saif, A.; March, S.; Wong, M.H.L.; Leung, S.; Miller, A.B.; Baker, D.A.; Alano, P.; et al. Antimalarial activity of primaquine operates via a two-step biochemical relay. *Nat. Commun.* **2019**, *10*, 3226. [CrossRef]
46. Adjalley, S.H.; Johnston, G.L.; Li, T.; Eastman, R.T.; Ekland, E.H.; Eappen, A.G.; Richman, A.; Sim, B.K.L.; Lee, M.C.S.; Hoffman, S.L.; et al. Quantitative assessment of Plasmodium falciparum sexual development reveals potent transmission-blocking activity by methylene blue. *Proc. Natl. Acad. Sci. USA* **2011**, *108*, E1214–E1223. [CrossRef]
47. Lelièvre, J.; Almela, M.J.; Lozano, S.; Miguel, C.; Franco, V.; Leroy, D.; Herreros, E. Activity of Clinically Relevant Antimalarial Drugs on Plasmodium falciparum Mature Gametocytes in an ATP Bioluminescence "Transmission Blocking" Assay. *PLoS ONE* **2012**, *7*, e35019. [CrossRef]
48. Newton, P.; van Vugt, M.; Teja-Isavadharm, P.; Siriyanonda, D.; Rasameesoroj, M.; Teerapong, P.; Ruangveerayuth, R.; Slight, T.; Nosten, F.; Suputtamongkol, Y.; et al. Comparison of Oral Artesunate and Dihydroartemisinin Antimalarial Bioavailabilities in Acute Falciparum Malaria. *Antimicrob. Agents Chemother.* **2002**, *46*, 1125–1127. [CrossRef]
49. Lichorowic, C.L.; Zhao, Y.; Maher, S.P.; Padín-Irizarry, V.; Mendiola, V.C.; de Castro, S.T.; Worden, J.A.; Casandra, D.; Kyle, D.E.; Manetsch, R. Synthesis of Mono- and Bisperoxide-Bridged Artemisinin Dimers to Elucidate the Contribution of Dimerization to Antimalarial Activity. *ACS Infect. Dis.* **2021**, *7*, 2013–2024. [CrossRef] [PubMed]
50. Meunier, B. Hybrid Molecules with a Dual Mode of Action: Dream or Reality? *Acc. Chem. Res.* **2008**, *41*, 69–77. [CrossRef] [PubMed]
51. Ncokazi, K.K.; Egan, T.J. A colorimetric high-throughput β-hematin inhibition screening assay for use in the search for antimalarial compounds. *Anal. Biochem.* **2005**, *338*, 306–319. [CrossRef] [PubMed]
52. Sanchez, B.A.; Mota, M.M.; Sultan, A.A.; Carvalho, L.H. Plasmodium berghei parasite transformed with green fluorescent protein for screening blood schizontocidal agents. *Int. J. Parasitol.* **2004**, *34*, 485–490. [CrossRef] [PubMed]

## 4.4 CAPÍTULO 2

1 O artigo intitulado “Avaliação do potencial farmacológico de híbridos baseados em artemisininas para o tratamento da malária” será submetido a revista Antimicrobial Agents Chemotherapy.

# Assessing the pharmacological potential of artemisinin hybrid-based drugs for the treatment of malaria

Helenita Costa Quadros,[a] Lars Herrmann, [b] Jeanne Manaranche,[c,d,e] Lucie Paloque,[c,d,e] Mariana C. Borges-Silva,[a] Godwin Akpeko Dziwornu,[f] Sarah D'Alessandro,[g] Kelly Chibale,[f] Nicoletta Basilico,[h] Françoise Benoit-Vical,[c,d,e]* Svetlana B. Tsogoeva,[b]* and Diogo Rodrigo M. Moreira[a]*

[a] Instituto Gonçalo Moniz, Fundação Oswaldo Cruz, Salvador 40296-710, Brazil.
[b] Organic Chemistry Chair I and Interdisciplinary Center for Molecular Materials (ICMM), Friedrich-Alexander University of Erlangen-Nürnberg, Nikolaus Fiebiger-Straße 10, 91058 Erlangen, Germany;
[c] LCC-CNRS, Laboratoire de Chimie de Coordination, Université de Toulouse, CNRS, Toulouse, France.
[d] MAAP, New antimalarial molecules and pharmacological approaches, Inserm ERL 1289, Toulouse, France.
[e] Institut de Pharmacologie et de Biologie Structurale (IPBS), Université de Toulouse, CNRS, Université Toulouse III - Paul Sabatier (UPS), Toulouse, France.
[f] South African Medical Research Council Drug Discovery and Development Research Unit, Department of Chemistry and Institute of Infectious Diseases and Molecular Medicine, University of Cape Town, Rondebosch 7701, South Africa.
[g] Dipartimento di Scienze Farmacologiche e Biomolecolari, Università degli Studi di Milano, 20133 Milan, Italy.
[h] Dipartimento di Scienze Biomediche, Chirurgiche e Odontoiatriche, Universitá degli Studi di Milano, 20133 Milan, Italy.

## Abstract

We previously shown that artemisinin (ART) hybrid-based drugs may offer the use of a single molecule while conserving the ART combination therapy (ACT) activity on multiple stages of *Plasmodium* life cycle. Here, we aimed to characterize the susceptibility of ART-sensitive or -resistant asexual blood-stage parasites for hybrids (**3**) and (**4**) and to correlate the phenotype-based activity with the chemical stability and the long-lasting duration of antiparasitic activity. Hybrids can display a parasite growth reduction which is as high as dihydroartemisinin (DHA) against a culture of *P. falciparum*. We further observed that rings and trophozoites are the maximally susceptible stages for hybrids, a period that coincide with extensive hemoglobin digestion and ARTs' peak in antimalarial activity. However, in the ring-stage survival assay (RSA), activity of DHA or hybrid (**3**) decreases while hybrid (**4**) activity persists; consistent to RSA data, $IC_{50}$ values shift from a continuous drug exposure in comparison to a short-pulse treatment, altogether suggesting that the dissimilarity in potency among compounds is due to the chemical stability and the duration of the drugs. In fact, hybrid (**4**) has a metabolic stability in liver microsomes similar to ARTs, but it has a superior chemical stability in erythrocytes and therefore a long-lasting duration on its antiparasitic activity, which is higher than DHA or hybrid (**3**). This is in agreement to the notion that the short half-life of ARTs is responsible for a loss in activity, while a prolonged half-life for hybrid (**4**) is responsible for its powerful activity. While the superior stability and long-lasting effects may warrant

a relevant antimalarial activity for this compound class against proliferating parasite stages, against ART-derived quiescent parasites, the antimalarial activity for hybrid (**4**) is relatively low. We have also found that the hybrids can display summation of activity when co-exposure to other antimalarials and based on this, we propose that hybrid may be suitable for replacing ART in ACT.

**Keywords**: *Plasmodium*; drug therapy, artemisinins; phenotype-based activity, delayed clearance phenotype, slow-clearing infection, heme activation.

## 1. Introduction

Artemisinins (ART) is a class of antimalarial endoperoxides which were game-changing drugs in the therapy (Liu et al., 2022; Ma et al., 2020; Wang et al., 2017). However, this has been treated by the phenomena of parasites with a decreased susceptibility to ART, also referred to as 'ART resistance' (Dondorp et al., 2009). The main hallmarks of this resistance are a delayed clearance phenotype (DCP) and single-nucleotide polymorphisms in the *Pf*k13 gene (Hassett & Roepe, 2019; Mok et al., 2021; Pacheco et al., 2019). A DCP is in part characterized by a prolongation of the ring stage in the intra-erythrocytic parasite development, also referred to as slow-clearing parasites (*i.e.*, long half-life parasites). However, not only parasites upon ART exposure can display a DCP but these enter a quiescent state of minimal cellular metabolism (Reyser et al., 2020). Approaches to overcome DCP are the temporizing solution by extending in days the duration of ACT therapy (Wang et al., 2019) and the triple ACT (T-ACT), where an additional third drug is added to the standard two-drugs therapy (Bassat et al., 2022; Hamaluba et al., 2021). Troublingly, the quiescent parasites present a reduced susceptibility to the heme detoxification suppressors' chloroquine (CQ), amodiaquine (AQ) and piperaquine, which are currently the most prominent drug partners of ACT (Reyser et al., 2020). This leaves few drug partners active against quiescent parasites to be added in the triple ACT, such as mefloquine (MFQ), lumefantrine and atovaquone (ATO) (typically not used in ACT), which are relatively slow-acting drugs in comparison to CQ (Reyser et al., 2020).

The elimination half-life in the plasma ($t_{1/2}$) is short for all ART drugs (Batty et al., 1998, 2008) and considered to be the bottleneck of this class of drugs. To overcome this, a next generation of endoperoxide drugs relying on the replacement of the ART's 1,2,4-trioxane by 1,2,4-trioxolane (ozonides OZ277 and OZ439) (Giannangelo et al., 2020; Straimer et al., 2017) and 1,2,4,5-tetraoxane (N205 and E209) (O' Neill et al., 2018; O'Neill et al., 2017) has been developed. One leading model is that while all these endoperoxide drugs can kill parasites by a radical-induced protein alkylation (RIPA) mechanism where proteins are alkylated, the dissimilarity in the half-live warrant some OZ and most tetraoxanes to have a peak of antimalarial activity that do not coincide with ART peak in activity, leveraging the possibility of alkylating proteins unaffected by ART (Siddiqui et al., 2022). Studies have shown that OZ439 ($t_{1/2}$ > 42 h) and tetraoxane E209 ($t_{1/2}$ > 24-30 h) can kill DCP parasites more efficiently than dihydroartemisinin (DHA, $t_{1/2}$ ~2 h) or OZ277 ($t_{1/2}$ ~2-4 h). Conceivably, both 1,2,4-trioxane and 1,2,4-trioxolane groups can react with heme by a pseudo first-order mechanism. However, a plausible explanation for the extended half-live of OZ439 vis-a-vis OZ277 is that by possessing a chemical group which affords a structural conformation whereas the peroxide group is not ready exposed to heme, OZ439 undergoes a bioreductive activation which is much more slowly than OZ277 and DHA in general (Blank et al., 2020; Giannangelo et al., 2019).

Via this reasoning of seeking new endoperoxide drugs, hybrid-based drugs of endoperoxide drugs presenting a second pharmacophoric group have been developed. Examples of the second pharmacophoric group are the quinolines to exert heme detoxification suppression (Çapcı et al., 2019), the vinyl phosphonates to inhibit cysteine proteases (Aratikatla et al., 2021) and the peptidomimetics to block the proteasomes (Zhan et al., 2021). In many examples of hybrid-based drugs, the chemical linker which is introduced to connect the endoperoxide with the second pharmacophoric group can indeed play a dual role, not only acting as a chemical bridge necessary for conjugation of pharmacophoric groups but also introducing a structural conformation whereas the peroxide group is not ready exposed to heme, warranting the potential of hybrids to present an extended half-life in comparison to parental ART.

In the course of this line of investigation, we previously exploited a library of ART hybrid drugs featuring cleavable and non-cleavable linkers hybridized to quinolines and non-quinolinic heterocyclics (Çapcı et al., 2019; Quadros et al., 2021). Quinolines can produce the CQ efficacy for heme detoxification suppression, which was considered for the design of 163A hybrid (**3**); and a non-quinolinic heterocyclic can assist in the steric hindrance to protect peroxide from a rapid heme-mediated bioactivation, which was considered for the design of LH70 hybrid (**4**) (**Figure 1**) (Lars et al., 2022, in submission). Here, we aimed to characterize the susceptibility profile of hybrids exposure to *in vitro* parasites, and underlying mechanisms of action involved in the dissimilar antiparasitic activity between hybrids *versus* parental ART drugs, such as DHA and artesunate (ARE).

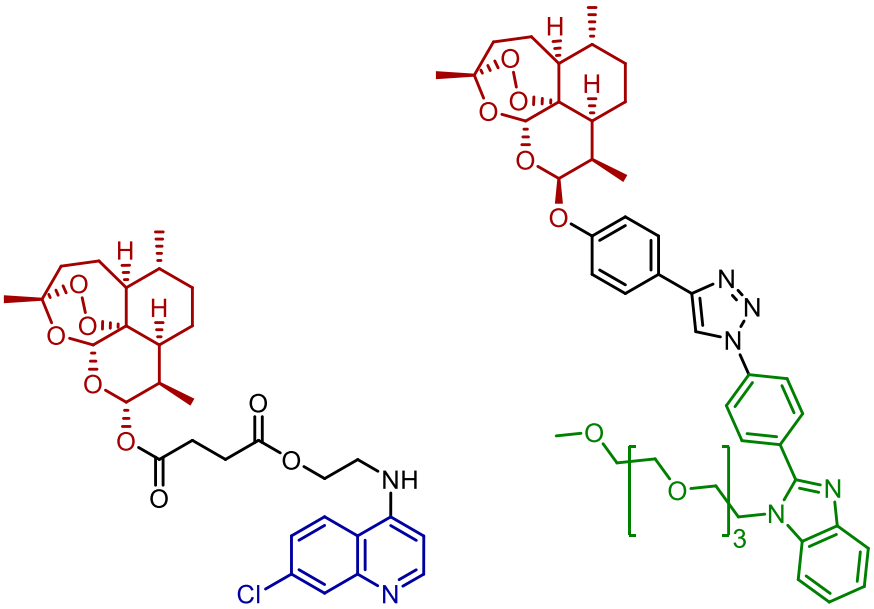


163A (**3**) LH70 (**4**)

**Figure 1**: Chemical structures of artemisinin hybrid-based drugs 163A (**3**) and LH70 (**4**). A red color highlights the artemisinin fragment.

## 2. Materials and Methods

### 2.1 Drugs

ATO, AQ, DHA and MFQ free base were obtained from Sigma-Aldrich (St. Louis, MO, USA). 163A (**3**) and LH70 (**4**) hybrid compounds were synthesized and gently provided by Dr. Svetlana B. Tsogoeva, and E209 experimental compound was a gift by Dr. Paul O'Neil. SYBR Green I nucleic acid staining dye was purchased from Molecular Probes. All other general chemicals and solvents were of analytical or HPLC grade.

### 2.2 *P. falciparum* cultures

The cultures of CQ-susceptible strain NF54 *Plasmodium falciparum* or its clone 3D7 were carried out according to Trager and Jensen, with minor modifications (Trager & Jensen, 1976). In general, the cultures were maintained at 5% hematocrit (human type O-positive red blood cells) in RPMI-1640 medium (EuroClone, Milan, Italy) supplemented with 1% AlbuMax (Invitrogen, Milan, Italy), 2 mM L-glutamine (Euroclone), 20 mM HEPES (Euroclone) and 0.37 mM hypoxanthine (Sigma-Aldrich). For parasite growth and experiments, the cultures were maintained at 37°C and in a standard gas mixture composed of 1% $O_2$, 5% $CO_2$, and 94% $N_2$. For ring stage survival assay (RSA) and quiescent-stage assay (QSA), ART-susceptible and -resistant strains were used. F32-ART is a laboratory strain resistant to ARTs obtained after several years of sequential and increasing ART pressures, while F32-TEM is its susceptible twin (Witkowski, Lelievre et al. 2010). F32-ART owns the M476I mutation on the *pfk*13 gene, responsible for its ART resistance (Ariey et al., 2014). They were both cultured in RPMI-1640 medium (Dutscher, France) at 2% hematocrit in human red blood cells (EFS, French Blood Bank) and 5% human serum (EFS, French Blood Bank) at 37°C under 5% $CO_2$ humidified atmosphere.

### 2.3. Activity against *P. falciparum* asexual blood stages

The asexual blood stages of CQ-susceptible strain (NF54 or 3D7) and CQ-resistant strain (W2) of *P. falciparum* were maintained in culture in RPMI-1640 supplemented with 10% human serum (Abcys S.A., Paris, France) and buffered with 25 mM 4-(2-hydroxyethyl)-1-piperazineethanesulfonic acid (HEPES) and 25 mM $NaHCO_3$. Parasites were grown in A-positive human blood (Etablissement Français du Sang, Marseille, France) under controlled atmospheric conditions of 10% $O_2$, 5% $CO_2$ and 85% $N_2$ at 37◦C with a humidity of 95%. For determination of antiparasitic activity, a volume of 25 µL/well of each hybrid and 200 µL/well of the parasitized red blood cells at final parasitemia of 0.5% and hematocrit of 1.5% were distributed into 96-well plates. The plates were incubated for 72 h at 37◦C in controlled atmosphere. After frozen and thawing the

plates, hemolyzed cultures were homogenized by vortexing the plates. Parasite growth was determined by measuring the activity of the parasite lactate dehydrogenase (pLDH) using a microplate reader Sinergy 4 (Biotek), and the concentration at which the drugs were able to inhibit 50% of parasite growth ($IC_{50}$) was calculated with the inhibitory sigmoid Emax model, with estimation of the $IC_{50}$ through nonlinear regression using a standard function of the R software (ICEstimator version 1.2). $IC_{50}$s were expressed as means of three to five experiments.

**2.4 Drug combination studies**

The antiplasmodium activity of drug combinations between experimental drugs (hybrids **3** and **4**) and MFQ or CQ were tested against NF54 strain *P. falciparum* using a fixed molar ratio. Drug concentration was based on the individual $IC_{50}$ values determined previously for each drug (Quadros et al., 2021). Serial two-fold dilutions were performed in duplicate in ratios of 1:1, 1:3 or 3:1 of hybrids and MFQ or CQ. As controls, MFQ or CQ alone were used at the same range of concentrations of its combinations. Parasite growth was determined by pLDH method using a microplate reader Sinergy 4 (Biotek), and the antimalarial activity was expressed as 50% inhibitory concentrations ($IC_{50}$). An isobologram was constructed by plotting a pair of fractional inhibitory concentrations (FIC) values for each combination and isolated drug. FICs were calculated by $IC_{50}$ when combined divided by $IC_{50}$ isolated drug. A dashed line was used to indicating additive effect, and also to distinguish antagonism (above of the dashed line) and synergism effect (below of the dashed line). Each $IC_{50}$ was calculated using Graph Pad Prism version 5.0.1 program (Graph Pad Software, San Diego, CA, USA). Three independent experiments were performed, and one single experiment was used to represent the result by the mean and confidence level (95% CI).

**2.5 Short pulse treatment and activity on different *P. falciparum* stages**

One hundred microliters of 163A (**3**) or LH70 (**4**) hybrid compounds previously suspended in dimethyl sulfoxide (DMSO) and diluted in seven different concentrations using RPMI-1640 medium were dispensed in duplicate in the respective wells into a 96-well flat-bottom microplate. After, 100 μL of NF54 strain on D-Sorbitol-synchronized ring stage or asynchronous culture at 1-1.5% parasitemia and 1% final hematocrit in RPMI-1640 were added into the microplates. Untreated parasite received 100 μL of medium. DHA and CQ were used as parental controls of both hybrids. Plates were incubated for 6 h (short pulse) plus 66 h or 72 h (continuous drug exposure) at 37°C with the standard gas mixture. Six hours after addition of drugs, plate was centrifuged, the medium was replaced, and the plates were returned to the incubator for more 66 h. The plates were processed using the pLDH method, and $IC_{50}$ values were calculated as the mean and standard error of mean of at least two independent experiments.

**2.6 Speed of antiplasmodium action**

For the test, 163A (**3**) and LH70 (**4**) hybrid compounds were suspended in DMSO and then diluted in serial two-fold dilutions in RPMI-1640 medium using 96-well flat-bottom microplates until achieving seven desired concentrations. Additionally, 100 µl of a NF54 strain asynchronous culture with 1-1.5% parasitemia and 1% final hematocrit were added into the plates containing 100 µl of each hybrid compound concentration in duplicate, and then incubated for 24, 48 and 72 h at 37°C and with gas mixture. DHA was used as positive control (fast-acting drug) and ATO was used as negative control (relatively slow-acting drug). Untreated parasite received 100 µL of medium. Parasite growth was determined by pLDH method using a microplate reader Sinergy 4 (Biotek), and the antimalarial activity was expressed as 50% inhibitory concentrations ($IC_{50}$), where each $IC_{50}$ value was represented as the mean and standard deviation of at least two independent experiments performed.

**2.7 Drug stability in erythrocyte culture**

The relative drug concentration of hybrids in the erythrocyte culture was estimated by measuring the antiplasmodium activity of supernatant harvested from erythrocyte culture as described previously (Yang et al., 2016). In brief, a 96-well flat-bottom microplate, 125 µL of hybrid (**3**), hybrid (**4**) or DHA were aliquoted in sextuplicate, and then 125 µL of uRBC (2% hematocrit) were added into the microplate. Drug E209 was employed as a long-lasting experimentally endoperoxide, while AQ was employed as a standard drug. Final concentration of all drugs was of at 500 nM. The plate was incubated at 37° and in the standard gas mixture for different times (0.16, 6 and 24 h). Untreated uRBCs incubated at the same times were used as negative controls. After each timepoint, supernatants were collected and stored until use.

Supernatants were diluted in medium for a serial two-fold dilutions and at least six different supernatant dilutions were aliquoted in the plate. The antiplasmodium activity of supernatant was determined by incubation of with 1-2% parasitemia and 2.5% hematocrit for 72 h at the same condition described above using 3D7 strain. After incubation, the plate was frozen at -80°C overnight, and then thawed at 37°C for 4 h. In addition, 100 µL of each respective well were transferred to a black sterile 96-well plate, and 100 µL of a SYBR Green I solution (0.2 µL of SYBR Green I per 1 mL of lysis buffer) were aliquoted. The plate was incubated at room temperature protected from light, and gently mixed using a shaker for 1 h. The fluorescence measurement was performed using excitation and emission wavelengths of 485 and 530 nm, respectively. Only the experiments where the $IC_{50}$ of supernatant harvested at 10 min displayed values similar to the $IC_{50}$ of a fresh drug dilution in the medium were considered for analysis of equivalent drug concentration. Therefore, by considering that the supernatant harvested at 10 min has a 500 nM of drug concentration, an

equivalent drug concentration was calculated as 500/$IC_{50}$ value for each indicated time. At least three independent experiments were performed.

### 2.8 *In vitro* metabolic stability assay

This assay was performed in duplicate using a 96-well microtiter plate. Hybrid compounds (0.1 μM) were incubated at 37°C in mouse and pooled human liver microsomes with a final protein concentration of 0.4 mg/ml$^{-1}$, XenoTech, Lenexa, KS suspended in 0.1 M phosphate buffer at pH 7.4 for predetermined time points. This was in the presence and absence of cofactor-reduced nicotinamide adenine dinucleotide phosphate (NADPH, 1.0 mM). The reactions were quenched by adding ice-cold MeCN containing an internal standard (carbamazepine, 0.0236 μg/mL). The samples were centrifuged, and the supernatant was analyzed via liquid chromatography−tandem mass spectrometry (LC−MS/MS) (Agilent Rapid Resolution HPLC, AB SCIEX 4500 MS). The relative loss of the parent compound with time was monitored, and plots were prepared for each compound of Ln% remaining versus time to determine the first-order rate constant for compound depletion. This was used to calculate the degradation half-life and subsequently to predict the in vitro intrinsic clearance ($CL_{int}$) and in vitro hepatic extraction ratio ($E_H$) (Bertrand et al., 2000).

### 2.9 Antiparasitic activity (potency) against sensitive and resistant *P. falciparum* strain

To evaluate the *in vitro* antimalarial activity of 163A (**3**) and LH70 (**4**) against F32-ART and F32-TEM, the SYBR Green I assay was carried out (Smilkstein, Sriwilaijaroen et al. 2004). Parasite cultures were synchronized with 5% D-sorbitol (Sigma-Aldrich) at the ring stage (Lambros and Vanderberg, 1979) and adjusted at 1% parasitemia. In a 96-well plate, parasites were exposed during 48h at 37°C to different concentrations of the drugs (0.1 nM, 1nM, 10nM, 100 nM and 1μM) in triplicate. The drugs were then removed by washing three times the parasite pellets in 1X PBS (Sigma-Aldrich) before freezing the red blood cells at -20°C overnight. The plates were then thawed, and the lysed parasites transferred in a black 96-well plate. SYBR Green I (Thermo Fisher) at a final concentration of 2X in a lysis buffer (20 mM Tris base pH 7.5, 20 mM EDTA, 0.008% w/v saponin, 0.08% w/v Triton X-100) was then added and the plates incubated for one hour at room temperature in the dark. Fluorescence was measured at 485 nm excitation/528 nm emission in the VICTOR Nivo plate reader (Perkin Elmer), and the $IC_{50s}$ were then calculated using GraphPad Prism 7 software. The inhibition percentages were calculated with the following formula:

$$\%\ inhibition = 100 - \frac{signal\ (molecule) - signal(red\ blood\ cells)}{signal\ (control) - signal\ (red\ blood\ cells)}$$

**2.10 Recrudescence assay**

A recrudescence assay was performed on F32-ART and F32-TEM in parallel to evaluate the potential cross-resistance of 163A (**3**) and LH70 (**4**) with ARTs by comparing the ability of the two strains to survive and proliferate after drug exposure (Ménard et al., 2015). Parasites synchronized at the ring stage (Lambros and Vanderberg, 1979), adjusted to 3% parasitemia and 2% hematocrit were treated during 48h in a 6-well plate. The parasites were then washed with RPMI-1640 before being placed in drug-free culture conditions with 10% human serum. The parasitemia was followed via blood smears until the cultures reached their starting parasitemia, defined as the recrudescence day. If no parasite recrudescence was observed for up to 30 days the data is censored in the Kaplan-Meier analysis.

**2.11 Ring stage survival assay (RSA)**

The RSA was performed, as previously described, to determine the ability of ring-stage parasites (0-3h old) to survive to a brief drug exposure, mimicking the pharmacokinetics of DHA, comparatively to untreated condition (Witkowski et al., 2013). Ring-stage parasites obtained after a Percoll-Sorbitol treatment were exposed to 700 nM of the drugs (163A (**3**), LH70 (**4**) and DHA) or 0.1% DMSO (control) for 6h in duplicate. The parasite pellets were then washed in RPMI-1640 before being placed in drug-free culture conditions with 10% human serum for 72h. The survival rates were determined by counting the parasitemia of each condition on 10,000 red blood cells by two independent microscopists.

**2.12 Quiescent-stage assay (QSA)**

The QSA was performed as previously described to determine the activity of 163A (**3**) and LH70 (**4**) on ART resistant parasites at the quiescent stage (Egwu et al., 2022). Parasites were synchronized at the ring stage (Lambros and Vanderberg, 1979) and adjusted to 3% parasitemia and 2% hematocrit. They were then exposed to DHA to induce quiescence or mock (condition C) during 6h. After a drug wash, parasites were treated either with DHA, or DHA + compound to be tested (163A (**3**), LH70 (**4**) or ATO as control) for 48h. The condition A is the control of recrudescence for quiescent parasites. The DHA treatment is kept in the condition B to make sure that quiescence is maintained. Conditions A and B will be compared to determine if a molecule is active on quiescent parasites. The condition C allows to check that the concentration at which the molecule is tested is active on proliferating parasites. At the end of the treatments, the parasite cultures were washed with RPMI-1640 medium and replaced in new wells in drug-free culture medium with 10% human serum. The parasitemia was followed via blood smear until the cultures reached their starting parasitemia

(3%), defined as the recrudescence day (Reyser, Paloque et al. 2020). If no parasite recrudescence was observed for up to 30 days, the data is censored in the Kaplan-Meier analysis.

**2.13 Statistic analysis**

Data are presented as median ± standard error of the mean (S.E.M.) or mean ± standard deviation (S.D.). Statistical analysis was performed using the Prism version 5.01 software (GraphPad Software, La Jolla, CA, USA). Statistical significance was assessed by performing the one-way analysis of variance (ANOVA) followed by post-test for multiple comparisons as indicated in each figure. Differences with $p$ values $< 0.05$ were considered significant.

## 3. Results

### 3.1 Hybrids can efficiently kill ring-stage parasites

It is well documented that a > 48-h drug exposure is a poor predictor of the ARTs efficacy, since these drugs display a much shorter *in vivo* exposure time. A time-dependent drug exposure study (short pulse *versus* continuous exposure) is important to mimic ART conditions *in vivo*, as well as to determine the specificity of a drug in killing each parasite stage. Therefore, we studied the stage specificity of antiparasitic activity against ART-sensitive parasites of NF54 strain of *P. falciparum*. Firstly, the antiparasitic activity was determined by incubating an asynchronous parasite culture with the drugs for a pulse of 6 h, a time that surpass the half-life of DHA (~1 to 3 h), followed by parasite washing and quantification of the % of parasite survival 66 h later by pLDH method. $IC_{50}$ values obtained under short-pulse treatment (6+66h) were compared to the values under continuous drug incubation (72 h).

In terms of $IC_{50}$ values for an asynchronous culture (rings, trophozoites, schizonts), the antiparasitic activity of hybrids and DHA under a short pulse (6 h) was similar in comparison to the activity determined in continuous drug incubation (72 h). In contrast, the potency of MFQ has decreased in three-folds from a short pulse in comparison to continuous incubation, since it is a stage-specific drug for early trophozoites (**Figure 2**).

The antiparasitic activity of hybrids assayed for a culture tightly synchronized in mid-ring stages was assayed as described above. Of note, a timeframe of 6 h coincides with the growth from mid-rings into early trophozoites (roughly 8 h). Using MFQ as a threshold, where a decrease in five-folds from a short pulse in comparison to continuous incubation is observed, the antiparasitic activity of hybrids and DHA for killing rings under a short pulse (6 h) was slightly decreased in comparison to the activity determined under continuous drug incubation (72 h). These findings are broadly consistent to a previous report showing that mid-ring stage of 3D7 strain has a lower sensitivity to a 6-h pulse exposure to DHA than at longer exposure times (> 48 h). This is in contrast to a slow-activated ozonide drug OZ439, which is significantly much less potent at a short pulse exposure than at longer exposure times (Yang et al., 2016).

Considering that the activity of hybrids against rings was higher than asynchronous and that the activity against asynchronous is not mitigated by a short pulse, we have inferred that hybrids and DHA are effective in killing ring and trophozoites stages of *P. falciparum*, while MFQ is only effective in killing trophozoite stages.

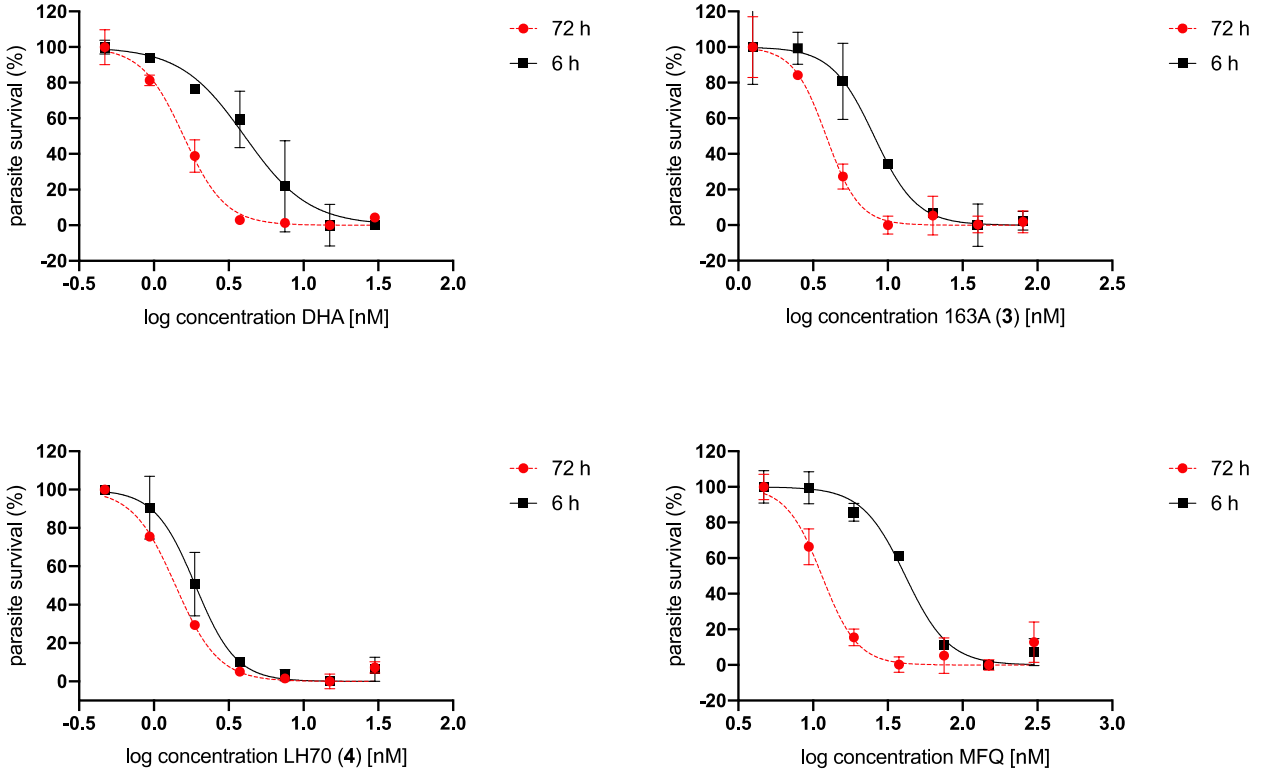


316

| Compounds | NF54 strain of *P. falciparum* ($IC_{50}$, nM)[a] | | | | | |
|---|---|---|---|---|---|---|
| | ring stage | | | asexual blood stages | | |
| | 72 h | 6+66 h | Ratio | 72 h | 6+66 h | Ratio |
| 163A (**3**) | 3.8±0.4 | 9.0±1.5 | 2.4 | 8.1±1.0 | 19.1±1.8 | 2.4 |
| LH70 (**4**) | 1.5±0.1 | 1.5±0.3 | 1.0 | 3.0±0.3 | 3.5±0.3 | 1.2 |
| DHA | 1.9±0.2 | 5.0±0.5 | 2.7 | 2.1±0.6 | 4.6±0.9 | 2.2 |
| MFQ | 10.3±2.6 | 47.2±5.2 | 4.6 | 20.2±1.3 | 61.6±11.9 | 3.0 |

317 **Figure 2**. Stage specificity of the antiparasitic activity of hybrid compounds (**3**) and (**4**) against ART-sensitive
318 strain of *P. falciparum*. [a] Values are the mean ± S.E.M. of two independent experiments, using each
319 concentration of compounds in duplicate. Ratio of each compound was calculated by $IC_{50}$ of short pulse (6+66
320 h) divided by $IC_{50}$ of continuous incubation of 72 h. MFQ = mefloquine. DHA = dihydroartemisinin. Graphics
321 disclosed above are for mid-ring stage experiments.

322

323 **3.2 Hybrids are useful in the drug combination**

324

325 In the clinic, ART-based drugs are used in drug combination with other partners, typically
326 presenting a different mechanism of action to avoid *P. falciparum* resistance or of long-lasting
327 duration in the plasma. In this context, we assessed whether hybrids (**3**) and (**4**) could present a
328 summation of antiplasmodium potency to the long-lasting drugs CQ (heme detoxification suppressor)

or MFQ (a pleiotropic antimalarial agent). To this end, assays were performed using different molar ratio of the drugs against synchronized *P. falciparum* ring-stage for 72 h.

The combination of hybrid (**3**) and MFQ presented a summation of antiplasmodium activity towards additivity (**Figure 3, panel A**). An explanation for the summation of antiplasmodium activity between hybrid (**3**) and MFQ is that these drugs have a dissimilar affinity for hematin, where MFQ is several folds less potent to binding to hematin than hybrid (**3**). In contrast, the combination of hybrid (**3**) and CQ did not present a summation of antiplasmodium activity (**Figure 3, panel B**). A plausible explanation for the antagonism of antiplasmodium activity is that both hybrid (**3**) and CQ have a strong affinity for hematin, giving rise to a competition of both drugs in suppressing the heme detoxification. This shed on light that the quinoline from hybrid (**3**) is participating and contributing to the mechanism underlying the antiplasmodium activity of hybrid (**3**). Except in one combination where an antagonism was observed, the hybrid (**4**) combined with MFQ presented a summation of antiplasmodium activity towards additivity (**Figure 3, panel C**); however, when combined with CQ, all molar ratio tested revealed a summation of antiplasmodium activity (**Figure 3, panel D**).

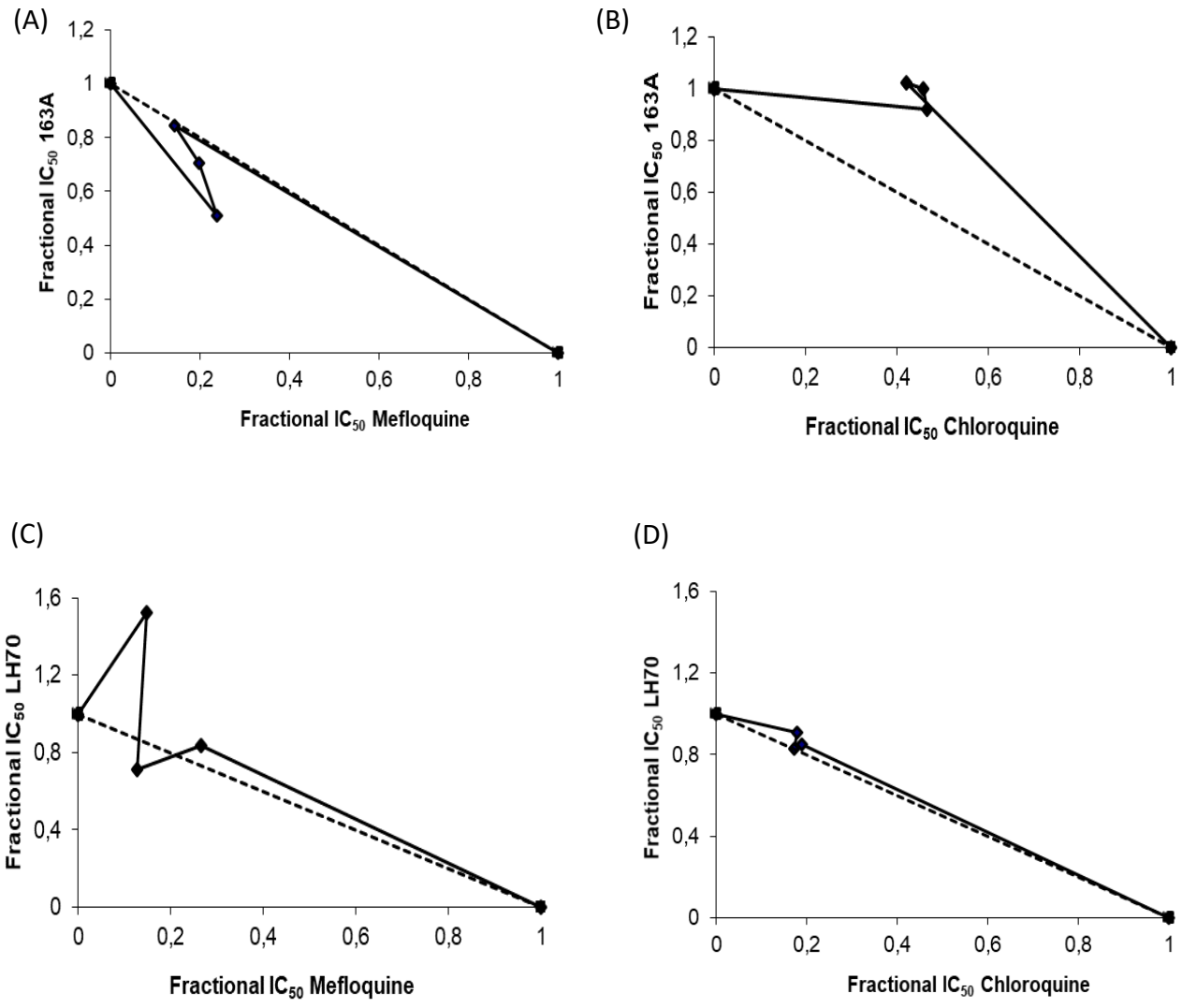

(E)

| Drug combination | 3:1 | 1:1 | 1:3 |
|---|---|---|---|
| Hybrid (**3**)-CQ | 1.4 | 1.5 | 1.4 |
| Hybrid (**3**)-MFQ | 1.0 | 0.9 | 0.7 |
| Hybrid (**4**)-CQ | 1.0 | 1.0 | 1.1 |
| Hybrid (**4**)-MFQ | 1.0 | 0.6 | 1.9 |

**Figure 3**. Antiplasmodium activity of the drug combination between the hybrids (**3**) and (**4**) and the aminoquinolines CQ and MFQ. The panels A and B shows the interaction of hybrid (**3**) and mefloquine or chloroquine, respectively. In the panels C and D, we showed the interaction of hybrid (**4**) and mefloquine or chloroquine. Values represents the FIC of each drug combination in one single experiment against NF54 strain of *P. falciparum*. Each concentration of compounds was tested in duplicate. In the graphics, the black solid line indicates FIC=1, or absolute additivity. FIC index <1 is synergistic, ~ 1 is additive, and >1 is antagonistic. FIC = fractional inhibitory concentration. CQ = Chloroquine; MFQ = Mefloquine. Values are represented by the mean and confidence level (95% CI) of one single experiment.

Regarding $IC_{50}$ values, all drug ratio of hybrid (**3**) and CQ in combination regimens resulted in similar potencies of approximately 5 nM. Additionally, independently of hybrid (**3**) moieties in the combinations or of the presence of CQ, the potency of all combinations to inhibit the parasitemia was similar. Of note, CQ did not sum the antiplasmodium activity in the drug combinations due to its presence in the hybrid (**3**) skeleton; indeed, both hybrid and CQ as drug partner pursuit the hemozoin inhibition as a common target on plasmodium asexual stage. While CQ did not perform an antiplasmodium summation of its activity, hybrid (**3**) plus MFQ presented a synergism in the parasitemia inhibition with drug ratio of 3 parts of hybrid (**3**) and 1 part of MFQ. Of note, we observed that in contrast to hybrid (**3**) and CQ, the combination with MFQ presented a longer activity, probably due not only to dissimilar mechanism of action, but also due to the long-action (longer half-life), which maintain its plasmatic levels and efficacy against the parasite on rings or early trophozoites stages for more time. Regarding to hybrid (**4**), we noted that the drug combinations with CQ or MFQ presented an equipotency to hybrid (**4**) isolated (**Table 1**).

**Table 1**. Potency of drugs alone or in combination therapies with CQ or MFQ as drug partners.

| **Ring stages of NF54 strain of *P. falciparum* ($IC_{50}$, nM)[a]** | | | | |
|---|---|---|---|---|
| drugs alone | | combination therapies | | |
| Hybrid (**3**) | CQ | 3 (**3**) : 1 CQ | 1 (**3**) : 1 CQ | 1 (**3**) : 3 CQ |
| 4.7 (4.6-4.8) | 10.4 (9.2-11.7) | 4.9 (4.5-5.2) | 4.8 (4.4-5.1) | 4.4 (3.7-5.1) |
| Hybrid (**3**) | MFQ | 3 (**3**) : 1 MFQ | 1 (**3**) : 1 MFQ | 1 (**3**) : 3 MFQ |
| 4.8 (4.5-5.1) | 17.0 (14.0-20.6) | 4.0 (3.8-4.3) | 3.4 (2.8-4.1) | 2.5 (2.0-2.9) |
| Hybrid (**4**) | CQ | 3 (**4**) : 1 CQ | 1 (**4**) : 1 CQ | 1 (**4**) : 3 CQ |
| 2.2 (2.0–2.4) | 10.5 (7.5-14.8) | 1.9 (1.6-2.1) | 1.8 (1.5-2.2) | 2.0 (1.7-2.3) |
| Hybrid (**4**) | MFQ | 3 (**4**) : 1 MFQ | 1 (**4**) : 1 MFQ | 1 (**4**) : 3 MFQ |
| 2.0 (1.9-2.2) | 10.3 (8.6-12.3) | 1.9 (1.7-2.0) | 1.5 (1.3-1.7) | 2.5 (2.0-3.1) |

[a] Values are the mean and confidence level (95% CI) of one single experiment using each concentration of compounds in duplicate. CQ = Chloroquine; MFQ = Mefloquine.

### 3.3 Hybrids are fast-acting antimalarial agents

The two hybrid compounds inhibited the growth of ART-sensitive strain of the asynchronous *P. falciparum* asexual blood stage assayed after 72 h of exposure. Hybrid (**4**) was an equipotent inhibitor of parasite survival as DHA, while hybrid (**3**) was approximately two folds less potent. In light of this, we first examined whether their *in vitro* speed in killing parasites is responsible for the dissimilar potency (**Figure 4**). As the controls, the slow-acting drug ATO and fast-acting drug DHA were included in this set of experiments. Differently from ATO, both hybrid compounds displayed a fast parasite killing capability, which was inferred by observing that the $IC_{50}$ values after 72 h are in the same magnitude of potency as after 24 h of drug exposure. In addition, we observed that after 24 h of parasite exposure, hybrid (**3**) and DHA were almost equipotent as inhibitors of parasite survival, while at 72 h of parasite exposure DHA became twice more potent than hybrid (**3**). In contrast, the potency of hybrid (**4**) remained the same at the different times of exposure.

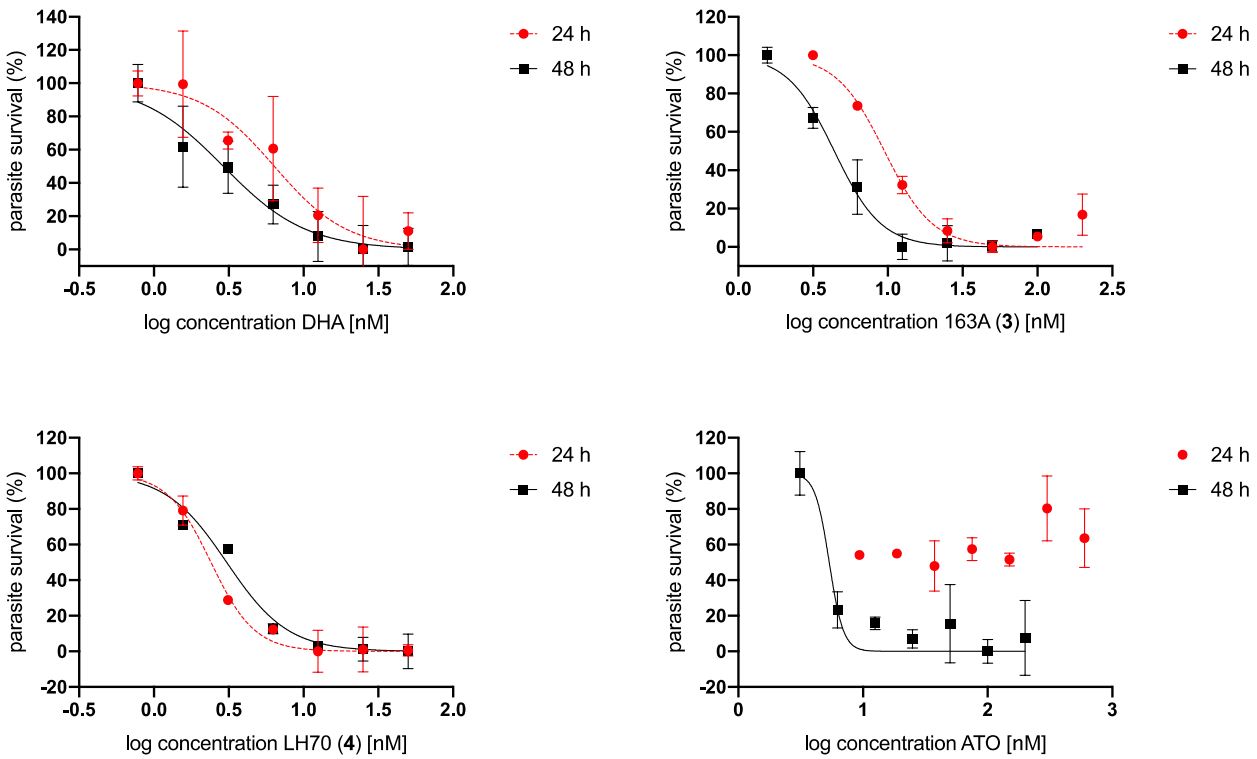


| Compounds | Asynchronous NF54 strain of *P. falciparum* ($IC_{50}$, nM)[a] | | | |
|---|---|---|---|---|
| | 24 h | 48 h | 72 h | Conclusion |
| 163A (**3**) | 9.4 (8.0-11.2) | 4.3 (3.8-5.0) | 5.6 (5.0-6.4) | Fast-acting |
| LH70 (**4**) | 2.4 (2.1-2.7) | 3.0 (2.6-3.5) | 2.0 (1.8-2.4) | Fast-acting |
| DHA | 8.3 (3.9-10) | 2.9 (2.0-4.1) | 2.7 (2.5-2.9) | Fast-acting |
| ATO | >600 | 5.3 (4.1-6.0) | 0.78 (0.39-0.91) | Slow-acting |

**Figure 4**. Antiparasitic activity of hybrids (**3**) and (**4**) against ART-sensitive strain of *P. falciparum* at different times of exposure. [a] Values are the mean and confidence level (95% CI) of one single experiment using each concentration of compounds in duplicate. DHA = dihydroartemisinin; ATO = atovaquone.

### 3.4 Chemical stability and host-mediated degradation

ART are *in situ* prodrugs where activation occurs at cellular compartments enriched in heme, such as the RBC and plasmodia. Therefore, we examined whether hybrids have the same half-live profile as observed for DHA. To infer this, we adapted a protocol (Yang et al., 2016) where drugs were incubated in uninfected RBC (uRBC), supernatants were harvested at different time points and the antiparasitic activity of the drug-containing supernatants were determined (**Figure 5, panel A**). AQ was used as a long-lasting drug, while DHA was used as a short-living drug. Experimental drug E209 was assayed in parallel, since it is an antimalarial peroxide of long-lasting property, where its pharmacokinetics in rodents has been determined (O'Neill et al., 2017).

Supernatant from DHA lost its antiparasitic activity after a 6 h timeframe, which is broadly consistent with previously reported stability in RBC (Yang et al., 2016) and DHA half-life of 1-3 h. Hybrid 163A (**3**) lost activity more slowly, remaining at 6 h but losing activity at a 24 h timeframe. In contrast, hybrid LH70 (**4**) was stable under culture conditions, with a loss of approximately 40 % after 24 h. In comparison to E209, a long-lasting peroxide drug, we can infer that hybrid 163A (**3**) is substantially less stable and of inferior long-lasting property, while hybrid LH70 (**4**) is substantially more stable and of superior long-lasting property than DHA or (**3**), but inferior to E209 (**Figure 5, panels B-E**).

Having examined their half-live at cellular level but given that these hybrid compounds presented efficacious *in vivo* antiparasitic activity against *P. berghei*-infected mice (Quadros et al., 2021; Lars et al., 2022, in submission), we thoroughly studied the stability of compounds in liver microsomes of mouse and human. As a threshold, compounds with more than 70 % remaining after 30 min of incubation with liver microsomes were considered stable. In comparison to artesunate as a representative ART drug, we observed that hybrid (**4**) was only slightly less stable in microsomal studies than Artesunate. In contrast, hybrid (**3**) was rapidly metabolized, which is characteristic of a cleavable prodrug.

(A)

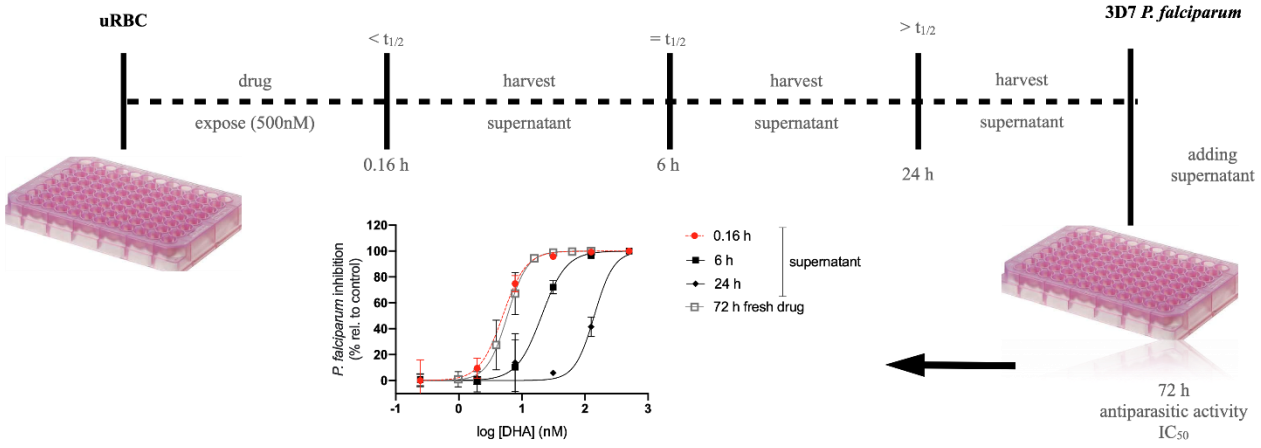


(B)

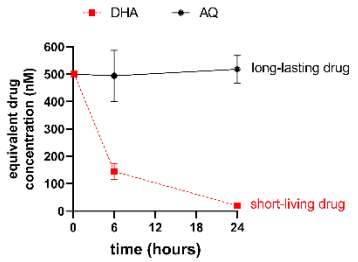


(C)

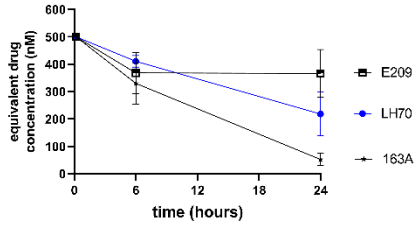


(D)

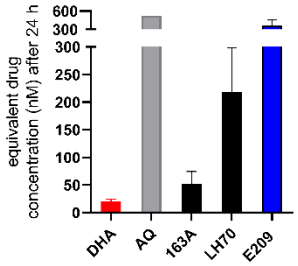


(E)

| Compounds | IC$_{50}$ (nM) from the supernatant of uRBC harvested at indicated time [a] | | | Fold change (24h /0.16 h) [b] |
|---|---|---|---|---|
| | 0.16 h | 6 h | 24 h | |
| Amodiaquine (AQ) [c] | 3.6 (3.3-4.3) | 3.8 (3.5-4.0) | 3.3 (2.2-3.4) | 1.0 |
| DHA | 6.7±2.5 | 22.7±3.1* | 147.3±10.3** | 25.9±4.7 |
| 163A (**3**) [c] | 2.8±0.51 | 4.3±0.74 | 29.0±6.9** | 10.7±4.1 |
| LH70 (**4**) [c] | 1.3±0.44 | 1.5±0.63 | 4.8±1.1 | 3.6±0.8 |
| E209 | 5.9±1.8 | 8.0±0.9 | 11.1±1.5 | 1.42±0.37 |

**Figure 5.** Hybrid compounds (**3**) and (**4**) can exceed the host-mediated degradation of ARTs on the cell culture. Panel A shows the experimental design of the uninfected red blood cells (uRBC) degradation assay and the analysis to estimate the chemical stability of drugs. Inset depicts a sigmoid curve of antimalarial potency 72 h after exposed to either supernatant harvested at indicated time (0.16, 6 or 24 h) or a fresh-diluted drug DHA. IC$_{50}$ values were generated and normalized to determine the equivalent drug concentration on the supernatants. Panel B shows the curves of the equivalent drug concentration on the supernatants from standard drugs DHA or AQ. Panel B shows the curves of the equivalent drug concentration on the supernatants from reference drugs DHA or AQ. Panel C shows the curves of the equivalent drug concentration on the supernatants from experimental drugs. Panel D shows a comparison of the equivalent drug concentration on the supernatants harvested 24 h after drug exposure. In panels B-D, values are mean and standard deviation. Panel E shows a table summarizing the values. Footnotes of Panel E: [a] The *in vitro* antiparasitic activity of supernatants against the 3D7 strain of *P. falciparum* determined 72 h after drug exposure to the parasites. [b] Calculated as the ratio between IC$_{50}$ values of 24 h / 0.16 h.[c] Values are expressed as mean (95 % CI) of one single experiment, each concentration in duplicate. Unpaired two-tailed *t*-test at 95% confidence interval: *$p < 0.05$; **$p < 0.0005$.

### 3.5 Hybrids are active on *P. falciparum* proliferative forms

Like DHA, both hybrid compounds (**3**) and (**4**) had IC$_{50}$ values inferior to 5 nM in the standard chemosensitivity assay whatever the *P. falciparum* strains tested *in vitro* (**Table 2**). No difference was observed between the ART-resistant strain F32-ART and the four tested ART-sensitive strains.

This result was expected since the mechanism of resistance to ARTs is mediated by a quiescence phenomenon (parasite cell cycle arrest during ART exposure). In fact, the $IC_{50}$ determination is important to confirm drug potency, but it is not relevant to discriminate the phenotype of fast-clearing *P. falciparum* infection caused by ART-sensitive parasites to the slow-clearing infection caused by ART-resistant ones (Witkowski, Lelievre et al. 2010).

**Table 2**. Chemosensitivity evaluation ($IC_{50}$) on different *P. falciparum* strains for ART, DHA, 163A (**3**) and LH70 (**4**).

| Compounds | **$IC_{50}$ (nM) against *P. falciparum*** | | | | |
|---|---|---|---|---|---|
| | **Slow-clearing infection phenotype. Mid-ring stages, 48 h incubation time[a,b]** | | **Fast-clearing infection phenotype. Asynchronous culture, 72 h incubation time [a,c]** | | |
| | F32-ART (ART-resistant) | F32-TEM (ART-sensitive) | 3D7 (CQ-sensitive) | Dd2 (CQ-resistant) | K1 (CQ-resistant) |
| ART | N.D. | N.D. | 26.8±2.4 | 11.3±1.8 | 5.4±0.5 |
| DHA | 0.8±0.8 | 1±1 | N.D. | N.D. | N.D. |
| 163A (**3**) | 4.5±2.5 | 4.8±1.2 | 4.5±0.5 | 2.3±0.6 | 1.7±0.3 |
| LH70 (**4**) | 4.2±1.3 | 2.6±0.6 | 3.0±0.2 | 3.0±0.3 | 1.8±0.1 |

[a] Activity determined using SYBR green I. CQ = Chloroquine. ART = Artemisinin. DHA = Dihydroartemisinin. N.D. = not determined.

### 3.6 Cross-resistance of the two hybrids with artemisinins

To determine if ART-resistance can impair the activity of 163A (**3**) and LH70 (**4**), a recrudescence assay was conducted (Witkowski, Lelievre et al. 2010, Ménard, Ben Haddou et al. 2015), by comparing the ability of ART-resistant and ART-sensitive parasites to recover after a 48h-drug exposure. Consistently, after the end of DHA exposure at 700 nM, F32-ART recovered faster than F32-TEM with a 8-days delay between strains (**Figure 6**). As 163A (**3**) and LH70 (**4**) are both ART derivatives, they were tested at the same dose as DHA. Analysis of parasites recovery after the end of drug exposure highlighted a delay in recrudescence time between F32-ART and F32-TEM (**Figure 6**) demonstrating that ART resistance impaired the activity of 163A (**3**) and LH70 (**4**). These data are in accordance with previously obtained results which highlighted cross-resistance between ARTs and molecules harboring an endoperoxide function (Straimer, Gnadig et al. 2017, Paloque, Witkowski et al. 2018, Ouji, Barnoin et al. 2020).

However, after LH70 (**4**) treatment, F32-ART and F32-TEM strains recovered respectively later than after DHA or 163A (**3**) treatment, suggesting a difference of parasite sensitivity to the different molecules. To explore this hypothesis, the Ring-stage Survival Assay ($RSA^{0-3h}$) was

conducted with 0-3 h old ring-stage parasites, the most resistant ones in ART-resistant parasites (Witkowski, Amaratunga et al. 2013).

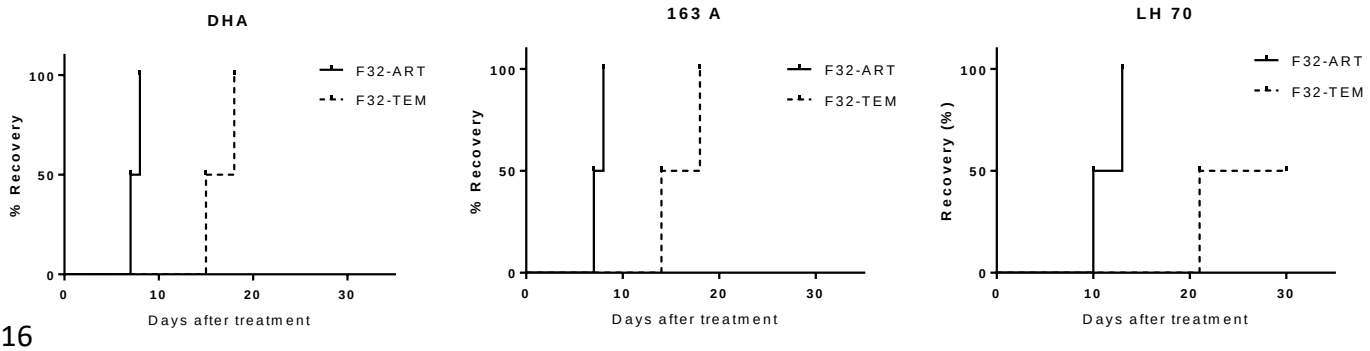


**Figure 6.** Kaplan-Meier analysis of recrudescence time of F32-ART (artemisinin-resistant) and F32-TEM (artemisinin-sensitive) parasites after a 48-hours treatment with 700 nM of DHA (as control condition), 163A and LH70. The final event was defined as the time necessary for treated cultured to reach D0 parasitaemia. Observations were considered to be censored if no recrudescence was observed at day 30. Two independent experiments were performed in parallel for F32-ART and F32-TEM in the same conditions to generate paired results.

## 3.7 LH70 is a more potent inhibitor of artemisinin-resistant parasites in $RSA^{0-3h}$ compared to DHA

As expected, survival rates of F32-TEM parasites were closed to 0 % after treatment with any of the three molecules (**Figure 7**) confirming the chemosensitivity of this strain and the ability of 163A (**3**) and LH70 (**4**) to act in less than 6 h like DHA. At the same time, F32-ART parasites had a mean survival rate of 10 % after DHA treatment consistent with its ART resistance. Interestingly, while F32-ART parasites treated with 163A (**3**) had a mean survival rate similar to the one obtained with DHA, parasites treated with LH70 (**4**) had a mean survival rate of only 2%. This result suggests a lower cross-resistance between ART and LH70 (**4**) than between ART and 163A (**3**). The difference in activity profiles of these two compounds can be explain by their metabolic stability. Indeed, the compound 163A (**3**), which is the combination of an ART moiety and a quinoline part, is highly cleavable mainly by parasite hydrolase enzymes, thus releasing a moiety corresponding to DHA, artemether or ARE according to the cutting site. That is why 163A (**3**) can be considered as a pro-drug delivering an ART entity. By contrast, LH70 (**4**) is much more stable and can truly be considered as a hybrid compound with two different pharmacophores. This could explain why, under RSA conditions but also in recrudescence assay, parasites present similar features when treated by 163A (**3**) and DHA, while the compound LH70 (**4**) appears to be more active, even against the ART-resistant strain F32-ART.

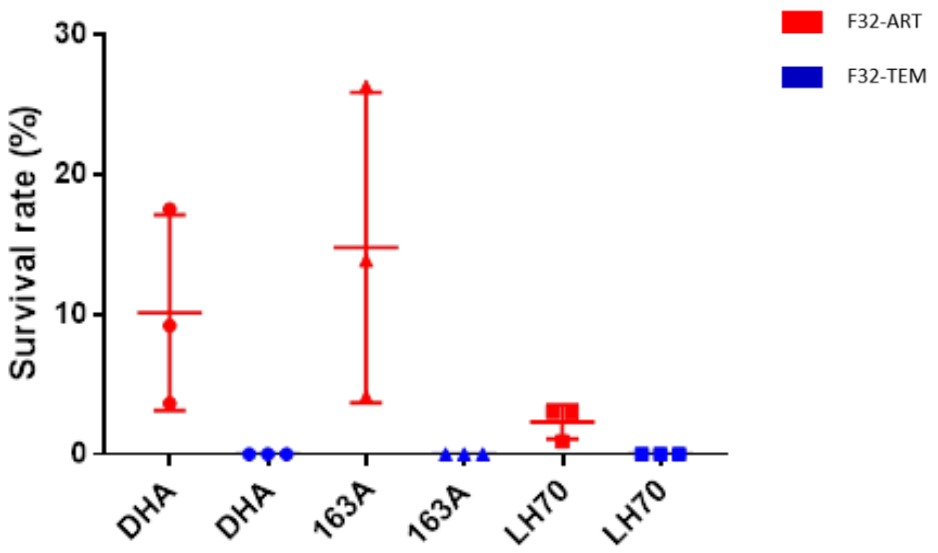


**Figure 7.** Efficiency of compounds on the ring stage survival assay (RSA). Mean survival rates (± SD) of artemisinin-resistant (F32-ART) and artemisinin-sensitive (F32-TEM) parasites in the $RSA^{0-3h}$ after different treatments compared to the control condition. All drugs were tested at 700 nM. Data correspond to three independent experiments. S.D. = standard deviation of the mean.

### 3.8 163A and LH70 present a weak activity on *P. falciparum* artemisinin-resistant parasites at the quiescent stage

Because during the quiescence state, the metabolism of parasites is modified, molecules that are active on *P. falciparum* proliferating forms (RSA) have also to be tested on quiescent forms (QSA) to fully evaluate their efficacy in the framework of ART resistance. The two hybrid compounds 163A (**3**) and LH70 (**4**) were thus tested on parasites resistant to ART at the quiescent stage. As a cut-off, it was determined that a molecule is active on quiescent parasites, when the delay of recrudescence is of at least 6 days between parasites only treated by DHA and parasites treated by DHA plus a drug of interest (Reyser, Paloque et al. 2020).

The blue curves (**Figure 8**) indicate that parasites for which quiescence was induced are then able to reach initial parasitemia between days 7 and 8 after the end of the treatment. When 163A (**3**) is added on quiescent parasites (green curve), the parasites reach 3% parasitemia only 2-days later comparatively to parasites only DHA treated. In parallel, when quiescent parasites are treated with LH70 (**4**), parasite recrudescence occurred 4-days later. The delays are thus inferior to the 6-days threshold for both molecules suggesting a weak activity of these compounds on quiescent parasites while these molecules are active on proliferating parasites (orange curves). As a positive drug control, ATO, known as active on quiescent parasites, was routinely tested in the laboratory in the QSA and shown a delay of recrudescence up to 10 days (data not shown) (Reyser, Paloque et al. 2020). Like for results obtained with recrudescence assay and RSA, LH70 (**4**) presented a better activity against

maintained quiescent parasites than 163A (**3**) in QSA conditions, certainly due to its chemical structure and its better stability.

(A)

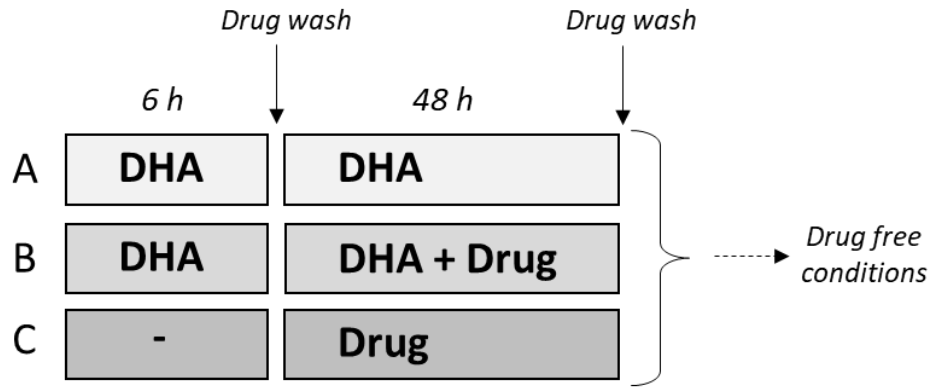


(B)

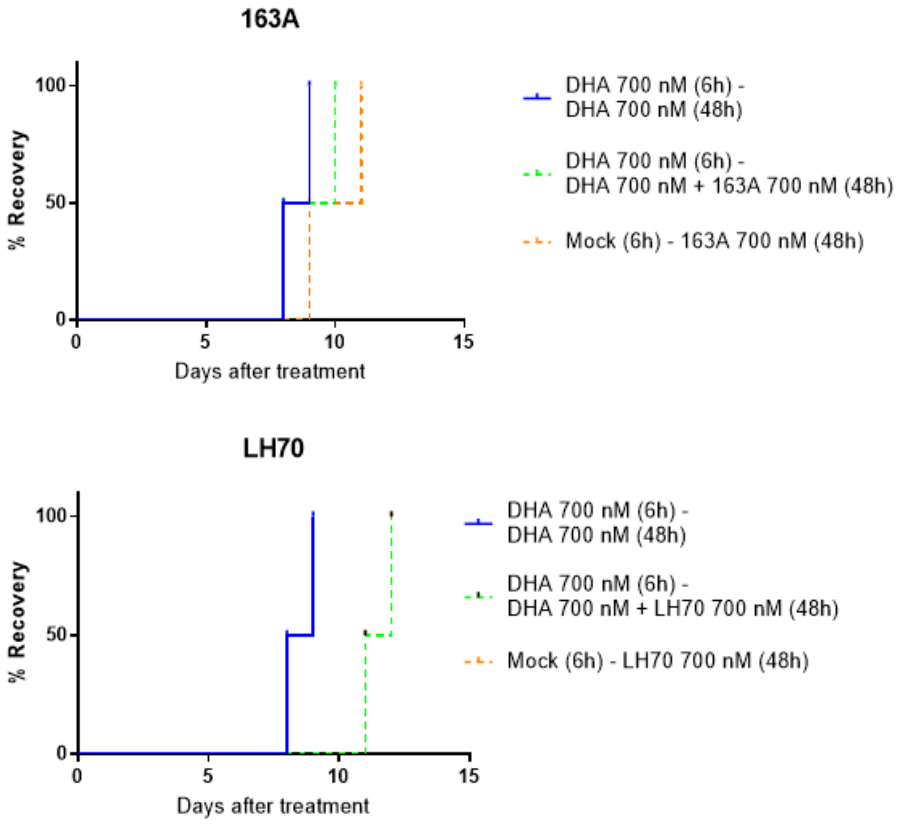


**Figure 8.** Efficiency of compounds on the Quiescent-stage Survival Assay (QSA). Panel (A) shows the treatment schedule for the QSA adapted from Reyser et al. 2020. Panel (B) shows the Kaplan-Meier analysis of recrudescence (in days) of quiescent parasites resistant to artemisinins after different treatments in the QSA. For LH70 (**4**), the orange curve is superposed to the green one. Data correspond to two independent experiments.

## 4 Discussion

Endoperoxide drugs are powerful antimalarial agents. These drugs are rapidly bio-activated by heme, which is rich in the plasmodia environment, into highly reactive radical species (Quadros et al., 2022). Parasite can evade endoperoxide treatment by arresting ring-stage growth and subsequently escaping the short-living radical species generated upon ART treatment. Here, we have addressed that hybrid compounds (**3**) and (**4**) can exceed the chemical stability and the host-mediated degradation of ARTs on the cell culture, resulting in a potency improvement in parasite killing; this might be beneficial for overcoming the spread of ART resistance (**Figure 9**).

Hybrid compound (**3**) is a less potent antimalarial than DHA against fast-clearing infection caused by CQ-sensitive and CQ-resistant strains of *P. falciparum*. However, it was previously shown to be highly active as a heme detoxification suppressor (Quadros et al., 2021) and a powerful protein alkylating agent (Aysun, 2019). Hybrid compound (**4**) is an equipotent antimalarial than DHA against fast-clearing infection caused by CQ-sensitive and CQ-resistant strains of *P. falciparum*. However, it was previously shown to be highly efficacious *in vivo* against *P. berghei*-infected mice, displaying efficacy twice higher than Artesunate (Lars et. al, 2022, in submission).

Despite some dissimilarities discussed above, both hybrid compounds can share some phenotype-based activity in common to each other and to DHA. First, it was observed that the speed of parasite killing is relatively fast in comparison to ATO. Second, it was observed that the specificity in killing each parasite stage – namely, ring, trophozoites or an asynchronous culture – was similar as observed under DHA treatment. Thereby, both hybrids are fast-acting antimalarial agents and they are mostly efficient to kill young stages within the asexual blood life cycle, where the processes of heme consummation, augmentation and subsequent heme detoxification are peaked (Murithi et al., 2020).

Since hybrid compounds (**3**) and (**4**) have a dissimilar antimalarial phenotype response, we have speculated that the endoperoxide activation by heme, their chemical stability or the ability to kill parasites might occur differently or at least at different times. From the data of host-mediated degradation of drugs on the cell culture, we have inferred that both hybrid compounds (**3**) and (**4**) can exceed the chemical stability of DHA. However, hybrid compound (**3**) can only exceed in few hours the chemical stability of DHA, meanwhile hybrid compound (**4**) can substantially surpass the chemical stability of DHA, albeit of magnitude inferior if compared to the long-lasting tetraoxane peroxide drug E209.

Currently, a prevailing hypothesis is that changes over the conformation-dependent activity of endoperoxides with heme can have an improvement effect on the phenotype of the antiparasitic activity, leveraging the possibility of developing endoperoxide variants of slow heme-mediated

bioactivation. This is the case for ozonide drugs OZ277 and OZ439 as well as the tetraoxane E209. A slow heme-mediated bioactivation of endoperoxides can clearly be beneficial for overcoming the spread of slow-clearing infection caused by ART-resistant parasites as inferred by reports on the superior activity on the RSA of these three drugs against ART-resistant parasites (Giannangelo et al., 2020; Straimer et al., 2017; O' Neill et al., 2018; O'Neill et al., 2017). However, a slow heme-mediated bioactivation of endoperoxides can also slow down the parasite killing capability. For instance, Straimer et al. (Straimer et al., 2017) have shown that in the RSA and at a bolus treatment of 700 nM, ozonide drugs OZ277 and OZ439 are more potent inhibitors of parasite survival than DHA, however, using a drug-concentration curve in the RSA, ozonide drugs OZ277 and OZ439 were less potent inhibitors of parasite survival than DHA. These authors speculated that a slow heme-mediated drug bioactivation for ozonides might be less efficient, resulting in a slower parasite killing (*i.e.*, reduced potency) in comparison to DHA. Despite of this slow parasite killing, this leverages these ozonide drugs to efficiently killing ART-resistant parasites of different backgrounds of resistance where DHA fails.

For the hybrids studied here, the underlying improved chemical stability against fast-clearing infection caused by proliferating parasite stages (RSA) is a matter of discussion. For hybrid (**3**), the improved stability is modest in comparison to DHA. In addition, its liver microsome stability is relatively low. Together, this might explain the reasons for hybrid (**3**) being less potent than DHA. For hybrid (**4**), it is possible that the equipotent activity *versus* DHA using a standard chemosensitivity evaluation ($IC_{50}$ values) is due to an improved drug stability. It is noticed that hybrid (**4**) is more efficient to kill parasites in the RSA than DHA or hybrid (**3**). The superior efficiency of hybrid (**4**) in the RSA coincides to the fact that it is of improved drug stability. Presumably, a slow heme-mediated drug bioactivation for hybrid (**4**) might be relevant in the context of RSA; this is also the case for ozonides and other next-generation peroxides.

The underlying improved stability of hybrid compounds for the activity against slow-clearing infection of non-proliferating parasite stages (quiescent) is also a matter of discussion. The literature describing endoperoxide variants killing quiescent parasites is relatively scarce. However, Reyser et al (Reyser et al., 2020) have compelling data that shown that the chemosensitivity of quiescent *versus* proliferating ART-resistant parasites are significantly different, namely, a drug able to kill proliferating parasites in the RSA is not necessarily able to kill quiescent parasites. Here, we observed that hybrid (**3**), which was devoid potent activity in the RSA was also devoid of parasite killing the quiescent ones. In contrast, we observed that hybrid (**4**), a potent agent in the RSA, was endowed with a promising capability of killing the quiescent ones, albeit of reduced potency. Much work is necessary to understand the underlying contribution of an improved stability of endoperoxide drugs and the capability of killing quiescent parasites.

An important remaining question is whether *in vitro* susceptibility data can correlate with drug stability (*i.e.*, a long-lasting drug can have a stronger efficiency for long half-life parasites). Here, we observed that hybrid (**4**) is as potent as DHA using a standard chemosensitivity evaluation ($IC_{50}$ values) against a panel of sensitive and resistant strains. Interestingly, hybrid (**4**)-derived supernatant is substantially more potent than DHA-derived supernatant, this is a quite convincing notion that hybrid (**4**) is more chemically stable than DHA. Based on this, it would to be expected hybrid (**4**) to be a more potent antimalarial agent against fast-clearing infection caused by parasites of 3D7, NF54 and W2 strains. In fact, DHA chemical speciation, heme-dependent bioactivation and subsequent antiparasitic activity is not recapitulated by any other antimalarial endoperoxides; explaining why no other endoperoxide drug is as potent as DHA for fast-clearing parasite strains. However, the superiority on the potency of hybrid (**4**) *versus* DHA was observed in the RSA, which is composed of slow-clearing and proliferating parasites (*i.e.*, long half-life parasites) (Witkowski et al., 2013).

Finally, an important aspect of developing hybrid drugs is to deploy them in drug combination therapy. Here, we have observed that hybrid compound (**3**) can present an antagonism of potency if combined to the heme detoxification suppressor CQ; this antagonism is most likely due to the competition of both quinolines for the same molecular targets and it is also suggestive that the quinoline pharmacophore presented on (**3**) is actively contributing to antimalarial activity. In contrast, hybrid compound (**3**) presented synergism of potency if combined to the pleiotropic antimalarial drug MFQ, indicating that these drugs do not compete for molecular targets. In the case of hybrid (**4**), it displayed additivity or synergism of potency when combined to CQ or MFQ; a plausible explanation is that the glycol benzimidazole group presenting in hybrid (**4**) does not add a second mechanism of action, but actually it confers a beneficial steric protection of peroxide to not be rapidly degraded by heme. While these results are promising, a limitation of these drug combination studies is whether or not a summation of potency can be observed against drug-resistant strains; further work is still necessary.

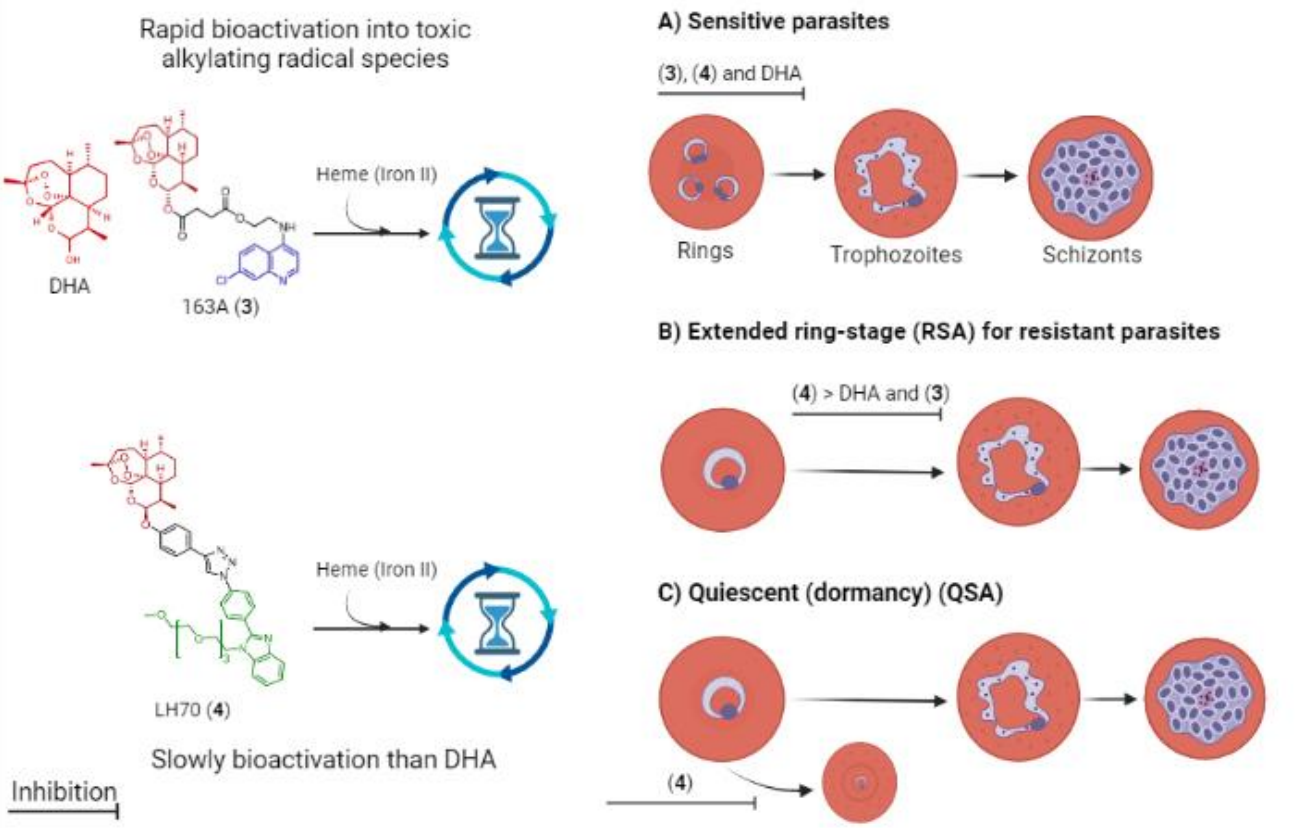


**Figure 9**: Proposed action of endoperoxide drugs against different phenotypes of the plasmodium. Peroxide bond is activated through a Fenton reaction with heme [Fe(II)PPIX], which produces radical species to alkylate multiple parasite targets. Presumably, this chemical reaction can be very fast (DHA) or more slowly (163A, LH70, ozonides, E209, etc). One consequence of the very fast bio-activation by a drug is to kill sensitive parasites but an inability to kill extended ring stage parasites. It is arguable that a more slowly bio-activation is the ability of a drug to potently kill extended ring stage parasites and partially affect parasite viability on dormancy stage.

## Acknowledgements

Study design, S.B.T., F.B.V., and D.R.M.M.; experimental work, H.C.Q., L.H., J.M., L.P., M.C.B.S., G.A.D., and S.D.-A.; writing—original draft preparation, H.C.Q. and D.R.M.M.; writing—review and editing, F.B.V., N.B., K.C., S.B.T., and D.R.M.M.; funding acquisition, F.B.V., N.B., K.C., S.B.T., and D.R.M.M.

## Funding

H.C.Q. work was supported through a CAPES doctoral scholarship (Finance Code 001, Brazil). S.B.T. acknowledges the Deutsche Forschungsgemeinschaft (DFG) for funding (grant number TS87/17-1; TS87/23-1, Germany) and the Bavarian State Ministry for Science, Research and Art (Germany). D.R.M.M. acknowledges CNPq (grants no. 305732/2019-6 and 440227/2022-4, Brazil), FAPESB (grant no. INCTIE 2625, Brazil), and Fiocruz/Proep (grant number IGM-002-FIO-20-2-25, Brazil). S.D.-A. and N.B. were supported by the by Fondazione Cariplo (grant number 2017−0846), the Ministero dell'Istruzione, dell'Università e della Ricerca (grant number PRIN 2015.4JRJPP_004), and the Ministero degli Affari Esteri e della Cooperazione Internazionale (Progetti di grande rilevanza,

753 grant number 00949–2018). J.M., L.P. and F.B.V. acknowledge the Fondation pour la Recherche
754 Médicale FRM "Équipe EQU202103012596", the Centre National de la Recherche Scientifique
755 (CNRS), and the Institut National de la Sante et de la Recherche Médicale (Inserm) for their support.

756

757 **Informed consent statement**

758 Blood donor consent was waived since erythrocytes were used for *P. falciparum* culture and no
759 personal data were collected.

760

761 **Acknowledgments**

762 S.D.-A. and N.B. thank AVIS Comunale Milano for providing blood samples for parasite culture.
763 H.C.Q. and D.R.M.M. thank the flow cytometry at Fiocruz for data acquisition. Jean-Michel
764 Augereau was acknowledged for fruitful discussions. We are thankful for Prof. Paul. M. O'Neill
765 (Department of Chemistry, The University of Liverpool) for kind gift of E209 drug.

766

767 **Conflicts of Interest:**

768 The authors declare no conflict of interest.

769 **References**

770 Ariey, F., Witkowski, B., Amaratunga, C., Beghain, J., Langlois, A.-C., Khim, N., Kim,
771 S., Duru, V., Bouchier, C., Ma, L., Lim, P., Leang, R., Duong, S., Sreng, S., Suon,
772 S., Chuor, C. M., Bout, D. M., Ménard, S., Rogers, W. O., … Ménard, D. (2014). A
773 molecular marker of artemisinin-resistant Plasmodium falciparum malaria. *Nature*,
774 *505*(7481), 50–55. https://doi.org/10.1038/nature12876
775 Bassat, Q., Maïga-Ascofaré, O., May, J., Clain, J., Mombo-Ngoma, G., Groger, M.,
776 Adegnika, A. A., Agobé, J.-C. D., Djimde, A., Mischlinger, J., & Ramharter, M.
777 (2022). Challenges in the clinical development pathway for triple and multiple drug
778 combinations in the treatment of uncomplicated falciparum malaria. *Malaria*
779 *Journal*, *21*(1), 61. https://doi.org/10.1186/s12936-022-04079-9
780 Batty, K. T., Anh Thu, L. T., Davis, T. M. E., Ilett, K. F., Xuan Mai, T., Canh Hung, N.,
781 Phuc Tien, N., Powell, S. M., van Thien, H., Quang Binh, T., & Kim, N. van. (1998).
782 A pharmacokinetic and pharmacodynamic study of intravenous vs oral artesunate
783 in uncomplicated falciparum malaria. *British Journal of Clinical Pharmacology*,
784 *45*(2), 123–129. https://doi.org/10.1046/j.1365-2125.1998.00655.x
785 Batty, K. T., Gibbons, P. L., Davis, T. M. E., & Ilett, K. F. (2008). Pharmacokinetics of
786 dihydroartemisinin in a murine malaria model. *The American Journal of Tropical*
787 *Medicine and Hygiene*, *78*(4), 641–642.
788 Bertrand, M., Jackson, P., & Walther, B. (2000). Rapid assessment of drug metabolism in
789 the drug discovery process. *European Journal of Pharmaceutical Sciences*, *11*, S61–
790 S72. https://doi.org/10.1016/S0928-0987(00)00165-2
791 Blank, B. R., Gonciarz, R. L., Talukder, P., Gut, J., Legac, J., Rosenthal, P. J., & Renslo,
792 A. R. (2020). Antimalarial Trioxolanes with Superior Drug-Like Properties and In

Vivo Efficacy. *ACS Infectious Diseases*, *6*(7), 1827–1835. https://doi.org/10.1021/acsinfecdis.0c00064

Çapcı, A., Lorion, M. M., Wang, H., Simon, N., Leidenberger, M., Borges Silva, M. C., Moreira, D. R. M., Zhu, Y., Meng, Y., Chen, J. Y., Lee, Y. M., Friedrich, O., Kappes, B., Wang, J., Ackermann, L., & Tsogoeva, S. B. (2019a). Artemisinin–(Iso)quinoline Hybrids by C−H Activation and Click Chemistry: Combating Multidrug-Resistant Malaria. *Angewandte Chemie International Edition*, *58*(37), 13066–13079. https://doi.org/10.1002/anie.201907224

Dondorp, A. M., Nosten, F., Yi, P., Das, D., Phyo, A. P., Tarning, J., Lwin, K. M., Ariey, F., Hanpithakpong, W., Lee, S. J., Ringwald, P., Silamut, K., Imwong, M., Chotivanich, K., Lim, P., Herdman, T., An, S. S., Yeung, S., Singhasivanon, P., … White, N. J. (2009). Artemisinin Resistance in *Plasmodium falciparum* Malaria. *New England Journal of Medicine*, *361*(5), 455–467. https://doi.org/10.1056/NEJMoa0808859

Egwu, C. O., Pério, P., Augereau, J.-M., Tsamesidis, I., Benoit-Vical, F., & Reybier, K. (2022). Resistance to artemisinin in falciparum malaria parasites: A redox-mediated phenomenon. *Free Radical Biology and Medicine*, *179*, 317–327. https://doi.org/10.1016/j.freeradbiomed.2021.08.016

Giannangelo, C., Anderson, D., Wang, X., Vennerstrom, J. L., Charman, S. A., & Creek, D. J. (2019). Ozonide Antimalarials Alkylate Heme in the Malaria Parasite *Plasmodium falciparum*. *ACS Infectious Diseases*, *5*(12), 2076–2086. https://doi.org/10.1021/acsinfecdis.9b00257

Hamaluba, M., van der Pluijm, R. W., Weya, J., Njuguna, P., Ngama, M., Kalume, P., Mwambingu, G., Ngetsa, C., Wambua, J., Boga, M., Mturi, N., Lal, A. A., Khuroo, A., Taylor, W. R. J., Gonçalves, S., Miotto, O., Dhorda, M., Mutinda, B., Mukaka, M., … Dondorp, A. M. (2021). Arterolane–piperaquine–mefloquine versus arterolane–piperaquine and artemether–lumefantrine in the treatment of uncomplicated Plasmodium falciparum malaria in Kenyan children: a single-centre, open-label, randomised, non-inferiority trial. *The Lancet Infectious Diseases*, *21*(10), 1395–1406. https://doi.org/10.1016/S1473-3099(20)30929-4

Hassett, M. R., & Roepe, P. D. (2019). Origin and Spread of Evolving Artemisinin-Resistant Plasmodium falciparum Malarial Parasites in Southeast Asia. *The American Journal of Tropical Medicine and Hygiene*, *101*(6), 1204–1211. https://doi.org/10.4269/ajtmh.19-0379

Liu, G., Xie, Y., Sun, Y., Zhang, K., Maa, J., & Huang, Y. (2022). *Research and development of traditional medicines in low- and middle-income countries: A case study of artemisinin discovery in China* (pp. 187–209). https://doi.org/10.1016/bs.apar.2022.01.002

Ma, N., Zhang, Z., Liao, F., Jiang, T., & Tu, Y. (2020). The birth of artemisinin. *Pharmacology & Therapeutics*, *216*, 107658. https://doi.org/10.1016/j.pharmthera.2020.107658

Ménard, S., ben Haddou, T., Ramadani, A. P., Ariey, F., Iriart, X., Beghain, J., Bouchier, C., Witkowski, B., Berry, A., Mercereau-Puijalon, O., & Benoit-Vical, F. (2015). Induction of Multidrug Tolerance in *Plasmodium falciparum* by Extended Artemisinin Pressure. *Emerging Infectious Diseases*, *21*(10), 1733–1741. https://doi.org/10.3201/eid2110.150682

Mok, S., Stokes, B. H., Gnädig, N. F., Ross, L. S., Yeo, T., Amaratunga, C., Allman, E., Solyakov, L., Bottrill, A. R., Tripathi, J., Fairhurst, R. M., Llinás, M., Bozdech, Z., Tobin, A. B., & Fidock, D. A. (2021). Artemisinin-resistant K13 mutations rewire Plasmodium falciparum's intra-erythrocytic metabolic program to enhance survival. *Nature Communications*, *12*(1), 530. https://doi.org/10.1038/s41467-020-20805-w

Murithi, J. M., Owen, E. S., Istvan, E. S., Lee, M. C. S., Ottilie, S., Chibale, K., Goldberg, D. E., Winzeler, E. A., Llinás, M., Fidock, D. A., & Vanaerschot, M. (2020). Combining Stage Specificity and Metabolomic Profiling to Advance Antimalarial Drug Discovery. *Cell Chemical Biology*, *27*(2), 158-171.e3. https://doi.org/10.1016/j.chembiol.2019.11.009

O' Neill, P. M., Stocks, P. A., Sabbani, S., Roberts, N. L., Amewu, R. K., Shore, E. R., Aljayyoussi, G., Angulo-Barturén, I., Belén, M., Jiménez-Díaz, Bazaga, S. F., Martínez, M. S., Campo, B., Sharma, R., Charman, S. A., Ryan, E., Chen, G., Shackleford, D. M., Davies, J., … Ward, S. A. (2018). Synthesis and profiling of benzylmorpholine 1,2,4,5-tetraoxane analogue N205: Towards tetraoxane scaffolds with potential for single dose cure of malaria. *Bioorganic & Medicinal Chemistry*, *26*(11), 2996–3005. https://doi.org/10.1016/j.bmc.2018.05.006

O'Neill, P. M., Amewu, R. K., Charman, S. A., Sabbani, S., Gnädig, N. F., Straimer, J., Fidock, D. A., Shore, E. R., Roberts, N. L., Wong, M. H.-L., Hong, W. D., Pidathala, C., Riley, C., Murphy, B., Aljayyoussi, G., Gamo, F. J., Sanz, L., Rodrigues, J., Cortes, C. G., … Ward, S. A. (2017a). A tetraoxane-based antimalarial drug candidate that overcomes PfK13-C580Y dependent artemisinin resistance. *Nature Communications*, *8*(1), 15159. https://doi.org/10.1038/ncomms15159

Pacheco, M. A., Kadakia, E. R., Chaudhary, Z., Perkins, D. J., Kelley, J., Ravishankar, S., Cranfield, M., Talundzic, E., Udhayakumar, V., & Escalante, A. A. (2019). Evolution and Genetic Diversity of the *k13* Gene Associated with Artemisinin Delayed Parasite Clearance in Plasmodium falciparum. *Antimicrobial Agents and Chemotherapy*, *63*(8). https://doi.org/10.1128/AAC.02550-18

Quadros, H. C., Çapcı, A., Herrmann, L., D'Alessandro, S., Fontinha, D., Azevedo, R., Villarreal, W., Basilico, N., Prudêncio, M., Tsogoeva, S. B., & Moreira, D. R. M. (2021a). Studies of Potency and Efficacy of an Optimized Artemisinin-Quinoline Hybrid against Multiple Stages of the Plasmodium Life Cycle. *Pharmaceuticals*, *14*(11), 1129. https://doi.org/10.3390/ph14111129

Quadros, H. C., Silva, M. C. B., & Moreira, D. R. M. (2022). The Role of the Iron Protoporphyrins Heme and Hematin in the Antimalarial Activity of Endoperoxide Drugs. *Pharmaceuticals*, *15*(1), 60. https://doi.org/10.3390/ph15010060

Reyser, T., Paloque, L., Ouji, M., Nguyen, M., Ménard, S., Witkowski, B., Augereau, J.-M., & Benoit-Vical, F. (2020a). Identification of compounds active against quiescent artemisinin-resistant Plasmodium falciparum parasites via the quiescent-stage survival assay (QSA). *Journal of Antimicrobial Chemotherapy*, *75*(10), 2826–2834. https://doi.org/10.1093/jac/dkaa250

Straimer, J., Gnädig, N. F., Stokes, B. H., Ehrenberger, M., Crane, A. A., & Fidock, D. A. (2017). *Plasmodium falciparum* K13 Mutations Differentially Impact Ozonide Susceptibility and Parasite Fitness *In Vitro*. *MBio*, *8*(2). https://doi.org/10.1128/mBio.00172-17

Trager, W., & Jensen, J. B. (1976). Human Malaria Parasites in Continuous Culture. *Science*, *193*(4254), 673–675. https://doi.org/10.1126/science.781840

Wang, J., Xu, C., Lun, Z.-R., & Meshnick, S. R. (2017). Unpacking 'Artemisinin Resistance.' *Trends in Pharmacological Sciences*, *38*(6), 506–511. https://doi.org/10.1016/j.tips.2017.03.007

Witkowski, B., Amaratunga, C., Khim, N., Sreng, S., Chim, P., Kim, S., Lim, P., Mao, S., Sopha, C., Sam, B., Anderson, J. M., Duong, S., Chuor, C. M., Taylor, W. R. J., Suon, S., Mercereau-Puijalon, O., Fairhurst, R. M., & Menard, D. (2013a). Novel phenotypic assays for the detection of artemisinin-resistant Plasmodium falciparum malaria in Cambodia: in-vitro and ex-vivo drug-response studies. *The Lancet Infectious Diseases*, *13*(12), 1043–1049. https://doi.org/10.1016/S1473-3099(13)70252-4

Yang, T., Xie, S. C., Cao, P., Giannangelo, C., McCaw, J., Creek, D. J., Charman, S. A., Klonis, N., & Tilley, L. (2016). Comparison of the Exposure Time Dependence of the Activities of Synthetic Ozonide Antimalarials and Dihydroartemisinin against K13 Wild-Type and Mutant Plasmodium falciparum Strains. *Antimicrobial Agents and Chemotherapy*, *60*(8), 4501–4510. https://doi.org/10.1128/AAC.00574-16

Zhan, W., Liu, Y. J., Yang, C., Zhang, H., Harris, J. C., Wang, R., Zhu, S., Sherman, J., Sukenick, G., Rodriguez, A., Deng, H., Nathan, C. F., Kirkman, L. A., & Lin, G. (n.d.). *Artemisinin-based hybrids produce intracellular proteasome inhibitors that overcome resistance in Plasmodium falciparum*. https://doi.org/10.1101/2021.06.21.449268

# 5 **DISCUSSÃO**

Diante dos processos de resistência desenvolvidos pelas espécies de plasmódio aos antimaláricos atuais, a busca por novos fármacos antimaláricos com mecanismos de ação em diferentes alvos do plasmódio e em múltiplos estágios tornou-se essencial e determinante para combater efetivamente à malária. Partindo desta premissa, a presente tese de doutorado trouxe resultados obtidos experimentalmente que evidenciam a noção de que os compostos híbridos são em geral agentes antimaláricos com potência *in vitro* ou eficácia *in vivo* superior aos fármacos antimaláricos de referência.

A superioridade da ação antimalárica de um composto híbrido em relação ao fármaco protótipo pode ser devido ao aspecto farmacodinâmico ou ao aspecto farmacocinético; aqui nós estudamos os aspectos farmacodinâmico de todos os compostos híbridos e quando o modelo farmacodinâmico por si só não foi capaz de explicar a superioridade da ação antimalárica, estudos subsequentes de farmacocinética foram conduzidos. A nível farmacodinâmico, o estudo foi conduzido tanto em relação a resposta fenotípica da atividade antiparasitária do composto híbrido em inibir o crescimento do plasmódio, quanto em relação a alvos moleculares do plasmódio, mais especificamente os processos de detoxificação do heme e da homeostasia redox de tióis. A nível farmacocinético, o estudo foi conduzido com o intuito de compreender a estabilidade química dos compostos híbridos no ambiente celular do plasmódio.

Os compostos híbridos MNCS59 (**1**) e MNCS60 (**2**) foram quimicamente planejados para combinar as características químicas das 4-aminoquinolinas CQ e AQ, e da 8-aminoquinolina PQ. O racional químico para o desenvolvimento destes híbridos foi baseado no tratamento atual para a malária não-complicada em áreas de transmissão por *P. vivax* ou *P. ovale*, no qual a terapia combinada de uma 4-aminoquinolina (CQ ou QN) e uma 8-aminoquinolina (PQ ou TFQ) é recomendada.

É interessante destacar que diferentemente de outras terapias combinadas, onde há somação/potencialização das atividades antiparasitárias frente ao estágio sanguíneo assexuado, neste tipo de terapia é descrito a somação/potencialização frente aos esquizontes teciduais, onde a 8-aminoquinolina PQ e TFQ é bastante ativa (CABRERA; CUI, 2015; GORKA; JACOBS; ROEPE, 2013). Por combinar dois grupos farmacofóricos distintos, presumiu-se que os compostos híbridos MNCS59 (**1**) e MNCS60 (**2**) poderiam apresentar uma ação fenotípica e um mecanismo de ação que englobassem ambos os grupos farmacofóricos. Outrossim, presumiu-se que os compostos híbridos pudessem ser ao menos equipotentes à terapia combinada atual, e que, além disso, pudessem apresentar eficácia com a administração dos dois

grupos farmacofóricos ao mesmo tempo, visto que ambos compõem os híbridos. A terapia combinada atual, por outro lado, é administrada com tempos de tratamento distintos, uma vez que o tempo de tratamento das 8-aminoquinolina PQ e TFQ é mais longo em relação a CQ.

A ação antimalárica *in vitro* e *in vivo* dos híbridos MNCS59 (**1**) e MNCS60 (**2**) revelou potência e eficácia em múltiplos estágios do ciclo de vida do plasmódio, caracterizando-os como fármacos experimentais com espectro de ação mais amplo do que os fármacos de referência. No estágio sanguíneo assexuado, a atividade antimalárica foi avaliada inicialmente *in vitro* contra cepa sensível à CQ (3D7) e cepa resistente à CQ (W2). Os dois híbridos apresentaram atividade em nanomolar e foram quase equipotentes aos seus fármacos de referência 4-aminoquinolinas CQ e AQ contra a 3D7. Contra a cepa W2, o MNCS59 (**1**) foi pelo menos duas vezes mais potente do que a CQ e equipotente à PQ. Já o MNCS60 (**2**) apresentou uma potência 154 vezes maior em relação à CQ, e 29 vezes maior do que a AQ frente à W2. Com relação à seletividade, o MNCS59 (**1**) apresentou-se tão seletivo quanto à PQ e duas vezes menos seletivo do que à CQ. Isto indica que este híbrido conserva a potência da CQ contra a cepa sensível e apresenta perfil semelhante a PQ contra a cepa resistente, a qual é tipicamente hipersensível a este tratamento. Já o MNCS60 (**2**) apresentou um índice de seletividade superior a PQ e similar a AQ.

Dada a potência antimalárica *in vitro* contra cepas do *P. falciparum* e a seletividade comparável aos fármacos de referência no estágio sanguíneo assexuado, subsequentemente nós avaliamos a eficácia antiparasitária *in vivo* dos híbridos como agentes esquizonticidas sanguíneos tanto pelo modelo de Peters de supressão da parasitemia quanto pelo modelo curativo de Thompson. O híbrido MNCS59 (**1**) foi eficaz em reduzir a parasitemia e aumentar a sobrevivência dos animais nas doses de 11 e 33 μmol/kg pela via subcutânea, além de modular a formação dos cristais de hemozoína e a produção do heme livre; a terapia combinada CQ+PQ apresentou eficácia similar em reduzir a parasitemia e aumentar a sobrevivência, entretanto a dose administrada foi cerca de 2 ou 10 vezes maior em relação à dose testada com o MNCS59 (**1**). Além disso, não apresentou eficácia em curar os animais no modelo de Thompson.

Ao consultar a literatura, sabe-se que a monoterapia ou até mesmo a terapia combinada onde um dos fármacos é de velocidade de ação lenta ou apresenta eficácia como esquizonticida sanguíneo baixa, as chances de curar os animais no modelo de Thompson são poucas (BIRRELL et al., 2015). Nesse sentido, nós especulamos que a ausência de cura está relacionada à ausência de uma propriedade antiparasitária de velocidade de ação rápida em relação a PQ nos híbridos.

Como evidenciamos a eficácia do MNCS59 (**1**) na dose de 11 µmol/kg, nós avaliamos o híbrido MNCS60 (**2**) com dose similar (10,8 µmol/kg) através da sua administração pelas vias oral (gavagem) e intraperitoneal, e comparamos com a terapia combinada AQ+PQ. O MNCS60 (**2**) apresentou eficácia similar ao MNCS59 (**1**) na dose de 10,8 µmol/kg pela via oral; já a terapia combinada AQ+PQ na mesma dose e mesma via apresentou uma eficácia cerca de 50% inferior em comparação com o híbrido MNCS60 (**2**); outrossim, a terapia combinada AQ+PQ não foi capaz de curar os animais. A PQ tem uma eficácia limitada contra as formas evolutivas do estágio sanguíneo assexuado, assim, a somação da co-administração da AQ+PQ aconteceria se uma alta dose da PQ fosse administrada.

Embora a eficácia do MNCS59 (**1**) tenha sido avaliada somente pela via subcutânea e a eficácia do MNCS60 (**2**) tenha sido avaliada tanto por via intraperitoneal quanto oral (gavagem), é possível discutir comparativamente os resultados dos dois híbridos. Quando administrados por via injetável (s.c. ou i.p.), ambos os híbridos apresentaram eficácia maior do que a monoterapia ou a terapia combinada. A eficácia superior de moléculas híbridas contendo PQ *versus* a terapia combinada já tem sido encontrada também em outros estudos (CAPELA et al., 2011; MIRANDA et al., 2014). Sabendo-se que a CQ e a AQ acumulam-se preferencialmente no vacúolo digestivo do plasmódio, pode-se especular que a PQ conjugada a CQ ou AQ resulte em um acúmulo da PQ nas células infectadas, no qual é maior no tratamento com os híbridos do que a monoterapia ou a terapia combinada.

Além de investigar a atividade dos híbridos no estágio sanguíneo eritrocítico, nós destacamos também as atividades antimaláricas frente aos estágios hepático e sexuado do plasmódio, os quais evidenciaram um espectro de ação mais amplo dos híbridos em relação a PQ, a qual é um antimalárico ativo frente a gametócitos e esporozoítos. No estágio hepático, tanto o MNCS59 (**1**) quanto o MNCS60 (**2**) apresentaram atividade em inibir em até 100% a taxa de infecção dos esporozoítos em hepatócitos, sem afetar o funcionamento e morfologia da célula hepática hospedeira. Em contrapartida, a terapia combinada AQ+PQ inibiu a infecção pelos esporozoítos às células hepáticas em 70%. A eficácia dos híbridos contra o estágio hepático sugere uma conservação das propriedades farmacológicas da PQ, a qual apresenta uma eficácia moderada contra os esporozoítos. No estágio sanguíneo sexuado, o MNCS60 (**2**) foi quase equipotente à DHA em inibir os estágios mais jovens dos gametócitos, e contra o estágio V (maduro), apresentou eficácia em micromolar; apesar de uma menor eficácia no estágio maduro, o híbrido foi superior aos seus parentais PQ e AQ.

É plausível sugerir que a potência melhorada do híbrido MNCS60 (**2**) frente aos gametócitos e esporozoítos em comparação com a terapia combinada é devido a cooperação das propriedades farmacológicas de dois fármacos quinolínicos com modos de ação distintos; a PQ, causando um aumento de espécies oxidantes tóxicas para o parasito, e a AQ, suprimindo a detoxificação do heme e diminuindo os níveis de GSH antioxidante durante a liberação dos esquizontes hepáticos e dos gametócitos jovens (CAMARDA et al., 2019; O'NEILL et al., 2009). Outro pressuposto é que, diferente da terapia combinada que não possui metal na sua constituição, a presença do ouro (I) na composição do híbrido afeta a homeostasia redox de tióis no parasito.

Além do que já fora discutido acima, os possíveis alvos moleculares dos híbridos MNCS59 (**1**) e MNCS60 (**2**) também foram investigados. O primeiro alvo a nível molecular estudado foi o DNA, onde observamos que o híbrido MNCS59 (**1**) atua como um intercalador reversível no DNA, aumentando a viscosidade do DNA de maneira concentração-dependente do híbrido. Em seguida, avaliamos se a ação dos compostos híbridos envolvia a inibição da via da detoxificação do heme do plasmódio. Medimos a afinidade (log*K*) dos compostos para se ligar a hemina, assim como a inibição da formação dos cristais de β-hematina usando a hematina (FeIII-PPIX) ou o heme (FeII-PPIX) como substratos da reação.

As afinidades dos híbridos MNCS59 (**1**) e MNCS60 (**2**) em se ligar a hemina foram similares entre si e similares aos fármacos quinolínicos CQ e AQ. A PQ e a ART, no entanto, não apresentaram afinidade de ligação a hemina. Uma vez que constatamos que estes híbridos interagem com a hemina, nós presumimos que seria possível observar também uma habilidade destes compostos em inibir a formação dos cristais de β-hematina. Nesse sentido, ao avaliarmos a atividade dos híbridos em inibir a formação dos cristais de β-hematina através dos ensaios de BHIA, observamos que tanto o MNCS59 (**1**) quanto o MNCS60 (**2**) foram capazes de inibir a formação da β-hematina, atuando também de forma similar as 4-aminoquinolinas de referência. Mais especificamente, a presença da 4-aminoquinolina (CQ ou AQ) na composição dos híbridos foi essencial para esta atividade, uma vez que os fármacos dessa classe possuem um nitrogênio quinolínico com alta afinidade pelo heme do plasmódio. A PQ, no entanto, é destituída de tal ação antimalárica.

No ensaio de inibição da β-hematina em ferro oxidado (FeIII-PPIX), o híbrido MNCS60 (**2**) mostrou uma potência duas vezes maior do que a CQ e foi quase equipotente à AQ; a PQ e a ART não apresentaram atividade inibitória. Já no ensaio realizado em heme (FeII-PPIX), o MNCS60 (**2**) e a AQ foram potentes em inibir a formação dos cristais de β-hematina, entretanto,

apresentaram uma potência inferior à ART, o qual é um inibidor potente neste ensaio. Com todos estes achados, podemos concluir que o híbrido (**2**) é um inibidor potente dos cristais β-hematina, o que é consistente com a sua forte ligação ao FeIII-PPIX.

Além da detoxificação do heme, é importante frisar os achados frente a enzima *Pf*TrxR. Ambos os compostos híbridos MNCS59 (**1**) e MNCS60 (**2**) contêm o ouro (I) na sua estrutura química, que é um componente importante em inibir a atividade da enzima *Pf*TrxR, como é observado com o auranofino, um fármaco contendo ouro na sua estrutura química (FENG et al., 2020; SSEMAGANDA et al., 2018). Embora ambos os híbridos apresentem ouro (I) na sua estrutura química, foi observado que o MNCS59 (**1**) é mais potente em inibir a atividade da enzima *Pf*TrxR do que o MNCS60 (**2**); esta dissimilaridade na inibição enzimática se explica devido a diferença na estrutura química de coordenação do ouro (I) nestes compostos; no composto MNCS59 (**1**), o ouro pode ser mais facilmente deslocado da quinolina quando interagindo com a *Pf*TrxR do que com o MNCS60 (**2**), no qual o ouro está mais estabilizado e é mais difícil de interagir com a *Pf*TrxR e inibi-la.

Em relação a contribuição da inibição da atividade da *Pf*TrxR para a atividade antimalárica destes compostos híbridos, nós observamos que o composto híbrido (**1**) foi mais potente em inibir a atividade da *Pf*TrxR mas não foi o mais potente em inibir o crescimento *in vitro* do plasmódio, uma vez que a potência em micromolar do MNC59 (**1**) em inibir a atividade da *Pf*TrxR não é o suficiente para contribuir com a inibição o crescimento *in vitro* do plasmódio, sendo apenas uma contribuição modesta do bloqueio da *Pf*TrxR para inibir o parasito. Consistente com isso, o fármaco de ouro auranofino é capaz de inibir a *Pf*TrxR na escala de nanomolar. Ainda a nível molecular, nós também determinamos a ligação dos híbridos à glutationa reduzida (GSH). Tanto o MNCS59 (**1**) quanto o MNCS60 (**2**) foram capazes de interagir com a GSH, sugerindo que a PQ, componente antimalárico presente na composição dois híbridos, possui um papel essencial na atividade antiparasitária mediada pela depleção da GSH.

Por fim, a nível farmacocinético, foi determinado que os híbridos (**1**) e (**2**) foram estáveis em DMSO e em meio de cultura RPMI (o meio de cultura do plasmódio), muito embora não se saiba sobre o perfil de distribuição celular e de concentrações plasmáticas, e suas semelhanças e diferenças em relação com os antimaláricos CQ, AQ e PQ. De fato, é importante citar que ambos os compostos foram mais estáveis em DMSO do que outros compostos de ouro, tais como o auranofino, que sofre transformações químicas nestas condições (PRATESI et al., 2018;

ZOPPI et al., 2020). Todavia, estudos farmacocinéticos futuros são necessários para compreender a biodisponibilidade e a distribuição celular destes dois compostos híbridos.

Os achados farmacológicos com os compostos híbridos MNCS59 (**1**) e MNCS60 (**2**) abriram um precedente para empregar as 4-aminoquinolinas como um componente químico a ser combinado com as ARTs. Nesse sentido, idealizamos o composto híbrido 163A. De fato, a exemplo dos compostos híbridos MNCS59 (**1**) e MNCS60 (**2**) que foram planejados a luz da terapia combinada, o composto híbrido 163A (**3**) foi concebido a luz da terapia combinada entre as ARTs e as aminoquinolinas, tais como ARS e MFQ, DHA e PPQ, dentre outras combinações úteis ao tratamento de pacientes infectados com cepas do *P. falciparum* resistentes aos fármacos (MUELLER et al., 2002; ZANI et al., 2014). Porém, diferentemente da terapia combinada entre CQ e PQ, no qual há pouca potencialização das atividades antiparasitárias frente ao estágio sanguíneo assexuado, neste tipo de terapia entre as ARTs e as aminoquinolinas há uma potencialização, do tipo adição, das atividades antiparasitárias frente ao estágio sanguíneo assexuado (RIBBISO et al., 2021). Todavia, a potencialização das atividades antiparasitárias da terapia combinada entre ARTs e aminoquinolinas frente aos esquizontes teciduais e gametócitos era até então pouco conhecida, e havia poucos relatos da ação antiparasitária de compostos híbridos frente a estes estágios evolutivos (BENOIT-VICAL et al., 2007).

Nosso estudo foi pioneiro em tentar compreender qual a origem, tanto a nível fenotípico quanto a nível molecular na via da detoxificação do heme, do espectro de ação antimicrobiano do composto híbrido 163A (**3**) em comparação com os seus componentes e aos fármacos de referência, ART e CQ. No estágio sanguíneo assexuado, o híbrido 163A (**3**) apresentou potência em nanomolar significativamente superior aos fármacos de referência, tanto frente às cepas sensíveis (3D7 e Dd2) quanto à cepa resistente à CQ (K1), e demonstrou citotoxicidade em micromolar frente a células de mamíferos; coletivamente, esses dados indicaram um índice de seletividade alto do híbrido (**3**), o qual apresentou-se tão seletivo quanto os fármacos de referência frente a linhagem de macrófago murino J774, e cerca de 3 a 4 vezes mais seletivo do que a CQ e ART, respectivamente, frente às células da linhagem HepG2.

Com esses achados a nível fenotípico, nós pressupomos que os componentes químicos do híbrido 163A (**3**) – 7-cloroquinolina e o endoperóxido – poderiam estar suprimindo a detoxificação do heme, o qual é um processo altamente ativo nos esquizontes sanguíneos. É conhecido que as 4-aminoquinolinas atuam de forma potente na supressão da detoxificação do heme e, mais recentemente, estudos vêm mostrando que os antimaláricos endoperóxidos, como as ARTs e os ozonídeos, além de apresentarem a capacidade de alquilar proteínas dos parasitos,

podem também levar a supressão da detoxificação do heme através do processo químico redox envolvendo a formação de conjugados químico heme-ART, os quais são moléculas antiparasitárias endógenas (QUADROS; SILVA; MOREIRA, 2022; RIBBISO et al., 2021).

De acordo com o que foi discutido acima, ao realizarmos os ensaios de BHIA com o híbrido (**3**), observamos uma potência elevada em inibir a formação da β-hematina partindo-se da hematina, tendo sido duas vezes mais potente do que a CQ; a ART, por outro lado, foi incapaz de inibi-la uma vez que ela é destituída de afinidade pela hematina. Já usando o heme como produto de partida, a CQ e o híbrido (**3**) foram equipotentes, e a ART foi pelo menos 2 vezes mais potente do que ambos; ressalva-se aqui que as ARTs possuem afinidade pelo heme mas não pela hematina. Mais uma vez, estes dados mostram-se consistentes com os resultados já encontrados, uma vez que as 4-aminoquinolinas e as ARTs podem atuar simultaneamente neste processo de detoxificação do heme.

Dentro desse contexto, o perfil antimalárico potente do 163A (**3**) pode estar relacionado parcialmente aos efeitos pleiotrópicos na detoxificação do heme, visto que o composto híbrido 163A (**3**) é capaz de se ligar a hemina; reagir, via bioativação redutiva, com o heme; se ligar a hematina; e suprimir a formação dos cristais de β-hematina em tampão ácido.

De modo a avaliar se a potência *in vitro* poderia ser translacionada *in vivo* em termos de eficácia, nós testamos sua atividade antimalárica *in vivo* através do método curativo de Thompson. Diferente da eficácia alta do 163A (**3**) observada quando administrado pela via subcutânea (ÇAPCI et al., 2019), aqui nós avaliamos a sua atividade pela via intraperitoneal, a qual é comumente empregada para a malária complicada. A via subcutânea favorece a alta absorção de fármacos lipofílicos como a ART, entretanto, até o momento não se conhecia como este híbrido se comportaria quando administrado pela via intraperitoneal. Outrossim, era importante comparar a eficácia do 163A (**3**) em relação ao tratamento com a terapia combinada.

O tratamento com o fármaco 163A (**3**) foi eficaz em reduzir a parasitemia, porém, os experimentos revelaram que a terapia com o híbrido foi menos eficaz do que com a terapia combinada CQ+ARS. Em geral, quando a potência *in vitro* de um fármaco não reflete numa eficácia elevada, aspectos associados a absorção, distribuição, metabolismo e excreção (ADME) podem estar envolvidos. Especulamos que o híbrido 163A (**3**) seja metabolizado *in vivo* de maneira extensiva e rápida, minimizando a quantidade necessária de um dos componentes a ser formado: quinolina ou o endoperóxido. De fato, o grupo químico ligante do híbrido 163A (**3**) é um éster no qual pode ser facilmente clivável.

Com o intuito de avaliar se o híbrido 163A (**3**) apresentaria potência em inibir as formas evolutivas responsáveis pela transmissão da doença (esporozoítos e gametócitos), ensaios frente aos ciclos hepático e sexual foram realizados. Nós observamos que a potência do híbrido 163A (**3**) em inibir os esquizontes hepáticos ocorre devido a presença do antimalárico endoperóxido na composição química do 163A (**3**), o qual é ativo contra esta forma evolutiva e é constituinte da estrutura do híbrido; já a quinolina, por outro lado, não possui tal atividade. Nesta mesma linha de achados científicos, um estudo prévio descrito por Capela et al. (CAPELA et al., 2011) observou que o híbrido de ART e PQ contendo um ligante clivável mostrou potência e eficácia superiores no estágio hepático, quando comparado ao híbrido análogo com ligante não-clivável ou com os fármacos parentais (ART e PQ).

No estágio sanguíneo sexuado, o híbrido 163A (**3**) apresentou potência em nanomolar para inibir a viabilidade dos gametócitos jovens, o que retarda ou inibe a maturação para gametócitos maduros. A potência para inibir os gametócitos jovens é quase equivalente a potência encontrada contra o estágio sanguíneo assexuado, o que pode levar a compreensão deste ser um híbrido capaz tanto de inibir as formas evolutivas do estágio assexuado, quanto de impedir a diferenciação para gametócitos. Nossos resultados são consistentes com o trabalho desenvolvido por Benoit-Vical e colaboradores (BENOIT-VICAL et al., 2007), os quais observaram uma potência elevada do composto híbrido do endoperóxido 1,2,4-trioxano e da quinolina em comparação com o seu componente endoperóxido.

Embora o híbrido 163A (**3**) seja capaz de afetar esporozoítos e gametócitos jovens na escala de nanomolar, o cenário é diferente quando analisado a ação frente aos gametócitos maduros (estágio V). Por serem metabolicamente menos ativos, como por exemplo, apresentarem uma menor metabolização do heme, o potencial antimalárico do 163A (**3**) frente os gametócitos maduros foi de menor potência, na escala de micromolar. É bem verdade que poucos compostos são potentes na escala em nanomolar frente aos gametócitos maduros, e uma das poucas exceções é o azul de metileno (D'ALESSANDRO et al., 2013; LELIÈVRE et al., 2012). Embora o híbrido 163A (**3**) e a DHA tenham apresentado potência inferior no estágio maduro, ambos apresentaram valores de $IC_{50}$ entre 2 e 5 µM.

Sabe-se que a concentração plasmática máxima da DHA em paciente é de aproximadamente 4 µM, uma concentração próxima dos valores de $IC_{50}$ necessários para eliminar os gametócitos maduros (NEWTON et al., 2002). Por conta disso, a falha em bloquear a transmissão é relativamente frequente sob o tratamento com a TCA. Por fim, é importante frisar que, muito embora a ação dos compostos híbridos frente aos diferentes estágios dos

gametócitos do *P. falciparum* tenham sido estudados aqui, sugerindo um potencial no bloqueio da transmissão ao vetor, ainda se faz necessária a realização de estudos de susceptibilidade nos estágios evolutivos do plasmódio nos anofelinos frente aos compostos híbridos.

Uma vez que os achados farmacológicos com o composto híbrido 163A (**3**) revelaram o seu perfil de ação fenotípica frente aos diferentes estágios evolutivos do plasmódio, outros questionamentos pertinentes surgiram no decorrer das pesquisas: (i) qual a ação fenotípica de compostos híbridos de ART frente a cepas do *P. falciparum* resistentes as ARTs?; (ii) como é o perfil de estabilidade química e de tempo de meia-vida de compostos híbridos em relação aos fármacos da classe das ARTs?

É uma prerrogativa pertinente que o fenômeno de resistência do plasmódio ao tratamento com as ARTs está correlacionado com o tempo de meia-vida plasmático relativamente curto dos fármacos desta classe (GIANNANGELO et al., 2019; MOK et al., 2015; TILLEY et al., 2016). Por esta classe de fármaco apresentar um t1/2 de cerca de 1 a 3 h, o plasmódio promove um atraso no seu ciclo evolutivo, a fim de contornar o pico plasmático das ARTs. Após a eliminação das ARTs, o plasmódio retorna o crescimento no seu ciclo evolutivo sanguíneo assexuado.

Portanto, para responder estas perguntas conceituais citadas acima, foram realizados ensaios farmacológicos específicos, assim como incluiu-se o composto híbrido LH70 (**4**), no qual diferentemente do 163A (**3**), é um composto híbrido não-clivável, mais estável e destituído de 4-aminoquinolina. Nós já tínhamos evidenciado que o híbrido (**3**) é ativo na supressão da detoxificação do heme e na alquilação de proteínas (QUADROS et al., 2021; AYSUN, 2019), enquanto que um destaque do híbrido (**4**) é que o mesmo possui eficácia *in vivo* duas vezes maior do que o ARS (LARS et al, 2022, em submissão). Estes achados sugerem que os híbridos possuem características tanto semelhantes quanto diferentes em relação as ARTs. Porém, o fenômeno de resistência do plasmódio as ARTs é complexo e multi-fatorial, exigindo assim um estudo frente a fenótipos diferentes do parasito. É importante destacar que o estudo subsequente se deu frente a três fenótipos de parasitos: infecção de eliminação rápida (“fast-clearing”) de parasitos sensíveis as ARTs ($CI_{50}$), infecção de eliminação lenta (“slow-clearing”) de parasito proliferativo (RSA) e a infecção de eliminação lenta de parasito não-proliferativo e quiescentes (QSA).

Em relação a infecção de eliminação rápida de parasitos sensíveis as ARTs ($IC_{50}$), os achados dos híbridos foram interessantes e merecem ser discutidos. Os híbridos foram mais potentes do que a ART em inibir as cepas do *P. falciparum* sensíveis e resistentes a CQ. No

caso do híbrido (**4**), o mesmo foi equipotente a DHA, no qual *in vitro*, é o fármaco da classe das ART de maior potência.

Em seguida, através dos ensaios de RSA e de sobrevivência destes parasitos como um indicador de resistência cruzada dos híbridos com as ARTs, nós avaliamos se os híbridos seriam capazes de reduzir a sobrevivência de anéis (RSA) e consequentemente impedir a recrudescência de cepas do *P. falciparum* sensíveis ou resistentes à ART. O híbrido (**3**) não foi capaz de reduzir a sobrevivência de anéis (RSA) com eficiência maior do que a DHA. Já o híbrido (**4**) foi capaz de reduzir a sobrevivência de anéis (RSA) com eficiência maior do que a DHA. Confirmando esse dado do RSA, nós observamos que o híbrido (**4**), mas não o (**3**), é capaz de causar um atraso na recrudescência dos parasitos sensíveis e resistentes a ART. Uma interpretação para isso é que a susceptibilidade de existir resistência cruzada com as ARTs é maior com o híbrido (**3**) do que com o híbrido (**4**). Estes dados estão de acordo com os resultados obtidos anteriormente que evidenciaram a susceptibilidade de existir resistência cruzada entre ARTs e moléculas que contêm um grupo peróxido (STRAIMER, GNADIG et al. 2017, PALOQUE, WITKOWSKI et al. 2018, OUJI, BARNOIN et al. 2020).

Dada a ação dos híbridos em inibir os parasitos resistentes à ART no RSA, nós também avaliamos as suas atividades contra os estágios de parasitas não-proliferativos (quiescentes) usando o ensaio de QSA. Nós observamos que o híbrido (**3**), que foi desprovido de atividade potente na RSA, também foi desprovido de potência para eliminar os parasitos quiescentes (QSA). Em contrapartida, observamos que o híbrido (**4**), que apresentou potência no ensaio de RSA, também foi dotado de uma capacidade promissora na eliminação dos parasitos quiescentes, embora com potência reduzida em relação a sua capacidade de afetar os parasitos em proliferação (RSA).

A literatura descrevendo a ação de fármacos nos ensaios de QSA é relativamente escassa. Entretanto, Reyser et al. (2020) demonstraram que a susceptibilidade dos parasitos quiescentes *versus* proliferativos ao tratamento podem ser significativamente diferentes, ou seja, um fármaco capaz de eliminar parasitos no RSA pode ser incapaz de eliminar parasitos quiescentes no QSA. Diante dos nossos resultados, presume-se que para um fármaco derivado de endoperóxido ser capaz de reduzir a infecção de eliminação lenta (“slow-clearing”) de parasitos proliferativos (RSA), deveria apresentar um t1/2 mais longo. Já para um fármaco ser capaz de reduzir a infecção de eliminação lenta de parasitos quiescentes (QSA), deveria apresentar um mecanismo de ação diferente das ARTs, visto que nos parasitos quiescentes, a detoxificação de heme e o fluxo de heme estão diminuídos e inoperantes.

Como os compostos híbridos (**3**) e (**4**) têm uma resposta fenotípica antimalárica diferente entre si, nós especulamos que essa distinta ação fenotípica poderia ser devido a ativação do peróxido mediada pelo heme, a estabilidade química ou a capacidade destes híbridos de eliminar parasitos ocorrer de formas diferentes ou pelo menos em momentos diferentes.

Nós observamos que o híbrido (**3**) possui uma estabilidade levemente maior do que a DHA, contudo, sua estabilidade nos microssomos hepáticos é relativamente baixa. Já o híbrido (**4**) possui uma estabilidade significativamente maior do que a DHA, assim como uma estabilidade nos microssomos hepáticos quase comparável ao ARS. De fato, a maior estabilidade química do híbrido (**4**) parece estar diretamente relacionada com a sua potência frente aos parasitos resistentes à ART no ensaio de sobrevivência dos anéis (RSA). Tanto o híbrido (**3**) como a DHA foram destituídos de atividade no RSA; ambos possuem uma estabilidade química menor, pois são rapidamente metabolizados. Esta mesma correlação tem sido observada para os fármacos ozonídeos (OZ277 e OZ439) (GIANNANGELO et al., 2020; STRAIMER et al., 2017) e os 1,2,4,5-tetraoxanos (N205 e E209) (O' NEILL et al., 2018; O'NEILL et al., 2017).

Em relação a capacidade dos híbridos em eliminar parasitos em momentos diferentes, nós avaliamos a velocidade de ação dos híbridos em eliminar as diferentes formas evolutivas dos parasitos do estágio sanguíneo assexuado em diferentes tempos (24, 48 e 72 horas). Em comparação com a ATQ, que é um antimalárico de velocidade de ação lenta, os híbridos (**3**) e (**4**) apresentaram uma velocidade de ação relativamente rápida e similar a DHA, o que evidência mais uma vez as características fenotípicas similares com as ARTs. O híbrido (**4**) apresentou equipotência em eliminar os parasitos nos diferentes tempos avaliados, enquanto o híbrido (**3**) e a DHA apresentaram potência menor do que o híbrido (**4**) em eliminar os parasitos com 24 horas; isto é, o híbrido (**4**) possui uma velocidade de ação mais rápida do que o híbrido (**3**) e DHA para eliminar os parasitos em menor tempo. Ressalva-se aqui, entretanto, que o ensaio de velocidade de ação com os métodos do SYBR green I ou pLDH não permitem distinguir parasitos não-viáveis dos parasitos dormentes. Em geral, para estabelecer com maior acurácia a velocidade de ação, é necessário usar a técnica de diluição limitante (SANZ et al., 2012). Todavia, em geral, os fármacos endoperóxidos têm velocidade de ação relativamente rápida, o que parece ser também o caso dos híbridos (**3**) e (**4**).

Por fim, nós investigamos se os híbridos apresentam sinergismo com antimaláricos já utilizados em terapias combinadas, e se podem funcionar como fármacos substitutos de tais

terapias combinadas. Assim, nós observamos que o híbrido (**3**) pode apresentar um antagonismo de potência se combinado com a CQ, um fármaco potente em suprimir a detoxificação do heme; este antagonismo se deve muito provavelmente à competição de ambas as quinolinas pelos mesmos alvos moleculares. Em contrapartida, o composto híbrido (**3**) apresentou sinergismo de potência quando combinado ao fármaco pleiotrópico MFQ, indicando que estes compostos não competem pelos mesmos alvos moleculares. Já o híbrido (**4**) apresentou aditividade ou sinergismo de potência quando combinado ao CQ ou MFQ; uma explicação plausível é que o grupo glicol benzimidazol apresentado no híbrido (**4**) não acrescenta um segundo mecanismo de ação, mas na verdade confere uma proteção estéril benéfica do peróxido para não ser rapidamente degradado pelo heme. Embora estes resultados sejam promissores, é necessário ainda investigar se a somação da combinação de fármacos também pode ser observada ou não contra cepas resistentes a fármacos; ainda é necessário mais trabalho.

# 6 **CONSIDERAÇÕES FINAIS**

Dado o volume de investigações criteriosas e evidências científicas apresentadas nesta tese, conclui-se que o desenvolvimento dos compostos híbridos (**1-4**) revelou um volume de dados que ratificam que estes fármacos conservam os mecanismos de ação dos endoperóxidos e/ou quinolinas; de fato, os híbridos são potentes e eficazes frente aos alvos moleculares da supressão da detoxificação do heme e a homeostasia de tióis. Além disso, estes fármacos experimentais também apresentaram um potencial terapêutico melhorado e um espectro de ação mais amplo do que a monoterapia ou a terapia combinada com as ARTs. Reitera-se também que os fármacos híbridos como componentes em terapias combinadas de fármacos podem ser de velocidade de ação rápida e de uma ação mais duradoura, e podem ser bastante ativos contra os parasitos sensíveis e resistentes às ARTs.

Através dos resultados apresentados nesta tese, podemos concluir que:

1. Os compostos híbridos MNCS59 (**1**) e MNCS60 (**2**), cuja composição farmacofórica inclui as aminoquinolinas PQ e CQ ou PQ e AQ ligadas pelo ouro (I), são bastante ativos na supressão da detoxificação do heme e na homeostasia de tióis; além disso, possuem um espectro de ação amplo, sendo potentes e eficazes contra os estágios sexuado e assexuados, incluindo o estágio hepático.
2. Os compostos híbridos MNCS59 (**1**) e MNCS60 (**2**) foram capazes de eliminar os esporozoítos (formas evolutivas responsáveis por iniciar a infecção no estágio hepático) e de eliminar os gametócitos (formas evolutivas não-proliferativas responsáveis pela transmissão da doença).
3. O composto híbrido 163A (**3**) é um endoperóxido cujos componentes da sua composição são a CQ e a ART. Assim como os híbridos (**1**) e (**2**), o híbrido (**3**) também é bastante ativo na supressão da detoxificação do heme. O híbrido (**3**) é potente e eficaz contra os parasitos dos estágios assexuados e sexuados. Além disso, é um fármaco experimental potente em alquilar proteínas do parasito, levando-o a morte.
4. Os híbridos 163A (**3**) e LH70 (**4**) são fármacos estáveis e de ação rápida contra os parasitos do *P. falciparum* sensíveis e resistentes a CQ ou a ART. Além disso, o híbrido LH70 (**4**) demonstrou potência elevada em eliminar parasitos resistentes a ART, bem como em eliminar os parasitos quiescentes resistentes a ART.

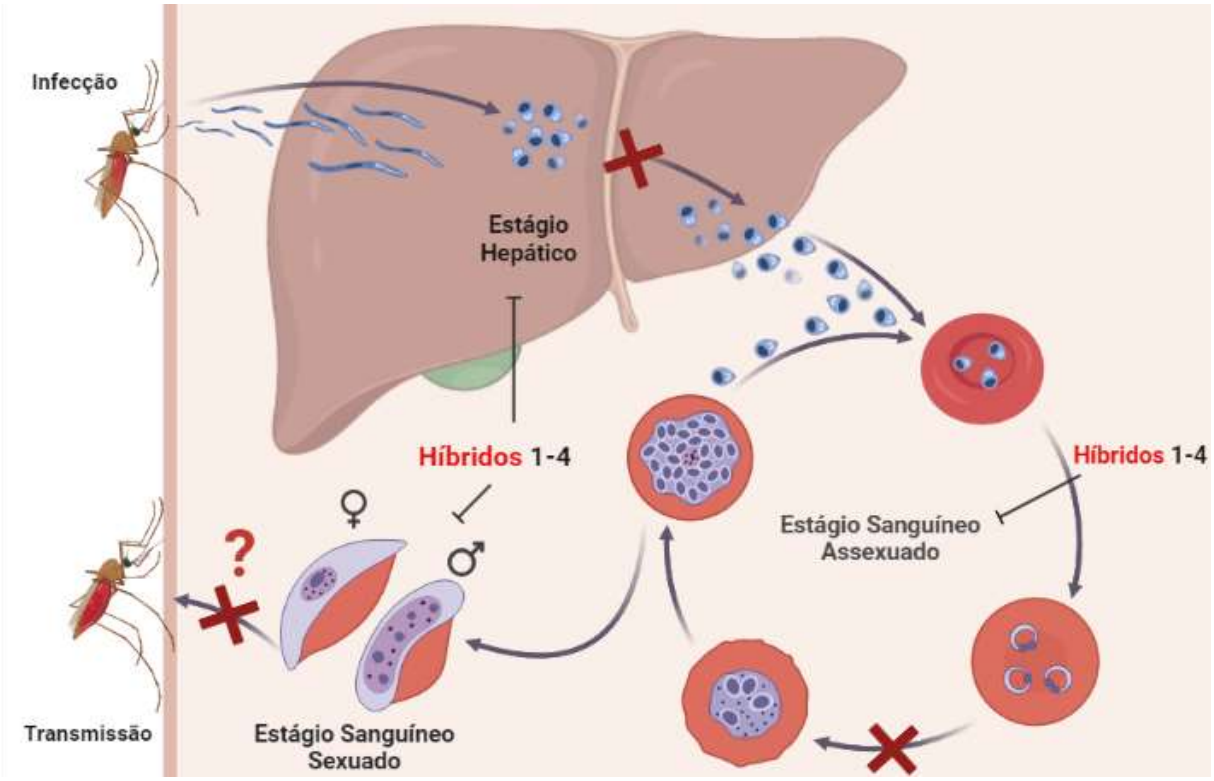


**Figura 12 -** Esquema demonstrativo da atividade antimalárica dos híbridos 1-4. Os híbridos estudados nesta tese demonstraram experimentalmente potência em todos os estágios evolutivos, indicando o amplo espectro de ação em múltiplos estágios. Além disso, foram eficazes contra o estágio sanguíneo assexuado, onde a homeostasia de tióis e detoxificação do heme livre são processos bastante ativos. A interrogação (?) no estágio sanguíneo sexuado indica uma possível atividade de bloqueio da transmissão dos gametócitos pelos híbridos.
**Fonte**: Elaborado pela autora

Através da conclusão apresentada nesta tese, podemos sugerir perspectivas experimentais futuras:

1. Realizar estudos para determinar a ação antiparasitária dos compostos híbridos frente ao *P. vivax*, especial no contexto da malária no Brasil.

2. Realizar estudos de susceptibilidade dos estágios evolutivos do *P. vivax* ou *P. falciparum* nos anofelinos, tais como o bloqueio da formação de oocinetos, frente aos compostos híbridos.

3. Verificar se a susceptibilidade do tratamento com os compostos híbridos gera parasitos resistentes (resistência adquirida).

## REFERÊNCIAS

ABLA, N. et al. Long-Lasting and Fast-Acting in Vivo Efficacious Antiplasmodial Azepanylcarbazole Amino Alcohol. **ACS Medicinal Chemistry Letters**, v. 8, n. 12, p. 1304–1308, 14 dez. 2017.

ACHAN, J. et al. Quinine, an old anti-malarial drug in a modern world: Role in the treatment of malaria. **Malaria Journal**, May 24;10:144, 2011.

ADOKE, Y. et al. A randomized, double-blind, phase 2b study to investigate the efficacy, safety, tolerability and pharmacokinetics of a single-dose regimen of ferroquine with artefenomel in adults and children with uncomplicated Plasmodium falciparum malaria. **Malaria Journal**, v. 20, n. 1, p. 222, 19 dez. 2021.

AGUIAR, A. C. C. et al. New approaches in antimalarial drug discovery and development - A Review. **Memorias do Instituto Oswaldo Cruz**, v. 107, n. 7, p. 831–845, 2012.

AHMAD, S. S. et al. Mefloquine as a prophylaxis for malaria needs to be revisited. **International Journal for Parasitology: Drugs and Drug Resistance**, v. 17, p. 23–26, dez. 2021.

ALVEN, S.; ADERIBIGBE, B. Combination Therapy Strategies for the Treatment of Malaria. **Molecules**, v. 24, n. 19, p. 3601, 7 out. 2019.

AMELO, W.; MAKONNEN, E. Efforts Made to Eliminate Drug-Resistant Malaria and Its Challenges. **BioMed Research International**, v. 2021, p. 1–12, 30 ago. 2021.

ANSBRO, M. R. et al. Modulation of Triple Artemisinin-Based Combination Therapy Pharmacodynamics by *Plasmodium falciparum* Genotype. **ACS Pharmacology & Translational Science**, v. 3, n. 6, p. 1144–1157, 11 dez. 2020.

ASHLEY, E. A.; PYAE PHYO, A.; WOODROW, C. J. Malaria. **The Lancet**, v. 391, n. 10130, p. 1608–1621, 2018.

AUTINO, B. et al. Epidemiology of malaria in endemic areas. **Mediterranean Journal of Hematology and Infectious Diseases**, v. 4, n. 1, 2012.

AYOUB, N. M. Editorial: Novel Combination Therapies for the Treatment of Solid Cancers. **Frontiers in Oncology**, v. 11, 18 jun. 2021.

BAIRD, J. K. 8-Aminoquinoline Therapy for Latent Malaria. **Clinical Microbiology Reviews**, v. 32, n. 4, p. 1–68, 31 jul. 2019.

BAKSHI, R. P. et al. Long-acting injectable atovaquone nanomedicines for malaria prophylaxis. **Nature Communications**, v. 9, n. 1, p. 315, 22 jan. 2018.

BARAGAÑA, B. et al. A novel multiple-stage antimalarial agent that inhibits protein synthesis. **Nature**, v. 522, n. 7556, p. 315–320, 2015.

BASSAT, Q. et al. Challenges in the clinical development pathway for triple and multiple drug combinations in the treatment of uncomplicated falciparum malaria. **Malaria Journal**, v. 21, n. 1, p. 61, 22 dez. 2022.

BELL, A. Antimalarial drug synergism and antagonism: Mechanistic and clinical significance. **FEMS Microbiology Letters**, v. 253, n. 2, p. 171–184, dez. 2005.

BENOIT-VICAL, F. et al. Trioxaquines Are New Antimalarial Agents Active on All Erythrocytic Forms, Including Gametocytes. **Antimicrobial Agents and Chemotherapy**, v. 51, n. 4, p. 1463–1472, abr. 2007a.

BENOIT-VICAL, F. et al. Trioxaquines Are New Antimalarial Agents Active on All Erythrocytic Forms, Including Gametocytes. **Antimicrobial Agents and Chemotherapy**, v. 51, n. 4, p. 1463–1472, abr. 2007b.

BERMAN, J. Toxicity of commonly used antimalarial drugs. **Travel Medicine and Infectious Disease**, v. 2, n. 3–4, p. 171–184, ago. 2004.

BIAMONTE, M. A.; WANNER, J.; LE ROCH, K. G. Recent advances in malaria drug discovery. **Bioorganic and Medicinal Chemistry Letters**, v. 23, n. 10, p. 2829–2843, 2013.

BIRRELL, G. W. et al. JPC-2997, a New Aminomethylphenol with High *In Vitro* and *In Vivo* Antimalarial Activities against Blood Stages of Plasmodium. **Antimicrobial Agents and Chemotherapy**, v. 59, n. 1, p. 170–177, jan. 2015.

BLAGBOROUGH, A. M. et al. Transmission-blocking interventions eliminate malaria from laboratory populations. **Nature Communications**, v. 4, n. 1, p. 1812, 7 out. 2013.

BLANK, B. R. et al. Antimalarial Trioxolanes with Superior Drug-Like Properties and In Vivo Efficacy. **ACS Infectious Diseases**, v. 6, n. 7, p. 1827–1835, 10 jul. 2020.

BLASCO, B.; LEROY, D.; FIDOCK, D. A. Parasite Biology To the Clinic. **Nature Medicine**, v. 23, n. 8, p. 917–928, 2017.

BRANCUCCI, N. M. B. et al. Lysophosphatidylcholine Regulates Sexual Stage Differentiation in the Human Malaria Parasite Plasmodium falciparum. **Cell**, v. 171, n. 7, p. 1532- 1544.e15, dez. 2017.
BURROWS, J. N. et al. New developments in anti-malarial target candidate and product profiles. **Malaria Journal**, v. 16, n. 1, p. 26, 13 dez. 2017.

BRASIL. Ministério da Saúde. Secretaria de Vigilância em Saúde. Departamento de Vigilância Epidemiológica. **Guia Prático de Tratamento de Malária no Brasil.** Brasília: Ministério da Saúde, 2010. (Série A. Normas e Manuais Técnicos) 2010. Disponivel em: <https://bvsms.saude.gov.br/bvs/publicacoes/guia_pratico_malaria.pdf> Acesso em: 01 dez.2022.

BYNUM, B. A history of malaria. **The Lancet**, v. 371, n. 9622, p. 1407–1408, abr. 2008.

CABRERA, M.; CUI, L. *In Vitro* Activities of Primaquine-Schizonticide Combinations on Asexual Blood Stages and Gametocytes of Plasmodium falciparum. **Antimicrobial Agents and Chemotherapy**, v. 59, n. 12, p. 7650–7656, dez. 2015.

CAMARDA, G. et al. Antimalarial activity of primaquine operates via a two-step biochemical relay. **Nature Communications**, v. 10, n. 1, p. 3226, 19 jul. 2019.

ÇAPCI, A. et al. Artemisinin–(Iso)quinoline Hybrids by C−H Activation and Click Chemistry: Combating Multidrug-Resistant Malaria. **Angewandte Chemie International Edition**, v. 58, n. 37, p. 13066–13079, 9 set. 2019.

CAPELA, R. et al. Design and Evaluation of Primaquine-Artemisinin Hybrids as a Multistage Antimalarial Strategy. **Antimicrobial Agents and Chemotherapy**, v. 55, n. 10, p. 4698–4706, out. 2011.

CENTERS FOR DISEASE CONTROL AND PREVENTION. **Malaria Distribution**. CDC, 2020. Disponível em: <https://www.cdc.gov/malaria/about/distribution.html> Acesso em: 12/12/2022.

CHARMAN, S. A. et al. Synthetic ozonide drug candidate OZ439 offers new hope for a single-dose cure of uncomplicated malaria. **Proceedings of the National Academy of Sciences**, v. 108, n. 11, p. 4400–4405, 15 mar. 2011.

CLOETE, T. T. et al. Synthesis, in vitro antiplasmodial activity and cytotoxicity of a series of artemisinin–triazine hybrids and hybrid-dimers. **European Journal of Medicinal Chemistry**, v. 76, p. 470–481, abr. 2014.

COTTRELL, G. et al. Emergence of Resistance to Atovaquone-Proguanil in Malaria Parasites: Insights from Computational Modeling and Clinical Case Reports. **Antimicrobial Agents and Chemotherapy**, v. 58, n. 8, p. 4504–4514, ago. 2014.

COWMAN, A. F. et al. Malaria: Biology and Disease. **Cell**, v. 167, n. 3, p. 610–624, out. 2016.
COX, F. E. G. Cox. History of the discovery of the malaria parasites and their vectors. **Parasites and Vectors**, v. 3, n. 5, p. 1–9, 2010.

CUI, L.; SU, X. Discovery, mechanisms of action and combination therapy of artemisinin. **Expert Review of Anti-infective Therapy**, v. 7, n. 8, p. 999–1013, 10 out. 2009.

D'ALESSANDRO, S. et al. A Plasmodium falciparum screening assay for anti-gametocyte drugs based on parasite lactate dehydrogenase detection. **Journal of Antimicrobial Chemotherapy**, v. 68, n. 9, p. 2048–2058, set. 2013.

DAMBUZA, N. S. et al. Antiplasmodial activity, in vivo pharmacokinetics and anti-malarial efficacy evaluation of hydroxypyridinone hybrids in a mouse model. **Malaria Journal**, v. 14, n. 1, p. 505, 16 dez. 2015.

DASH, M. et al. Gametogenesis in Plasmodium: Delving Deeper to Connect the Dots. **Frontiers in Cellular and Infection Microbiology**, v. 12, 15 jun. 2022.

DEGAREGE, A. et al. Improving socioeconomic status may reduce the burden of malaria in sub–Saharan Africa: A systematic review and meta-analysis. **PLoS ONE**, v. 14, n. 1, p. 1–26, 2019.

DELVES, M. et al. The Activities of Current Antimalarial Drugs on the Life Cycle Stages of Plasmodium: A Comparative Study with Human and Rodent Parasites. **PLoS Medicine**, v. 9, n. 2, p. e1001169, 21 fev. 2012.

DINI, S. et al. Investigating the Efficacy of Triple Artemisinin-Based Combination Therapies for Treating Plasmodium falciparum Malaria Patients Using Mathematical Modeling. **Antimicrobial Agents and Chemotherapy**, v. 62, n. 11, nov. 2018.

DOUGLAS, N. M. et al. Artemisinin combination therapy for vivax malaria. **The Lancet Infectious Diseases**, v. 10, n. 6, p. 405–416, jun. 2010.

DUBAR, F. et al. Ferroquine, an Ingenious Antimalarial Drug –Thoughts on the Mechanism of Action. **Molecules**, v. 13, n. 11, p. 2900–2907, 20 nov. 2008.

DUFFY, S. et al. Large-scale production of Plasmodium falciparum gametocytes for malaria drug discovery. **Nature Protocols**, v. 11, n. 5, p. 976–992, 2016.

DZIEKAN, J. M. et al. Identifying purine nucleoside phosphorylase as the target of quinine using cellular thermal shift assay. **Science Translational Medicine**, v. 11, n. 473, 2 jan. 2019.
FAIRHURST, R. M.; DONDORP, A. M. Artemisinin-Resistant *Plasmodium falciparum* Malaria. **Microbiology Spectrum**, v. 4, n. 3, 6 maio 2016.

F. HOFFMANN-LA ROCHE LTD. **Mefloquine hydrochloride**. New Jersy, 2009. Disponível em: <https://www.accessdata.fda.gov/drugsatfda_docs/label/2009/019591s026s028lbl.pdf>. Acesso em: 01/12/2022.

FAN, Y.-L. et al. Antiplasmodial and antimalarial activities of quinolone derivatives: An overview. **European Journal of Medicinal Chemistry**, v. 146, p. 1–14, fev. 2018.

FENG, L. et al. Repurposing Auranofin and Evaluation of a New Gold(I) Compound for the Search of Treatment of Human and Cattle Parasitic Diseases: From Protozoa to Helminth Infections. **Molecules**, v. 25, n. 21, p. 5075, 1 nov. 2020.

FIDOCK, D. A. et al. Antimalarial drug discovery: Efficacy models for compound screening. **Nature Reviews Drug Discovery**, v. 3, n. 6, p. 509–520, 2004.

FRAMPTON, J. E. Tafenoquine: First Global Approval. **Drugs**, v. 78, n. 14, p. 1517–1523, 2018.

FREL, UL et al. The Effectiveness of Combinations of Antileukemic Agents in Inducing and Maintaining Remission in Children with Acute Leukemia. **Blood**, 26(5):642-56, 1965.

GIANNANGELO, C. et al. Ozonide Antimalarial Activity in the Context of Artemisinin-Resistant Malaria. **Trends in Parasitology**, v. 35, n. 7, p. 529–543, jul. 2019.

GOLENSER, J. et al. Current perspectives on the mechanism of action of artemisinins. **International Journal for Parasitology**, v. 36, n. 14, p. 1427–1441, 2006.

GORKA, A. P.; JACOBS, L. M.; ROEPE, P. D. Cytostatic versus cytocidal profiling of quinoline drug combinations via modified fixed ratio isobologram analysis. **Malaria Journal**, v. 12, n. 1, p. 332, 18 dez. 2013.

GROBUSCH, M. P. et al. Travel-related infections presenting in Europe: A 20-year analysis of EuroTravNet surveillance data. **The Lancet Regional Health - Europe**, v. 1, p. 100001, fev. 2021.

HANBOONKUNUPAKARN, B.; WHITE, N. J. Advances and roadblocks in the treatment of malaria. **British Journal of Clinical Pharmacology**, v. 88, n. 2, p. 374–382, fev. 2022.

HELD, J. et al. Ferroquine and artesunate in African adults and children with Plasmodium falciparum malaria: A phase 2, multicentre, randomised, double-blind, dose-ranging, non-inferiority study. **The Lancet Infectious Diseases**, v. 15, n. 12, p. 1409–1419, 2015.

HOEFNAGEL, J. G. M.; MASSAR, K.; HAUTVAST, J. L. A. Non-adherence to malaria prophylaxis: The influence of travel-related and psychosocial factors. **Journal of Infection and Public Health**, v. 13, n. 4, p. 532–537, abr. 2020.

ISLAHUDIN, F. et al. The antimalarial drug quinine interferes with serotonin biosynthesis and action. **Scientific Reports**, v. 4, 2014.

JOSLING, G. A.; LLINÁS, M. Sexual development in Plasmodium parasites: Knowing when it's time to commit. **Nature Reviews Microbiology**, v. 13, n. 9, p. 573–587, 2015.

KAPISHNIKOV, S. et al. Mode of action of quinoline antimalarial drugs in red blood cells infected by *Plasmodium falciparum* revealed in vivo. **Proceedings of the National Academy of Sciences**, v. 116, n. 46, p. 22946–22952, 12 nov. 2019.

KAPISHNIKOV, S. et al. Malaria Pigment Crystals: The Achilles′ Heel of the Malaria Parasite. **ChemMedChem**, v. 16, n. 10, p. 1515–1532, 18 maio 2021.

KATO, N. et al. Diversity-oriented synthesis yields novel multistage antimalarial inhibitors. **Nature**, v. 538, n. 7625, p. 344–349, 2016.

KIM, H. S.; HAMMILL, J. T.; GUY, R. K. Seeking the Elusive Long-Acting Ozonide: Discovery of Artefenomel (OZ439). **Journal of Medicinal Chemistry**, v. 60, n. 7, p. 2651–2653, 13 abr. 2017.

KOKO, D. C. et al. Analysis of attitudes and practices influencing adherence to seasonal malaria chemoprevention in children under 5 years of age in the Dosso Region of Niger. **Malaria Journal**, v. 21, n. 1, p. 375, 6 dez. 2022.

LAURENS, M. B. RTS, S/AS01 vaccine (Mosquirix™): an overview. **Human Vaccines & Immunotherapeutics**, v. 16, n. 3, p. 480–489, 3 mar. 2020.

LAWRENSON, A. S. et al. Study of the antimalarial activity of 4-aminoquinoline compounds against chloroquine-sensitive and chloroquine-resistant parasite strains. **Journal of Molecular Modeling**, v. 24, n. 9, 2018.
LELIÈVRE, J. et al. Activity of Clinically Relevant Antimalarial Drugs on Plasmodium falciparum Mature Gametocytes in an ATP Bioluminescence "Transmission Blocking" Assay. **PLoS ONE**, v. 7, n. 4, p. e35019, 13 abr. 2012.

LIGUORI, I. et al. Oxidative stress, aging, and diseases. **Clinical Interventions in Aging**, v. Volume 13, p. 757–772, abr. 2018.

LIN, J. et al. Replication of Plasmodium in reticulocytes can occur without hemozoin formation, resulting in chloroquine resistance. **Journal of Experimental Medicine**, v. 212, n. 6, p. 893–903, 1 jun. 2015.

LLANOS-CUENTAS, A. et al. Antimalarial activity of single-dose DSM265, a novel plasmodium dihydroorotate dehydrogenase inhibitor, in patients with uncomplicated Plasmodium falciparum or Plasmodium vivax malaria infection: a proof-of-concept, open-label, phase 2a study. **The Lancet Infectious Diseases**, v. 18, n. 8, p. 874–883, ago. 2018.

LLANOS-CUENTAS, A. et al. Tafenoquine versus Primaquine to Prevent Relapse of *Plasmodium vivax* Malaria. **New England Journal of Medicine**, v. 380, n. 3, p. 229–241, 17 jan. 2019.

LLANOS-CUENTAS, A. et al. Tafenoquine for the treatment of *Plasmodium vivax* malaria. **Expert Opinion on Pharmacotherapy**, v. 23, n. 7, p. 759–768, 3 maio 2022.

LLORÀ-BATLLE, O. et al. Conditional expression of PfAP2-G for controlled massive sexual conversion in *Plasmodium falciparum*. **Science Advances**, v. 6, n. 24, 12 jun. 2020.

MA, W. et al. A second mechanism employed by artemisinins to suppress Plasmodium falciparum hinges on inhibition of hematin crystallization. **Journal of Biological Chemistry**, v. 296, p. 100123, jan. 2021.

MACE, K. E.; LUCCHI, N. W.; TAN, K. R. Malaria Surveillance — United States, 2018. **MMWR. Surveillance Summaries**, v. 71, n. 8, p. 1–35, 2 set. 2022.

MACEDO, T. S. et al. Chloroquine-containing organoruthenium complexes are fast-acting multistage antimalarial agents. **Parasitology**, v. 143, n. 12, p. 1543–1556, 21 out. 2016.

MACEDO, T. S. et al. Platinum (<scp>ii</scp>)–chloroquine complexes are antimalarial agents against blood and liver stages by impairing mitochondrial function. **Metallomics**, v. 9, n. 11, p. 1548–1561, 2017.

MAGUIRE, J. D. et al. Mefloquine is highly efficacious against chloroquine-resistant Plasmodium vivax malaria and Plasmodium falciparum malaria in Papua, Indonesia. **Clinical Infectious Diseases**, v. 42, n. 8, p. 1067–1072, 2006.

MAIRET-KHEDIM, M. et al. Clinical and In Vitro Resistance of *Plasmodium falciparum* to Artesunate-Amodiaquine in Cambodia. **Clinical Infectious Diseases**, v. 73, n. 3, p. 406–413, 2 ago. 2021.

MCCARTHY, J. S. et al. Safety, tolerability, pharmacokinetics, and activity of the novel long-acting antimalarial DSM265: a two-part first-in-human phase 1a/1b randomised study. **The Lancet Infectious Diseases**, v. 17, n. 6, p. 626–635, jun. 2017.

MIRANDA, D. et al. Novel Endoperoxide-Based Transmission-Blocking Antimalarials with Liver- and Blood-Schizontocidal Activities. **ACS Medicinal Chemistry Letters**, v. 5, n. 2, p. 108–112, 13 fev. 2014.

MOK, S. et al. Population transcriptomics of human malaria parasites reveals the mechanism of artemisinin resistance. **Science**, v. 347, n. 6220, p. 431–435, 23 jan. 2015.

MOKHTARI, R. B. et al. Combination therapy in combating cancer. **Oncotarget**, v. 8, n. 23, p. 38022–38043, 6 jun. 2017.

MUELLER, E. A. et al. Artesunate and mefloquine given simultaneously for three days via a prepacked blister is equally effective and tolerated as a standard sequential treatment of uncomplicated acute Plasmodium falciparum malaria: randomized, double-blind study in Thailand. **The American Journal of Tropical Medicine and Hygiene**, v. 67, n. 5, p. 465–472, 1 nov. 2002.

MÜLLER, I. B.; HYDE, J. E. Antimalarial drugs: modes of action and mechanisms of parasite resistance. **Future Microbiology**, v. 5, n. 12, p. 1857–1873, dez. 2010.

NEWTON, P. N. et al. Comparison of Oral Artesunate and Dihydroartemisinin Antimalarial Bioavailabilities in Acute Falciparum Malaria. **Antimicrobial Agents and Chemotherapy**, v. 46, n. 4, p. 1125–1127, abr. 2002.

NGOTHO, P. et al. Revisiting gametocyte biology in malaria parasites. **FEMS Microbiology Reviews**, v. 43, n. 4, p. 401–414, 2019.

O' NEILL, P. M. et al. Synthesis and profiling of benzylmorpholine 1,2,4,5-tetraoxane analogue N205: Towards tetraoxane scaffolds with potential for single dose cure of malaria. **Bioorganic & Medicinal Chemistry**, v. 26, n. 11, p. 2996–3005, jul. 2018.

O'NEILL, P. M. et al. Synthesis, Antimalarial Activity, and Preclinical Pharmacology of a Novel Series of 4′-Fluoro and 4′-Chloro Analogues of Amodiaquine. Identification of a Suitable "Back-Up" Compound for *N-tert* -Butyl Isoquine. **Journal of Medicinal Chemistry**, v. 52, n. 7, p. 1828–1844, 9 abr. 2009.

O'NEILL, P. M. et al. A tetraoxane-based antimalarial drug candidate that overcomes PfK13-C580Y dependent artemisinin resistance. **Nature Communications**, v. 8, n. 1, p. 15159, 24 maio 2017.

ORGANIZAÇÃO MUNDIAL DE SAÚDE. **Malária**, 2022. <https://www.who.int/news-room/fact-sheets/detail/malaria>. Acesso em: 01 jan. 2022.

OUJI, M., G. et al. Hybrid Gold(I) NHC-Artemether Complexes to Target Falciparum Malaria Parasites. **Molecules**, v. 25, n. 12, 2020.

PALOQUE, L. et al. Endoperoxide-based compounds: cross-resistance with artemisinins and selection of a Plasmodium falciparum lineage with a K13 non-synonymous polymorphism. **J Antimicrob Chemother**, 73(2): 395-403, 2018.
PANNU, A. K. Malaria today: advances in management and control. **Tropical Doctor**, v. 49, n. 3, p. 160–164, 2019.

PARROCHE, P. et al. Malaria hemozoin is immunologically inert but radically enhances innate responses by presenting malaria DNA to Toll-like receptor 9. **Proceedings of the National Academy of Sciences**, v. 104, n. 6, p. 1919–1924, 6 fev. 2007.

PATON, D. G. et al. Exposing Anopheles mosquitoes to antimalarials blocks Plasmodium parasite transmission. **Nature**, v. 567, n. 7747, p. 239–243, 27 mar. 2019.

PEREIRA, M. L. M.; MARINHO, C. R. F.; EPIPHANIO, S. Could Heme Oxygenase-1 Be a New Target for Therapeutic Intervention in Malaria-Associated Acute Lung Injury/Acute Respiratory Distress Syndrome? **Frontiers in Cellular and Infection Microbiology**, v. 8, 16 maio 2018.

PETER, S. et al. Artemisinin and Derivatives-Based Hybrid Compounds: Promising Therapeutics for the Treatment of Cancer and Malaria. **Molecules**, v. 26, n. 24, p. 7521, 11 dez. 2021.

PETO, T. J. et al. Triple therapy with artemether–lumefantrine plus amodiaquine versus artemether–lumefantrine alone for artemisinin-resistant, uncomplicated falciparum malaria: an open-label, randomised, multicentre trial. **The Lancet Infectious Diseases**, v. 22, n. 6, p. 867–878, jun. 2022.

PHILLIPS, M. A. et al. Malaria. **Nature Reviews Disease Primers**, v. 3, 2017.

PILLAT, M. M. et al. Insights in Chloroquine Action: Perspectives and Implications in Malaria and <scp>COVID</scp> -19. **Cytometry Part A**, v. 97, n. 9, p. 872–881, 21 set. 2020.

PINHEIRO, L. C. S. et al. Current antimalarial therapies and advances in the development of semi-synthetic artemisinin derivatives. **Anais da Academia Brasileira de Ciencias**, v. 90, n. 1, p. 1251–1271, 2018.

PINO, P. et al. A multistage antimalarial target the plasmepsins IX and X essential for invasion and egress. **Science**, v. 358, n. 6362, p. 522–528, 27 out. 2017.

PORTUGALIZA, H. P. et al. Artemisinin exposure at the ring or trophozoite stage impacts Plasmodium falciparum sexual conversion differently. **eLife**, v. 9, 21 out. 2020.

PORTUGALIZA, H. P. et al. Plasmodium falciparum sexual conversion rates can be affected by artemisinin-based treatment in naturally infected malaria patients. **eBioMedicine**, v. 83, p. 104198, set. 2022.

PRATESI, A. et al. Reactions of Auranofin and Its Pseudohalide Derivatives with Serum Albumin Investigated through ESI-Q-TOF MS. **Inorg. Chem**. v. 57, 10507–10510, 2018.

PRICE, R. N. et al. Mefloquine resistance in Plasmodium falciparum and increased pfmdr1 gene copy number. **The Lancet**, v. 364, n. 9432, p. 438–447, jul. 2004.

PRICE, R. N. et al. Global extent of chloroquine-resistant Plasmodium vivax: a systematic review and meta-analysis. **The Lancet Infectious Diseases**, v. 14, n. 10, p. 982–991, out. 2014.

QUADROS, H. C.; SILVA, M. C. B.; MOREIRA, D. R. M. The Role of the Iron Protoporphyrins Heme and Hematin in the Antimalarial Activity of Endoperoxide Drugs. **Pharmaceuticals**, v. 15, n. 1, p. 60, 4 jan. 2022.

RAMOS, S. et al. Renal control of disease tolerance to malaria. **Proceedings of the National Academy of Sciences**, v. 116, n. 12, p. 5681–5686, 19 mar. 2019.

REAL, E.; MANCIO-SILVA, L. Single-cell views of the Plasmodium life cycle. **Trends in Parasitology**, v. 38, n. 9, p. 748–757, set. 2022.

RECHT, J. et al. Malaria in Brazil, Colombia, Peru and Venezuela: Current challenges in malaria control and elimination. **Malaria Journal**, v. 16, n. 1, p. 1–18, 2017.

REYSER, T. et al. Identification of compounds active against quiescent artemisinin-resistant Plasmodium falciparum parasites via the quiescent-stage survival assay (QSA). **Journal of Antimicrobial Chemotherapy**, 75(10), 2826–2834, 2020.

RIBBISO, K. A. et al. Artemisinin-Based Drugs Target the Plasmodium falciparum Heme Detoxification Pathway. **Antimicrobial Agents and Chemotherapy**, v. 65, n. 4, 18 mar. 2021.

RICCI, F. Social implications of malaria and their relationships with poverty. **Mediterranean Journal of Hematology and Infectious Diseases**, v. 4, n. 1, 2012.

ROE, M. S.; O'FLAHERTY, K.; FOWKES, F. J. I. Can malaria parasites be spontaneously cleared? **Trends in Parasitology**, v. 38, n. 5, p. 356–364, maio 2022.

SANZ, L. M. et al. P. falciparum In Vitro Killing Rates Allow to Discriminate between Different Antimalarial Mode-of-Action. **PLoS ONE**, v. 7, n. 2, p. e30949, 23 fev. 2012.

SAUNDERS, D. L.; VANACHAYANGKUL, P.; LON, C. Dihydroartemisinin–Piperaquine Failure in Cambodia. **New England Journal of Medicine**, v. 371, n. 5, p. 484–485, 31 jul. 2014.

SEIXAS, E. et al. Heme oxygenase-1 affords protection against noncerebral forms of severe malaria. **Proceedings of the National Academy of Sciences**, v. 106, n. 37, p. 15837–15842, 15 set. 2009.

SHAH, S. S.; FIDOCK, D. A.; PRINCE, A. S. Hemozoin Promotes Lung Inflammation via Host Epithelial Activation. **mBio**, v. 12, n. 1, 23 fev. 2021.

SHERIDAN, C. M. et al. The Plasmodium falciparum cytoplasmic translation apparatus: a promising therapeutic target not yet exploited by clinically approved anti-malarials. **Malaria Journal**, v. 17, n. 1, p. 1–13, 2018.

SSEMAGANDA, A. et al. Gold( <scp>i</scp> ) phosphine compounds as parasite attenuating agents for malaria vaccine and drug development. **Metallomics**, v. 10, n. 3, p. 444–454, 2018.
SURYAPRANATA, F. S. T. et al. Malaria in long-term travelers: Infection risks and adherence to preventive measures – A prospective cohort study. **Travel Medicine and Infectious Disease**, v. 49, p. 102406, set. 2022.

SUTHERLAND, C. J. et al. Mutations in the Plasmodium falciparum cytochrome b gene are associated with delayed parasite recrudescence in malaria patients treated with atovaquone-proguanil. **Malaria Journal**, v. 7, n. 1, p. 240, 20 dez. 2008.

TARNING, J. et al. Pitfalls in estimating piperaquine elimination. **Antimicrobial Agents and Chemotherapy**, v. 49, n. 12, p. 5127–5128, 2005.

TILLEY, L. et al. Artemisinin Action and Resistance in Plasmodium falciparum. **Trends in Parasitology**, v. 32, n. 9, p. 682–696, set. 2016.

TRAMPUZ, A. et al. Clinical review: Severe malaria. **Critical Care**, v. 7, n. 4, p. 315–323, 2003.

TSE, E. G.; KORSIK, M.; TODD, M. H. The past, present and future of anti-malarial medicines. **Malaria Journal**, v. 18, n. 1, p. 93, 22 dez. 2019.

VAN DER PLUIJM, R. W. et al. Triple artemisinin-based combination therapies versus artemisinin-based combination therapies for uncomplicated Plasmodium falciparum malaria: a multicentre, open-label, randomised clinical trial. **The Lancet**, v. 395, n. 10233, p. 1345–1360, abr. 2020.

VARO, R.; CHACCOUR, C.; BASSAT, Q. Update on malaria. **Medicina Clínica**, v. 155, n. 9, p. 395–402, nov. 2020.

VASQUEZ, M.; ZUNIGA, M.; RODRIGUEZ, A. Oxidative Stress and Pathogenesis in Malaria. **Frontiers in Cellular and Infection Microbiology**, v. 11, 30 nov. 2021.

VENNERSTROM, J. L. et al. Identification of an antimalarial synthetic trioxolane drug development candidate. **Nature**, v. 430, n. 7002, p. 900–904, ago. 2004.

VENUGOPAL, K. et al. Plasmodium asexual growth and sexual development in the haematopoietic niche of the host. **Nature Reviews Microbiology**, v. 18, n. 3, p. 177–189, 9 mar. 2020.

VERHAVE, J. P. **Robert Koch, malaria pioneer**. 2021.

WALTER, K.; JOHN, C. C. Malaria. **JAMA**, v. 327, n. 6, p. 597, 8 fev. 2022.

WANG, J. et al. A Temporizing Solution to “Artemisinin Resistance”. **New England Journal of Medicine**, v. 380, n. 22, p. 2087–2089, 30 maio 2019.

WATSON, J. A.; NEKKAB, N.; WHITE, M. Tafenoquine for the prevention of Plasmodium vivax malaria relapse. **The Lancet Microbe**, v. 2, n. 5, p. e175–e176, maio 2021.

WEISS, D. J. et al. Mapping the global prevalence, incidence, and mortality of Plasmodium falciparum, 2000–17: a spatial and temporal modelling study. **The Lancet**, v. 394, n. 10195, p. 322–331, jul. 2019.

WEISS, D. J. et al. Indirect effects of the COVID-19 pandemic on malaria intervention coverage, morbidity, and mortality in Africa: a geospatial modelling analysis. **The Lancet Infectious Diseases**, v. 21, n. 1, p. 59–69, jan. 2021.

WHITE, M. T. et al. Plasmodium vivax and Plasmodium falciparum infection dynamics: re-infections, recrudescences and relapses. **Malaria Journal**, v. 17, n. 1, p. 170, 17 dez. 2018.

WHITE, N. J. et al. Malaria. **The Lancet**, v. 383, n. 9918, p. 723–735, 2014.

WONG, W. et al. Mefloquine targets the Plasmodium falciparum 80S ribosome to inhibit protein synthesis. **Nature Microbiology**, v. 2, 2017.

WOODLEY, C. M. et al. Enantioselective Synthesis and Profiling of Potent, Nonlinear Analogues of Antimalarial Tetraoxanes E209 and N205. **ACS Medicinal Chemistry Letters**, v. 12, n. 7, p. 1077–1085, 8 jul. 2021.

YAHIYA, S. et al. The antimalarial screening landscape—looking beyond the asexual blood stage. **Current Opinion in Chemical Biology**, v. 50, p. 1–9, 2019.

ZANI, B. et al. Dihydroartemisinin-piperaquine for treating uncomplicated *Plasmodium falciparum* malaria. **Cochrane Database of Systematic Reviews**, 20 jan. 2014.

ZAVALA, F. RTS, S: the first malaria vaccine. **Journal of Clinical Investigation**, v. 132, n. 1, 4 jan. 2022.

ZOPPI, C. et al. ESI MS studies highlight the selective interaction of auranofin with protein free thiols. **Dalt. Trans**. v. 49, 5906–5913, 2020.

**Apêndice**: Lista de artigos publicados ou submetidos durante o doutorado

1. **HELENITA C. QUADROS**; MARIANA C. B. SILVA; DIOGO R. M. MOREIRA. The Role of the Iron Protoporphyrins Heme and Hematin in the Antimalarial Activity of Endoperoxide Drugs. PHARMACEUTICALS, v. 15, p. 1-18, 2022 (Publicado na revista Pharmaceuticals; DOI: 10.3390/ph15010060).

2. SOUSA, C. C.; DZIWORNU, G. A.; **HELENITA C. QUADROS**; ARAUJO-NETO, J. H.; CHIBALE, K.; MOREIRA, D. R. M. Antimalarial Pyrido [1,2- a ]benzimidazoles Exert Strong Parasiticidal Effects by Achieving High Cellular Uptake and Suppressing Heme Detoxification, 2022 (Artigo de colaboração publicado na revista ACS infectious diseases; DOI: 10.1021/acsinfecdis.2c00326).

3. **QUADROS, HELENITA COSTA**; DE MACÊDO FERREIRA SANTOS, LAÍS; MEIRA, CÁSSIO SANTANA; KHOURI, MARIANA IVO; MATTEI, BRUNO; SOARES, MILENA BOTELHO PEREIRA; DE CASTRO-BORGES, WILLIAM; FARIAS, LEONARDO PAIVA; FORMIGA, FABIO ROCHA. Development and in vitro characterization of polymeric nanoparticles containing recombinant adrenomedullin-2 intended for therapeutic angiogenesis, 2019 (Artigo publicado na revista International Journal of Pharmaceutics; DOI: 10.1016/j.ijpharm.2019.118997).

4. LARS HERRMANN, MARIA LEIDENBERGER, ROMAN POPOV, **HELENITA C. QUADROS**, BENEDIKT W. GRAU, FELIX JENNE, GIRISH K. SHANKARA, OLIVER FRIEDRICH, DIOGO R. M. MOREIRA, ALEXANDER NESTEROV-MÜLLER, * BARBARA KAPPES,* AND SVETLANA B. TSOGOEVA*. Fluorescent benzimidazole-artemisinin hybrids via metal-free click reactions: In Vitro and In Vivo studies of antimalarial activity (O artigo foi submetido à revista JACS em 2022).

5. ZILYANE CARDOSO DE SOUZA, FRANCISCO HUMBERTO XAVIER JÚNIOR, IRAPUAN OLIVEIRA PINHEIRO, JULIANA DE SOUZA REBOUÇAS, BRENDA OLIVEIRA DE ABREU, **HELENITA COSTA QUADROS**, TIAGO MANUEL FERNANDES MENDES, PAUL NGUEWA, SILMARA MARQUES ALEGRETTI5, LEONARDO PAIVA FARIAS, FABIO ROCHA FORMIGA*. Ameliorating the antiparasitic activity of the multifaceted drug ivermectin through a polymer nanocapsule formulation (O artigo foi submetido à revista International Journal of Pharmaceutics em 2022).

6. MACÊDO FERREIRA SANTOS, LAÍS DE; CARDIM BARRETO, BRENO; **COSTA QUADROS, HELENITA**; SANTANA MEIRA, CÁSSIO; SIQUEIRA FERRAZ-CARVALHO, RAFAELA DE; SOUZA REBOUÇAS, JULIANA DE; GARCIA MACAMBIRA, SIMONE; FRAGA VASCONCELOS, JULIANA; FREITAS SOUZA, BRUNO SOLANO DE; BOTELHO PEREIRA SOARES, MILENA; STELA SANTOS-MAGALHÃES, NEREIDE; ROCHA FORMIGA, FABIO. Tissue response and retention of micro- and nanosized liposomes in infarcted mice myocardium after ultrasound-guided transthoracic injection, 2022 (Artigo de colaboração publicado na revista European Journal of Pharmaceutics and biopharmaceutics; DOI: 10.1016/j.ejpb.2022.03.005).

7. CRUZ, KERCIA P.; PATRICIO, BEATRIZ F. C.; PIRES, VINÍCIUS C.; AMORIM, MARINA F.; PINHO, ALAN G. S. F.; **QUADROS, HELENITA C.**; DANTAS, DIANA A. S.; CHAVES, MARCELO H. C.; FORMIGA, FABIO R.; ROCHA, HELVÉCIO V. A.; VERAS, PATRÍCIA S. T. Development and Characterization of PLGA Nanoparticles Containing 17-DMAG, an Hsp90 Inhibitor, 2021 (Artigo de colaboração publicado na revista Frontiers in Chemistry; DOI: 10.3389/fchem.2021.644827).

8. ROCHA, VINÍCIUS; **QUADROS, HELENITA**; MEIRA, CÁSSIO; SILVA, LAÍS; CARVALHO, DAHARA; HODEL, KATHARINE; MOREIRA, DIOGO; SOARES, MILENA. Potential of Triterpenic Natural Compound Betulinic Acid for Neglected Tropical Diseases New Treatments, 2022 (Artigo publicado na revista Biomedicines; DOI: 10.3390/biomedicines10040831).

9. SALES, DANILO K.S.; SIMPLÍCIO, LÍLIAN M.T.; DA SILVA, CARLOS D.S.; ENJU, CAROLINA M.B.; SILVA, VANESSA B.; PAULO, TÉRCIO DE F.; SANTOS, IVANILSON P.; **QUADROS, HELENITA C.**; MEIRA, CÁSSIO S.; SOARES, MILENA B.P.; LOPES, LUIZ G. DE F.; DE SOUSA, EDUARDO H.S.; DE SÁ, DENISE S. A bis-indazolic ruthenium(II) complex: Reactivity and biological studies on cancer cells, 2021 (Artigo publicado na revista Inorganica Chimica Acta; DOI: 10.1016/j.ica.2020.120125).

10. VINÍCIUS ROCHA*, **HELENITA QUADROS***, LUANA GONÇALVES, ANTÔNIO MÁRCIO FERNANDES, BRUNA MACHADO, MILENA SOARES. Alternative methods for SARS-CoV-2 neutralizing antibodies measurement (O artigo está em fase de submissão à revista Viruses).